

**Studies on Power Plant Blue-Green Alga for
CO₂ Capture and Production of Oil,
Pigments and Biochar**

**Thesis Submitted by
Sumona Das**

Doctor of Philosophy (Engineering)

**Chemical Engineering Department
Faculty Council of Engineering & Technology
Jadavpur University
Kolkata, India**

2023

Dedicated to “Pillars of my life”

Mr. Ganesh Chandra Das (Father)

Mrs. Purnima Das (Mother)

&

Mr. Amit Kumar Das (Elder Brother)

JADAVPUR UNIVERSITY
KOLKATA 700032, INDIA

INDEX No. 145/17/E

- 1. Title of the thesis: Studies on Power Plant Blue-Green Alga for CO₂ Capture and Production of Oil, Pigments and Biochar**

- 2. Name, Designation & Institution of the Supervisor/s:**
 - **Name:** Ranjana Chowdhury

 - **Designation:** Professor

 - **Department:** Chemical Engineering Department

 - **Institute:** Jadavpur University, Kolkata-700032

Certificate from the Supervisor

*This is to certify that the thesis entitled "Studies on Power Plant Blue-Green Alga for CO₂ Capture and Production of Oil, Pigments and Biochar" submitted by **Sumona Das**, who got her name registered on **04/04/2017** for the award of Ph. D. (Engg.) degree of Jadavpur University is absolutely based upon his own work under the supervision of **Prof. Ranjana Chowdhury** and that neither his thesis nor any part of the thesis has been submitted for any degree or any other academic award anywhere before.*

Dr. Ranjana Chowdhury
Professor
Chemical Engineering Department
JADAVPUR UNIVERSITY
Kolkata-700 032

Ranjana Chowdhury 18/5/2023

Signature of the supervisor and date with office seal

“Statement of Originality”

I **Sumona Das** registered on **04/04/2017** do hereby declare that this thesis entitled” “**Studies on Power Plant Blue-Green Alga for CO₂ Capture and Production of Oil, Pigments and Biochar**” contains literature survey and original research work done by the undersigned candidate as part of Doctoral studies.

All information in this thesis have been obtained and presented in accordance with existing academic rules and ethical conduct. I declare that, as required by these rules and conduct, I have fully cited and referred all materials and results that are not original to this work.

I also declare that I have checked this thesis as per the “Policy on Anti Plagiarism, Jadavpur University, 2019”, and the level of similarity as checked by iThenticate software is 6%.

Sumona Das

Signature of Candidate:

Date: *19/05/2023*

Dr. Ranjana Chowdhury
Professor
Chemical Engineering Department
JADAVPUR UNIVERSITY
Kolkata-700 032

Certified by Supervisor(s):

(Signature with date, seal)

1. *Ranjana Chowdhury 18/5/2023*

List of Publications

| Serial no. | Publication Details | Publication category |
|------------|---|----------------------|
| 1 | Das, S., Nath, K., & Chowdhury, R. (2021). Comparative studies on biomass productivity and lipid content of a novel blue-green algae during autotrophic and heterotrophic growth. Environmental Science and Pollution Research, 28, 12107-12118. Doi: 10.1007/s11356-020-09577-4 | Research article |
| 2 | Das, S., Nath, K., Gupta, V. K., & Chowdhury, R. (2021). Studies on power plant algae: assessment of growth kinetics and bio-char production from slow pyrolysis process. Indian Chemical Engineer, 63(2), 129-138. Doi: https://doi.org/10.1080/00194506.2020.1845987 | Research article |
| 3 | Chowdhury, R., Das, S., & Ghosh, S. (2018). CO ₂ Capture and Utilization (CCU) in Coal-Fired Power Plants: Prospect of In Situ Algal Cultivation. Sustainable Energy Technology and Policies: A Transformational Journey, Volume 1, 231-254. Doi: https://link.springer.com/chapter/10.1007/978-981-10-7188-1_10 | Book chapter |

List of Presentations in National/International Conferences

| Serial no. | Details of Presentations |
|------------|---|
| 1 | Indo-Japan Bilateral Symposium on Future Perspective of Bioresource Utilization in North-Eastern Region (IJBS 17) ~ February 01-04, 2018 Guwahati, India. Bio-capture of CO ₂ using Blue Green Algae – Growth Kinetics and Characterization of High-Value Biochemicals Sumona Das ¹ , Ritwick Kali ¹ , Ranjana Chowdhury |
| 2 | 11th International Exergy, Energy and Environment Symposium (IEEEES-11), July 14-18, 2019, Chennai, India. Comparative studies on biomass productivity and lipid content of a novel blue-green algae during autotrophic and heterotrophic growth. Sumona Das, Kaustav Nath, *Ranjana Chowdhury Jadavpur University, Faculty of Engineering and Technology, Chemical Engineering Department, 188, Raja S.C. Mallick Rd, Kolkata, 700032, India |
| 3 | International Workshop on Hybrid Technologies for Conversion of Lignocellulosic Biomass to Biofuel (December 11-13, 2019) Sponsored by: DST, India. Chemical Engineering Department, Jadavpur University Kolkata 700032. Studies on Power Plant Algae: Assessment of growth kinetics and bio-char production from slow pyrolysis process. Sumona Das, Vivek Kumar Gupta, *Ranjana Chowdhury |
| 4 | 70th Annual Session of Indian Institute of Chemical Engineers CHEMCON – 2017 VERSATILITY OF CHEMICAL ENGINEERING TO MEET SOCIETAL CHALLENGES December 27 – 30, 2017 Dept. of Chemical Engineering, Haldia Institute of Technology. Studies on growth kinetics of Power plant blue-green algae with potential CO ₂ fixation efficiency and biomass productivity. Sumona Das, Ritwick Kali, Ritwick Bhattacharya, Ranjana Chowdhury* Chemical Engineering Department, Jadavpur University, Kolkata,700032, India |

Acknowledgement

It is my privilege to express my sincere thanks and gratitude to Prof. Ranjana Chowdhury, Chemical Engineering Department, Jadavpur University (Kolkata-700032) who has given me this opportunity to work in her research laboratory and constantly gave me invaluable guidance throughout the research work. She also encouraged me in accomplishing the PhD research work and without her support it would not have been possible to complete my PhD thesis.

Also I must express my gratitude to my Lab mates PhD research scholars, for their support and help during my PhD research work which proved to be a constant source of inspiration to me.

I also highly appreciate the prompt help and co-operation extended by the other scholars, faculty members and staff of Department of Chemical Engineering, Jadavpur University (Kolkata) at the various phases of the experimental work.

Above all, I want to express my special tribute of gratitude to my family members for their encouragement and constant support throughout the PhD research work.

Thanks to almighty for all his blessings and wish for accomplishing this work.

Sumona Das

List of Tables

| Table No. | Table Title | Page No. |
|-----------|---|----------|
| 2.1. | Photoautotrophic growth of Blue green algae/cyanobacteria | 18-31 |
| 2.2 | 2.2 Photoautotrophic growth of Microalgae | 31-43 |
| 2.3 | Photoheterotrophic and Photomixotrophic Growth of Blue-green Algae/ Cyanobacteria | 43-45 |
| 2.4 | Photoheterotrophic and Photomixotrophic Growth of Microalgae | 46-50 |
| 2.5 | Pyrolysis of blue green algae for production of Pyro-Char, Pyro-oil and Pyro-Gas. | 50-52 |
| 2.6 | Pyrolysis of microalgae for production of Pyro-Char, Pyro-oil and Pyro- Gas | 53-54 |
| 4.1 | Composition of Modified-18 media | 67-68 |
| 4.2 | List of Chemical used in the experimental work and procurement details. | 68-69 |
| 4.3 | Carbon, Hydrogen and Nitrogen contents(% w/w) of algal biomass cultivated under photoautotrophic and photoheterotrophic growth. | 75 |
| 5.1 | The experimental values of $\frac{w_R(t \rightarrow \infty)}{w_V(t \rightarrow \infty)}$ at different reaction temperatures | 90 |
| 6.1 | Lower and Upper limits of values of input variables (A: CO ₂ concentrations (g/L), B: NaNO ₃ concentrations (g/L) and C: light intensities (kLux). | 97 |
| 6.2 | The values of coded variables in the seventeen sets of experiments, designed using Box-Behnken method. | 98 |
| 6.3 | Calculated values of equilibrium concentration of CO ₂ and glycerol (C ₃ H ₈ O ₃) in aqueous phase corresponding to each gas phase concentration in CO ₂ -air mixture | 101 |
| 6.4 | Values of pH against CO ₂ concentrations (% v/v) of bubbling gas | 105 |

| Table No. | Table Title | Page No. |
|------------------|---|-----------------|
| 6.5 | Experimental values of biomass concentrations (g/L) and productivities (g/L/d) of <i>L.subtilis</i> JUCHE1 have been observed against each time intervals at different CO ₂ concentrations(% v/v) under photo-autotrophic growth mode. | 105 |
| 6.6 | Time histories of relative molar concentrations of oxygen (O _R) at different inlet-CO ₂ concentrations (5-20% v/v). | 106 |
| 6.7 | Experimental values of Specific growth rates at different substrate concentrations(g/L). | 108 |
| 6.8 | Haldane model parameters using Method-I and Method-II along with RMSE values | 109 |
| 6.9 | Calculated values of CO ₂ -Fixation rates(g/L/d) of <i>L.subtilis</i> JUCHE1 under photo-autotrophic condition. | 111 |
| 6.10 | Values of % carbon capture (CC) of <i>L.subtilis</i> JUCHE1 under photo-autotrophic growth. | 111 |
| 6.11 | Comparison of the CO ₂ fixation rate of <i>Leptolyngbya subtilis</i> JUCHE1 with other algal strains. | 113- 114 |
| 6.12 | Experimental values of biomass concentrations (g/L) and productivities (g/L/d) against each time intervals at individual NaNO ₃ concentrations(g/L) as nitrogen source. | 116 |
| 6.13 | Comparison of effect of NaNO ₃ concentration on biomass productivity of <i>Leptolyngbya subtilis</i> JUCHE1 with literature data on other algal strains. | 117 |
| 6.14 | The calculated values of Specific growth rate, μ (d ⁻¹) at different NaNO ₃ concentrations under photo-autotrophic growth condition. | 119 |
| 6.15 | CO ₂ fixation rate of different algal strains varying nitrogen concentrations. | 121 |

| Table No. | Table Title | Page No. |
|------------------|--|-----------------|
| 6.16 | The experimental values of biomass concentrations and productivities at each time intervals under the irradiance of light intensities having range of 145-3.2kLux. | 123 |
| 6.17 | Values of CO ₂ fixation rate (g/L/d) at each time intervals under the irradiance of light intensities having range of 145-3.2kLux. | 124 |
| 6.18 | Statistical Analysis for the validation of predictive growth models using calculated/assumed constant parameters. | 126 |
| 6.19 | Normalized experimental and calculated values of specific growth rates, $\mu_{Norm,I}$ for three different growth models such as Steele, Aiba and Bernard and Remond varying light intensities in the range of 1.45- 3.2 kLux. | 127 |
| 6.20 | Normalized values of μ , (d ⁻¹) with respect to each NaNO ₃ concentrations from 1-2.5 g/L. | 129 |
| 6.21 | The ANOVA table for the quadratic model. | 132 |
| 6.22 | Fit statistics summary | 133 |
| 6.23 | The comparison of experimental values of set of “ μ ” with the prediction of Kinetic Model and the Quadratic Model Equation using Box–Behnken Design method | 133 |
| 6.24 | Experimental values of biomass concentrations (g/L) against each time intervals at different gas phase CO ₂ equivalent glycerol concentrations under photoheterotrophic growth mode. | 137 |
| 6.25 | Values of % carbon capture (CC) of <i>L.subtilis</i> JUCHE1 under photo-heterotrophic growth. | 138 |
| 6.26 | The calculated values of Specific growth rate, μ (d ⁻¹) at each individual inlet-CO ₂ equivalent glycerol concentrations under photo-heterotrophic growth condition. | 139 |

| Table No. | Table Title | Page No. |
|------------------|--|-----------------|
| 6.27 | Values of glycerol consumption, X_{gly} against each time intervals at time (t) under photo-heterotrophic growth. | 142 |
| 6.28 | Experimental values of biomass concentrations at each time interval under mixotrophic growth using CO ₂ and glycerol as carbon sources. | 143 |
| 6.29 | Biomass concentration (g/L) of various algal strains under mixotrophic growth. | 145-146 |
| 6.30 | Calculated values of specific growth rates at each equivalent carbon concentrations (mg-atom/L) for three growth modes (photoautotrophic, photoheterotrophic and mixotrophic). | 148 |
| 7.1 | Time history of Lipid content and productivity under photoautotrophic growth mode with the variation of inlet gas-phase CO ₂ concentrations | 160 |
| 7.2 | Fatty acid profile of <i>Leptolyngbya subtilis</i> JUCHE1 | 161 |
| 7.3 | Experimental values of Lipid content and productivity of <i>Leptolyngbya subtilis</i> JUCHE1 varying concentrations of NaNO ₃ from 1-2.5g/L at each time intervals. | 164 |
| 7.4 | Comparison of the influence of variation of NaNO ₃ concentration on the performance of algal strains with respect to lipid production | 165-166 |
| 7.5 | Experimental values of lipid content at each time intervals varying light intensities from (1.45-3.2kLux). | 168 |
| 7.6 | Experimental values of Lipid content (%w/w) and Lipid productivities (g/L/d) with respect to time under photo-heterotrophic growth. | 170 |
| 7.7 | Identified compounds from extracted lipid of <i>L.subtilis</i> JUCHE1 under photo-heterotrophic growth using glycerol (as carbon source) | 173 |
| 7.8 | Lipid content and lipid productivities of algal strains in both autotrophic and heterotrophic conditions. | 174-175 |

| Table No. | Table Title | Page No. |
|------------------|--|-----------------|
| 7.9 | Experimental values of lipid content and productivities at different Carbon concentrations CO ₂ :Glycerol (1:1 ratio) under mixotrophic growth. | 178 |
| 7.10 | The values of Lipid content (%w/w) of various algal strains under mixotrophic growth. | 179 |
| 7.11 | Pigment contents(% wt.) of different algal strains under different growth conditions (Photoautotrophic , Photoheterotrophic and Photomixotrophic). | 182 |
| 8.1 | Observed values of biomass concentration and productivities of <i>L.subtilis</i> JUCHE1 at each time interval under different wavelengths of light (yellow, green, red and blue). | 193 |
| 8.2 | Values of maximum biomass concentration, biomass productivity and specific growth rate of <i>L. subtilis</i> JUCHE1 obtained for different wavelengths of light. | 193 |
| 8.3 | Comparison of biomass concentration under different wavelength at 6 th day with literature data. | 195 |
| 8.4 | Experimental values of lipid content(%w/w) and productivities (g/L/d) under irradiance of varying different wavelengths of light | 198 |
| 8.5 | Lipid content(%w/w) of algal strains in different spectrums of light | 198- 199 |
| 8.6 | Values of CO ₂ Fixation Rate (g/L/d) at each time intervals for all the wavelengths of light. | 201 |
| 8.7 | The values of Chlorophyll (a+b) and Carotenoid content (%w/w) of <i>L.subtilis</i> JUCHE1 at each time intervals from 0-6 days under the irradiation of different wavelengths of light (Yellow, Blue, Green and Red) | 204 |
| 8.8 | Observed values of biomass concentrations at each time interval under yellow light using IEIGPBR in the semi-continuous mode. | 206 |

| Table No. | Table Title | Page No. |
|------------------|---|-----------------|
| 8.9 | Values of Lipid content (%w/w) and Lipid productivity g/L/d at each time intervals under yellow light using IEIGPBR in the semi-continuous mode. | 208 |
| 8.10 | Values of CO ₂ Fixation rate of <i>L. subtilis</i> JUCHE1 at each time interval under yellow light using IEIGPBR in the semi-continuous mode. | 209 |
| 9.1 | Observed values of Weight of residual biomass (W _R , g) and Weight of volatile matter (W _V , g) at each time intervals varying reaction temperatures (300, 500, 700°C). | 216 |
| 9.2 | The experimental values of $\frac{w_R(t \rightarrow \infty)}{w_V(t \rightarrow \infty)}$ at different reaction temperatures | 217 |
| 9.3 | Experimental values of W _c with respect to individual time intervals at different temperatures 300 °C, 500 °C and 700 °C. | 218 |
| 9.4 | Maximum yields values of Pyro-char (% wt.), Pyro-oil(%wt.) and Pyro-Gas (%wt.) of different Algae at different reaction temperatures | 221 |
| 9.5 | Calculated values of ln W _{un} at each reaction time varying different temperatures | 223 |
| 9.6 | Values of rate constants at different temperatures | 224 |
| 9.7 | Values of the rate constants of formation of volatiles at different temperatures | 225 |
| 9.8 | Calculated values of weight of volatile matters and (1-Exp(-kt)) at different temperatures and time intervals. | 226 |
| 9.9 | Values of k, k _v , k _c , ln (k), ln(k _v) at different temperatures (300, 500 and 700 °C). | 227 |
| 9.10 | Values of activation energies and pre-exponential factors | 227 |
| 9.11 | Characterization of pyro-oil using GC-MS analysis | 231 |

List of Figures

| Figure No. | Figure Title | Page No. |
|------------|--|----------|
| 1.1 | Different growth metabolism of phototrophic microorganism “Algae”. | 3 |
| 1.2 | Schematic representation of Biomass, Lipid, Amino acids (Chlorophyll), Carbohydrate synthesis through different pathways (photosynthesis, oxidative phosphorylation, pentose phosphate pathway, glycolysis) in algae by utilization of both inorganic carbon source (CO ₂) and Organic carbon source (Glycerol). | 5 |
| 1.4 | Biochemical process of CO ₂ sequestration and biomass conversion through algal biorefinery concept | 8 |
| 1.5 | Integrated scheme of a coal-fired thermal power plant and algal biorefinery | 9 |
| 4.1 | CO ₂ sparging into the aquarium containing M-18 medium for cultivation of <i>Leptolyngbya subtilis</i> JUCHE1. | 67 |
| 4.2 | Photographs of instruments used in the experimental study: (A) Incubator, (B) Centrifuge, (C) Hot air Oven | 70 |
| 4.3 | Photograph of Elemental Analyzer (C-H-N-S). | 71 |
| 4.4 | Photograph of Gas chromatography mass spectrophotometry (GC-MS) | 71 |
| 4.5 | Photograph of Lux meter. | 72 |
| 4.6 | Photograph of pH meter. | 72 |
| 4.7 | Photograph of Spectrophotometer. | 73 |
| 6.1 | Small scale bioreactor set up for batch experiments under Photoautotrophic growth mode. | 95 |
| 6.2 | Experimental set-up of the batch study for 0-5 days at different concentrations of NaNO ₃ as nitrogen substrate | 96 |

| Figure No. | Figure Title | Page No. |
|------------|---|----------|
| 6.3 | Culture tubes for the batch experiments under photoheterotrophic condition | 100 |
| 6.4 | Micrographs of <i>Leptolyngbya subtilis</i> JUCHE1 with different magnifications as shown in: (A) 600x magnification and (B) 5000x magnification. | 102 |
| 6.5 | Growth curve of <i>Leptolyngbya subtilis</i> JUCHE1 under photoautotrophic condition varying inlet CO ₂ concentrations from 5-20(% v/v). | 104 |
| 6.6 | Algal growth of <i>L.subtilis</i> JUCHE1 at 4th day varying different inlet-CO ₂ concentrations from 5-20%. | 104 |
| 6.7 | (A) Experimental growth curve of <i>Leptolyngbya subtilis</i> JUCHE1 with variation of CO ₂ concentration (μ against Initial liquid phase CO ₂ concentration); Figure 6.7 (B) Double reciprocal plot ($1/\mu$ versus $1/C_{CO_2}$) | 104 |
| 6.8 | Simulated and experimental values of specific growth rate " μ " against Initial liquid phase CO ₂ concentration | 109 |
| 6.9 | CO ₂ fixation rate of <i>Leptolyngbya subtilis</i> JUCHE1 under photoautotrophic growth by varying inlet CO ₂ concentrations. | 110 |
| 6.10 | Experimental set up for batch study varying NaNO ₃ concentrations from 1-2.5g/L as substrate. | 115 |
| 6.11 | Effect of different NaNO ₃ concentrations (1 - 2.5g/L of NaNO ₃) on the cell growth of <i>Leptolyngbya subtilis</i> JUCHE1. | 116 |
| 6.12 | (A) Specific growth rate against initial NaNO ₃ concentrations (1-2.5 g/L) and (B) Double reciprocal plot of $1/\mu$ against $1/C_{NaNO_3}$. | 119 |
| 6.13 | CO ₂ fixation rate of <i>L.subtilis</i> JUHE1 with the variation of NaNO ₃ concentration | 120 |

| Figure No. | Figure Title | Page No. |
|------------|---|----------|
| 6.14 | Growth curve of <i>L.subtilis</i> JUCHE1 varying light intensities from 1.45-3.2 kLux for 0-4 days under photoautotrophic growth. | 122 |
| 6.15 | Biomass productivities (g/L/d) of <i>L.subtilis</i> JUCHE1 for all light intensities for 0-4 days. | 123 |
| 6.16 | Time histories plot of CO ₂ fixation rate of <i>L.subtilis</i> JUCHE1 varying light intensities from 1.45-3.2kLux | 124 |
| 6.17 | Graphical plots of : (A) Experimental variation of μ against light intensity and (B) Comparison of observed and simulated values of $\mu_{Norm,I}$ using Steele model against light intensity | 127 |
| 6.18 | Growth curve of the normalized values of specific growth rate of experimental and simulated models of Steele, Aiba and Bernard and Remond have been compared. | 128 |
| 6.19 | The growth kinetic plots: (A) f_{NaNO_3} verses each concentration of NaNO ₃ (C_{NaNO_3}) and (B) Double reciprocal plot of $\frac{1}{f_{NaNO_3}}$ versus $\frac{1}{C_{NaNO_3}}$. | 129 |
| 6.20 | Comparison between experimental and simulated (Steele model) trend of f_I against light intensity. | 130 |
| 6.21 | Predicted verses Actual plot of specific growth rate, μ (d ⁻¹) | 132 |
| 6.22 | The change of μ according to AB: CO ₂ concentration (g/L) and NaNO ₃ concentrations (g/L) , BC: NaNO ₃ concentrations (g/L) and Light intensities (kLux) and AC: CO ₂ concentrations (g/L) and Light intensities (kLux) using Box–Behnken method (a, c, e) 3-D model graphs, (b, d, f) Contour Graphs. | 134 |
| 6.23 | Biomass concentration time histories of <i>L.subtilis</i> JUCHE1 under photo-heterotrophic mode of growth. | 136 |
| 6.24 | Algal growth at different CO ₂ equivalent carbon concentrations of glycerol under photo heterotrophic growth. | 137 |

| Figure No. | Figure Title | Page No. |
|-------------------|---|-----------------|
| 6.25 | The growth kinetic plots (A, B and C) of <i>Leptolyngbya subtilis</i> JUCHE1 under photoheterotrophic growth using glycerol as organic carbon source: (A) Graphical representation of specific growth rates at different CO ₂ equivalent glycerol concentrations (g/L), (B) Double reciprocal plot of 1/ μ versus 1/C _{gly} , (C) Simulated and experimental values of specific growth rate “ μ ” against different CO ₂ equivalent glycerol concentrations. | 139 |
| 6.26 | Glycerol consumption of <i>Leptolyngbya subtilis</i> JUCHE1 at different time intervals under photo-heterotrophic growth. | 141 |
| 6.27 | Biomass concentrations of <i>L.subtilis</i> JUCHE1 at each time intervals varying carbon concentrations under mixotrophic growth. | 142 |
| 6.28 | Biomass productivities (g/L/d) of <i>L.subtilis</i> JUCHE1 at each time intervals varying Carbon concentrations under mixotrophic growth. | 144 |
| 6.29 | Specific growth rate of <i>L.subtilis</i> JUCHE1 against each equivalent Carbon concentrations under three growth modes (photoautotrophic, photoheterotrophic and mixotrophic). | 147 |
| 7.1 | Overall flow diagram of lipid extraction process from algal biomass. | 156 |
| 7.2 | Overall solvent extraction process for pigment extraction from algal biomass of <i>L.subtilis</i> JUCHE1. | 157 |
| 7.3 | Effect of inlet CO ₂ concentrations (5-20% v/v) on time history of Lipid content under photo- autotrophic growth | 159 |
| 7.4 | Effect of inlet CO ₂ concentrations (5-20% v/v) on time history of Lipid productivity under photo- autotrophic growth | 160 |
| 7.5 | GC-MS chromatogram of extracted lipid of <i>L.subtilis</i> JUCHE1 | 162 |
| 7.6 | GC-MS chromatogram of identified DHA from the extracted lipid of <i>L.subtilis</i> JUCHE1 | 162 |

| Figure No. | Figure Title | Page No. |
|-------------------|--|-----------------|
| 7.7 | Dependence of time history of lipid content of <i>Leptolyngbya subtilis</i> JUCHE1 on NaNO ₃ concentration (1-2.5g/L) | 163 |
| 7.8 | Dependence of time history of Lipid productivity of <i>Leptolyngbya subtilis</i> JUCHE1 on NaNO ₃ concentration (1-2.5g/L) | 164 |
| 7.9 | Bar plot of (A)Lipid content(%w/w) and (B) Lipid productivity of <i>L.subtilis</i> JUCHE1 at each time intervals i.e. 0-4th days for different light intensities having range of 1.45-3.2kLux. | 168 |
| 7.10 | Lipid content(%w/w) of <i>Leptolyngbya subtilis</i> JUCHE1 varying different equivalent glycerol concentrations | 170 |
| 7.11 | Lipid productivities(g/L/d) of <i>Leptolyngbya subtilis</i> JUCHE1 varying different equivalent glycerol concentrations. | 171 |
| 7.12 | Reaction pathway for fatty acid synthesis under mixotrophic growth of alga using CO ₂ and glycerol. | 171 |
| 7.13 | Chromatogram of extracted lipid under photoheterotrophic growth using glycerol as organic carbon source. | 172 |
| 7.14 | Lipid production (g/L) by <i>L.subtilis</i> JUCHE1 varying C-concentrations under mixotrophic growth. | 177 |
| 7.15 | Lipid productivities (g/L/d) of <i>L.subtilis</i> JUCHE1 against each time intervals varying different C-concentrations under mixotrophic growth. | 177 |
| 7.16 | Maximum values of Lipid content (%w/w) and productivity (g/L/d) under photoautotrophic, photomixotrophic and photoheterotrophic growth. | 178 |
| 7.17 | Bar plot of Chlorophyll (a+b) and Carotenoid contents (%w/w) of <i>L.subtilis</i> JUCHE1 observed under different growth condition (Photoautotrophic, Photoheterotrophic and Photomixotrophic) on 4-5 th day of culture period. | 180 |

| Figure No. | Figure Title | Page No. |
|-------------------|--|-----------------|
| 8.1 | Small scale bioreactor set up for batch experiments varying different wavelengths of light. | 188 |
| 8.2 | The schematic diagram of Internally-Externally Illuminated Gas lift Photobioreactor (IEIGPBR) using yellow wavelength for algal cultivation. | 191 |
| 8.3 | Time histories of photoautotrophic biomass growth of <i>L. subtilis</i> JUCHE1 under irradiation of varying wavelength of light (Blue, Green, Yellow and Red). | 192 |
| 8.4 | Time histories of lipid accumulation by <i>L. subtilis</i> JUCHE1 under irradiation of varying wavelength of light (blue, green, yellow and red). | 197 |
| 8.5 | Values of CO ₂ fixation rate of <i>L. subtilis</i> JUCHE1 under irradiation of varying wavelength of light (blue, green, yellow and red). | 201 |
| 8.6 | Bar plot of Chlorophyll contents (%w/w) of <i>L.subtilis</i> JUCHE1 against each time intervals from 0-6 days under the irradiation of different wavelengths of light (Yellow, Blue, Green and Red). | 203 |
| 8.7 | Bar plot of Carotenoid contents (%w/w) of <i>L.subtilis</i> JUCHE1 against each time intervals from 0-6 days under the irradiation of different wavelengths of light (Yellow, Blue, Green and Red). | 203 |
| 8.8 | Maximum value of Chlorophyll (a+b) and Carotenoid content(% w/w) under the irradiation of different wavelengths of light (Yellow, Blue, Green and Red). | 204 |
| 8.9 | Photograph of IEIGPBR under operation | 205 |
| 8.10 | Time history of Algal biomass concentration in IEIGPBR | 205 |
| 8.11 | Time histories of lipid content and the productivity in IEIGPBR | 207 |
| 8.12 | Time history of CO ₂ Fixation rate of <i>L. subtilis</i> JUCHE1 in IEIGPBR | 208 |
| 9.1 | Dry algal biomass of <i>L.subtilis</i> JUCHE1. | 214 |

| Figure No. | Figure Title | Page No. |
|-------------------|--|-----------------|
| 9.2 | Graphical representation of weight of residue W_R and W_v with respect to reaction time by variation of temperature from 700°C to 300°C. | 215 |
| 9.3 | Experimental and model fit plot of Weight of char (W_c) of <i>L. subtilis</i> JUCHE1 at different temperatures (300°C, 500°C and 700°C) in respective reaction time. | 217 |
| 9.4 | Photographs of Pyro char of <i>Leptolyngbya subtilis</i> JUCHE1 at different pyrolysis temperatures (A) Dry algal biomass, (B) 300°C , (C)500°C, (D) 700°C. | 219 |
| 9.5 | Yields of Bio-char, oil and gas of <i>Leptolyngbya subtilis</i> JUCHE1 at each time intervals and different reaction temperatures (300°C to 700°C). | 219 |
| 9.6 | Graphical representation of the plot of $\ln W_{un}$ with respect to each to intervals at different reaction temperatures: (A) 300, (B) 500 and (C) 700 °C. | 223 |
| 9.7 | Graphical representation of the plot of $(1-\text{Exp}(-kt))$ vs W_v at different reaction temperatures (A)300, (B) 500 and (C) 700 °C. | 225 |
| 9.8 | Determination of activation energies and pre-exponential factors (A: for k ; B: for k_p) | 227 |
| 9.9 | Thermo-Gravimetric Analysis (TGA) of Dry Algal biomass at different heating rate 10, 15, 20, 25 and 30 °C/min | 228 |
| 9.10 | Thermogravimetric Analysis (TGA) of Pyro-char at 500 °C . | 229 |
| 9.11 | Thermogravimetric Analysis (TGA) of Pyro-char at 700 °C. | 229 |
| 9.12 | Chromatogram of Pyro-oil obtained at 500°C. | 230 |

CONTENTS

| Content | Page No. |
|--|----------|
| List of Tables | i-vi |
| List of Figures | vii-xii |
| Chapter 1. Introduction | 1-16 |
| 1.1 Preamble | 1-2 |
| 1.2 Phototrophic Algae | 2 |
| 1.2.1 Photoautotrophic growth of Algae | 2-5 |
| 1.2.2 Photoheterotrophic and Photomixotrophic Growth of Algae | 6 |
| 1.3 Prospect of generation of specialty Biochemicals and biofuels from algae | 6-10 |
| 1.3.1 Biochemicals from algae | 6-7 |
| 1.3.2 Biofuels from algae | 7-8 |
| 1.3.3 Algal Carbon Capture and Utilization | 8-10 |
| Chapter 1 Bibliography | 11-16 |
| Chapter 2. Literature Review | 17 |
| 2.1 Photoautotrophic growth of Blue green algae/cyanobacteria | 18-31 |
| 2.2 Photoautotrophic growth of Microalgae | 31-43 |
| 2.3 Photoheterotrophic and Photomixotrophic Growth of Blue green algae/cyanobacteria | 43-45 |
| 2.4 Photoheterotrophic and Photomixotrophic Growth of Microalgae | 45-50 |
| 2.5 Pyrolysis of blue green algae for production of Pyro-Char, Pyro-oil and Pyro-Gas | 50-52 |
| 2.6 Pyrolysis of microalgae for production of Pyro-Char, Pyro-oil and Pyro-Gas | 53-54 |

| Content | Page No. |
|--|-----------------|
| Chapter 2 Bibliography | 55-60 |
| Chapter 3. Aim and Objective | 61-66 |
| Chapter 4. Materials and methods | 67-75 |
| 4.1. Materials and methods | 67 |
| 4.1.2. Algal strain collection and identification | 67 |
| 4.1.3 Growth medium | 67-68 |
| 4.1.4. Chemicals | 68-69 |
| 4.1.5 Equipment's and apparatus | 69-70 |
| 4.2. Determination of algal cell mass | 70-74 |
| 4.3. Analytical Methods | 70 |
| 4.3.1. Field Emission Scanning Electron Microscope (FESEM) | 70-71 |
| 4.3.2 CHN analysis | 71 |
| 4.3.3 GC-MS analysis | 72 |
| 4.3.4 Lux Meter | 72 |
| 4.3.5 pH meter | 73 |
| 4.3.6 Spectrophotometric analysis | 73 |
| 4.3.6.1 Quantification of Glycerol concentration | 73 |
| 4.3.6.2 Detailed method for glycerol determination | 74 |
| 4.3.6.3 Preparation of calibration curve | 74 |
| 4.3.6.4 Sample analysis | 74 |
| 4.3.7 Quantification of Pigment concentration | 74 |
| 4.4 Elemental analysis of <i>L.subtilis</i> JUCHE1 | 75 |

| Content | Page No. |
|--|-----------------|
| Chapter 4 Bibliography | 76 |
| Chapter 5. Theoretical Analysis | 77-92 |
| 5.1.1 Determination of liquid phase CO ₂ Concentration under equilibrium | 77 |
| 5.1.2 Biomass Production rate | 78 |
| 5.1.3 Assessment of CO ₂ Bio-fixation Rate | 78 |
| 5.1.4 Determination of the relative molar concentration of Oxygen (O _R) | 78-79 |
| 5.1.5 Specific growth rate | 79 |
| 5.1.6 Determination of growth kinetic parameters | 79-81 |
| 5.1.7 Mathematical models for Algal growth | 81 |
| 5.1.7.1 Dependence on CO ₂ and NaNO ₃ | 81 |
| 5.1.7.2 Dependence on Light Intensity | 81-82 |
| 5.1.7.3 Multi-Variate (CO ₂ -NaNO ₃ -I) Kinetics | 82-83 |
| 5.1.7.3 Statistical analysis | 83-84 |
| 5.1.8 Response surface methodology (RSM) | 84 |
| 5.1.9 Determination of equivalent glycerol concentration against each gas phase concentration of CO ₂ | 85-86 |
| 5.1.9.1 Conversion of Glycerol | 85-86 |
| 5.1.10 Carbon capture | 86 |
| 5.1.11 Estimation of Lipid content | 86 |
| 5.1.11.1 Lipid production rate (P _L) | 87 |
| 5.1.12 Calculation of content of extracted Pigment | 87 |
| 5.1.13 Lumped Kinetics Pyrolysis of Algal biomass | 87-88 |

| Content | Page No. |
|---|-----------------|
| 5.1.13.1 Determination of overall rate constants (k , k_v) at different temperatures | 88-89 |
| 5.1.13.2 Activation energies and pre-exponential factors | 89 |
| 5.1.13.3 Determination of Pyrolysis Products | 89-91 |
| 5.1.13.3.1 Volatiles | 89 |
| 5.1.13.3.2 Pyro-oil | 89 |
| 5.1.13.3.3 Pyro-gas | 90 |
| 5.1.13.3.4 Pyro-char and unreacted algal mass | 90-91 |
| Chapter 5 Bibliography | 92 |
| Chapter 6 Growth Performance of isolated blue green alga under photoautotrophic (CO ₂)- photoheterotrophic(Glycerol)-photo-mixotrophic (CO ₂ +Glycerol) conditions | 93-154 |
| 6.1 Growth under photoautotrophic condition | 93 |
| 6.1.1 Experimental | 93 |
| 6.1.1.1 Maintenance and Growth Culture medium | 93-94 |
| 6.1.1.2 Experimental setup | 94 |
| 6.1.1.3 Batch experiments for CO ₂ as substrate under Photoautotrophic growth mode | 94-95 |
| 6.1.1.4 Batch studies for Growth kinetics on Nitrogen Substrate | 95-96 |
| 6.1.1.5 Determination of dependence of Growth kinetics on Light Intensity | 96 |
| 6.1.1.6 Dependence of Growth simultaneously on CO ₂ - NaNO ₃ -I | 96 |
| 6.1.1.7 Experimental Design | 99-100 |
| 6.2 Growth under Photoheterotrophic condition | 99 |
| 6.2.1 Experimental | 99 |

| Content | Page No. |
|--|-----------------|
| 6.2.1.1 Maintenance and Growth Culture medium | 99 |
| 6.2.1.2 Batch experiments under Photoheterotrophic condition | 99-100 |
| 6.3 Growth under Photomixotrophic condition | 100-101 |
| 6.3.1 Experimental | 100 |
| 6.3.1.1 Maintenance and Growth Culture medium | 100 |
| 6.3.1.2 Batch experiments under mixotrophic condition | 100-101 |
| 6.5 Results and discussions | 102 |
| 6.5.1 Morphological characterization of Power Plant Blue Green Alga | 102 |
| 6.5.2 Effect of CO ₂ bubbling on medium pH | 102-103 |
| 6.5.3 Equilibrium aqueous phase concentration of CO ₂ | 103 |
| 6.5.4 Effect of inorganic carbon source (CO ₂) on algal growth | 103-106 |
| 6.5.4.1 Growth kinetic study | 107-109 |
| 6.5.4.2 CO ₂ fixation rate of <i>L. subtilis</i> JUCHE1 | 110-114 |
| 6.5.4.3 Effect of different nitrogen concentrations on algal growth | 114-118 |
| 6.5.4.3.1 Growth kinetics | 118-119 |
| 6.5.4.3.2 CO ₂ fixation rate of <i>L. subtilis</i> JUCHE1 | 119-123 |
| 6.5.4.4 Effect of different light intensities having range of 1.45-3.2 kLux on algal growth | 123 |
| 6.5.4.4.1 CO ₂ fixation rate of <i>L. subtilis</i> JUCHE1 under different light intensities | 123-124 |
| 6.5.4.5 Predictive modeling and simulation | 125 |
| 6.5.4.5.1 Statistical validation of mathematical growth models | 125-126 |
| 6.5.4.6 Effect of light intensity on algal growth | 127-128 |

| Content | Page No. |
|---|-----------------|
| 6.5.4.7 Growth kinetics incorporating Combined effects of CO ₂ - NaNO ₃ -I | 128 |
| 6.5.4.7.1 Correction factor for NaNO ₃ | 128-129 |
| 6.5.4.7.2 Correction factor for Light Intensity | 130 |
| 6.5.4.8 Response surface methodology (RSM) | 130-135 |
| 6.5.4.8.1 Effect of the interaction of coded variables: (A) CO ₂ Concentration, (B) NaNO ₃ Concentration and (C) Light Intensity on the specific growth rate | 134-135 |
| 6.5.5 Effect of organic carbon source (Glycerol) on growth of algal biomass under photo-heterotrophic condition | 135-138 |
| 6.5.5.1 Growth kinetics | 138-141 |
| 6.5.5.2. Glycerol Consumption | 141-142 |
| 6.5.6 Effect of mixture of inorganic + organic carbon source (CO ₂ :Glycerol) in (1:1 ratio) on growth of algal biomass under mixotrophic condition | 142-146 |
| 6.5.7 Algal growth rate under three different modes of cultivation (Photo-autotrophic, Photo-heterotrophic and Photo-mixotrophic) | 147-148 |
| Chapter 6 Bibliography | 149-154 |
| Chapter 7 Studies on lipid and pigments (Chlorophyll and Carotenoid) production by alga under Photoautotrophic, Photoheterotrophic and Photomixotrophic conditions using white light | 155 |
| 7.1 Materials and Methods | 155 |
| 7.1.1 Chemicals | 155 |
| 7.1.2 Lipid extraction | 155 |
| 7.1.3 Pigment extraction | 156 |
| 7.1.4 Characterization of Lipid | 157 |
| 7.2 Experimental conditions | 157 |

| Content | Page No. |
|---|-----------------|
| 7.2.1 Lipid | 157 |
| 7.2.2 Pigment | 158 |
| 7.3 Results and Discussion | 158 |
| 7.3.1 Lipid accumulation of <i>L.subtilis</i> JUCHE1 under Photoautotrophic growth | 158-160 |
| 7.3.1.2 Characterization of Lipid | 160-162 |
| 7.3.1.3 Lipid production varying inlet-CO ₂ concentrations (%v/v) under photoautotrophic mode of cultivation | 162-166 |
| 7.3.1.4. Effect of Sodium nitrate concentrations on lipid accumulation | 167-168 |
| 7.3.2 Lipid accumulation of <i>L.subtilis</i> JUCHE1 under Photoheterotrophic growth | 169 |
| 7.3.2.1 Lipid production varying CO ₂ equivalent glycerol concentrations under photoheterotrophic mode of cultivation | 169-171 |
| 7.3.2.2 Characterization of Lipid | 172-173 |
| 7.3.3 Comparison of lipid production of <i>L.subtilis</i> JUCHE1 under both photoauto and heterotrophic growth condition | 174-175 |
| 7.3.4 Lipid accumulation of <i>L.subtilis</i> JUCHE1 under mixotrophic growth | 175 |
| 7.3.4.1 Effect of both organic and inorganic C-source on Lipid accumulation of <i>L.subtilis</i> JUCHE1 under mixotrophic growth | 175-179 |
| 7.3.5 Content of Photosynthetic pigments (Chlorophyll and Carotenoid) under Photoautotrophic, heterotrophic and mixotrophic growth | 179-182 |
| Chapter 7 Bipligraphy | 183-186 |
| Chapter 8 Study the effect of different light wavelengths on algal growth and lipid accumulation by Blue-Green Alga <i>L.subtilis</i> JUCHE | 187 |
| 8.1 Materials and methods | 187 |
| 8.1.1 Nutrient medium | 187 |

| Content | Page No. |
|--|-----------------|
| 8.1.2 Batch mode cultivation of <i>L.subtilis</i> JUCHE1 with the variation of light wavelength | 188 |
| 8.1.3 Semi-Continuous Operation of mode of Gas-lift Photobioreactor | 189-191 |
| 8.2 Results and discussion | 191-209 |
| 8.2.1 Batch mode cultivation of <i>L. subtilis</i> JUCHE1 | 191 |
| 8.2.1.1 Growth of <i>L. subtilis</i> JUCHE1 under variation of wavelength of light | 191-196 |
| 8.2.1.2 Effect of four different spectrums of light on lipid accumulation of <i>L.subtilis</i> JUCHE1 | 196-199 |
| 8.2.1.3 CO ₂ fixation rate of <i>L. subtilis</i> JUCHE1 under variation of wavelength of light | 200-201 |
| 8.2.1.4 Effect of different spectrum of lights on photosynthetic activity for pigment production of <i>L.subtilis</i> JUCHE1 | 201-204 |
| 8.2.2 Semi-Continuous Operation of mode of Gas-lift Photobioreactor | 204 |
| 8.2.2.1 Visual appearance of IEIGPBR in operating condition | 205 |
| 8.2.2.2 Time history of Algal biomass in IEIGPBR | 205-207 |
| 8.2.2.3 Time histories of lipid content and the productivity in IEIGPBR | 207-208 |
| 8.2.2.4 Time history of CO ₂ Fixation rate of <i>L. subtilis</i> JUCHE1 in IEIGPBR | 208-209 |
| Chapter 8 Bipligraphy | 210-212 |
| Chapter 9 Studies on Power plant blue-green alga <i>Leptolyngbya subtilis</i> JUCHE1 for production of Biochar through slow pyrolysis. | 213 |
| 9.1 Materials and methods | 213 |
| 9.1.1 Pyrolysis of Algal biomass | 213 |
| 9.2. Results and discussion | 215-231 |
| 9.2.1 Pyrolysis of algal biomass <i>L. subtilis</i> JUCHE1 | 215-221 |

| Content | Page No. |
|---|-----------------|
| 9.2.2 Rate constants | 222 |
| 9.2.2.1 Determination of overall rate constants (k) at different temperatures | 222-224 |
| 9.2.2.2 Determination of rate constants of formation of volatiles (k_v) at different temperatures | 224-226 |
| 9.2.2.3 Determination of activation energies and pre-exponential factors | 226-227 |
| 9.2.3 Thermo-gravimetric analysis (TGA) | 228-229 |
| 9.2.4 GC-MS analysis of Pyro-Oil | 230-231 |
| Chapter 9. Bibliography | 232 |
| Chapter 10 | 233-240 |
| Future scope | 241 |
| Appendix | |

Chapter 1

1. Introduction

1.1 Preamble

Currently, there is a threat of global warming due to high extent of CO₂ emission in the atmosphere worldwide by industry and transport sectors. Intergovernmental Panel on Climate Change (IPCC) released the Special Report on “Global Warming of 1.5 °C above pre-industrial levels and the related emissions pathways” in October 2018. According to this report, “Reaching and sustaining net zero global anthropogenic CO₂ emissions and declining net non-CO₂ radiative forcing would halt anthropogenic global warming on multi-decadal time scales (high confidence)” [1]. The IPCC report described CO₂ as a long-lived greenhouse gas (GHG) meaning that warming effect of this type of GHG depends on its cumulative emission over the entire industrial epoch [1]. Therefore, limiting the global warming to 1.5°C needs zero anthropogenic emission of CO₂. Therefore, anthropogenic CO₂ emission has been given special attention and is considered to be the single most deleterious factor for global warming [2,3]. CO₂ emission is largely caused by combustion of hydrocarbon fossil fuels like coal, oil and natural gas in thermal power plants as primary sources of energy to produce the more easily utilizable secondary energy sources, namely; heat and electricity [4]. According to the recent report of International Energy Agency (IEA), coal contributed 40% of the total CO₂ emission, amounting to 15.3 billion tons in 2021[5]. Natural gas and oil are the other contributors reaching the CO₂ emission of 7.5 and 10.7 billion tons respectively in 2021[5]. According to a worrisome data published by the IEA, CO₂ emission was again on the rise, 2% higher compared to 2019 level, in December, 2020 despite a global decline in CO₂ emission by 2 billion tonnes in 2020 March [6]. This was because of the economic struggle to bounce back after a year of COVID-caused contraction [6]. Presently the thermal power plants, particularly, the coal fired ones are adversely regarded as one of the major point sources of extensive emission of anthropogenic CO₂ throughout the world [7,8]. In India, coal based thermal power plants, perhaps, are responsible for majority of the country’s huge CO₂ emission footprint [9-11]. Average low calorific value, high levels of non-organic impurities and high ash content of Indian coals further worsen the CO₂ emission scenario of coal-fired power plants by manifolds [12]. Immediate remedial measures should be undertaken for reduction of the CO₂ emission from coal combustion as well as post-combustion CO₂ capture from the atmosphere to notably cut down the current CO₂ emission loads of the country [12, 13]. Joint administration of clean

coal technologies (CCT), carbon capture and storage (CCS) and/or carbon capture and utilization (CCU) techniques as mitigation strategies to lower the emission of CO₂ from coal-fired thermal power plants are viewed as necessary action plans for India [12,13].

Although, several physical and chemical-based processes are commonly used for CCS, their impacts are not always certain, regarding several technical, economic and environmental barriers [14,15,16]. Among different routes based on absorption, adsorption, membrane, hydrate and cryogenics, absorption-based technology is the most mature one (14, 15,17,18,19). However, high energy penalty during the regeneration of solvent becomes a challenge to meet the target of 2 MJ/kg CO₂ [20]. Again, the geological storage capacity of most of the leading CO₂ emitting countries is not sufficient and further, the storage itself is just a ‘stopgap’ management, not completely ‘leakage-proof’ [7,14]. Moreover, according to Daneshvar et al, capture of CO₂ can be made attractive in three ways: (1) economic incentives within existing carbon markets, (2) preventing costly environmental and humanitarian disasters resulting from uncontrolled climate change, and (3) upgrading a damaging waste product into valuable products and renewable energy” [6]. From this perspective, the utilization of the captured carbon in place of storing it, is grabbing a lot of interest worldwide, paving the way for CCU as a complementing technology for CCS [13,15]. Biological CCU using different strains of algae offers an eco-friendly route of capturing post-combustion CO₂ and its further utilization through conversion to various added value products [15]. The novel aspects of algal bio-CCU are the simplicity, cost effectiveness and adaptability towards diversity of climatic condition, and techno-economic scales [6]. The potential for the production of lipids and other high-value bio-molecules and green energy from the cell biomass are other attractions of the algal route of post-combustion CO₂ capture. Thus, integration of algal CCUs with power plants can mitigate CO₂ simultaneously with the production of algal oils and bio-chemicals. Some strategies like the decrease in the ratio of N:C has been reported to be beneficial for the enhancement of the production of algal oil production [21,22,23]. In many instances, the algal species, capable of capturing CO₂ can also assimilate organic carbon sources like glucose, acetate, lactate, glycerol etc. following photo-heterotrophic growth [24,25, 26,27]. Some reports are also available claiming the enhancement of lipid production using organic carbon source [24,25,26,27]. Literature data are available on mixotrophic growth of algae using both inorganic (CO₂, Na₂CO₃, NaHCO₃ etc) and organic (glucose, acetate, lactate, glycerol etc.) carbon sources. Recently, the concept of integration of Bioenergy set-ups with algal CO₂

capture, popularly known as “Algae with Bioenergy Carbon Capture and Storage (ABECCS)” has also been developed and proved as a feasible sustainability option [28, 29].

1.2 Phototrophic Algae

Algae follow several mechanisms for production of biomass as well as lipid and can be grown under different metabolic modes: (i) photo-autotrophic (with light energy and inorganic carbon source e.g., CO₂, Na₂CO₃, NaHCO₃ etc.); (ii) photo-heterotrophic growth (with light energy and organic carbon source e.g. Glucose, Glycerol etc.) (iii) Mixotrophic mode (with light energy and carbon sources of both organic and inorganic ones) [24-26,30,31]. In any phototrophic pathway, light energy is utilised for producing ATP and NADPH. The metabolic pathway of algae under different modes under phototrophic condition has been represented schematically in the following Figure 1.1.

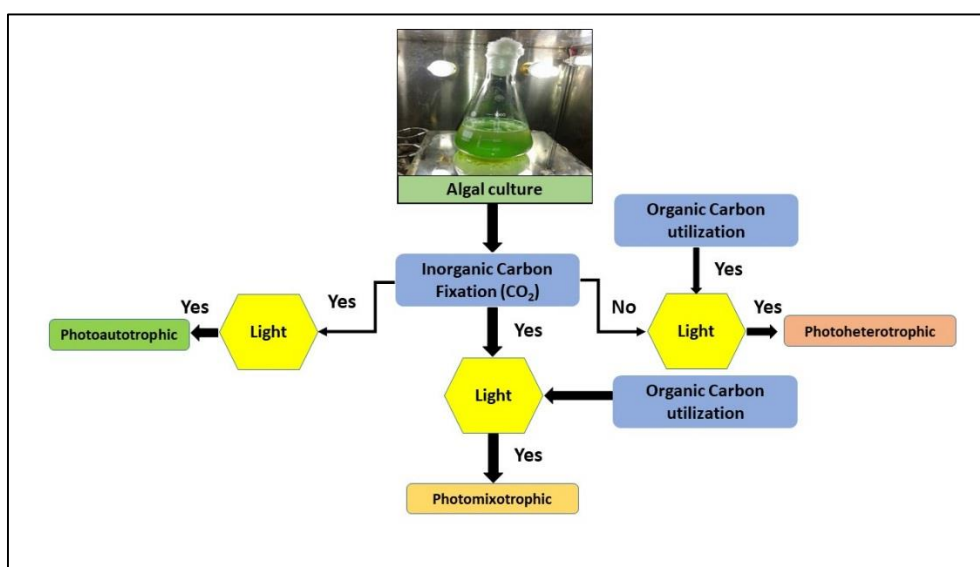


Figure 1.1 Different growth metabolism of phototrophic microorganism “Algae”.

1.2.1 Photoautotrophic growth of Algae

Photoautotrophic algae, both micro and macro, conduct oxygenic photosynthesis alike the terrestrial plants [32,33,34]. While the photo-biochemical process is mainly driven by the energy obtained from light (in nature sunlight), CO₂ serves as an important inorganic reactant for the biosynthesis of several biomolecules and biomass [32, 34]. Like the terrestrial plants, algae conduct oxygenic photosynthesis in which the inorganic CO₂ is converted to organic compounds and molecular oxygen is produced as an end product [34]. The general biochemical reaction of photosynthesis process can be represented as the following equation:



Photosynthesis in algae is divided into two distinct stages, i.e., light-dependent and light-independent. Light dependent stage is the primary one in which the light energy is captured by the antenna complexes of Chlorophyll and other carotenoids present in Photosystem I or Photosystem II of chloroplast [32]. At the expense of the captured light energy ADP and NADP⁺ are respectively converted to the energy carriers ATP and NADPH through the transfer of electrons via the electron transport chain (ETC) and oxygen is produced as the end product [32,34]. Different wavelength can have variable effects on the growth and lipid production dynamics of algae under photoautotrophic condition [35,36,37]. The light dependent Photosystem I or Photosystem II have been shown in Figure 1.2. CO₂ is used in the light-independent phase of photosynthesis. Dissolved CO₂ enters the algal cells as either HCO₃⁻ or as CO₂ through the specific transporters present in the cell membrane and chloroplast membrane [32]. The bio-fixation or the sequestration of the inorganic carbon from CO₂ is conducted via the redox reactions of the Calvin-Benson cycle [38]. When CO₂ is assimilated to form sugar, ATP and NADPH act respectively as energy source and reducing agents in the light independent Calvin cycle occurring in the stroma part of chlorophyll. In Calvin-Benson cycle, each molecule of CO₂ gets condensed with ribulose 1,5-bisphosphate (a 5-carbon compound) to produce two molecules of 3-carbon compound 3-phosphoglycerate (3-PGA) through the action of the enzyme ribulose 1,5-bisphosphate carboxylase-oxygenase (RuBisCO) using the ATP and NADPH produced in the light dependent stage [32,34,38]. From the produced 3-phosphoglycerate the starting compound ribulose 1,5-bisphosphate is cyclically regenerated through a series of intermediate compounds [32,34]. 3-phosphoglycerate also serves as the precursor for the biosynthesis of biomass component in form of glucose through the intermediate compound glyceraldehyde-3-phosphate (G-3P/GAP) [32]. The produced glucose is transported to the cytoplasm and gets stored in form of starch molecules. This is the overall procedure of the sequestration of carbon of CO₂ via assimilation into biomass of algae. This 3-phosphoglycerate (PGA) is converted into glyceraldehyde-3 phosphate (GAP) and transported from chloroplast to cytosol to be used in the synthesis of biomass, lipid, carbohydrate, amino acids etc. [39, 40]. As shown in the Figure 1.2, glyceraldehyde-3 phosphate (GAP) is the end product of photosynthesis process and it enters into glycolysis pathway which is subdivided into two parts: (i) Lower glycolysis and (ii) Upper glycolysis [39,40].

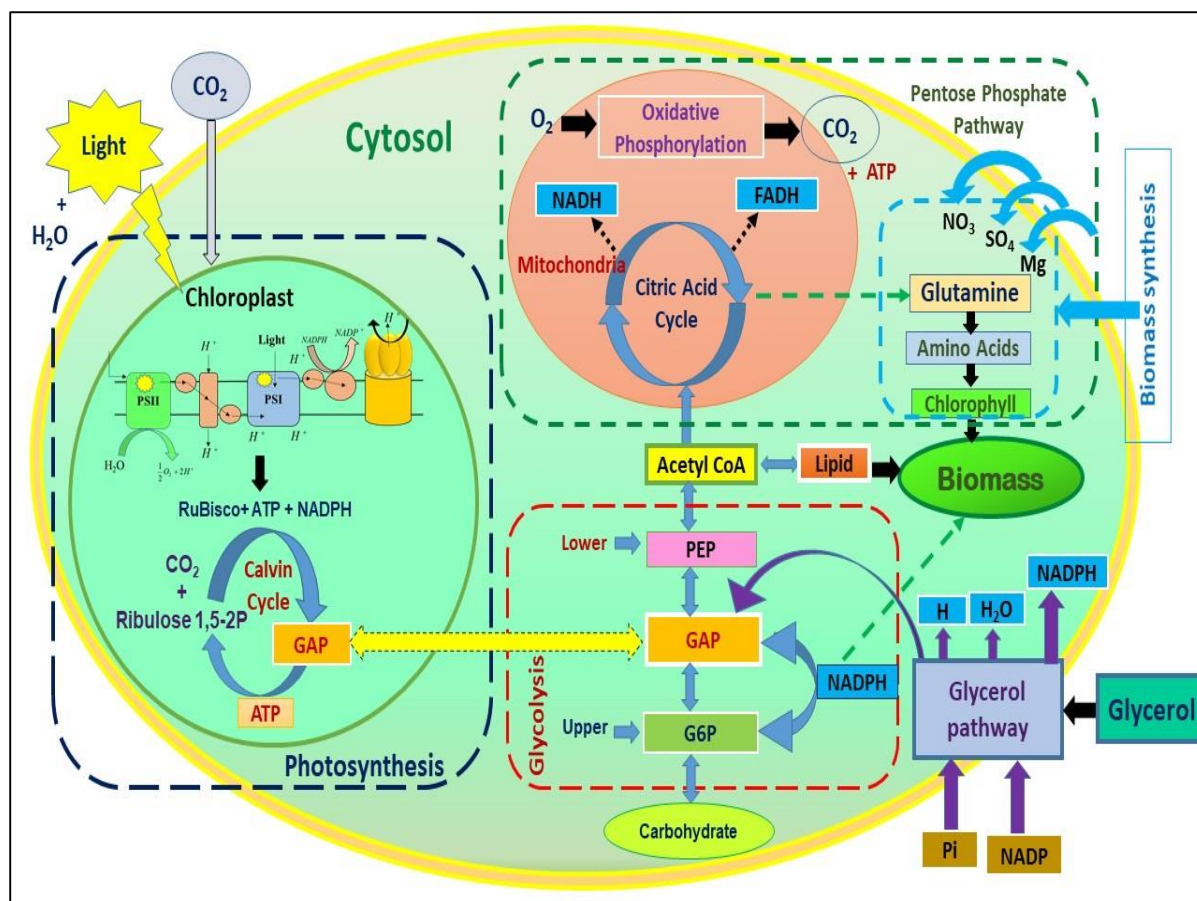


Figure 1.2 Schematic representation of Biomass, Lipid, Amino acids (Chlorophyll), Carbohydrate synthesis through different pathways (photosynthesis, oxidative phosphorylation, pentose phosphate pathway, glycolysis) in algae by utilization of both inorganic carbon source (CO_2) and Organic carbon source (Glycerol).

In upper glycolysis process, through reverse glycolysis the glyceraldehyde- 3 phosphate (GAP) is converted to Glucose 6- phosphate (G6P) to produce carbohydrates (carbon storage compounds/complex sugar) [39]. In case of lower glycolysis process, GAP is transformed into phosphoenolpyruvate (PEP) as the end product of the pathway. Using PEP as the precursor of acetyl-coA the lipid synthesis is carried out. This process also involves use of metabolites formed through citric acid cycle for biomass synthesis which consists of formation of precursors of carbohydrates, proteins, amino acids, chlorophyll etc [39]. The biomass synthesis is supported by the metabolic precursors formed in citric acid cycle, oxidative phosphorylation and pentose phosphate pathway as well as assimilation of N, S and Mg in the cytosol [39]. The stored carbohydrates of algae can be harnessed and used for the production of several biofuels through specific conversion routes.

1.2.2 Photoheterotrophic and Photomixotrophic Growth of Algae

Photoheterotrophic algae use organic compounds such as glycerol as carbon and light as energy sources respectively for growth. As represented in Figure 1.2, utilization of glycerol as organic carbon source is facilitated through the glycerol pathway conducted in cytosol for biomass synthesis [40]. Glycerol is converted to glyceraldehyde-3 phosphate (GAP) and through the synthesis of precursor metabolites and utilizing several elemental inputs (O_2 , NH_4 , Mg, SO_4 , NO_3 , NADPH, P_i etc.) it is converted to biomass, as shown in Figure 1.2[40]. Under the mixotrophic mode of growth both types of carbon sources i.e., inorganic (CO_2 , Na_2CO_3 , $NaHCO_3$ etc) or organic (glycerol, organic acids, glucose etc.) are consumed and metabolized through specific pathways (as collectively shown in Figure 1.2.) for their conversion to biomass and lipid.

Phototrophic growth of algae, whether autotrophs, heterotrophs or mixotrophs, involves light dependent photosynthetic metabolic pathway occurring in the thylakoid membrane producing ATP and NADPH. In photoheterotrophic mode, ATP and NADPH produced in the thylakoid enable algae to utilise the energy efficient active transport of the available organic carbon source. The light dependent products can also be utilised in cellular metabolic pathways and can be used for accumulation of energy rich storage products, namely fatty acids and TAGs [41]. Organic carbon sources like glucose, xylose, acetate, lactate, glycerol and waste water with high load of organic carbon can be utilized by different algae under photoheterotrophic and/or photomixotrophic growth condition.

1.3 Prospect of generation of specialty biochemicals and biofuels from algae

1.3.1 Biochemicals from algae

By using photosynthesis process, algae efficiently convert solar energy into chemical energy and store it in the cells. Other than biofuels, algal biomass is a potential source of different type of biochemicals [42-47]. The major biochemicals are mainly categorized as Polyunsaturated omega 3 fatty acids, namely, Docosahexaenoic acid (DHA), Docosapentanoic acid (DPA), Eicosapentanoic acid (EPA), α -linolenic acid (ALA) and stearic acid (SDA) etc. and pigments such as chlorophyll, carotenoids (lutein, β -carotene), xanthophyll, astaxanthin etc. [42,48,49]. Polyunsaturated fatty acids (PUFAS) are mainly present in algal oil/lipid [16]. Among all the PUFAS, DHA is the most crucial due its medicinal properties [50]. Its consumption as a food additive may lower the risk of cancer, cardiovascular diseases (reduces the high blood pressure and stimulates blood circulation), Alzheimer's disease etc. [50]. Due to its high utility in

pharmaceutical industries, these biochemicals are very expensive [50,51]. EPA is a biochemical with proven anti-inflammatory activity, enhances lipid metabolism and overall neural health [52]. DPA also helps in the storage of EPA and DHA in human body. According to table 3, it has been observed that many of the algal strains produces DHA, ALA, SDA, EPA and DPA as fractions of the product omega 3 fatty acids [42]. Other categories of biochemicals extracted from algae are pigments, namely; chlorophyll (chl a and chl b), carotenoid (carotene, lutein) etc. Algal strains contain chlorophyll a, chlorophyll b and chlorophyll c, depending on the species [48, 49]. Green algae mostly contain chlorophyll a and chlorophyll b, red algae contain chlorophyll a only and diatoms mainly contain chlorophyll c [53]. Due to its use in food and cosmetic industries, chlorophyll is a valuable biochemical. Carotenoids, which are tetra-terpenoids in nature, are pigments of red, orange and yellow color. Different carotenoids are lutein, beta-carotene, xanthophyll's, astaxanthin etc. are found in algal biomass [44,49].

1.3.2 Biofuels from algae

Algae are considered as a potential renewable resource for biofuel production. As a part of their metabolism, some algae can produce high amount of lipids/fats in their cells as storage materials. This 'oil fraction' can be separated from the algal biomass using particular solvent extraction method [53]. After extracting the oil-soluble biochemicals (the omega 3 fatty acids), the residual algal oil is converted to biodiesel through trans-esterification process [53]. The oil-extracted solid biomass fraction, rich in storage carbohydrates (mainly algal starch of the cell wall) can serve as feedstock for production of different other biofuels. Absence of lignin in algal biomass makes it a favorable substrate for conversion to biofuels via biochemical routes [54]. Besides biochemical routes algal biomass has been considered as an attractive feedstock in thermochemical bioenergy process. Algal biomass can be directly fed to anaerobic digestion process for its conversion to biomethane/biogas [55]. The mixed microbes of the anaerobic digestion process can efficiently perform the necessary hydrolysis of the biomass and subsequent conversion to biogas [56]. The algal biomass, after mild chemical treatment to facilitate release of simple sugars, can be converted to ethanol or hydrogen through fermentative routes conducted by dedicated microbes [57]. Biodiesel, biomethane, bioethanol and biohydrogen are greatly valued as promising renewable energy vectors. Production of these biofuels from algal biomass are classified under third generation of biofuels. Production of biodiesel from residual algal-oil is also a third generation process due to the non-edibility.

Recently, the algal biomass has been popularly used in the thermochemical processes like pyrolysis and gasification [58]. In these processes the residual algal biomass, after deriving the

oil and biochemicals, is used as feedstock. In pyrolysis the algal biomass is converted to pyro-oil, pyro-gas and pyro-char [59, 60]. The pyro-oil is considered as a promising drop-in option for petro-fuels for the transportation sector.

1.3.3 Algal Carbon Capture and Utilization

Sequestration of CO₂ using microalgae and its conversion to fuels and chemicals can be considered as a promising CCU platform. Algal bio-sequestration of CO₂ is a completely eco-friendly green route for carbon capture. Operation at ambient temperature and pressure makes the process less energy intensive, although indoor operations require energy investment for CO₂ Capture and Utilization (CCU) in Coal-Fired Power Plants to provide either solar or electrical illumination to the photobioreactors [61]. Since it holds the prospect of production of low-emission renewable biofuels from the algal biomass, the overall process can become CO₂ neutral/negative [62]. On the economical front, most of the biochemicals, derived from the algal cells are high-value products, which will compensate the high cost of algal biodiesel in comparison to conventional petro-fuels. As stated by IEA, algal biorefinery, as represented in Figure 1.4, is mainly conversion of biomass to produce bioenergy (3-G biofuel such as, biodiesel, bio-oil etc.) and beneficial biochemicals (ex. Chlorophyll, β- carotene extracted from pigments and omega 3 fatty acids like in oil etc.).

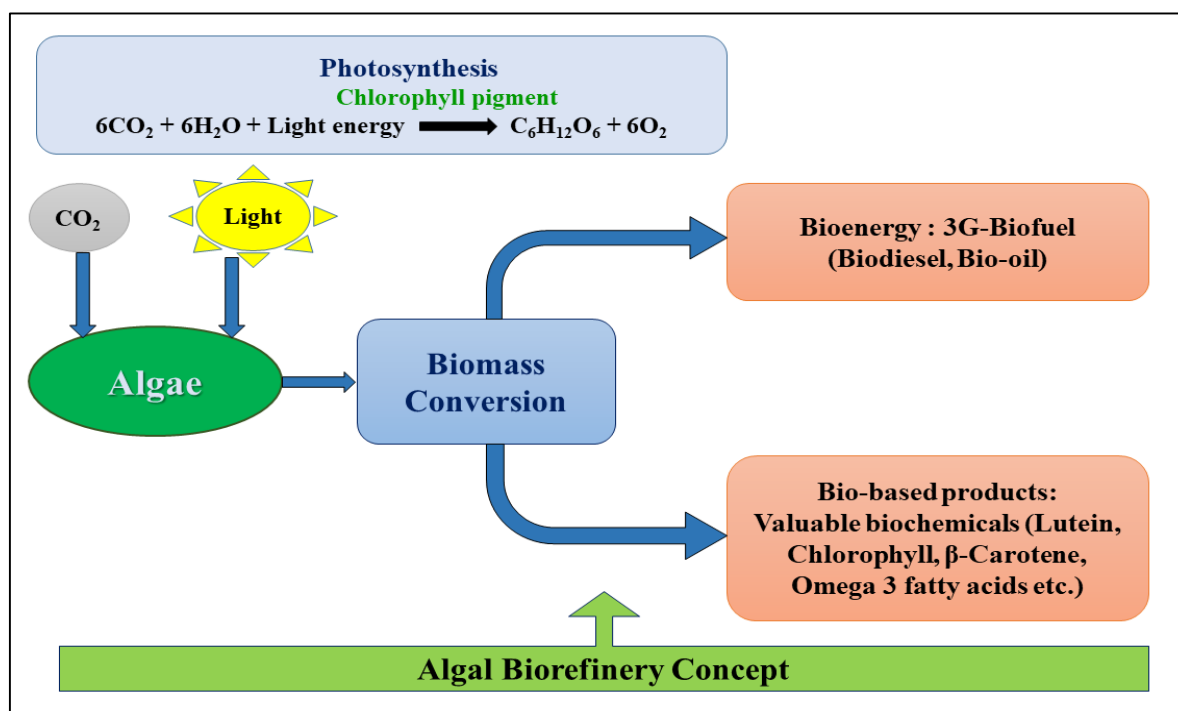


Figure 1.4: Biochemical process of CO₂ sequestration and biomass conversion through algal biorefinery concept.

Considering the potential of algae to generate both biofuels and biochemicals by the assimilation of CO₂ from any emitting source, an integrated scheme of power plant and algal CCU, based on bio-refinery concept, and hence an ABECCS unit, can be represented in Figure 1.5

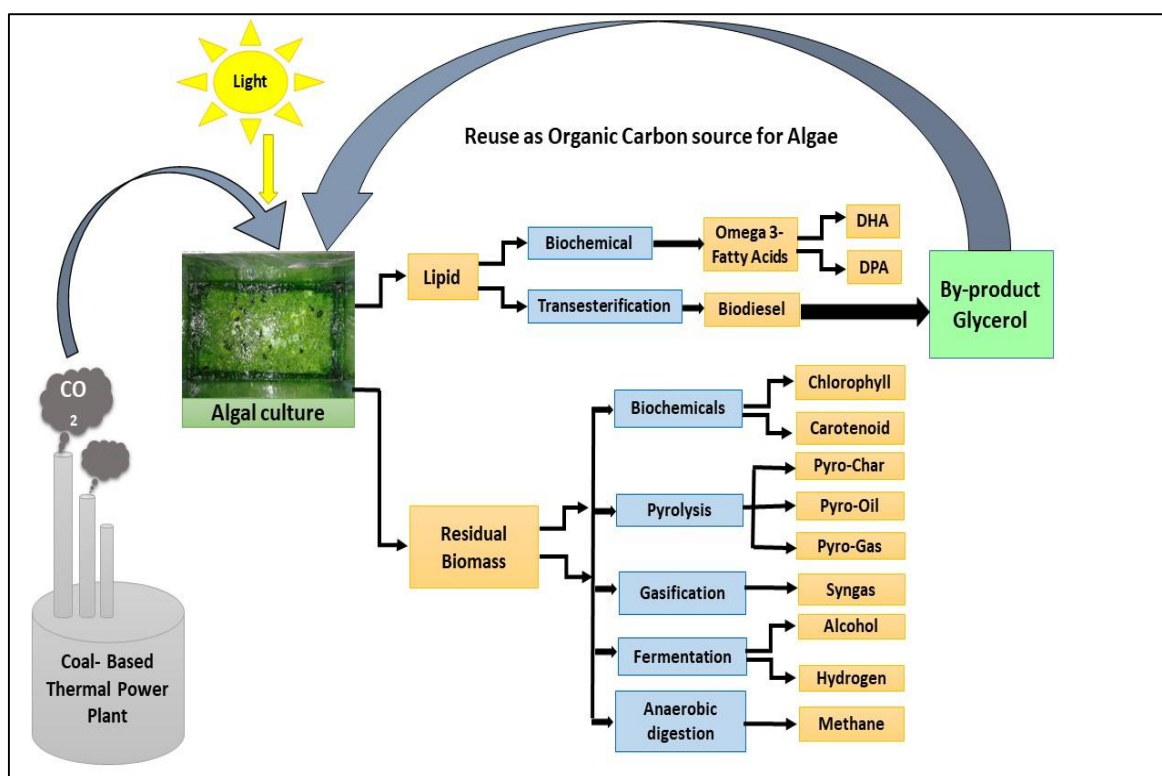


Figure 1.5 Integrated scheme of a coal-fired thermal power plant and algal biorefinery.

The algae which have the capability of growing in different growth modes (autotrophic, heterotrophic, mixotrophic) are good candidates for ABECCS. In an algae-based ABECCS, integrated with power plant, a part of algal oil produced by autotrophic assimilation of CO₂, emitted from power plant, can be used for the production of biodiesel through transesterification process. In the same unit there is a scope for assimilation of the by-product of trans-esterification process, namely, glycerol, by the algae in heterotrophic and mixotrophic mode. For proper implementation of algal CCUs in Indian perspective, their suitability for integration with CO₂-emitting power plants is a necessity. Although the typical value of CO₂ concentration in the flue gas lies in the range of 10-15%, common algal strains are suitable for low CO₂ concentration, typically 5%,[63]. Therefore, proper screening of algal strains, capable of assimilating CO₂ in the range of 10-15% (v/v), is required. The algal strains isolated from power plant water sources are very efficient in capturing CO₂ and can withstand high CO₂ concentration up to 20%(v/v).

Therefore, recognizing the bright prospect of integration of algal CCU with the Indian power plants for the mitigation of CO₂ emission, the present research studies will be focused in the following directions: (I) Isolation of a suitable power plant algal strain, capable of withstanding high CO₂ levels; (II) determination of detailed growth dynamics of the suitable algal strain under photoautotrophic condition; assessment of potential of CO₂ capture; dynamics of production of lipid and biomolecules like pigments etc. ; (III) evaluation of growth behaviour of the suitable algal strain under different light condition to divulge important information about its utilization in large photobioreactor; (IV) determination of detailed growth dynamics of the same algal strain in heterotrophic and mixotrophic conditions; (V) The thermochemical utilization of the residual algal biomass after the extraction of lipids and other valuable biochemicals to facilitate the assessment of the isolated algal strain for the setting up of a sustainable biorefinery or ABECCS unit with zero waste.

References

1. https://www.ipcc.ch/site/assets/uploads/sites/2/2019/06/SR15_Full_Report_High_Res.pdf.%20IPCC%20report%20described%20CO2
2. Intergovernmental Panel on Climate Change (2015) Climate change 2014: mitigation of climate change, vol 3, Cambridge University Press
3. Ajmi AN, Hammoudeh S, Nguyen DK, Sato JR (2015) On the relationships between CO₂ emissions, energy consumption and income: the importance of time variation. *Energ Econ*49:629–638.
4. Vernon C, Thompson E, Cornell S (2011) Carbon dioxide emission scenarios: limitations of the fossil fuel resource. *Procedia Environ Sci* 6:206–215
5. <https://iea.blob.core.windows.net/assets/c3086240-732b-4f6a-89d7-db01be018f5e/GlobalEnergyReviewCO2Emissionsin2021.pdf>
6. Daneshvar, E., Wicker, R. J., Show, P. L., & Bhatnagar, A. (2022). Biologically-mediated carbon capture and utilization by microalgae towards sustainable CO₂ biofixation and biomass valorization—A review. *Chemical Engineering Journal*, 427, 130884.
7. Rahman, F. A., Aziz, M. M. A., Saidur, R., Bakar, W. A. W. A., Hainin, M. R., Putrajaya, R., & Hassan, N. A. (2017). Pollution to solution: Capture and sequestration of carbon dioxide (CO₂) and its utilization as a renewable energy source for a sustainable future. *Renewable and Sustainable Energy Reviews*, 71, 112-126.
8. Board CIA (2010) Power generation from coal: measuring and reporting efficiency performance and CO₂ emissions. CIAB International Energy Agency, Paris, Report:OECD/IEA2010, pp 1–114
9. Sethi M (2015) Location of greenhouse gases (GHG) emissions from thermal power plants in India along the urban-rural continuum. *J Clean Prod* 103:586–600.
10. Mittal ML, Sharma C, Singh R (2012) Estimates of emissions from coal fired thermal power plants in India. In: 2012 International emission inventory conference, pp 13–16.
11. Ito O (2011) Emissions from coal fired power generation. In: Workshop on IEA high efficiency low emissions coal technology roadmap, vol 29.

12. www.teriin.org/projects/green/pdf/India-CCT.pdf2015. Greengrowth and clean coal technologies in India. The Energy and Resources Institute, New Delhi.
13. Goel M (2017) CO₂ Capture and utilization for the energy industry: outlook for capability development to address climate change in India. In: Carbon utilization, Springer, Singapore, pp 3–33.
14. Leung DY, Caramanna G, Maroto-Valer MM (2014) An overview of current status of carbon dioxide capture and storage technologies. *Renew Sustain Energy Rev* 39:426–443
15. Cuéllar-Franca RM, Azapagic A, (2015) Carbon capture, storage and utilisation technologies: a critical analysis and comparison of their life cycle environmental impacts. *J CO₂ Utilization* 9:82–102.
16. Viebahn P, Vallentin D, Höller S (2014) Prospects of carbon capture and storage (CCS) in India’s power sector—an integrated assessment. *Appl Energy* 117:62–75.
17. Mishra MK, Khare N, Agrawal AB (2015) Scenario analysis of the CO₂ emissions reduction potential through clean coal technology in India’s power sector: 2014–2050. *Energy Strategy Rev* 7:29–38
18. Chang S, Zhuo J, Meng S, Qin S, Yao Q (2016) Clean coal technologies in China: current status and future perspectives. *Engineering* 2:447–459
19. Goel M (2010) Implementing clean coal technology in India.
20. Song, C., Liu, Q., Deng, S., Li, H., & Kitamura, Y. (2019). Cryogenic-based CO₂ capture technologies: State-of-the-art developments and current challenges. *Renewable and Sustainable Energy Reviews*, 101, 265-278.
21. Tagliaferro, G.V., Izário Filho, H.J., Chandel, A.K., da Silva, S.S., Silva, M.B. and dos Santos, J.C., 2019. Continuous cultivation of *Chlorella minutissima* 26a in a tube-cylinder internal-loop airlift photobioreactor to support 3G biorefineries. *Renewable Energy*, 130, pp.439-445.
22. Sánchez-García, D., Resendiz-Isidro, A., Villegas-Garrido, T. L., Flores-Ortiz, C. M., Chávez-Gómez, B., & Cristiani-Urbina, E. (2013). Effect of nitrate on lipid production by *T. suecica*, *M. contortum*, and *C. minutissima*. *Central European Journal of Biology*, 8, 578-590.

23. Yodsuwan, N., Sawayama, S., & Sirisansaneeyakul, S. (2017). Effect of nitrogen concentration on growth, lipid production and fatty acid profiles of the marine diatom *Phaeodactylum tricornutum*. *Agriculture and Natural Resources*, 51(3), 190-197.
24. Li, T., Zheng, Y., Yu, L., & Chen, S. (2014). Mixotrophic cultivation of a *Chlorella sorokiniana* strain for enhanced biomass and lipid production. *Biomass and Bioenergy*, 66, 204-213.
25. Lin, T. S., & Wu, J. Y. (2015). Effect of carbon sources on growth and lipid accumulation of newly isolated microalgae cultured under mixotrophic condition. *Bioresource technology*, 184, 100-107.
26. Cheirsilp, B., & Torpee, S. (2012). Enhanced growth and lipid production of microalgae under mixotrophic culture condition: effect of light intensity, glucose concentration and fed-batch cultivation. *Bioresource technology*, 110, 510-516.
27. Baldisserotto, C., Popovich, C., Giovanardi, M., Sabia, A., Ferroni, L., Constenla, D., ... & Pancaldi, S. (2016). Photosynthetic aspects and lipid profiles in the mixotrophic alga *Neochloris oleoabundans* as useful parameters for biodiesel production. *Algal Research*, 16, 255-265
28. Beal, C. M., Archibald, I., Huntley, M. E., Greene, C. H., & Johnson, Z. I. (2018). Integrating algae with bioenergy carbon capture and storage (ABECCS) increases sustainability. *Earth's Future*, 6(3), 524-542.
29. Choi, Y. Y., Patel, A. K., Hong, M. E., Chang, W. S., & Sim, S. J. (2019). Microalgae Bioenergy with Carbon Capture and Storage (BECCS): An emerging sustainable bioprocess for reduced CO₂ emission and biofuel production. *Bioresource Technology Reports*, 7, 100270.
30. Zeng, J., Wang, Z., & Chen, G. (2021). Biological characteristics of energy conversion in carbon fixation by microalgae. *Renewable and Sustainable Energy Reviews*, 152, 111661.
31. Paranjape, K., Leite, G. B., & Hallenbeck, P. C. (2016). Strain variation in microalgal lipid production during mixotrophic growth with glycerol. *Bioresource technology*, 204, 80-88.

32. Zhao, B., & Su, Y. (2014). Process effect of microalgal-carbon dioxide fixation and biomass production: a review. *Renewable and Sustainable Energy Reviews*, 31, 121-132.
33. Aresta, M., Dibenedetto, A., & Barberio, G. (2005). Utilization of macro-algae for enhanced CO₂ fixation and biofuels production: Development of a computing software for an LCA study. *Fuel processing technology*, 86(14-15), 1679-1693.
34. Cardol P, Forti G, Finazzi G (2011) Regulation of electron transport in microalgae. *Biochimica et Biophysica Acta (BBA)-Bioenerg* 1807:912–918.
35. Mohsenpour, S. F., & Willoughby, N. (2013). Luminescent photobioreactor design for improved algal growth and photosynthetic pigment production through spectral conversion of light. *Bioresource technology*, 142, 147-153.
36. Mattos, E. R., Singh, M., Cabrera, M. L., & Das, K. C. (2015). Enhancement of biomass production in *Scenedesmus bijuga* high-density culture using weakly absorbed green light. *Biomass and Bioenergy*, 81, 473-478.
37. Niizawa, I., Heinrich, J. M., & Irazoqui, H. A. (2014). Modeling of the influence of light quality on the growth of microalgae in a laboratory scale photo-bio-reactor irradiated by arrangements of blue and red LEDs. *Biochemical engineering journal*, 90, 214-223.
38. Jablonsky J, Bauwe H, Wolkenhauer O (2011) Modeling the Calvin-Benson cycle. *BMC Syst Biol* 5:185
39. Baroukh, C., Muñoz-Tamayo, R., Steyer, J. P., & Bernard, O. (2014). DRUM: a new framework for metabolic modeling under non-balanced growth. Application to the carbon metabolism of unicellular microalgae. *PloS one*, 9(8), e104499.
40. Pessi, B. A., Baroukh, C., Bacquet, A., & Bernard, O. (2023). A universal dynamical metabolic model representing mixotrophic growth of *Chlorella sp.* on wastes. *Water Research*, 229, 119388.
41. Abomohra, A. E. F., Eladel, H., El-Esawi, M., Wang, S., Wang, Q., He, Z., ... & Hanelt, D. (2018). Effect of lipid-free microalgal biomass and waste glycerol on growth and lipid production of *Scenedesmus obliquus*: Innovative waste recycling for extraordinary lipid production. *Bioresource technology*, 249, 992-999.

42. Ryckebosch, E., Bruneel, C., Termote-Verhalle, R., Goiris, K., Muylaert, K., & Foubert, I. (2014). Nutritional evaluation of microalgae oils rich in omega-3 long chain polyunsaturated fatty acids as an alternative for fish oil. *Food chemistry*, 160, 393-400.
43. Wei, D., Chen, F., Chen, G., Zhang, X., Liu, L., & Zhang, H. (2008). Enhanced production of lutein in heterotrophic *Chlorella protothecoides* by oxidative stress. *Science in China Series C: Life Sciences*, 51, 1088-1093.
44. Del Campo, J. A., Rodriguez, H., Moreno, J., Vargas, M. A., Rivas, J., & Guerrero, M. G. (2004). Accumulation of astaxanthin and lutein in *Chlorella zofingiensis* (Chlorophyta). *Applied microbiology and biotechnology*, 64, 848-854.
45. Yeh, T. J., Tseng, Y. F., Chen, Y. C., Hsiao, Y., Lee, P. C., Chen, T. J., ... & Lee, T. M. (2017). Transcriptome and physiological analysis of a lutein-producing alga *Desmodesmus sp.* reveals the molecular mechanisms for high lutein productivity. *Algal research*, 21, 103-119.
46. Chen, C. Y., Hsieh, C., Lee, D. J., Chang, C. H., & Chang, J. S. (2016). Production, extraction and stabilization of lutein from microalga *Chlorella sorokiniana* MB-1. *Bioresource technology*, 200, 500-505.
47. Sánchez, J. F., Fernández, J. M., Acién, F. G., Rueda, A., Pérez-Parra, J., & Molina, E. (2008). Influence of culture conditions on the productivity and lutein content of the new strain *Scenedesmus almeriensis*. *Process Biochemistry*, 43(4), 398-405.
48. Molnár, É., Rippel-Pethő, D., & Bocsi, R. (2013). Solid-liquid extraction of chlorophyll from microalgae from photoautotroph open-air cultivation. *Hungarian Journal of Industry and Chemistry*, 119-122.
49. Whyte, J. N. (1987). Biochemical composition and energy content of six species of phytoplankton used in mariculture of bivalves. *Aquaculture*, 60(3-4), 231-241.
50. Tang, S., Qin, C., Wang, H., Li, S., & Tian, S. (2011). Study on supercritical extraction of lipids and enrichment of DHA from oil-rich microalgae. *The Journal of Supercritical Fluids*, 57(1), 44-49.
51. <http://www.sigmaaldrich.com/india.html>
52. Swanson, D., Block, R., & Mousa, S. A. (2012). Omega-3 fatty acids EPA and DHA: health benefits throughout life. *Advances in nutrition*, 3(1), 1-7.

53. Johnson, M. B., & Wen, Z. (2009). Production of biodiesel fuel from the microalga *Schizochytrium limacinum* by direct transesterification of algal biomass. *Energy & Fuels*, 23(10), 5179-5183.
54. Welker, C. M., Balasubramanian, V. K., Petti, C., Rai, K. M., DeBolt, S., & Mendu, V. (2015). Engineering plant biomass lignin content and composition for biofuels and bioproducts. *Energies*, 8(8), 7654-7676.
55. Sialve, B., Bernet, N., & Bernard, O. (2009). Anaerobic digestion of microalgae as a necessary step to make microalgal biodiesel sustainable. *Biotechnology advances*, 27(4), 409-416.
56. Park, J. H., Cheon, H. C., Yoon, J. J., Park, H. D., & Kim, S. H. (2013). Optimization of batch dilute-acid hydrolysis for biohydrogen production from red algal biomass. *International Journal of Hydrogen Energy*, 38(14), 6130-6136.
57. Harun, R., Jason, W. S. Y., Cherrington, T., & Danquah, M. K. (2011). Exploring alkaline pre-treatment of microalgal biomass for bioethanol production. *Applied Energy*, 88(10), 3464-3467.
58. Duman, G., Uddin, M. A., & Yanik, J. (2014). Hydrogen production from algal biomass via steam gasification. *Bioresource technology*, 166, 24-30.
59. Choia, J. H., Woob, H. C., & Suha, D. J. (2014). Pyrolysis of seaweeds for bio-oil and bio-char production. *Chem Eng*, 37, 121-126.
60. Chaiwong, K., Kiatsiriroat, T., Vorayos, N., & Thararax, C. (2012). Biochar production from freshwater algae by slow pyrolysis. *Maejo International Journal of Science and Technology*, 6(2), 186.
61. Zhao, B., & Su, Y. (2014). Process effect of microalgal-carbon dioxide fixation and biomass production: a review. *Renewable and Sustainable Energy Reviews*, 31, 121-132.
62. Moreira, D., & Pires, J. C. (2016). Atmospheric CO₂ capture by algae: negative carbon dioxide emission path. *Bioresource technology*, 215, 371-379.
63. Song, C., Liu, Q., Qi, Y., Chen, G., Song, Y., Kansha, Y., & Kitamura, Y. (2019). Absorption-microalgae hybrid CO₂ capture and biotransformation strategy—A review. *International Journal of Greenhouse Gas Control*, 88, 109-117.

Chapter 2

2. Literature review

In the context of understanding and analyzing the background of the present research extensive literature review have been conducted and the research gaps have been identified. As discussed in Chapter-I, the present research studies will be focused in the following directions: (I) Isolation of a suitable power plant algal strain, capable of withstanding high CO₂ levels; (II) determination of detailed growth dynamics of the suitable algal strain under photoautotrophic condition; assessment of potential of CO₂ capture; dynamics of production of lipid and biomolecules like pigments etc. ; (III) evaluation of growth behaviour of the suitable algal strain under different light condition to divulge important information about its utilization in large photobioreactors; (IV) determination of detailed growth dynamics of the same algal strain in heterotrophic and mixotrophic conditions; (V) The thermochemical utilization of the residual algal biomass after the extraction of lipids and other valuable biochemicals to facilitate the assessment of the isolated algal strain for the setting up of a sustainable biorefinery or ABECCS unit with zero waste. Therefore, the literature review has been conducted to identify the research gaps on the aspects I-V to be focused under the present research.

From an overall literature review using standard publication sources [1, 2] on algal research over 2014-2022 it has been observed that the micro algal strains, namely, *Chlorella vulgaris*, *Scenedesmus* sp., *Chlorella minutissima*, *Nannochloropsis gaditana*, *Scenedesmus obliquus*, *Scenedesmus abundans* are mostly used in experimental studies. Comparatively much less number of literatures is available on blue green algal strains [1,2]. Therefore, more research data are to be generated on cyanobacteria or blue green algal strains. In order to identify the research gaps in the area of blue green algae the literature database on these types of algae have been analyzed in this review. As it is understandable that the data on relevant research studies on the micro-algal strains is equally important to identify the overall research gap, general literature review on micro-algal research is also being included. Moreover, as the high level of CO₂ tolerance of algal strains is one of the focuses of this research, one sub-section is also dedicated to the review of high CO₂-tolerant algal strains (irrespective of their types, i.e., both microalgae and cyanobacteria/blue green algae of power plant and non-power plant sources.

2.1 Photoautotrophic growth of Blue green algae/cyanobacteria

| Publication years | Literature review and findings | References |
|-------------------|--|------------|
| 2022 | <ul style="list-style-type: none"> • Strain: <i>Spirulina platensis</i> LEB-52 • Source: Not mentioned • Scale of operation: 500 mL Erlenmeyer flask • Study on CO₂ Fixation: No • Study on Lipid Production: Yes • Study on Chlorophyll Production: Yes • Study on carotenoid Production: No • Kinetic study on Growth with respect to Carbon source: No • Kinetic study on Growth with respect to Nitrogen source: No • Kinetic study on Growth with respect to light source: No • Kinetic study on Growth simultaneously with respect to C and N-Source and light: No • Study on the effect of wavelength: No • Characterization of Lipid: No • Study in photo-bioreactor of capacity $\geq 2L$: No • Optimization of operation: No • Different carbon (NaHCO₃ to Na₂CO₃,) and nitrogen sources (NH₄Cl, and NH₂CONH₂) were used in Zarrou'k media but the concentration remains constant i.e. 0.214 M of C and 0.029 M of N. • The cultures were incubated at 27 °C for 16 days under 13 hrs continuous illumination having light intensity of 156 $\mu\text{mol m}^2/\text{s}$. • The maximum biomass concentrations of 0.8 g/L and 0.75 g/L respectively obtained for NaHCO₃ and Na₂CO₃ as carbon source whereas the nitrogen source in the media is NaNO₃. | 3 |

| | | |
|------|--|---|
| | <ul style="list-style-type: none"> The highest lipid content was found to be 34.08 mg/L and 54.50 mg/L using NaHCO₃ and Na₂CO₃. The maximum value of chlorophyll content was achieved on 14th days for both carbon sources and the values were 20.90 mg/L (NaHCO₃) and 11.86 mg/L(Na₂CO₃). | |
| 2022 | <ul style="list-style-type: none"> Strains: <i>Acaryochloris marina</i>, <i>Chlorogloeopsis sp. PCC 9212</i>, <i>Arthrospira platensis</i>, <i>Thermosynechococcus elongates</i>, <i>Halomicronema hongdechloris</i>, <i>Arthrospira platensis</i>, <i>Aphanocapsa sp. KCl</i>, <i>Synechococcus sp. PCC 7335</i>, <i>Synechocystis sp. CALU 1173</i>, <i>Chlorogloeopsis fritschii PCC 6912</i>, <i>Halomicronema hongdechloris C2206</i>, <i>Cyanobium sp.</i>, <i>Anabaena sp.</i>, <i>Prochlorococcus sp.</i>, <i>Nostoc calcicola (MACC-612)</i>, <i>Arthrospira platensis F&M-C260</i>, <i>C. fritschii CALU 759</i>, <i>Leptolyngbya sp. AO-1</i>, <i>Spirulina sp. LEB 18</i>, Source: Not mentioned Scale of operation: No Study on CO₂ Fixation: No Study on Lipid Production: No Study on Chlorophyll Production: Yes Study on Carotenoid Production: No Kinetic study on Growth with respect to Carbon source: No Kinetic study on Growth with respect to Nitrogen source: No Kinetic study on Growth with respect to light source: No Kinetic study on Growth simultaneously with respect to C and N-Source and light: No Study on the effect of wavelength: No Characterization of Lipid: No Study in photoreactor of capacity $\geq 2L$: No Optimization of operation: No | 4 |

| | | |
|------|---|---|
| | <ul style="list-style-type: none"> • S.K. Sandybayeva et al.2022, reviewed the pigment production ability of cyanobacteria/ blue green algae and also different extraction techniques were used. • The article reported that some cyanobacterial species have high Chlorophyll d and f content and the name of the species are <i>Acaryochloris marina</i>, <i>Arthrospira platensis</i>, <i>Thermosynechococcus elongates</i>, <i>Halomicronema hongdechloris</i>, <i>Aphanocapsa sp. KCl</i>, <i>Synechococcus sp. PCC 7335</i>, <i>Synechocystis sp.CALU 1173</i>, <i>Chlorogloeopsis fritschii PCC 6912</i>, <i>Chlorogloeopsis sp. PCC 9212</i>, <i>C. fritschii CALU 759</i>, <i>Halomicronema hongdechloris C2206</i>, <i>Leptolyngbya sp. AO-1</i>. • Some species such as <i>Thermosynechococcus elongatus</i>, <i>Anabaena</i>, <i>Nostoc punctiforme</i>, <i>Gloeobacter violaceus</i>, <i>Gloeotheca</i>, <i>Aphanothece</i>, <i>Synechocystis salina</i>, <i>Nodosilinea nodulosa</i> are rich in β-carotene. • It was also reported that the maximum carotenoid yield of 10.7 mg/gDW was obtained for <i>Phormidium spp.</i> using Pressurized liquid extraction method. Whereas, using Supercritical Fluid Extraction based on the CO₂ technique, the β-carotene yield of 0.49 ± 0.10 mg/gDW was obtained for <i>Synechococcus sp.</i> | |
| 2021 | <ul style="list-style-type: none"> • Strain: <i>Anabaena circinalis</i> FSS 124 and <i>Cylindrospermopsis raciborskii</i> FSS 127 • Source: Not mentioned • Scale of operation: 250 mL Borosilicate glass conical flasks • Study on CO₂ Fixation: No • Study on Lipid Production: Yes • Study on Chlorophyll Production: Yes • Study on carotenoid Production: No • Kinetic study on Growth with respect to Carbon source: No | 5 |

| | | |
|--|---|--|
| | <ul style="list-style-type: none"> • Kinetic study on Growth with respect to Nitrogen source: No • Kinetic study on Growth with respect to light source: No • Kinetic study on Growth simultaneously with respect to C and N-Source and light: No • Study on the effect of wavelength: No • Characterization of Lipid: No • Study in photo-bioreactor of capacity $\geq 2L$: No • Optimization of operation: No • A. Sarkar¹ et al. 2021, conducted the experiment varying NaNO_3 concentrations from 6-20 mg/L and cultured for 21 days at 23 ± 3 °C under the photo period of 12 hrs. with constant illumination having light intensity of $50 \mu\text{mol photons m}^{-2} \text{ s}^{-1}$. • The experiment was performed to study the effect of nitrogen source(NaNO_3) on growth, lipid as well as chlorophyll and carotenoid synthesis of both blue- Green Algal strains (<i>Anabaena circinalis</i> FSS 124 and <i>Cylindrospermopsis raciborskii</i> FSS 127). • The study reported that the maximum biomass concentration was achieved for <i>C. raciborskii</i> FSS 127 as compared to <i>A.circinalis</i> FSS 124. The value of highest biomass concentration was achieved i.e 2.47 g/L at 30 mg/L of NaNO_3 concentration beyond that growth was inhibited. • The highest chlorophyll content of $1.39 \mu\text{g ml}^{-1} \pm 0.069$ was observed for <i>Anabaena circinalis</i> FSS 124 at 30 mg/L NaNO_3 concentrations which is higher as compared to <i>Cylindrospermopsis raciborskii</i> FSS 127 i.e. $1.27 \mu\text{g ml}^{-1} \pm 0.009$ • The maximum lipid content (%) of $22.22\% \pm 0.067$ and $33.22\% \pm 0.057$ are obtained for <i>A.circinalis</i> FSS 124 and <i>C.raciborskii</i> FSS 127 in lower nitrogen concentration of 6 mg/L. | |
|--|---|--|

| | | |
|------|---|---|
| | <ul style="list-style-type: none"> From the FAME analysis it was reported that among all the fatty acid methyl esters the maximum value of 50.17% pentadecanoic acid (C15:0).and 27.78 % palmitic acid (C16:0) were obtained in <i>A.circinalis</i> FSS 124 and <i>C.raciborskii</i> FSS 127 respectively. | |
| 2021 | <ul style="list-style-type: none"> Strain:<i>Leptolyngbya foveolarum</i> HNBGU001 Source: Waterbodies of thermal springs, of Garhwal Himalaya Scale of operation: 250 mL Erlenmeyer flask Study on CO₂ Fixation: No Study on Lipid Production: Yes Study on Chlorophyll Production: No Study on carotenoid Production: No Kinetic study on Growth with respect to Carbon source: No Kinetic study on Growth with respect to Nitrogen source: No Kinetic study on Growth with respect to light source: No Kinetic study on Growth simultaneously with respect to C and N-Source and light: No Study on the effect of wavelength: No Characterization of Lipid: Yes Study in photoreactor of capacity $\geq 2L$: No Optimization of operation: No The blue green algal strain "<i>Leptolyngbya foveolarum</i> HNBGU001" was used to conduct the experiments for optiizaion of some nutrients as parameters to achieve the biomass and lipid productivity. For optimization of input parameters, Box-Behnken method of Response surface methodology was performed. The article reported that the maximum biomass and lipid productivity was found to be 55.60 ± 2.74 and 07.30 ± 0.29 | 6 |

| | | |
|------|--|---|
| | mg/L/d respectively under non-optimal condition. Whereas, under optimum condition, the values of 154.80 ± 3.60 and 49.60 ± 0.70 mg/L/d respectively were achieved. | |
| 2021 | <ul style="list-style-type: none"> • Strains: <i>Leptolyngbya tenuis</i> • Source: Not mentioned • Scale of operation: 250 mL Erlenmeyer conical flask • Study on CO₂ Fixation: Yes • Study on Lipid Production: Yes • Study on Chlorophyll Production: Yes • Study on carotenoid Production: Yes • Kinetic study on Growth with respect to Carbon source: No • Kinetic study on Growth with respect to Nitrogen source: No • Kinetic study on Growth with respect to light source: No • Kinetic study on Growth simultaneously with respect to C and N-Source and light: No • Study on the effect of wavelength: No • Characterization of Lipid: No • Study in photoreactor of capacity $\geq 2L$: No • Optimization of operation: No • The experiments were performed by co-cultivation of with and <i>Chlorella ellipsoidea</i>, a microalgal strain for the enhancement of biomass productivity, pigment content, lipid accumulation efficiency and CO₂ fixation rate. • From the study it was found that the highest value of biomass yield <i>Leptolyngbya tenuis</i>, <i>Chlorella ellipsoidea</i> and Co culture (<i>Leptolyngbya tenuis</i> + <i>Chlorella ellipsoidea</i>) are 0.92 ± 0.03 g/L and 2.11 ± 0.15 g/L and to 3.35 ± 0.04 g/L respectively obtained on 15th day. • In the same culture period, the maximum lipid content(% dcw) values for three different cultures: <i>Leptolyngbya tenuis</i>, | 7 |

| | | |
|------|--|---|
| | <p><i>Chlorella ellipsoidea</i> and Co culture (<i>Leptolyngbya tenuis</i> + <i>Chlorella ellipsoidea</i>) are $\pm 0.58\%$ and $9.98 \pm 0.34\%$ and $18.10 \pm 0.27\%$ respectively found on 12th day culture period.</p> <ul style="list-style-type: none"> • The highest value of chlorophyll content ($\mu\text{g/mL}$) was reported for <i>Leptolyngbya tenuis</i> and the value is $\pm 0.25 \mu\text{g/mL}$ as compare to the chlorophyll content of <i>Chlorella ellipsoidea</i> and Co culture i.e. $2.53 \pm 0.12 \mu\text{g/mL}$ and $6.54 \pm 0.36 \mu\text{g/mL}$. • Whereas, the maximum value of carotenoid content was reported for Co culture i.e. $3.30 \pm 0.10 \mu\text{g/mL}$ on 12th day. • In FAME analysis it was found that the saturated and unsaturated fatty acids are obtained for Co culture as compared to pure cultures. | |
| 2019 | <ul style="list-style-type: none"> • Strain: <i>Spirulina platensis</i> (SP.PL) and mixed algal culture (M.X) • Source: Not mentioned • Scale of operation: 1.50 L Erlenmeyer flasks • Study on CO₂ Fixation: Yes • Study on Lipid Production: No • Study on Chlorophyll Production: No • Study on carotenoid Production: No • Kinetic study on Growth with respect to Carbon source: Yes • Kinetic study on Growth with respect to Nitrogen source: No • Kinetic study on Growth with respect to light source: No • Kinetic study on Growth simultaneously with respect to C and N-Source and light: No • Study on the effect of wavelength: No • Characterization of Lipid: No • Study in photoreactor of capacity $\geq 2L$: No • Optimization of operation: No • Characterization of lipid: No | 8 |

| | | |
|------|--|---|
| | <ul style="list-style-type: none"> • The experimental study was performed using both <i>Spirulina platensis</i> (SP.PL) and mixed algal culture (M.X) algal cultures varying different CO₂ concentrations from 2to20% v/v to investigate the effect on biomass production and CO₂ fixation ability. • The study reported that with increase in CO₂ concentrations from 2 to 10 %, the value of maximum specific growth rate increases from 0.45-0.79 on day-1 for <i>Spirulina platensis</i> and 0.48 to 0.86 day⁻¹ for mixed culture. • The maximum CO₂ fixation rate of 0.360 g/L/d and 0.460 g/L/d respectively were achieved for <i>Spirulina platensis</i> and mixed culture. • The highest biomass productivities of 0.246 g/L/d for <i>Spirulina platensis</i> and 0.384 g/L/d for mixed culture were reported. | |
| 2019 | <ul style="list-style-type: none"> • Strain: Arthronema sp. ASW2 • Source:Secondary waste water sewage treatment plant (aerated lagoons) • Scale of operation: 500 mL Erlenmeyer flask • Study on CO₂ Fixation: Yes • Study on Lipid Production: Yes • Study on Chlorophyll Production: No • Study on carotenoid Production: No • Kinetic study on Growth with respect to Carbon source: No • Kinetic study on Growth with respect to Nitrogen source: No • Kinetic study on Growth with respect to light source:No • Kinetic study on Growth simultaneously with respect to C and N-Source and light :No • Study on the effect of wavelength: No • Characterization of Lipid: Yes | 9 |

| | | |
|------|---|----|
| | <ul style="list-style-type: none"> • Study in photoreactor of capacity $\geq 2L$: No • Optimization of operation: No • The experimental study was conducted by using the blue green alga to study the effect of different concentrations (0, 20, 30, 50, 100 and 150 mM) of carbon source NaHCO₃ (Bicarbonate:) and photo period variation of light:dark cycle (24:0, 12:12, 18:6, 20:4, 6:18 and 10:14) on algal growth and lipid accumulation. The CO₂ fixation rate of the algal strain was also studied. • From the experimental study it was reported that the higher biomass growth of 430 mg/L is obtained on 20th day incubation period for blue green alga <i>Arthronema sp.</i> ASW2 as compared to <i>Chlorella sp.</i> ASW1 i.e. 180 mg/L under optimum NaHCO₃ concentration of 50 mM • The maximum values of biomass concentration of 475 and 180 mg/L were reported for <i>Arthronema sp.</i> ASW2 and <i>Chlorella sp.</i> ASW1 respectively under 24h illumination having light intensity of 300 $\mu\text{mol m}^{-2} \text{s}^{-1}$. • The highest lipid yield (%) of 32.14 was obtained for <i>Arthronema sp.</i> ASW2 and was higher than <i>Chlorella sp.</i> where the maximum value of lipid was 29.6%. • The maximum CO₂ fixation rate for <i>Arthronema sp.</i> ASW2 was 52.64 mg L⁻¹ and was higher than <i>Chlorella sp.</i> ASW1 of which the value was 31.02 mg L⁻¹. | |
| 2017 | <ul style="list-style-type: none"> • Strain: <i>Synechococcus spp</i> • Source :Not mentioned • Scale of operation: open pond tanks made of thermos-plastic material of 850 L • Study on CO₂ Fixation: Yes • Study on Lipid Production: No • Study on Chlorophyll Production: No • Study on Carotenoid Production: No | 10 |

| | | |
|------|--|-----------|
| | <ul style="list-style-type: none"> • Kinetic study on Growth with respect to Carbon source: No • Kinetic study on Growth with respect to Nitrogen source: No • Kinetic study on Growth with respect to light source: No • Kinetic study on Growth simultaneously with respect to C and N-Source and light: No • Study on the effect of wavelength: No • Characterization of Lipid: No • Study in photoreactor of capacity $\geq 2L$: No • Optimization of operation: No • Characterization of lipid: No • The study conducted the experimental design varying input parameters (TIC, TOC, DIC, DOC and T) to optimization of output variable under photo auto trophic growth. . • The maximum values of biomass productivity, lipid content and lipid productivity were 18.3g/L/h , 11.78%w/w and 2.09 mg/L/h respectively and were less than those (35.1g/L/h, 27.2% w/wand 5.25 mg/L/h) of <i>Chlorella vulgaris</i>. | |
| 2017 | <ul style="list-style-type: none"> • Strain: <i>Tetraselmis suecica</i>. • Source: Not mentioned • Scale of operation: • Study on CO₂ Fixation: Yes • Study on Lipid Production: No • Study on Chlorophyll Production: No • Study on carotenoid Production: No • Kinetic study on Growth with respect to Carbon source: Yes • Kinetic study on Growth with respect to Nitrogen source: No • Kinetic study on Growth with respect to light source: No | 11 |

| | | |
|------|--|----|
| | <ul style="list-style-type: none"> • Kinetic study on Growth simultaneously with respect to C and N-Source and light: No • Study on the effect of wavelength: No • Characterization of Lipid: No • Study in photo-bioreactor of capacity $\geq 2L$: Yes • Optimization of operation: No • Kassim and Meng et. al (2017), investigated the growth rate and CO₂ fixation ability of the algal strains namely <i>Chlorella sp.</i> and <i>Tetraselmis suecica</i>. • The experiments were conducted by using four different concentrations of CO₂ (0.04, 5, 15 and 30% (v/v)) and nitrogen sufficient condition using 1.7 g/L of sodium nitrate. The cultures were incubated at 30.0±2.0 °C under constant illumination of 450 $\mu\text{mol}^{-2} \text{s}^{-1}$. • For <i>Tetraselmis suecica</i>.. the highest value of specific growth rate was 0.29 d⁻¹ and was less than <i>Chlorella sp.</i> for which the value 0.25 d⁻¹ at 15%CO₂ concentration. At 30% CO₂ concentration the growth was inhibited. • The research article reported that the biomass concentration as well as CO₂ fixation rate of <i>Tetraselmis suecica</i> were 0.72 g/L and 111.26 mg/L/d respectively at 15% CO₂. Whereas the maximum biomass concentration of 0.64 g/ L and CO₂ fixation rate of 96.89 mg L¹/d respectively were observed for <i>Chlorella sp.</i> at 5% CO₂ concentration. • From the research article it has been found that in case of both the algal strains <i>Tetraselmis suecica</i> and <i>Chlorella sp.</i>, the highest biomass production obtained at pH 7. And it has also been notified that at higher pH or alkaline range the growth was inhibited. | |
| 2016 | <ul style="list-style-type: none"> • Strain: <i>Spirulina platensis</i> • Source : Not mentioned • Scale of operation: 10 L Flat plates glass bioreactor • Study on CO₂ Fixation: Yes | 12 |

| | | |
|------|--|----|
| | <ul style="list-style-type: none"> • Study on Lipid Production: No • Study on Chlorophyll Production: No • Study on carotenoid Production: No • Kinetic study on Growth with respect to Carbon source: Yes • Kinetic study on Growth with respect to Nitrogen source: No • Kinetic study on Growth with respect to light source: No • Kinetic study on Growth simultaneously with respect to C and N-Source and light: No • Study on the effect of wavelength: No • Characterization of Lipid: No • Study in photo-bioreactor of capacity $\geq 2L$: Yes • Optimization of operation: No • As reported in the literature, the microalga <i>Chlorella vulgaris</i> and blue green algae "<i>Spirulina platensis</i>" were cultivated in a 10L flat plate photobioreactor. Four different inlet CO₂ concentration (0.03%, 2%, 5% and 10%) were used. • The maximum value of specific growth rate for <i>Chlorella vulgaris</i> and <i>Spirulina platensis</i> were found to be 0.17 and 0.153 respectively for 10% CO₂ as inlet concentration. • The study reported that with increase in inlet-CO₂ concentrations from 0.03-10%, exhibits an increasing trend of CO₂ fixation rate for both the strains. The highest CO₂ fixation rate of 0.419g/L/d was obtained at 10 % (v/v) for <i>Spirulina platensis</i>. However, the CO₂ fixation rate of <i>Chlorella vulgaris</i> varied from 0.041-0.055g/L/d as the inlet CO₂ concentration was increased from 0.03-10% (v/v) which was comparatively lower than <i>Spirulina platensis</i>. | |
| 2013 | <ul style="list-style-type: none"> • Strain: <i>Gloeotheca membranacea</i> • Source: Water bodies of waste solvent biofilter • Scale of operation: 450mL Bubble column photobioreactors | 13 |

| | | |
|--|---|--|
| | <ul style="list-style-type: none"> • Study on CO₂ Fixation: No • Study on Lipid Production: No • Study on Chlorophyll Production: yes • Study on carotenoid Production: No • Kinetic study on Growth with respect to Carbon source: No • Kinetic study on Growth with respect to Nitrogen source: Yes • Kinetic study on Growth with respect to light source: No • Kinetic study on Growth simultaneously with respect to C and N-Source and light: No • Study on the effect of wavelength: Yes • Characterization of Lipid: No • Study in photo-bioreactor of capacity $\geq 2L$: No • Optimization of operation: No • Characterization of lipid: No • The algal strains namely: <i>Gloeothece membranacea</i> (blue-green algae) <i>Chlorella vulgaris</i> (CCAP 211/79) were used to study the effect of different spectrum of light such as blue, green, yellow, orange and red on algal growth and pigment synthesis ability. • The batch mode experiments were conducted using Bubble column photo-bioreactors having working volume of 450ml capacity. The culture was continuously sparged with compressed sterile air at 2LPM flow rate. • From the experimental study it was found that among all the spectrum of lights (blue, green, yellow, orange and red) the maximum biomass concentration of 2.05g/L was obtained under red light illumination and was higher than that obtained for <i>chlorella vulgaris</i> under same condition using low density seed culture. | |
|--|---|--|

| | | |
|--|--|--|
| | <ul style="list-style-type: none"> • Similarly, in case of high density seed culture, the highest biomass concentrations of <i>Gloeothece membranacea</i> was 2.27g/L and was higher than <i>Chlorella vulgaris</i> for which the value was 1.92 g/L. • The maximum chlorophyll content of 1.98 and 1.17%w/w were obtained for <i>chlorella vulgaris</i> under green light cultivation for both low and high cell density seed culture. • The maximum values of chlorophyll content of 0.37 and 0.75%w/w respectively were obtained for <i>Gloeothece membranacea</i> using low and high cell density seed culture in red light illumination. For low and high cell density seed culture, comparatively higher values of maximum chlorophyll content of 1.98 and 1.17%w/w respectively were obtained for <i>chlorella vulgaris</i> under green light condition. | |
|--|--|--|

2.2 Photoautotrophic growth of Microalgae

- [Ref. 14] In a study reported by H. Leflay et al.2021, the experiments using the fresh water microalga “*Chlorella sp.*” were conducted. The effect of different inlet-CO₂ concentrations (5, 10 and 15%v/v) on algal growth, CO₂ fixation rate and CO₂ removal efficiency of the algal strain were investigated in 1 L conical flask. It has been reported that the highest biomass concentration of 2.11g/L was obtained at 5% CO₂ concentration after two weeks of cultivation period. The values of maximum CO₂ fixation rate and CO₂ removal efficiency of 0.21 g/L/d and 17.27% (monitored RE.) respectively were obtained at 5% inlet-CO₂ concentration. However, they did not report any data on lipid production as well as the characterization of lipid sample was not done. They did not report any data on Chlorophyll and carotenoid Production. No data were reported on Kinetic study on Growth with respect to Carbon source, Nitrogen source and light intensity. Photo -bioreactor having capacity $\geq 2L$ was operated. Optimization studies were also not conducted.
- [Ref.15] In a study reported by Li et al. 2021, experimental study using the algal strain “*Chlamydomonas reihardtii* WT CC-125” under white, blue and red-orange wavelengths of light was investigated in 250 mL baffled flasks. For the enrichment

of algal biomass Tris-Acetate-Phosphate media(TAP) was used. The effect of wavelengths (blue and red-orange) of light as well as different temperatures (range 24-32 °C) on the growth rate and lipid synthesis of microalga were investigated. It was reported that the biomass productivity of *Chlamydomonas reihardtii* WT CC-125 under the irradiance of red-orange wavelength was 38% higher as compared to blue wavelength at 24 °C temperature. However, under blue light illumination the biomass productivity of *C. reihardtii* WT CC-125 was 13% higher than red-orange wavelength at 32 °C. The maximum lipid content of approximately 5.5% was reported for red-orange wavelength and was higher than blue and white light at 32 °C. However, they did not characterize the lipid. They did not report any data on Chlorophyll and carotenoid Production. No data were also reported on Kinetic study on Growth with respect to Carbon source, Nitrogen source, light intensity. No photo-bioreactor having capacity $\geq 2L$ was operated. Optimization studies were also not conducted.

- **[Ref.16]** In a study reported by Chu B Q, et al.2021, the batch mode experiments were performed by using fresh water microalgae “*Chlorella pyrenoidosa* (FACHB-9)” under the irradiance of different wavelengths of light such as white light (380-760 nm), blue (460-470 nm), purple (400-410 nm), yellow (590-600 nm) green (525-550 nm), and red (620-630 nm) in Smart artificial climate chest (PRX-450C, Shanghai Joyn Electronic Co., Ltd., China). The batch experiments were conducted for 0-13 days. It was reported that among all the wavelengths of light (white, blue, purple, yellow, green and red) the highest value of biomass concentration i.e. 2076.3 ± 66.9 mg/L was obtained on 13th day under the illumination of red light. However, the highest lipid yield of 192.0 ± 5.5 mg/g on 13th day was obtained under the irradiance of green color. They did not report any data of CO₂ fixation rate, chlorophyll production and carotenoid production. No data were also reported on Kinetic study on Growth with respect to Carbon source, Nitrogen source, light intensity. Optimization studies were also not conducted.
- **[Ref.17]** In a study reported by J.-B. Beigbeder et al.2021, the green microalga “*Parachlorellakessleri* BOW-13C” was used to conduct the experiments varying different concentrations of bicarbonate (NaHCO₃) from 0-25g/L. The algal cultivation was conducted in two different experimental set up: (1) 1L Erlenmeyer conical flask and (2) 3.5 L bubble column photobioreactors (BCPs) using BBM

media as growth medium. The cultures were constantly aerated with the mixture of 5% CO₂ and 95% air and illuminated at 100 μmol/m²/s. It was reported that the maximum specific growth rate of 0.33d⁻¹ and 0.32 d⁻¹ were obtained at 5 and 10 g/L NaHCO₃ concentrations. However, the maximum biomass productivity and CO₂ fixation rate of 112.9 mg/L/d and 57.7 mg/L/d respectively were reported for 10 g/L concentration of NaHCO₃. The maximum lipid content of 17.1 ± 1.1% w/w was obtained on 34th day culture period as reported in the article. No data were reported on Kinetic study on Growth with respect to Carbon source, Nitrogen source, light intensity. Optimization studies were also not conducted. Also the characterization of lipid was not done. They did not report any data of chlorophyll production and carotenoid production.

- **[Ref. 18]** In the article reported by Baidya et al.2021, the effect of different colour of light (white, green, blue and red) on green algae *Chlorella ellipsoidea* for the production of biomass, lipid and pigment was studied by performing batch experiments in Erlenmeyer flasks having capacity of 1L. It was reported that, the highest biomass concentration of 60 mg/L was obtained under blue light on 15th day culture period. However, the highest values of chlorophyll a, chlorophyll b and carotenoid were found to be 7.31 ±0.03, 2.73 ±0.13 and 0.39 ±0.04 μg/mL respectively obtained on 15th day. The highest value of lipid content was obtained under the irradiance of blue color light and the value is 11.32 ± 0.10% w/w. No data were reported for CO₂ fixation rate different of light. No data were reported on Kinetic study on Growth with respect to Carbon source, Nitrogen source, light intensity. Optimization studies were also not conducted. Also the characterization of lipid was not done. No photo-bioreactor having capacity ≥ 2L was operated.
- **[Ref.19]** In a study reported by Hwang and N. Maier et. al 2019, the micro algae “*N. oleoabundans* (UTEX 1185)” was used to study the effect of red and white light on alga growth rate and fatty acid production. It has been reported that Aiba model is valid due to photo-inhibition at higher light intensity. It was reported that the values of kinetic parameters were determined using Aiba equation through non-linear regression. It was reported that two individual 1L capacity reactors were used to conduct the experiments having controllable incident light intensity (LI0) in the range of 47.8 to 634 μEm⁻² s⁻¹(white LED) and 58.5 to 792.6 μEm⁻² s⁻¹(red LED). The highest value of lipid yield of 25.2 ± 0.2% w/w was achieved for red-light

spectra (630–700 nm). The values of half-maximum-rate light irradiance (K_L) for both white and red spectra i.e. $35 \mu\text{E m}^{-2} \text{s}^{-1}$ and $37 \mu\text{E m}^{-2} \text{s}^{-1}$ were obtained. The values of half-inhibition-rate light irradiance (K_I) were found to be 299 and 502 $\mu\text{E m}^{-2} \text{s}^{-1}$ under the illumination of white and red spectra. . No data were reported on kinetic study on growth with respect to Carbon source, Nitrogen source. Optimization studies were also not conducted. Also the characterization of lipid was not done. Photo-bioreactor having capacity $\geq 2\text{L}$ was not operated. They did not report any data of chlorophyll production and carotenoid production.

- **[Ref 20]** In a study reported by Tagliaferro et al. 2019, the experiment was conducted by using microalgae “*Chlorella minutissima* 26a” varying NaNO_3 concentrations from 0.075- 0.225 g/L for production of biomass and lipid under both batch and continuous cultivation system in 3.8 L volume capacity of Tubecylinder airlift Photobioreactor. Nitrogen concentrations of 0.075, 0.150 and 0.225 g/L were supplemented in f/2 growth medium for enrichment of algal cultures and incubated at 30°C under the illumination having light intensity $130 \pm 2 \mu\text{mol m}^{-2} \text{s}^{-1}$. It was reported that, the maximum biomass concentrations of 0.25 g/L, 0.40 g/L and 0.6 g/L were obtained for NaNO_3 concentrations (75 mg/L, 150 mg/L and 225 mg/L) on 7th day of culture were obtained under batch mode experiment. The maximum biomass concentration and productivity of 1.4 g/L and 188.6 mg/L/d were obtained at 225 mg/L of NaNO_3 concentration under continuous mode of experiment. The maximum lipid productivity of 92.8 mg/L/g was obtained at highest NaNO_3 concentration (225 mg/L) under continuous cultivation in airlift photobioreactor. No data were reported on Kinetic study on Growth with respect to Carbon source, Nitrogen source and light intensity. Optimization studies were also not conducted. Also the characterization of lipid was not done. They did not report any data of chlorophyll production and carotenoid production.
- **[Ref.21]** In a study reported by D. Jain et al.2019, the algal strain *Chlorella vulgaris* NIOCCV was used to conduct the experiment in continuous mode varying different inlet- CO_2 concentrations (5, 10 and 20%) in 13 L tubular PBR. The aquaculture wastewater was used as growth medium for algal cultures and incubated at 28°C under the irradiance of $100 \mu\text{mol m}^{-2} \text{s}^{-1}$ (Light intensity). It was reported that the maximum value of biomass concentration, biomass productivity and specific growth (μ) rate of 1.65 g/L, $264.58 \pm 8.8 \text{ mg /L/ d}$, 0.46 d^{-1} respectively were

obtained at 10% inlet-CO₂ concentration. The highest CO₂ fixation rate of 430 mg/L/d was obtained for 10% in-let CO₂ concentration. No data were reported on Kinetic study on Growth with respect to Carbon source, Nitrogen source and light intensity. Optimization studies were also not conducted. Also the characterization of lipid was not done. They did not report any data of chlorophyll production and carotenoid production

- **[Ref. 22]** In a study reported by Eloka-Eboka & Inambao et al. 2017, different wavelengths of light such as blue, green, yellow and red LEDs were used to perform the batch experiments using the micro algal strain "*Scenedesmus quadricauda*". The effect of different wavelengths of light ((blue, green, yellow and red) on the algal growth and pigment production were investigated. Two different types of reactors: (1) cylindrical Photobioreactor having maximum capacity of 2 L and (2) Biofermentor having maximum capacity of 3 L were used to conduct the experiments. All the cultures were incubated at an ambient temperature (lies between 25-30 °C). It was reported that, the highest value of biomass concentration and productivity of 0.325g/L and 0.03438 g/L//d respectively on 12th day were obtained for blue color wavelength in a 2 L Photobioreactor. However, the highest biomass productivity of 0.09482 g/L/d was achieved under full spectrum of light (multiple- color) using 3L fermenter. The maximum chlorophyll concentration and productivity of 10 g/L and 0.00109 g/L/d respectively were obtained under the irradiance of blue wavelength on 8th day culture period. Whereas, the maximum chlorophyll productivity of 0.00270g/L/d was achieved under the illumination of full spectrum of light in 3L biofermentor. No data were reported on Kinetic study on Growth with respect to Carbon source, Nitrogen source and light intensity. Optimization studies were also not conducted. Also the characterization of lipid was not done. They did not report any data on CO₂ fixation, lipid production and carotenoid production
- **[Ref. 23]** In a study reported by Mooij et al.2016, different wavelength of light such as warm white, orange-red (642 nm), deep-red (661 nm), blue (458 nm), and yellow light (596 nm) were used to perform the experiment. Micro alga "*Chlamydomonas reinhardtii* CC-1690" was cultivated in bench-scale flat plate photobioreactors having 0.4 L working volume, pH 6.7 and incubation temperature at 25°C under the constant illumination having light intensity of 1500 μmol photons

$\text{m}^{-2} \text{s}^{-1}$. It was reported that the maximum biomass concentration of 1 g/L and 1.3 g/L were achieved for the strongly absorbing light spectrums (blue and deep red color). Whereas, the higher biomass concentration of 2.8 g/L was obtained under the irradiation of yellow spectrum. Among other spectra of light, the maximum biomass productivity of $54 \text{ g m}^{-2} \text{ d}^{-1}$ was obtained for yellow color. Therefore it has been reported that the yellow color spectrum of light is suitable for *Chlamydomonas reinhardtii* CC-1690 for biomass production. No photo-bioreactor having capacity $\geq 2\text{L}$ was operated. No data were reported on Kinetic study on Growth with respect to Carbon source, Nitrogen source and light intensity. Optimization studies were also not conducted. Also the characterization of lipid was not done. They did not report any data on CO_2 fixation and production of lipid, chlorophyll and carotenoid.

- [Ref. 24] In a study reported by Ra et al. 2016, six different wavelengths of lights such as red, purple, green, yellow, blue and fluorescent white were used to investigate the effect on growth and lipid production of "*Picochlorum atomus*". The batch experiments were performed in 2 L flasks as photobioreactor and the cultures were continuously aerated by supplying sterile air (0.04% CO_2). It was reported that the highest value of biomass concentration of 0.42 g/L was obtained under the illumination of red wavelength on 21st day of culture period. However, the highest value of lipid content i.e. 50.3% w/w was obtained under the irradiance of green wavelength during 2nd phase culture period. Therefore, it was reported that under the irradiance of red wavelength (strong light absorbing wavelength) the highest biomass concentration was achieved as compared to the weak absorbing wavelength for green light. However, the higher lipid accumulation by *Picochlorum atomus* was achieved under green color wavelength. The fatty acid composition through FAME analysis of lipid sample under different wavelengths of light was reported. Among all the fatty acids the highest values of linolenic acid (C18:3) i.e. 47.84, 44.08 and 45.22% were obtained respectively under the irradiance of green, red and blue wavelengths of light. No data were reported on kinetic study on growth with respect to carbon source and nitrogen source and light intensity. Optimization studies were also not conducted. They did not report any data on CO_2 fixation, chlorophyll production and carotenoid production.

- [Ref.25] In the study reported by Adameczyk et al. 2016, the algal strains “*Chlorella vulgaris*” and “*Nannochloropsisgaditana*” were used to study biomass production. Two photobioreactor having capacity of 15 L were used for growing the algal strains. It was reported that that the biomass concentration for both the algal cultures were increased monotonically along with the culture period and reached the maximum level on 10th day of culture period. The maximum biomass concentrations of 4.05 and 4.02 g/L were respectively obtained on 10th day for *Nannochloropsisgaditana* at 4% and 8% inlet CO₂ concentration. These values were comparatively higher than the maximum biomass concentrations of 3.15g/L and 3.33g/L obtained for *Chlorella sp.* at same inlet CO₂ concentration on 10th day. *Nannochloropsisgaditana* species exhibited higher CO₂ fixation rate (average more than 0.55 g/L/day). However, the differences between the values of growth rate coefficient K_c (d⁻¹) for *Chlorella sp* and *Nannochloropsisgaditana* were not so high. The highest CO₂ fixation rate of 1.7 g/L/day was obtained for *N. gaditana*. No data were reported on kinetic study on growth with respect to carbon source and nitrogen source and light intensity. Optimization studies were also not conducted. They did not report any data on chlorophyll production and carotenoid production.
- [Ref. 26] In the study reported by E.R. Mattos et al., 2015, the batch experiments were conducted by using the algal strain “*Scenedesmus bijuga*”, which was isolated from water bodies of waste water. The algal cultures were enriched using BG-11 growth medium and cultivated in 500 ml conical flask. The cultures were illuminated under different spectrums of light (white, red: 655 nm; blue: 470 nm and green: 530 nm) having intensity of 300 $\mu\text{mol}/\text{m}^2/\text{s}$. Two carbon sources namely 5% v/v CO₂ and 0.02 g/L of Na₂CO₃ were used to grow the alga for 28 days. It was found that among all the spectrums of light (white, red, green and blue) the maximum biomass concentration of 0.18 ± 0.02 g/L was obtained under the irradiance of green light on 6th day. It was also reported that the green wavelength is considered as the weakly absorbed light which has an ability to penetrate deeper in high density cultures due to which the biomass production increased significantly. Photo-bioreactor having capacity ≥ 2 L was not operated. No data were reported on kinetic study on growth with respect to carbon source and nitrogen source and light intensity. Optimization studies were also not conducted. They did

not report any data on CO₂ fixation, chlorophyll production and carotenoid production.

- **[Ref .27]** In a study reported by Vadiveloo et al. 2015, the experiments were conducted by using *Nannochloropsis sp.* (MUR 266) varying different wavelengths of light (white, blue, blue-green, pink, red and green) in 1 L Erlenmeyer flasks. The effect of different wavelengths on algal growth, lipid and pigment production were investigated. The algal cultures were cultivated using F/2 culture medium and aerated continuously at 150 rpm flow rate of air. The algal cultures were illuminated under 200 $\mu\text{mol}/\text{m}^2/\text{s}$. It was reported that the maximum biomass productivity of 132.4 ± 19.1 g/L/d was obtained under the illumination of white light. However, the maximum values of biomass productivities of 28.9 ± 2.12 , 12.9 ± 1.47 , 86.2 ± 8.81 , 101 ± 15.6 mg/L/d were respectively obtained for blue, blue-green, red and pink wavelengths of light. The value of highest lipid and chlorophyll a content of 60 %w/w and 1.5 pg/cell were obtained under the irradiance of blue light. Photo-bioreactor having capacity $\geq 2L$ was not operated. No data were reported on Kinetic study on Growth with respect to Carbon source, Nitrogen source and light intensity. Optimization studies were also not conducted. They did not report any data on CO₂ fixation and carotenoid production.
- **[Ref. 28]** In a study reported by Pradhan et.al (2015), the growth kinetics of the power plant microalgae “*Rhizoclonium hieroglyphicum* JUCHE2” was determined with respect to varying concentrations of inlet CO₂ and light intensity. The growth experiments were conducted in a 1.8L Flat Plate Photobio-Bubble-Reactor by varying wide range of light intensity ($82 \mu\text{mol}\cdot\text{m}^{-2}\cdot\text{s}^{-1}$ to $398.71 \mu\text{mol}\cdot\text{m}^{-2}\cdot\text{s}^{-1}$) and inlet-CO₂ (5% to 25 % (v/v)). It was observed that the *Rhizoclonium hieroglyphicum* JUCHE2 showed significant CO₂ capturing potential. The values of kinetic parameters μ_{max} , K_s , K_I for CO₂ and K_E (light inhibition constant) of 0.996 d^{-1} , $1.25 \times 10^{-7} \text{ Mol/L}$, 0.00165 Mol/L and $120 \mu\text{mol}/\text{m}^2/\text{s}$ were determined. It was reported that inhibition model was valid. The PBR operation was optimized through the use of standard statistical software based optimization. Photo-bioreactor having capacity $\geq 2L$ was not operated. No data were reported on kinetic study on growth with respect to nitrogen source. The characterization of lipid was not done. They did not report any data on CO₂ fixation, chlorophyll production and carotenoid production.

- [Ref. 29] In a study reported by Feng et al. 2014, growth experiments on the microalgae "*Scenedesmus Obliquus*" was performed in a 2-stage cultivation process with inlet-CO₂ concentrations varying from 0.5-20% v/v. In indoor system, 0.5 L glass vessel was used as the PBR. Whereas, in 2nd stage the algal culture was grown in a 80 L outdoor PBR system. It was reported that the maximum biomass concentration and productivity of 4.11 ± 0.29 g/L and 493 ± 33 g/L/d were obtained in the indoor cultivation system. The outdoor cultivation system, yielded the maximum biomass concentration and productivity of 4.36 ± 0.18 g/L and 525 ± 57 g/L/d respectively. The highest specific growth rate " μ " of 2.09 d⁻¹ was obtained at 5% inlet-CO₂ concentration. The maximum lipid contents of 49.6% w/w and $40.1 \pm 0.9\%$ w/w were achieved respectively in outdoor and indoor cultivation systems. It was reported that as compared to the indoor system, the lipid productivity was maximum in case of outdoor cultivation i.e. 151-193 mgL⁻¹d⁻¹. No data were reported on the kinetic study on growth with respect to nitrogen source and light intensity. They did not report any data on CO₂ fixation, chlorophyll production and carotenoid production.
- [Ref 30] In a study reported by Dhup et al. 2014, the algal strain "*Monoraphidium sp.* T4X" was used. The growth studies were conducted by varying NaNO₃ concentrations in the range 0.5-2 g/L in 1 L Erlenmeyer flask. It was reported that the highest value of biomass concentration, biomass productivity and specific growth rate, μ (d⁻¹) were respectively obtained as 0.083 d⁻¹, 0.23 ± 0.02 g/L and 15.3 mg/L/d at 1.5g/L NaNO₃ concentration (1.09 NO⁻³ concentration mg/L). The maximum lipid content and productivity of $18.42 \pm 0.4\%$ w/w and 0.18 g/L/d were obtained at 0.5g/L of NaNO₃ concentration. Therefore, it was reported that the high lipid content of *Monoraphidium sp.* T4X was achieved under nitrogen-stressed condition. Photo-bioreactor having capacity ≥ 2 L was not operated. No data were reported on the kinetic study on growth with respect to carbon source, nitrogen source and light intensity. Optimization study was not conducted. They did not report any data on CO₂ fixation, chlorophyll production and carotenoid production.
- [Ref. 31] In a study reported by Mandotra et al. 2014, batch experiments were conducted using fresh water microalgae "*Scenedesmus abundans*" varying different concentrations of KNO₃ as inorganic nitrogen source (0.0 gL⁻¹, 0.08 gL⁻¹, 0.16 gL⁻¹, 0.24 gL⁻¹, 0.32 gL⁻¹ and 0.4 gL⁻¹). It was reported that the maximum biomass

productivity of 167.23 ± 6.89 mg/L/d was obtained at 0.32 g/L of KNO_3 concentration. While the maximum lipid content of 67.59 ± 2.17 %w/w was obtained under absence of nitrogen source KNO_3 (nitrogen starvation condition). Under nitrogen limited/stressed condition the lipid content was 61.97 ± 1.94 % obtained at 0.08 g/L KNO_3 concentration. It was reported that with increase in nitrogen concentration the biomass production rate also increased up to 0.32g/L of KNO_3 concentration and inhibited at 0.4g/L of KNO_3 concentration. However, under nitrogen stressed condition the lipid accumulation of *Scenedesmus abundans* was increased. The characterization of lipid was done. Photo-bioreactor having capacity $\geq 2L$ was not operated. No data were reported on the kinetic study on growth with respect to carbon source, nitrogen source and light intensity. Optimization studies were not conducted. They did not report any data on CO_2 fixation, chlorophyll production and carotenoid production.

- [Ref.32] In a the study reported by Wang et al. 2014, growth experiments were conducted using algal strain "*Chlorella ellipsoidea*" in three photobioreactors : 1) 2L photo bioreactor, 2) bubble column reactor (volume capacity of 20 L) and 3) outdoor cultivation (volume capacity of 200 L). It was reported that due to better light and temperature supply, in the outdoor cultivation system, the higher biomass productivity of 0.03155 g/L/d was obtained. The value of highest specific growth rate of 0.168 ± 0.006 d⁻¹ was reported for 2L indoor photobioreactor. Whereas, specific growth rate values of 0.162 ± 0.011 and 0.145 ± 0.026 d⁻¹ were obtained for 20 L indoor and 200L outdoor reactors. The total fatty acid content of $36.14 \pm 1.63\%$, $36.95 \pm 1.83\%$ and $38.90 \pm 3.21\%$ were achieved respectively in 2L indoor, 20L indoor and 200L outdoor cultivation system. It was reported that the overall cost for the biomass production of the outdoor cultivation was less than the indoor cultivation. The characterization of lipid was not done. Photo-bioreactor having capacity $\geq 2L$ was operated. No data were reported on the kinetic study on growth with respect to carbon source, nitrogen source and light intensity. Optimization studies were not conducted. They did not report any data on CO_2 fixation, lipid production, chlorophyll production and carotenoid production.
- [Ref 33] In a study reported by Kim et al. 2014, the effect of red and blue color wavelength lights on biomass growth and lipid accumulation of "*Chlorella vulgaris*" were investigated. The experiment was conducted with *Chlorella*

vulgaris under the irradiance of red and blue color wavelength in 1L Erlenmeyer conical flasks under the illumination intensity of $100 \mu\text{mol}/\text{m}^2/\text{s}$. It was reported the highest biomass productivity of $1.05 \text{ mg}/\text{L}/\text{d}$ was obtained for red color wavelength and $1.2 \text{ mg}/\text{L}/\text{d}$ approximately was obtained under the irradiance of mixed color spectrum (incubated under blue light for 2 days and then incubated under red light for 3 days). The highest value of chlorophyll content of $3 \text{ mg}/\text{L}$ was achieved on the 4th day under the illumination of blue light. The characterization of lipid was not done. Photo-bioreactor having capacity $\geq 2\text{L}$ was not operated. No data were reported on the kinetic study on growth with respect to carbon source, nitrogen source and light intensity. Optimization study was not conducted. They did not report any data on CO_2 fixation, lipid production and carotenoid production.

- [Ref. 34] in a study reported by, Tang et al.2011, the algal strains namely “*Scenedesmus obliquus* SJTU-3” and “*Chlorella pyrenoidosa*” were used in batch experiments. The experiments were conducted by varying CO_2 concentrations from 0.03-50%(v/v) in 1 L Erlenmeyer flasks. It was reported that the maximum values of biomass concentrations of 1.84 ± 0.01 and $1.55 \pm 0.01 \text{ g}/\text{L}$ were respectively obtained for *Scenedesmus obliquus* SJTU-3 and *Chlorella pyrenoidosa* at 10% CO_2 concentration. The maximum CO_2 fixation rate of $0.29 \text{ g}/\text{L}/\text{d}$ and $0.26 \text{ g}/\text{L}/\text{d}$ were achieved respectively for *Scenedesmus obliquus* SJTU-3 and *Chlorella pyrenoidosa* at 10%(v/v) inlet CO_2 concentration. The highest values of specific growth rates of $0.943 \pm 0.021 \text{ d}^{-1}$ and $0.993 \pm 0.082 \text{ d}^{-1}$ were obtained for *Scenedesmus obliquus* SJTU-3 and *Chlorella pyrenoidosa* at 5% and 10% CO_2 concentrations, respectively. The study reported that the highest lipid content of 24.4% w/w and 26.75% were respectively achieved for *Scenedesmus obliquus* SJTU-3 and *Chlorella pyrenoidosa* at 50%(v/v) inlet CO_2 concentration. The characterization of lipid was done. Photo-bioreactor having capacity $\geq 2\text{L}$ was not operated. No data were reported on the kinetic study on growth with respect to carbon source, nitrogen source and light intensity. The optimization study was not conducted. They did not report any data on chlorophyll production and carotenoid production.
- [Ref 35] In a study reported by Ho et al. 2012, biomass growth studies were conducted on the algal strain “*Scenedesmus obliquus* CNW-N” by varying the CO_2 concentrations (0.03-5%) and CO_2 flow rate (0.05- 0.8 vvm) in 1L tubular PBR operated under a light intensity range varied from 30–300 $\mu\text{mol}/\text{m}^2/\text{s}$. RSM

(Response surface methodology) was used to optimize the major input parameters (CO₂ concentrations and CO₂ flow rate). It was reported that the highest specific growth rate (μ , d⁻¹) and CO₂ fixation rate of 1.113 d⁻¹ and 560.1g/L/d were respectively obtained at optimum values of input parameters (2.5% CO₂ and 0.4 vvm flow rate). Under the semi-batch operation mode, the biomass productivity, photosynthesis efficiency and CO₂ fixation rate of 1030 mgL⁻¹d⁻¹, 10.5% and 1782 mgL⁻¹d⁻¹ respectively were achieved. The characterization of lipid was not done. Photo-bioreactor having capacity $\geq 2L$ was operated. No data were reported on kinetic study on growth with respect to carbon source, nitrogen source and light intensity. Optimization studies were conducted. They did not report any data on lipid production, chlorophyll production, and carotenoid production.

- [Ref.36] In a study reported by Chui et al. 2009, the algal strain “*Chlorella sp.* NCTU-2” was used to conduct the experiments in three different types of airlift photobioreactors (Bubble column, Centric-tube photo and Porous centric-tube) having capacity of 4L. The culture was aerated continuously with 5% CO₂ at a flow rate of 1LPM. It was reported that the maximum specific growth rates (μ) of 0.180 d⁻¹, 0.226 d⁻¹, 252 d⁻¹ were obtained bubble column, centric-tube photo and porous centric-tube photo-bioreactors. The maximum biomass productivity, CO₂ removal efficiency of 0.61 g/L and 63% were achieved in the porous centric-tube photo-bioreactor. The characterization of lipid was not done. No data were reported on kinetic study on growth with respect to carbon source, nitrogen source and light intensity. Optimization study was not conducted. They did not report any data on lipid production, chlorophyll production, and carotenoid production.
- [Ref. 37] In a study reported by De Moris et al. 2007, the growth of the algal strains “*Chlorella kessleri*” and “*Scenedesmus obliquus*” was investigated. The algal strains were isolated from the water samples collected from a coal-fired thermoelectric power plant. The experiments were done by varying inlet-CO₂ concentrations (0.038, 6, 12 and 18% v/v) as a parameter for algal growth and cultivated in 2 L conical flask as photobioreactors. It was reported that *Scenedesmus obliquus* produced higher biomass as compared to *Chlorella kessleri* at 6, 12 and 18% inlet-CO₂ concentrations. The maximum biomass concentration of 1.14 g/L at 12%v/v CO₂ was obtained for *Scenedesmus obliquus* whereas the maximum biomass concentration of 1.45 \pm 0.01g/L was obtained at 0.038% CO₂. The

maximum biomass productivity of 0.085 ± 0.002 g/L/d was obtained at 6% inlet- CO_2 concentration for *Scenedesmus obliquus*, whereas, the highest biomass productivity of 0.090 ± 0.001 g/L/d was observed for 0.38% v/v CO_2 . The characterization of lipid was not done. No data were reported on kinetic study on growth with respect to carbon source, nitrogen source and light intensity. Optimization study were not conducted. They did not report any data on lipid production, chlorophyll production, and carotenoid production

2.3 Photoheterotrophic and Photomixotrophic Growth of Blue-green Algae/ Cyanobacteria

| Publication year | Literature review and findings | References |
|------------------|---|------------|
| 2016 | <ul style="list-style-type: none"> • Strain: <i>Chroococcus sp.</i> (HA1A1*), • Origin: Not Mentioned • Scale of operation: Microplates • Type of Growth: Mixotrophic • Carbon source: Glycerol and 2% CO_2 • Study on Lipid Production: Yes • Study on Chlorophyll Production: No • Study on carotenoid Production:No • Kinetic study on Growth with respect to Carbon source:No • Characterization of Lipid: Yes • Study in photo-bioreactor of capacity $\geq 2L$: No • The experiment was conducted by using 10 different algal strains namely <i>Chlorella sp.</i> (MA2H1, MA2H4, PCH03, PCH04, PCH10, PCH37), <i>Chroococcus sp.</i> (HA1A1*), <i>Scenedesmus sp.</i> (HA1B1*), <i>Desmodesmus sp.</i> (PCH19) or <i>Botrydiopsis sp.</i> (PCH22). • The algal strains were cultivated in both photo- autotrophic and heterotrophic growth | 38 |

| | | |
|--|--|-----------|
| | <p>mode. In case of photoautotrophic mode 2% CO₂ was supplied to the medium. Similarly, in case of photoheterotrophic growth glycerol concentration of 25 mM was supplied to BBM media.</p> <ul style="list-style-type: none"> • The algal cultures were incubated at low temperature i.e. 10°C and illuminated at 64.34 μmol/m²/s approximately for 0-24 days. • Wang et al reported that among all the algal strains, <i>Chlorella sp.</i> PCH10 produces maximum biomass concentration of 398.19 and 558.12 mg/L respectively for both the growth mode photoautotrophic and heterotrophic growth. • Under photoheterotrophic growth, <i>Desmodesmus sp.</i> (PCH19) and <i>Chlorella sp.</i> PCH37 accumulate 28.3 and 31 % of lipid content. Whereas, under photoautotrophic growth, among all the highest lipid accumulation of 20.7% was obtained for <i>Desmodesmus sp.</i> (PCH19). | |
| | <ul style="list-style-type: none"> • Strain: <i>Spirulina platensis</i> • Origin: Blue green algae • Scale of operation: 250 mL conical flasks • Type of Growth: Photo hetero trophic and Mixotrophic • Carbon source: glycerol and sodium bicarbonate • Study on Lipid Production: Yes • Study on Chlorophyll Production: Yes • Study on carotenoid Production: No | 39 |

| | | |
|--|--|--|
| | <ul style="list-style-type: none"> • Kinetic study on Growth with respect to Carbon source: No • Characterization of Lipid:Yes • Study in photo-bioreactor of capacity \geq 2L:No • The cyanobacterium species of <i>Spirulina platensis</i> was used for production of biomass, lipid and pigments (chlorophyll a and phycocyanin) using glycerol as organic carbon substrate under photoheterotrophic growth. • 2.5 mM L⁻¹ of glycerol concentration was supplemented in Zarrouk's medium, the algal cultures were incubated at 25 °C and illuminated under 16.98 kLux. • The research article revealed that the maximum lipid content of <i>Spirulina platensis</i> obtained using glycerol as only carbon source without addition of bicarbonate in the medium. And the value is 8.29±0.54(%DCW). • Whereas, the maximum biomass of 14.589±0.65mg/100ml was obtained for both glycerol and 2g bicarbonate supplemented medium. On the other hand, the higher content of chlorophyll and phycocyanin i.e. 2.309±0.13 and 24.039±2.2 (%DCW) respectively obtained by using 16.8g of bicarbonate supplemented medium. | |
|--|--|--|

2.4 Photoheterotrophic and Photomixotrophic Growth of Microalgae

- [Ref 40] In a study reported by Rana, & Prajapati et al.2021, biomass and lipid production by *C. pyrenoidosa* using glycerol as organic carbon source was studied in a 4L cylindrical photobioreactor. The batch experiments were performed by varying glycerol concentrations from 0-5g/L. Two types of growth medium were used: (1) synthetic wastewater (SWW) and (2) BBM. It was reported that in glycerol supplemented SWW media, *C. pyrenoidosa* removed 79.88% of COD after 15days of incubation period. The highest biomass concentration of $1.43 \pm 0.02 \text{ gL}^{-1}$ was obtained using 3g/L of glycerol supplemented in BBM media. The maximum value of lipid content of $30.76 \pm 0.93\%$ was achieved when 3g/L glycerol was supplemented in SWW media. The maximum chlorophyll concentration of $5.83 \pm 0.18 \mu\text{gL}^{-1}$ was obtained from the 15th day grown culture. It was reported that the highest specific growth rate of 0.57 d^{-1} was obtained using 3 gL^{-1} of glycerol. The characterization of lipid was done. Photo-bioreactor having capacity $\geq 2\text{L}$ was operated. No data were reported on kinetic study on growth with respect to carbon source, nitrogen source and light intensity. Optimization studies were not conducted. They did not report any data on chlorophyll production and carotenoid production.
- [Ref 41] In a study reported by Lacroux, et al.2020, five different algal strains namely *Acutodesmus obliquus*, *Auxenochlorella protothecoïdes*, *Chlorella sorokiniana*, *Chlamydomonas reinhardtii* CC-124 and *Chlamydomonas reinhardtii* CC-400 were used to conduct the experiments on mixotrophic growth under varying concentrations of acetic acid (0.16 to $8.6 \text{ g}\cdot\text{L}^{-1}$ of total acetate) and butyric acid (0.08 to $3.8 \text{ g}\cdot\text{L}^{-1}$ of total butyrate) as organic carbon sources. Other than organic carbon source, pH of the media was also varied in the range 5-10. The algal cultures were continuously agitated at 130 rpm and incubated at 25 °C under constant illumination of $100 \mu\text{mol}/\text{m}^2/\text{s}$. It was reported that highest values of biomass yields of $1.17 \pm 0.03 \text{ g/g}$, $1.07 \pm 0.03 \text{ g/g}$, $1.49 \pm 0.10 \text{ g/g}$, $0.63 \pm 0.08 \text{ g/g}$ and $3.88 \pm 0.3 \text{ g/g}$ were respectively obtained for *A. obliquus*, *A. protothecoïdes*, *C. reinhardtii* 124, *C. reinhardtii* 400 and *C. sorokiniana* at pH 9 and 0.5 gL^{-1} of acetate concentration. The characterization of lipid was not done. Photo-bioreactor having capacity $\geq 2\text{L}$ was not operated. No data were reported on kinetic study on growth with respect to carbon source, nitrogen source and light intensity. Optimization study was not conducted. They did not report any data on chlorophyll production and carotenoid production.

- [Ref 42] In a study reported by Abomohra et al. 2018, the algal strain *Scenedesmus obliquus* was used to conduct the experiments on photoheterotrophic growth using lipid free hydrolysate (LFAH) and waste glycerol (WG) as carbon substrates. Their impacts on biomass growth and lipid accumulation ability of the alga was investigated. Different concentrations of both lipid free hydrolysate (0, 5, 10 and 15%) and waste glycerol (0, 5, 10 and 20gL⁻¹) were used to conduct the experiment in 1 L Erlenmeyer flask. The algal cultures were incubated at 25 ± 1 °C under 18:6 hrs light: dark cycle of photoperiod with light intensity of 100 μmol photons m⁻² s⁻¹. It was reported that mixture of both 15% LFAH with 5, 10 and 20 gL⁻¹ concentrations of WG resulted in higher biomass yields of 27.4, 30.5 and 28.9%. The highest lipid productivity of 59.66 mgL⁻¹d⁻¹ was achieved at mixed proportion of LFAH(15g/L):WG(10g/L). The characterization of lipid was done. Photo-bioreactor having capacity ≥ 2L was not operated. No data were reported on kinetic study on growth with respect to carbon source, nitrogen source and light intensity. Optimization studies were not conducted. They did not report any data on chlorophyll production and carotenoid production.
- [Ref 43] In a study reported by Khanra et al. 2017, the effects of crude glycerol as organic carbon source on algal growth for enhancement of the lipid production in *Euglena gracilis* were investigated. The experiment was conducted under mixotrophic growth by supplying both organic (glycerol) and inorganic carbon (CO₂ in air) in the growth medium. The algal cultures were incubated at 28 °C under the light intensity 60 μmol/m²/s. The highest value of biomass concentration and lipid content of 2.63 g/L and 27.64% w/w were obtained under mixotrophic condition. The study also reported the effect of biodiesel derived glycerol on lipid accumulation (49.46%) and 93.45% of FAMES (consisting appropriate quantities of saturated as well as unsaturated C16-C18 fatty acids). The highest biomass and lipid concentration of 3.18 g/L and 1.573 g/L were respectively obtained for crude glycerol. The characterization of lipid was done. Photo-bioreactor having capacity ≥ 2L was not operated. No data were reported on kinetic study on growth with respect to carbon source, nitrogen source and light intensity. Optimization studies were not conducted. They did not report any data on chlorophyll production, and carotenoid production.
- [Ref 44] In a study reported by Leite et al. 2015, the *Chlorella sp.* LB1H09 was used to conduct the heterotrophic growth experiments in microtiter plates using BBM media as growth media supplemented with 20 mM xylose or 20mM glycerol. The algal culture

was incubated for 17 days and illuminated under photoperiod of light/dark cycle of 12 h at approximately $190 \mu\text{E}/\text{m}^2/\text{s}$ light intensity. It was reported that all the strains of *Chlorella sp.* produced biomass in the range of 0.4-0.8 g/L at 20 mM concentration of glycerol. The maximum specific growth rate of 1.52d^{-1} was reported for 20 mM glycerol concentration for *Chlorella sp.* PCH03. Using the same concentration of xylose i.e. 20 mM the highest value of specific growth rate of 1.10d^{-1} was obtained for *Chlorella sp.* LB1H10. The maximum lipid content of 16.5% under photoheterotrophic growth was achieved for *Chlorella sp.* LB1H09 using glycerol as organic substrate. The characterization of lipid was done. Photo-bioreactor having capacity $\geq 2\text{L}$ was not operated. No data were reported on kinetic study on growth with respect to carbon source, nitrogen source and light intensity. Optimization studies were not conducted. No data on chlorophyll production, and carotenoid production were reported.

- [Ref. 45] In a study reported by kumar et al.2014, *Chlorella sp.* KR-1 was grown in 500 mL bubble-column photo-bioreactor using mixed organic and inorganic carbon sources in modified N8 medium. The cultures were continuously aerated with 10% CO_2 and 90% sterile air mixture and glucose was used as organic carbon source for mixotrophic growth. The culture was incubated at 28-31 °C under the illumination of $170 \mu\text{E}/\text{m}^2/\text{s}$ light intensity. It was reported that the maximum biomass productivity and FAME productivity of 561 mg/L/d and 168 mg/L/d were achieved under mixotrophic growth. The maximum biomass concentration of 2.80 g/L was achieved from fed-batch mode of culture at 1g/L glucose concentration under mixotrophic growth. The characterization of lipid was done. Photo-bioreactor having capacity $\geq 2\text{L}$ was operated. No data were reported on kinetic study on growth with respect to carbon source, nitrogen source and light intensity. Optimization studies were not conducted. No data on chlorophyll production, and carotenoid production were reported.
- [Ref. 46] In a study reported by das et al. 2011, the autotrophic and mixotrophic growth of the microalgal strain "*Nannochloropsis sp.*" was investigated under different spectrums of lights (Red, Green, White and Blue). The experiments were performed in 250 ml culture flasks containing growth media supplemented with 2 g/L glycerol as well as sodium bicarbonate (Na_2CO_3) as inorganic carbon source (0.5-2 g/L). Also, the light intensity was varied in between 400-1200 Lux. It was reported that the maximum value of specific growth rates of 0.64 and 0.66d^{-1} were obtained for photoautotrophic and mixotrophic growth under the irradiance of blue light. The maximum biomass

concentration of 373 ± 10.74 mg/L was obtained for blue color spectrum under photoautotrophic condition. Under mixotrophic condition the highest biomass density of 578 ± 17.72 mg/L was achieved for blue light spectrum. The highest yield values of FAME of 55.13 mg/L and 111.96 mg/L were respectively obtained in photoautotrophic and mixotrophic growth under blue light. The characterization of lipid was done. Photo-bioreactor having capacity $\geq 2L$ was not operated. No data were reported on kinetic study on growth with respect to carbon source, nitrogen source and light intensity. Optimization studies was not conducted. They did not report any data on chlorophyll production and carotenoid production.

- **[Ref 47]** In a study reported by Yang et al. 2010, the algal strain *Chlorella minutissima* UTEX2341 was grown under photoheterotrophic condition using glycerin as organic carbon source for production of biomass and lipid. The experiments were conducted in a 2 L photobioreactor having 1.5L of working volume to culture the algal cells. The growth medium was supplemented with different concentrations of glycerin (9.02–25.2 g of C L⁻¹) and casein concentration (8.13 g /L). It was reported that the maximum biomass concentration of 7.42 /L was obtained at 9.02 g/L concentration of glycerin. Whereas the maximum value of specific growth rate of 0.408 d⁻¹ was achieved at a higher glycerin concentration (25.2 g/L). The highest lipid yield ($Y_{p/s}$) g/g of 0.1012 g/g was achieved for higher glycerin concentration (25.2g/L). The characterization of lipid was done. Photo-bioreactor having capacity $\geq 2L$ was operated. No data were reported on kinetic study on growth with respect to carbon source, nitrogen source and light intensity. Optimization studies was not conducted. No data on chlorophyll production, and carotenoid production were reported.
- **[Ref. 48]** In a study reported by Garcia et al. 2005, growth studies on the microalga *Phaeodactylum tricornutum* were conducted under variation of concentrations of glycerol (0.005, 0.01, 0.05 and 0.1 M). Cultures were grown with continuous supply of sterile air in the media for continuous aeration. The microalga was cultivated in 1 L conical flasks and incubated at 20°C under the illumination of 165 $\mu\text{Em}^{-2} \text{s}^{-1}$. It was reported that the maximum biomass concentrations of 2.4 g/L were obtained at 0.1M glycerol concentration. Maximum biomass productivity and specific growth rates were 17.5 mg L⁻¹ h⁻¹ and 1.13 d⁻¹ respectively obtained at 0.1 M and 0.01M Glycerol concentrations. The highest fatty acid yield of 16.98 % w/w was obtained from *Phaeodactylum tricornutum*. The highest EPA productivity of 33.5 mg L⁻¹ d⁻¹ was

obtained from the cultures supplemented with 0.1M glycerol. The characterization of lipid was done. Photo-bioreactor having capacity $\geq 2L$ was operated. No data were reported on kinetic study on growth with respect to carbon source, nitrogen source and light intensity. Optimization studies was not conducted. No data on chlorophyll production, and carotenoid production were reported.

2.5 Pyrolysis of Blue green algae for production of Pyro-Char, Pyro-oil and Pyro-Gas.

| Publication year | Literature review and findings | References |
|------------------|--|------------|
| 2021 | <ul style="list-style-type: none"> • Algal strain: <i>Spirulina platensis</i> • Pyrolysis type: Fast pyrolysis • Pyrolysis temperature range: 300, 400, 500, 600°C • Study on Thermal characterization: No • Reactor type: Horizontal fixed bed semi preparative reactor • Study on Product yield: Yes • Characterization of products: Yes • The pyrolysis process was carried out in horizontal fixed bed semi preparative reactor having equipped with tube furnace having temperature controller device. The algal sample weight of 0.20 g was used. • The oxygen free nitrogen flow rate of 0.1 mLs⁻¹ was supplied in the system. • The extracted oil was characterized using GC-MS analyzer. • The article reported that the maximum yield of pyrochar is 55% obtained at 300 °C for <i>Pithophora sp.</i> whereas, the pyrochar yields of 35 and 49% were reported for <i>Botryococcus braunii</i>, and <i>Spirulina platensis</i>. | 49 |

| | | |
|------|--|----|
| | <ul style="list-style-type: none"> • The maximum yield of pyro-oil and gas i.e. 65(at 500) and 59% wt. (at 600) are obtained for <i>Botryococcus brauni</i> and <i>Pithophora sp.</i> • From the GC-MS analysis of pyro –oil of three algal strains (<i>Botryococcus braunii</i>, <i>Spirulina platensis</i>, and <i>Pithophora sp</i>) it was found that themaximum amount groups of Alkane, Nitrogenates and Oxygenates are present in pyro-oil. Whereas, Alkenes, Aromatics and Anhydrosugars are present in less amount. | |
| 2015 | <ul style="list-style-type: none"> • Algal strain: <i>Spirulina sp. and Spirogyra</i> • Pyrolysis type: Slow and fast pyrolysis • Pyrolysis temperature range: 500°C • Study on Thermal characterization: Yes • Reactor type: Stainless steel reactor • Study on Product yield: Yes • Characterization of products: Yes • In experimental study the pyrolysis process was conducted in both the modes but the heating temperature was remaining constant at 500°C and the N₂ flow rate was maintained at 1 l.min⁻¹. • The characterization of pyrochar was analyzed by CHNSO analyzer and the characterization of pyo-oil was done by FTIR. • For <i>Spirulina sp.</i> under slow pyrolysis process, the maximum values of Pyro-char, Pyro-oil and Pyro-gas are 31, 21 and 23%wt. In case of fast pyrolysis the yields are 31, 29, and 40% of Pyro-char, Pyro-oil and Pyro-gas was obtained having same temperature at 500°C. • Similarly in case of <i>Spirogyra</i> , under slow pyrolysis process, the maximum values of Pyro-char, Pyro-oil and Pyro-gas are 27, 16 and 41%wt. | 50 |

| | | |
|------|--|----|
| | <p>whereas, in fast pyrolysis process, the maximum yields of Pyro-char, Pyro-oil and Pyro-gas are 32, 15, 55% respectively.</p> | |
| 2012 | <ul style="list-style-type: none"> • Algal strain: <i>Spirulina sp.</i>, <i>Spirogyra</i> and <i>Cladophora sp.</i> • Pyrolysis type: Slow pyrolysis • Pyrolysis temperature range: 550°C • Study on Thermal characterization: Yes • Reactor type: Fixed-Bed Pyrolysis • Study on Product yield: Yes • Characterization of products: Yes • The experimental study was conducted by using the dry biomass of 125 g sample of three blue green algal strain namely <i>Spirulina sp.</i> , <i>Spirogyra</i> and <i>Cladophora sp.</i> was used. • In Slow pyrolysis process was conducted by maintaining the temperature at 550 °C, the nitrogen flow rate was 30 ml/min. for 30 min having heating rate of 8°C/min. • Thermogravimetric analysis (TGA),having prograded (50-135°C (10 °C /min.); constant at a 135 °C (5 min.); 135-900°C,(100 °C /min) was also conducted for the analysis of thermal decomposition of rate of change of weight algal biomass with respect to heating temperature and time as well. • From the study it was found that the highest yield of Pyro-char, Pyro-oil and Pyro-gas are 31%, 46% and 23% was reported for <i>Spirulina sp.</i> as compared to <i>Spirogyra</i> and <i>Cladophora sp.</i> | 51 |

2.6 Pyrolysis of Microalgae for production of Pyro-Char, Pyro-oil and Pyro-Gas

- [Ref. 52] In a study reported by Gautam et al. 2019 pyrolysis of algal biomass was conducted using a non-off multimode domestic microwave oven (Whirlpool 20 L Magicook GW). Three different heating temperatures of 340°C, 320°C and 280°C were used to conduct the pyrolysis process using the algal biomass of three different algal strains: *Kappaphycus alvarezii*, *Sargassum wightii* and *Turbinaria ornate*. Maximum yield of pyro char (33.3%wt) was obtained for *Sargassum wightii* at pyrolysis temperature of 320°C. Whereas the maximum yields of pyro-oil (32.4%) and pyro-gas (45.6%) were obtained for *Kappaphycus alvarezii* at 340°C. GC-MS analysis of obtained pyro-oil was conducted and high amount of furan derivatives and aromatics were identified. The characterization of lipid was done. The thermal characterization of biomass was also done.
- [Ref.53] In a study reported by Adamczyk et al. 2015, pyrolysis of algal biomass was conducted in a the fixed-bed pyrolyzer using the dry biomass of *Nannochloropsis gaditana*. The pyrolyzer furnace was equipped with stainless steel retort (0.07 m diameter and 0.24 m height). The heating temperatures varied in the range 400-600°C. The nitrogen flow rate was maintained at 50 cm³/h during the pyrolysis process and a fixed heating rate of 20 K/min was used. The pyro-gas was analyzed in a GC-MS analyzer. It was reported that the highest yield of pyro-char of 55wt% was obtained at 400°C. Whereas, the value of maximum yield of pyro-oil of 39%wt was obtained at 600°C. The highest value of pyro gas was obtained at 400°C i.e. approximately 31%wt. The GC-MS analysis identified the presence of different aromatic hydrocarbons, heterocyclic compounds, phenols, amines, amides, indoles, alkanes, and nitriles groups in the algal pyro oil. The thermal characterization of biomass/char was not done. The characterization of lipid was done.
- [Ref. 54] In a study reported by Yuan et al. 2015, pyrolysis was performed using the algal biomass of the microalgae “*Chlorella vulgaris*” in a fixed-bed pyrolyzer under variation of temperature from 300°C to 900°C. The algal biomass was crushed and sieved to a particle size range of 74–140 µm before pyrolysis. TGA method was used for 10 mg algal biomass for thermal degradation study. Different heating rates were used as 5, 10, and 20 °C/min and the temperature profile included room temperature to 800°C. The nitrogen flow rate was maintained at 100 mL/min. It was reported that the maximum yields of pyro-char (43.46%w/w) and pyro-oil (32.69%w/w) were

respectively obtained at 400 °C and 500 °C. Whereas the maximum value of yield of 58.29%w/w was obtained for pyro-gas at 900°C. The characterization of products was done. The thermal characterization of biomass was also conducted.

- **[Ref. 55]** In a study reported by S.W. Kim et al. 2014, fast pyrolysis was conducted in a fluidized bed reactor using dry algal biomass of *Scenedesmus sp.* as the feedstock. The fast pyrolysis process was conducted at a temperature of 440°C under maintained nitrogen flow rates of 33 L/min at 25°C. The characterization of pyro-oil was conducted by GC-MS analysis. It was reported that the maximum yields of pyro-char, pyro-oil and pyro-gas was obtained as 26%w/w, 41.54%w/w and 21.8%w/w, respectively. It was also reported that palmitic acid (C₁₆H₃₂O₂) was identified as the major fatty acid from the fatty acids profile with maximum yield of 7.38%. Thermal characterization of biomass and char was not done.
- **[Ref. 56]** In a study reported by wang et al 2013, experiments on fast pyrolysis was conducted in lab-scale, atmospheric-pressure fluidized bed reactor using residual algal biomass of *Chlorella vulgaris*. Solvent extraction technique was used to extract the lipid from the algal biomass and the lipid free residual algal biomass was used for pyrolysis. The reactor used in the pyrolysis process was made of 316 stainless steel tube arrangements having 0.31m length and 38.1 mm diameter. The pyrolysis temperature was maintained at 500°C. It was reported that the maximum yields of pyro-char, pyro-oil and pyro-gas were respectively obtained as 31%w/w, 53%w/w and 10%w/w. The Thermal characterization was not done. The characterization of lipid was done using GC-MS analysis.
- **[Ref. 57]** In a study reported by Kirtania et al. 2013, pyrolysis was conducted using a TGA analyzer for the dry algal biomass of *Chlorococcum humicola*, to estimate the rate of weight loss with change in reaction temperature under non-isothermal condition. Temperature was raised in a two-phase heating, initially at a heating rate of 5 K min⁻¹ up to 200°C followed by raising up to 1000°C at rate of 10 K min⁻¹. The flow rate of nitrogen was maintained at 0.02 L min⁻¹. The fixed carbon content of 33% w/w was obtained for the algal biomass. The TGA profile revealed that the decomposition of algal biomass was started at 200°C and after 500 °C the rate of weight loss attained constant values. Therefore, the pyrolysis temperature for algal biomass was claimed to be lying between 200-500°C. The highest reactivity for algae was reported at 310 °C.

Reference

1. <https://www.sciencedirect.com/>
2. <https://scholar.google.com/>
3. Rosero-Chasoy, G., Rodríguez-Jasso, R. M., Aguilar, C. N., Buitrón, G., Chairez, I., & Ruiz, H. A. (2022). Growth kinetics and quantification of carbohydrate, protein, lipids, and chlorophyll of *Spirulina platensis* under aqueous conditions using different carbon and nitrogen sources. *Bioresource Technology*, 346, 126456.
4. Sandybayeva, S. K., Kossalbayev, B. D., Zayadan, B. K., Sadvakasova, A. K., Bolatkhan, K., Zadneprovskaya, E. V., ... & Chang, J. S. (2022). Prospects of cyanobacterial pigment production: Biotechnological potential and optimization strategies. *Biochemical Engineering Journal*, 187, 108640.
5. Sarkar, A., Rajarathinam, R., & Venkateshan, R. B. (2021). A comparative assessment of growth, pigment and enhanced lipid production by two toxic freshwater cyanobacteria *Anabaena circinalis* FSS 124 and *Cylindrospermopsis raciborskii* FSS 127 under various combinations of nitrogen and phosphorous inputs. *Environmental Science and Pollution Research*, 28(13), 15923-15933.
6. Singh, P., & Kumar, D. (2021). Biomass and lipid productivities of cyanobacteria-*Leptolyngbya foveolarum* HNBGU001. *BioEnergy Research*, 14, 278-291.
7. Satpati, G. G., & Pal, R. (2021). Co-Cultivation of *Leptolyngbya tenuis* (Cyanobacteria) and *Chlorella ellipsoidea* (green alga) for biodiesel production, carbon sequestration, and cadmium accumulation. *Current microbiology*, 78, 1466-1481.
8. Almomani, F., Judd, S., Bhosale, R. R., Shurair, M., Aljaml, K., & Khraisheh, M. (2019). Intergraded wastewater treatment and carbon bio-fixation from flue gases using *Spirulina platensis* and mixed algal culture. *Process Safety and Environmental Protection*, 124, 240-250.
9. Maheshwari, N., Krishna, P. K., Thakur, I. S., & Srivastava, S. (2020). Biological fixation of carbon dioxide and biodiesel production using microalgae isolated from sewage waste water. *Environmental Science and Pollution Research*, 27, 27319-27329.
10. Eloka-Eboka, A. C., & Inambao, F. L. (2017). Effects of CO₂ sequestration on lipid and biomass productivity in microalgal biomass production. *Applied Energy*, 195, 1100-1111.

11. Kassim, M. A., & Meng, T. K. (2017). Carbon dioxide (CO₂) biofixation by microalgae and its potential for biorefinery and biofuel production. *Science of the total environment*, 584, 1121-1129
12. Shabani, M. (2016). CO₂ bio-sequestration by *Chlorella vulgaris* and *Spirulina platensis* in response to different levels of salinity and CO₂. *Proceedings of the International Academy of Ecology and Environmental Sciences*, 6(2), 53.
13. Mohsenpour, S. F., & Willoughby, N. (2013). Luminescent photobioreactor design for improved algal growth and photosynthetic pigment production through spectral conversion of light. *Bioresource technology*, 142, 147-153.
14. Leflay, H., Pandhal, J., & Brown, S. (2021). Direct measurements of CO₂ capture are essential to assess the technical and economic potential of algal-CCUS. *Journal of CO₂ Utilization*, 52, 101657
15. Li, X., Huff, J., Crunkleton, D. W., & Johannes, T. W. (2021). LED alternating between blue and red-orange light improved the biomass and lipid productivity of *Chlamydomonas reinhardtii*. *Journal of Biotechnology*, 341, 96-102.
16. Chu, B., Zhao, J., Zheng, H., Gong, J., Chen, K., Zhang, S., ... & He, Y. (2021). Performance of LED with mixed wavelengths or two-phase culture on the growth and lipid accumulation of *Chlorella pyrenoidosa*. *International Journal of Agricultural and Biological Engineering*, 14(1), 90-96.
17. Beigbeder, J. B., Sanglier, M., de Medeiros Dantas, J. M., & Lavoie, J. M. (2021). CO₂ capture and inorganic carbon assimilation of gaseous fermentation effluents using *Parachlorella kessleri* microalgae. *Journal of CO₂ Utilization*, 50, 101581.
18. Baidya, A., Akter, T., Islam, M. R., Shah, A. A., Hossain, M. A., Salam, M. A., & Paul, S. I. (2021). Effect of different wavelengths of LED light on the growth, chlorophyll, β -carotene content and proximate composition of *Chlorella ellipsoidea*. *Heliyon*, 7(12), e08525.
19. Hwang, J. H., & Maier, N. (2019). Effects of LED-controlled spatially-averaged light intensity and wavelength on *Neochloris oleoabundans* growth and lipid composition. *Algal Research*, 41, 101573.
20. Tagliaferro, G. V., Izário Filho, H. J., Chandel, A. K., da Silva, S. S., Silva, M. B., & dos Santos, J. C. (2019). Continuous cultivation of *Chlorella minutissima* 26a in a tube-

- cylinder internal-loop airlift photobioreactor to support 3G biorefineries. *Renewable Energy*, 130, 439-445.
21. Jain, D., Ghonse, S. S., Trivedi, T., Fernandes, G. L., Menezes, L. D., Damare, S. R., ... & Gupta, V. (2019). CO₂ fixation and production of biodiesel by *Chlorella vulgaris* NIOCCV under mixotrophic cultivation. *Bioresource technology*, 273, 672-676.
 22. Eloka-Eboka, A. C., & Inambao, F. L. (2017). Effects of CO₂ sequestration on lipid and biomass productivity in microalgal biomass production. *Applied Energy*, 195, 1100-1111.
 23. de Mooij, T., de Vries, G., Latsos, C., Wijffels, R. H., & Janssen, M. (2016). Impact of light color on photobioreactor productivity. *Algal research*, 15, 32-42.
 24. Ra, C. H., Kang, C. H., Jung, J. H., Jeong, G. T., & Kim, S. K. (2016). Enhanced biomass production and lipid accumulation of *Picochlorum atomus* using light-emitting diodes (LEDs). *Bioresource technology*, 218, 1279-1283
 25. Adamczyk, M., Lasek, J., & Skawińska, A. (2016). CO₂ biofixation and growth kinetics of *Chlorella vulgaris* and *Nannochloropsis gaditana*. *Applied biochemistry and biotechnology*, 179, 1248-1261.
 26. Mattos, E. R., Singh, M., Cabrera, M. L., & Das, K. C. (2015). Enhancement of biomass production in *Scenedesmus bijuga* high-density culture using weakly absorbed green light. *Biomass and Bioenergy*, 81, 473-478
 27. Vadiveloo, A., Moheimani, N. R., Cosgrove, J. J., Bahri, P. A., & Parlevliet, D. (2015). Effect of different light spectra on the growth and productivity of acclimated *Nannochloropsis* sp.(Eustigmatophyceae). *Algal research*, 8, 121-127
 28. Pradhan, L., Bhattacharjee, V., Mitra, R., Bhattacharya, I., & Chowdhury, R. (2015). Biosequestration of CO₂ using power plant algae (*Rhizoclonium hieroglyphicum* JUCHE2) in a Flat Plate Photobio-Bubble-Reactor—Experimental and modeling. *Chemical Engineering Journal*, 275, 381-390.
 29. Feng, P., Yang, K., Xu, Z., Wang, Z., Fan, L., Qin, L., ... & Hu, L. (2014). Growth and lipid accumulation characteristics of *Scenedesmus obliquus* in semi-continuous cultivation outdoors for biodiesel feedstock production. *Bioresource technology*, 173, 406-414

30. Dhup, S., & Dhawan, V. (2014). Effect of nitrogen concentration on lipid productivity and fatty acid composition of *Monoraphidium sp.* *Bioresource technology*, 152, 572-575.
31. Mandotra, S. K., Kumar, P., Suseela, M. R., & Ramteke, P. W. (2014). Fresh water green microalga *Scenedesmus abundans*: a potential feedstock for high quality biodiesel production. *Bioresource Technology*, 156, 42-47
32. Wang, S. K., Hu, Y. R., Wang, F., Stiles, A. R., & Liu, C. Z. (2014). Scale-up cultivation of *Chlorella ellipsoidea* from indoor to outdoor in bubble column bioreactors. *Bioresource technology*, 156, 117-122.
33. Kim, D. G., Lee, C., Park, S. M., & Choi, Y. E. (2014). Manipulation of light wavelength at appropriate growth stage to enhance biomass productivity and fatty acid methyl ester yield using *Chlorella vulgaris*. *Bioresource technology*, 159, 240-248.
34. Tang, D., Han, W., Li, P., Miao, X., & Zhong, J. (2011). CO₂ biofixation and fatty acid composition of *Scenedesmus obliquus* and *Chlorella pyrenoidosa* in response to different CO₂ levels. *Bioresource technology*, 102(3), 3071-3076.
35. Ho, S. H., Lu, W. B., & Chang, J. S. (2012). Photobioreactor strategies for improving the CO₂ fixation efficiency of indigenous *Scenedesmus obliquus* CNW-N: statistical optimization of CO₂ feeding, illumination, and operation mode. *Bioresource technology*, 105, 106-113.
36. Chiu, S. Y., Tsai, M. T., Kao, C. Y., Ong, S. C., & Lin, C. S. (2009). The air-lift photobioreactors with flow patterning for high-density cultures of microalgae and carbon dioxide removal. *Engineering in life sciences*, 9(3), 254-260.
37. de Moraes, M. G., & Costa, J. A. V. (2007). Isolation and selection of microalgae from coal fired thermoelectric power plant for biofixation of carbon dioxide. *Energy Conversion and management*, 48(7), 2169-2173.
38. Wang, Y. Z., Hallenbeck, P. C., Leite, G. B., Paranjape, K., & Huo, D. Q. (2016). Growth and lipid accumulation of indigenous algal strains under photoautotrophic and mixotrophic modes at low temperature. *Algal Research*, 16, 195-200.
39. Narayan, M. S., Manoj, G. P., Vatchravelu, K., Bhagyalakshmi, N., & Mahadevaswamy, M. (2005). Utilization of glycerol as carbon source on the growth,



- pigment and lipid production in *Spirulina platensis*. International journal of food sciences and nutrition, 56(7), 521-528.
40. Rana, M. S., & Prajapati, S. K. (2021). Stimulating effects of glycerol on the growth, phycoremediation and biofuel potential of *Chlorella pyrenoidosa* cultivated in wastewater. Environmental Technology & Innovation, 24, 102082.
 41. Lacroux, J., Trably, E., Bernet, N., Steyer, J. P., & van Lis, R. (2020). Mixotrophic growth of microalgae on volatile fatty acids is determined by their undissociated form. Algal Research, 47, 101870.
 42. Abomohra, A. E. F., Eladel, H., El-Esawi, M., Wang, S., Wang, Q., He, Z., ... & Hanelt, D. (2018). Effect of lipid-free microalgal biomass and waste glycerol on growth and lipid production of *Scenedesmus obliquus*: Innovative waste recycling for extraordinary lipid production. Bioresource technology, 249, 992-999.
 43. Khanra, A., Vasistha, S., & Rai, M. P. (2017). Glycerol on lipid enhancement and fame characterization in algae for raw material of biodiesel. International Journal of Renewable Energy Research (IJRER), 7(4), 1970-1978.
 44. Leite, G. B., Paranjape, K., Abdelaziz, A. E., & Hallenbeck, P. C. (2015). Utilization of biodiesel-derived glycerol or xylose for increased growth and lipid production by indigenous microalgae. Bioresource technology, 184, 123-130.
 45. Praveen kumar, R., Kim, B., Choi, E., Lee, K., Park, J. Y., Lee, J. S., ... & Oh, Y. K. (2014). Improved biomass and lipid production in a mixotrophic culture of *Chlorella* sp. KR-1 with addition of coal-fired flue-gas. Bioresource technology, 171, 500-505.
 46. Das, P., Lei, W., Aziz, S. S., & Obbard, J. P. (2011). Enhanced algae growth in both phototrophic and mixotrophic culture under blue light. Bioresource technology, 102(4), 3883-3887.
 47. Yang, J., Rasa, E., Tantayotai, P., Scow, K. M., Yuan, H., & Hristova, K. R. (2011). Mathematical model of *Chlorella minutissima* UTEX2341 growth and lipid production under photoheterotrophic fermentation conditions. Bioresource Technology, 102(3), 3077-3082.
 48. Cerón Garcí, M. C., Fernández Sevilla, J. M., Acien Fernandez, F. G., Molina Grima, E., & García Camacho, F. (2000). Mixotrophic growth of *Phaeodactylum tricornutum*





- on glycerol: growth rate and fatty acid profile. *Journal of Applied Phycology*, 12, 239-248.
49. Piloni, R. V., Daga, I. C., Urcelay, C., & Moyano, E. L. (2021). Experimental investigation on fast pyrolysis of freshwater algae. Prospects for alternative bio-fuel production. *Algal Research*, 54, 102206.
50. Chaiwong, K., & Kiatsiriroat, T. (2015). Characterizations of bio-oil and bio-char products from algae with slow and fast pyrolysis. *Int J Environ Bioenergy*, 10, 65-76.
51. Chaiwong, K., Kiatsiriroat, T., Vorayos, N., & Thararax, C. (2012). Biochar production from freshwater algae by slow pyrolysis. *Maejo International Journal of Science and Technology*, 6(2), 186.
52. Gautam, R., Shyam, S., Reddy, B. R., Govindaraju, K., & Vinu, R. (2019). Microwave-assisted pyrolysis and analytical fast pyrolysis of macroalgae: product analysis and effect of heating mechanism. *Sustainable Energy & Fuels*, 3(11), 3009-3020.
53. Adamczyk, M., & Sajdak, M. (2018). Pyrolysis behaviours of microalgae *Nannochloropsis gaditana*. *Waste and biomass valorization*, 9, 2221-2235.
54. Yuan, T., Tahmasebi, A., & Yu, J. (2015). Comparative study on pyrolysis of lignocellulosic and algal biomass using a thermogravimetric and a fixed-bed reactor. *Bioresource Technology*, 175, 333-341.
55. Kim, S. W., Koo, B. S., & Lee, D. H. (2014). A comparative study of bio-oils from pyrolysis of microalgae and oil seed waste in a fluidized bed. *Bioresource technology*, 162, 96-102.
56. Wang, K., Brown, R. C., Homsy, S., Martinez, L., & Sidhu, S. S. (2013). Fast pyrolysis of microalgae remnants in a fluidized bed reactor for bio-oil and biochar production. *Bioresource technology*, 127, 494-499.
57. Kirtania, K., & Bhattacharya, S. (2013). Pyrolysis kinetics and reactivity of algae-coal blends. *Biomass and Bioenergy*, 55, 291-298.



Chapter 3






4. Aims and Objectives:





The research gap identified through the literature review on algal CO₂ capture, clearly indicates that mostly freshwater and marine algal strains collected from ponds/lakes or seawater have been extensively studied from the perspectives of CO₂ capture. Some articles also reported studies on production of lipid and bio-chemicals. Although coal-based power plant water is a source of algae, only a few studies have been reported on power plant algae. It is reported in the literature that algae can be grown on heterotrophic mode for high lipid production. However, no attempt has so far been made to study the performance of heterotrophic growth of power plant. Although blue green algae have been reported to show better performance regarding CO₂ capture and lipid production, no report on the study of power plant blue green algae is available. As Indian power sector is mostly based on coal, present research intends to address overall research gaps towards the utilization of blue green algae of Indian power plant with the following aims and objectives:





| Aims 1: Isolation and Characterization of Power Plant Blue green Alga | | |
|--|---|---|
| Objectives | | Work plan |
| Selection of source for isolation |  | <ul style="list-style-type: none"> • Collection of Water samples, already contaminated with algae, from a coal-fired Power plant of West Bengal |
| Isolation and identification of algal strain. |  | <ul style="list-style-type: none"> • Enrichment of collected power plant algal samples in a suitable growth medium • Identification of the blue green algal strain, by expert algologists. • Morphological characterization of identified alga under FESEM analysis of biomass. • The elemental (C-H-N) analysis of dry algal biomass. |

| Aim 2: Studies on the performance of the isolated blue green alga with respect to CO₂ fixation and its growth kinetics under photoautotrophic condition using white light. | | |
|--|---|--|
| Objectives | | Work plan |
| Determination of CO ₂ fixation rate |  | <ul style="list-style-type: none"> • Determination of CO₂ fixation rate of the isolated blue green alga at different inlet concentration of CO₂ under constant temperature and light intensity. |
| Determination of growth kinetics of isolated blue green alga by varying inlet-CO ₂ concentrations. |  | <ul style="list-style-type: none"> • Performance of batch mode experiments for the growth of the isolated blue green alga using inlet-CO₂ concentration as a parameter under constant concentration of nitrogen source and light intensity. • Determination of the kinetic parameters for different growth models using the specific growth rate data obtained at different inlet concentration of CO₂ |
| Determination of growth kinetics of isolated blue green alga by varying initial concentrations of nitrogen source (NaNO ₃). |  | <ul style="list-style-type: none"> • Performance of batch mode experiments for the growth of the isolated blue green alga using initial concentrations of nitrogen source as a parameter under constant values of inlet concentration of CO₂ and light intensity. • Determination of the kinetic parameters for different growth models using the specific growth rate data obtained at different initial concentrations of nitrogen source |
| Determination of growth kinetics of isolated blue green alga by varying light intensity |  | <ul style="list-style-type: none"> • Performance of batch mode experiments for the growth of the isolated blue green alga using light intensity as a parameter under constant values of inlet concentration of CO₂ and initial concentrations of nitrogen source. • Determination of the kinetic parameters for different growth models using the specific |

| | | |
|--|---|--|
| | | growth rate data obtained at different intensity of light. |
| Determination of growth kinetics of isolated blue green alga by simultaneously varying inlet-CO ₂ concentrations, initial concentrations of nitrogen source and light intensity |  | <ul style="list-style-type: none"> • Performance of batch mode experiments for the growth of the isolated blue green alga simultaneously varying inlet-CO₂ concentrations, initial concentrations of nitrogen source and light intensity. • Determination of the growth kinetics as a function of inlet-CO₂ concentrations, initial concentrations of nitrogen source and light intensity by multi-variable mathematical modelling and statistical modeling using response surface methodology. |
| Aim 3: Studies on the growth kinetics of the isolated blue green alga under photoheterotrophic (Glycerol) and photomixotrophic (CO₂+Glycerol) conditions using white light | | |
| Objectives | | Work plan |
| Determination of growth kinetics using glycerol as organic carbon source |  | <ul style="list-style-type: none"> • Study of Performance of batch mode experiments using initial concentration of glycerol as the parameter and maintaining constant values of initial concentrations of nitrogen source and light intensity. • Determination of the growth kinetic parameters for different growth models using the specific growth rate data obtained at different initial concentrations of glycerol. • Calculation of yield coefficient by using the data on generation of biomass and consumption of glycerol over same period of growth. |
| | | <ul style="list-style-type: none"> • Batch mode experiments conducted by supplying both gaseous CO₂ as well as glycerol. |

| | | |
|--|---|--|
| <p>Determination of growth kinetics using mixture of CO₂ and Glycerol</p> |  | <ul style="list-style-type: none"> • Determination of growth kinetic parameters using the specific growth rates under mixotrophic condition |
| <p>Comparison of growth under photoautotrophic, photoheterotrophic and photomixotrophic conditions</p> |  | <ul style="list-style-type: none"> • Comparison of the data on specific growth rate of the alga under photoautotrophic, photoheterotrophic and photomixotrophic conditions using same amount of carbon moles supplied by CO₂ and Glycerol and CO₂ +Glycerol respectively at same quantity of nitrogen source and light intensity are done. |
| <p>Aim4: Studies on Lipid production by alga under photoautotrophic, photoheterotrophic and photomixotrophic conditions using white light</p> | | |
| <p>Determination of Lipid content and productivity under photoautotrophic, photoheterotrophic and photomixotrophic conditions using white light</p> |  | <ul style="list-style-type: none"> • Extraction of lipid using mixture of solvents (Chloroform: Methanol) from dry algal biomass obtained under photoautotrophic, photoheterotrophic and photomixotrophic conditions using same amount of carbon moles supplied by CO₂ and Glycerol and CO₂ +Glycerol respectively at same quantity of nitrogen source and light intensity. |
| <p>Comparison of lipid production</p> |  | <ul style="list-style-type: none"> • Comparison of Lipid content of <i>L.subtilis</i> JUCHE1 under photoautotrophic, photoheterotrophic and photomixotrophic conditions are done. |
| <p>Characterization of lipid under photoautotrophic, photoheterotrophic and photomixotrophic conditions using white light</p> |  | <ul style="list-style-type: none"> • Lipid obtained from algal mass grown under photoautotrophic, photoheterotrophic and photomixotrophic conditions using white light are characterized through chromatographic analysis. |

| Aim 5: Studies on pigment production by alga under photoautotrophic, photoheterotrophic and photomixotrophic conditions using white light | | |
|--|---|---|
| Determination of chlorophyll and carotenoid content under photoautotrophic, photoheterotrophic and photomixotrophic conditions using white light |  | <ul style="list-style-type: none"> • Extraction of chlorophyll and carotenoid from algal biomass obtained under photoautotrophic, photoheterotrophic and photomixotrophic conditions using white light using 80% Acetone . |
| Comparison of chlorophyll and carotenoid content under photoautotrophic, photoheterotrophic and photomixotrophic conditions using white light |  | <ul style="list-style-type: none"> • Comparison of chlorophyll and carotenoid content of <i>L.subtilis</i> JUCHE1 under photoautotrophic, photoheterotrophic and photomixotrophic conditions are done. |
| Aim 6: Study the effect of different light wavelengths on algal growth, lipid accumulation and pigment production by Blue-Green Alga <i>L.subtilis</i>JUCHE | | |
| Determination of biomass growth by varying different wavelengths of light |  | <ul style="list-style-type: none"> • Conduction of batch experiments by varying four different wavelengths of light: Blue, Green, Yellow and Red for 0-6 days in 250 ml conical flasks. • Calculation of growth rate of alga at different time intervals for individual wavelengths of light. • Identification of the wavelength for which algal growth is maximum |
| Determination of Lipid content of alga |  | <ul style="list-style-type: none"> • Extraction of algal lipid for all the wavelengths of light under study. • Identification of the wavelength for which lipid accumulation is the highest |

| | | |
|---|---|---|
| <p>Determination of Chlorophyll and Carotenoid content different wavelength of light</p> |  | <ul style="list-style-type: none"> • Extraction of Chlorophyll and carotenoid from algal biomass obtained under photoautotrophic condition using different wavelength of light • Identification of the wavelength for which pigment production is the highest |
| <p>Study on the performance of Airlift photobioreactor using the most suitable wavelength with respect to Biomass and Lipid</p> |  | <ul style="list-style-type: none"> • Determination of performance of airlift photobioreactor with respect to biomass growth and accumulation of lipid using the most suitable wavelength with respect to Biomass and lipid |
| <p>Aim 7: Studies on Power plant Blue-Green Alga “<i>Leptolyngbya subtilis</i> JUCHE1” for production of biochar through slow pyrolysis.</p> | | |
| <p>Pyrolysis of algal biomass</p> |  | <ul style="list-style-type: none"> • Experiments in semi-batch pyrolyser under isothermal condition in the temperature range of 300-700°C are performed. • Yields (w/w%) of pyrochar/biochar and pyrooil are determined. |
| <p>Characterization of pyro char and oil</p> |  | <ul style="list-style-type: none"> • Characterization of pyrochar/biochar and pyro oil is performed. |

Chapter 4

4.1. Materials and methods

4.1.1 Algal strain collection and identification

A blue-green alga, *Leptolyngbya subtilis* JUCHE1, isolated from water bodies of a Coal-fired power plant situated in Sagardighi, Berhampur, West Bengal, was used under the present research study. Modified 18 medium was used as the minimal salt medium for all batch experiments [1]. The unknown Algal sample was identified by Dr. R.K. Gupta (Algologist) Central National Herbarium, Botanical Survey of India, Botanical Garden, Shibpur, Howrah, West Bengal, India. Figure 4.1 represents the photographs of algal biomass cultivation of *Leptolyngbya subtilis* JUCHE1 in the aquarium as well as in 250 ml conical flasks.

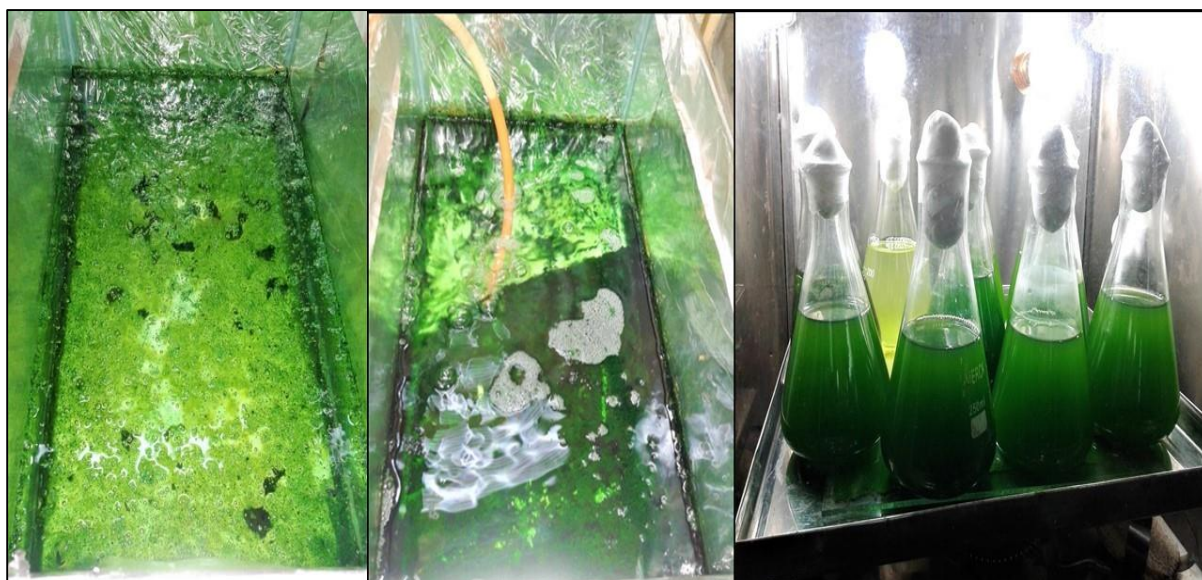


Figure 4.1 CO₂ sparging into the aquarium containing M-18 medium for cultivation *Leptolyngbya subtilis* JUCHE1.

4.1.2 Growth medium

The composition of Modified-18 (M18) is as follows (Basis 1L)[1]:

Table 4.1. Composition of Modified-18 media.

| Serial no. | Components | Quantity (basis- 1L) (g) |
|------------|--------------------------------------|-----------------------------|
| 1 | NaNO ₃ | 1.5 |
| 2 | MgSO _{4.7} H ₂ O | 0.38 |

| Serial no. | Components | Quantity (basis- 1L) (g) |
|------------|----------------------------|-----------------------------|
| 3 | K_2HPO_4 | 0.12 |
| 4 | $CaCl_2 \cdot 2H_2O$ | 0.11 |
| 5 | NaCl | 0.07 |
| 6 | $Fe_2(SO_4)_3 \cdot 4H_2O$ | 0.01 |
| 7 | $Na_2MoO_4 \cdot 2H_2O$ | 0.009 |
| 8 | H_3BO_3 | 0.003 |
| 9 | $MnSO_4 \cdot 4H_2O$ | 0.002 |
| 10 | $ZnSO_4 \cdot 7H_2O$ | 0.0003 |
| 11 | $CuSO_4 \cdot 5H_2O$ | 0.00008 |
| 12 | $CoCl_2 \cdot 6H_2O$ | 0.00004g |

The pH was maintained/ adjusted to 7. The cultures were grown in an incubator at 37°C with a light intensity of 2.5 kLux.

4.1.3 Chemicals

Table 4.2. List of Chemical used in the experimental work and procurement details.

| Inorganic Salts and Solvents | Name of the Company |
|------------------------------|---------------------|
| $NaNO_3$ | Merck, India |
| $MgSO_4 \cdot 7H_2O$ | |
| K_2HPO_4 | |
| $CaCl_2 \cdot 2H_2O$ | |
| NaCl | |
| $Fe_2(SO_4)_3 \cdot 4H_2O$ | |
| $Na_2MoO_4 \cdot 2H_2O$ | |
| H_3BO_3 | |
| $MnSO_4 \cdot 4H_2O$ | |
| $ZnSO_4 \cdot 7H_2O$ | |
| $CuSO_4 \cdot 5H_2O$ | |
| $CoCl_2 \cdot 6H_2O$ | |
| NaOH | |
| Sodium meta periodate | |

| Inorganic Salts and Solvents | Name of the Company |
|------------------------------|---|
| Glycerol Acetic acid | |
| Acetyl acetone | |
| Ammonium acetate | |
| Glycerol | |
| Acetone | |
| Chloroform | CDH (Central Drug House Pvt. Limited), India |
| Methanol | |
| | |

4.1.4 Equipment's and apparatus:

- Digital weighing balance (Sartorius, Germany).
- Digital Lux-meter (LT Lutron LX 101A)
- Digital pH meter (SS AUTOMATIONS 0.01 Ph controller)
- Autoclave (G.B. Enterprises, Kolkata, India)
- Hot air oven (G.B. Enterprises, Kolkata, India)
- B. O. D. incubator (G.B. Enterprises, Kolkata, India)
- Homogenizer (REMI ELEKTROTECHNIK LTD. VASAI-401208, India)
- Micro-Centrifuge (Spinwin, India)
- Laminar air flow chamber (G.B. Enterprises, Kolkata, India)
- Internally -Externally Illuminated Gas-Lift Photobioreactor
- Peristaltic pumps
- Vacuum pump
- Gas sensor
- Pyrolyzer
- Refrigerator (Whirlpool; Corona Deluxe, India)

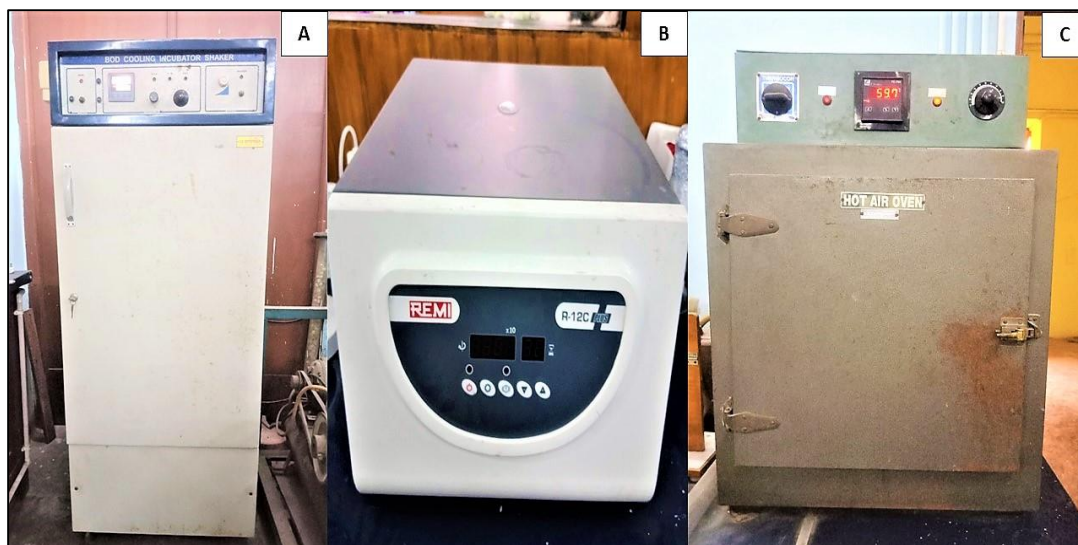


Figure 4.2 Photographs of instruments used in the experimental study: (A) Incubator, (B) Centrifuge, (C) Hot air Oven

4.2. Determination of algal cell mass

The algal sample filtered using muslin cloth was transferred in a petri-dish which is finally placed inside the hot air oven at 100-105 °C for complete removal of moisture from the wet algal biomass [2]. The weight of the dry algal biomass was measured using a digital balance (CPA225D Sartorius AG, Germany). The weight of dry algal biomass is calculated by subtracting the initial weight of the blank petri-dish from the final weight containing dry biomass.

4.3. Analytical Methods

4.3.1. Field Emission Scanning Electron Microscope (FESEM)

The analysis of algal surface morphology was done by conducting FESEM. The algal biomass was washed and dried overnight using a hot air oven at a temperature of 100°C to remove all the unbound moisture content present in the sample. The samples were then thinly coated with gold. The analysis was done using INSPECT F50 at 600-5000x magnification. The analysis was mainly done to observe the surface morphology and the particle size distribution.

4.3.2 CHN analysis

The CHNS elemental analyzer (Perkin Elmer 2400 series II) was used for elemental analysis of dry algal biomass. The analysis was performed by the experts of Indian Association for the Cultivation of Science (IACS) and Jadavpur University, Kolkata.



Figure 4.3 Photograph of Elemental Analyzer (C-H-N-S).

4.3.3 GC-MS analysis

The fatty acid analysis was carried out using GC-MS analyzer (Thermo-Scientific) in TR-WAX column ($30\text{m} \times 0.25\text{mm} \times 0.25\mu\text{m}$). The oven temperature was set at $175\text{ }^{\circ}\text{C}$ for 5 min and then raised to $230\text{ }^{\circ}\text{C}$. The injector and MS detector temperatures were set at $230\text{ }^{\circ}\text{C}$ and $280\text{ }^{\circ}\text{C}$ respectively. Helium was used as a carrier gas. The mass line range was programmed from 25- 800 amu (Mandotra et al. 2014) [2]. The photograph of GC-MS analyzer (Thermo-Scientific) is represented in Figure 4.4



Figure 4.4 Photograph of Gas chromatography mass spectrophotometry (GC-MS)

4.3.4 Lux Meter

The electronic instrument namely Digital Lux meter (LT Lutron LX 101A) was used to measure the light intensities as represented in figure 4.5.



Figure 4.5 Photograph of Lux meter.

4.3.5 pH meter

The electronic pH meter (S.S. AUTOMATIONS, Model no.PH8A, Accuracy: 0.01pH) connected with a pH probe has been used to measure the pH of the algal media during batch study to observe the pH change.



Figure 4.6 Photograph of pH meter.

4.3.6 Spectrophotometric analysis



Figure 4.7 Photograph of Spectrophotometer.

4.3.6.1 Quantification of Glycerol concentration

The glycerol concentrations in the culture medium (M-18) sample was quantified using spectrophotometric analysis as per the protocol suggested by Bondioli et al. (2005) [3]. The spectrophotometric analysis was carried out in UV-Vis spectrophotometer (PerkinElmer). The detailed method is provided below.

4.3.6.2 Detailed method for glycerol determination

Reagents preparation method is as follows: 1.6 M (9.6 g/ 100ml) Acetic acid stock solution, 4.0 M (30.8 g/100 mL) Ammonium acetate stock solution. Both the prepared stocks were mixed in equal proportion by volume and maintained at a pH of 5.5. For preparation of 0.2 M Acetylacetone stock solution 200 μ L (195 mg) of acetylacetone solution was dissolved in a mixture of 5mL acetic acid stock solution and 5mL ammonium acetate stock solution. 10mM Sodium periodate stock solution contained 21 mg of sodium meta periodate which is similarly added in a mixture of 5ml of acetic acid stock solution and 5 ml of ammonium acetate stock solution. These reagents were prepared on regular basis and stored at 0 °C. Finally, the working solvent were prepared by adding equal volumes of distilled water and 95% ethanol. These solvents are used for sample extraction, reaction and pure glycerol reference solutions. Glycerol reference stock solution were prepared using different glycerol concentrations for calibration curve.

4.3.6.3 Preparation of calibration curve

For plotting of calibration curve, different glycerol concentrations of 0.0 g/L, 0.05456 g/L, 0.1091 g/L, 0.16368 g/L, 0.2178 g/L of standard stock solutions were prepared in a 10 ml test tubes. Each standard solution containing different glycerol concentrations were diluted with the working solvent in such a way to get a final volume of 2 ml in each test tube. After dilution, 1.2 ml of 10 mM sodium periodate solution is added and shake for 30 seconds. 1.2 ml of acetylacetone solution is added again and finally put in a water bath at 70 °C for 1 minute. After 1 minute, the test tubes were immediately transferred in a beaker containing tap water for cooling down. Then, the prepared samples were used to measure the absorbance value at 410 nm in a spectrophotometer (UV-VIS PerkinElmer).

4.3.6.6 Sample analysis

As previously mentioned in the procedure for preparation of calibration curve, a similar method has been used for sample preparation. At first, 0.5 ml of sample is transferred in a 10 ml test tube. In similar manner, 1.2 mL of a 10mM sodium periodate solution is added in the test tube and shaken for 30 s. After that, 1.2 ml of 0.2 M acetylacetone solution is added and stirred properly. After mixing, the test tube is immediately placed in a water bath at 70 °C for 1 minute. Finally, after reaction time is over, the sample is cooled by placing the test tube in a beaker containing tap water at ambient temperature. The sample was placed in spectrophotometer to measure the absorbance value at 410nm wavelength.

4.3.7 Quantification of Pigment concentration

The extracted pigments like chlorophyll a, b and carotenoid concentrations of the algal biomass were quantified through spectrophotometric analysis, following the process suggested by Sumanta et al.2014 [4]. The absorbance of the extracted sample was measured in a UV-vis spectrophotometer (PerkinElmer). Further the determination of pigmented concentration was calculated from the equations which has been provided in equations (4.1), (4.2), and (4.3).

For 80% Acetone as solvent for extraction of pigments, the following equations was used to determine the concentration of Chlorophyll a, Chlorophyll b and total carotenoids ($\mu\text{g/mL}$) present in the sample provided below [4,5]:

$$Ch_a = 12.25A_{663.2} - 2.79A_{646.8} \quad (4.1)$$

$$Ch_b = 21.5A_{646.8} - 5.1A_{663.2} \quad (4.2)$$

$$C_{Carotrniod} = \frac{1000A_{470} - 1.82Ch_a - 85.02Ch_b}{198} \quad (4.3)$$

4.4 Elemental analysis of *L.subtilis* JUCHE1

The dry algal biomass weight of 2.056 mg was used in CHN analyser. The moisture content of algal mass was found to be 90% (w/w). The C, H, and N content (% wt) in dry algal mass was found to be 35.03%, 5.75% and 6.69% w/w respectively under photoautotrophic growth. The same has been also provided in a tabulated format. Under photoheterotrophic growth, the C, H, and N content (%w/w) in dry algal mass was determined to be 44.75%, 7.289% and 7.63% respectively.

Table 4.3 Carbon, Hydrogen and Nitrogen contents(%w/w) of algal biomass cultivated under photoautotrophic and photoheterotrophic growth.

| Growth mode | Carbon source | Carbon (%) | Hydrogen (%) | Nitrogen (%) |
|---------------------------|----------------------|-------------------|---------------------|---------------------|
| Photoautotrophic | CO ₂ | 35.03 | 5.75 | 6.69 |
| Photoheterotrophic | Glycerol | 44.75 | 7.289 | 7.63 |

References

1. Pradhan, L., Bhattacharjee, V., Mitra, R., Bhattacharya, I., & Chowdhury, R. (2015). Biosequestration of CO₂ using power plant algae (*Rhizoclonium hieroglyphicum* JUCHE2) in a Flat Plate Photobio-Bubble-Reactor–Experimental and modeling. *Chemical Engineering Journal*, 275, 381-390.
2. Mandotra SK, Kumar P, Suseela MR, Ramteke PW (2014) Fresh water green microalga *Scenedesmus abundans*: a potential feedstock for high quality biodiesel production. *Bioresour Technol* 156:42–47. <https://doi.org/10.1016/j.biortech.2013.12.127>
3. Bondioli P, Della Bella L (2005) An alternative spectrophotometric method for the determination of free glycerol in biodiesel. *Eur J Lipid Sci Technol* 107(3):153–157. <https://doi.org/10.1002/ejlt.200401054>
4. Sumanta, N., Haque, C. I., Nishika, J., & Suprakash, R. (2014). Spectrophotometric analysis of chlorophylls and carotenoids from commonly grown fern species by using various extracting solvents. *Res J Chem Sci*, 2231, 606X.
5. Porra, R. J., Thompson, W. A., & Kriedemann, P. E. (1989). Determination of accurate extinction coefficients and simultaneous equations for assaying chlorophylls a and b extracted with four different solvents: verification of the concentration of chlorophyll standards by atomic absorption spectroscopy. *Biochimica et Biophysica Acta (BBA)-Bioenergetics*, 975(3), 384-394.

Chapter 5

5.1 Theoretical Analysis

5.1.1 Determination of liquid phase CO₂ Concentration under equilibrium

Assuming the validity of Henry's law and the aqueous phase concentration of CO₂ corresponding to different inlet concentration or partial pressure of CO₂ in the inlet air-CO₂ mixture [1].

$$C_{LCO_2}^* = H_{CO_2}^{CP} p_{CO_2} \quad (5.1)$$

Where, $C_{LCO_2}^*$ =Liquid phase concentration of CO₂ under equilibrium, M

p_{CO_2} = Partial pressure of CO₂ in gas phase, kPa

$H_{CO_2}^{CP}$ = Henry's constant for CO₂, moles-L⁻¹/kPa

Temperature dependence of

$$H_{CO_2} = H_{CO_2}^{Ref} \exp \left[\frac{-\Delta H_{SolCO_2}}{R} \left(\frac{1}{T} - \frac{1}{T^{Ref}} \right) \right] \quad (5.2)$$

Here,

$$T^{Ref} = 298K$$

$H_{CO_2}^{Ref}$ = Henry's constant at 298K

From standard table (Sander 2015),

$$H_{CO_2}^{Ref} = 3.3 \times 10^{-4} \text{ M/kPa}$$

$$\frac{-\Delta H_{SolCO_2}}{R} = \frac{d \ln H_{CO_2}}{d \left(\frac{1}{T} \right)} = 2400K \quad (5.3)$$

Using Equation (5) the value of $H_{CO_2}^{310K}$ has been calculated to be 2.448×10^{-4} M/LkPa. The values of equilibrium concentration of CO₂ in aqueous phase, as calculated using Equation 5.1, corresponding to each gas phase concentration in CO₂-air mixture are provided in Table 5.2.

5.1.2 Biomass Production rate

The biomass production rate (P_x) has been defined as follows:

$$P_x = \frac{(m_x(t) - m_{x0})}{t * V_R} \quad (5.4)$$

Where,

$m_x(t)$ = mass of biomass (g) at time, t

m_{x0} = mass of biomass (g) at time, t_0

V_R = liquid volume in the reactor, L

t = culture time, day

5.1.3 Assessment of CO₂ Bio-fixation Rate

The CO₂ fixation rate of *Leptolyngbya subtilis*JUCHE1 was assessed using the experimental data obtained using inlet CO₂ concentration as a parameter (5-20%(v/v)) and at NaNO₃ concentration = 1.5 g/L and I= 2.5kLux. The CO₂ fixation rate (g/L/d) was calculated from the elemental analysis of the biomass, using equation 5.5,

$$R_{CO_2} = C_C \times P_{Biomass} \times \frac{M_{CO_2}}{M_C} \quad (5.5)$$

Where,

R_{CO_2} = CO₂ Biofixation Rate (g/L/d),

C_C is the carbon content (w/w %) in the cell and was calculated from the elemental composition of the cell, $P_{Biomass}$ is biomass productivity (g/L/d), M_{CO_2} is molecular weight (44.01 g/mol) of carbon dioxide and M_C molecular weight of carbon(12.01g/mol) [2].

5.1.4 Determination of the relative molar concentration of Oxygen (O_R)

O_R has been defined in equation 5.6,

$$O_R = \frac{O_f}{O_i} \quad (5.6)$$

Where, O_f = oxygen concentration in head space any time t

O_i = initial oxygen concentration in head space

5.1.5 Specific growth rate

The specific growth rate (μ) can be calculated using equation (5.7),

$$\mu = \frac{1}{C_{x,average}} \frac{dC_x}{dt} \quad (5.7)$$

Where,

C_x = biomass concentration; $C_{x,average}$ = average biomass concentration

$$C_{x,average} = \frac{C_x(t) + C_x(t + \Delta t)}{2} \quad (5.8)$$

5.1.6 Determination of growth kinetic parameters

The Monod type and Haldane type growth models have been used for the uninhibited and substrate inhibited growth respectively. For inhibited growth, power law type equation has been used if Haldane model does not fit [Drapcho]. These are as follows:

Monod Model

$$\mu = \frac{\mu_{max} C_s}{K_s + C_s} \quad (5.9)$$

Where,

μ = Specific growth rate, d^{-1}

C_s = Initial substrate concentration, g/L

The kinetic parameters, namely, μ_{max} and K_s can be determined by making double reciprocal plot, generated by graphing plotting inverse values of μ against inverse of initial substrate concentration.

Haldane Model

$$\mu = \frac{\mu_{max} C_s}{K_s + C_s + \frac{C_s^2}{K_i}} \quad (5.10)$$

Where, μ_{max} is maximum specific growth rate (d^{-1}), C_s is substrate concentration (g/L), K_s is half-saturation constant (g/L) and K_i is substrate inhibition (g/L).

$$C_{Smax} = \sqrt{K_s K_i} \quad (5.11)$$

Where C_{Smax} is maximum substrate concentration (g/L).

As mentioned in section 2.4., the dry cell weight of *Leptolyngbya subtilis* JUCHE1 were measured respectively on daily basis. The specific growth rate (μ) was determined from the slope of the biomass vs time curve during the exponential growth phase. Both Monod and Haldane growth kinetic equations, mentioned above in eq. 5.9, 5.10 and 5.11, have been used to evaluate kinetic parameters (μ_{\max} , K_s , K_I). The following two methods have been followed to determine μ_{\max} , K_s and K_I .

Method I:

In this method the values of μ_{\max} and K_s have been determined using the μ versus C_S data of uninhibited zone to be identified from the analysis of experimental data. Actually, μ_{\max} and K_s have been determined by making double reciprocal plot, generated by graphing the inverse values of μ against inverse of initial substrate concentration in the uninhibited zone. The $C_{S_{\max}}$ is the substrate concentration at which the highest value of μ is obtained experimentally. The value of $C_{S_{\max}}$ has been determined from the plot of μ versus C_S . Afterwards, the value of K_I has been determined using equation 5.11.

Method II:

Based on the highest value of μ , i.e., μ'_{\max} experimentally obtained at $C_{S_{\max}}$, all the values of μ are normalized leading to μ_{norm} , where, $\mu_{norm} = \frac{\mu}{\mu'_{\max}}$. Through non-linear regression of the dataset of μ_{norm} and C_S over the entire substrate concentration regime spanning over uninhibited and inhibited growth using "fitnlm" of MATLAB, K_S and K_I have been determined. The regression has been repeated by adjusting the value of μ'_{\max} in a narrow range around the experimental μ'_{\max} until the Root mean square error (RMSE), represented in Equation 5.1.7.3 is less than 0.02. The final value of μ'_{\max} is considered as μ_{\max} of the Haldane equation. The values of K_S and K_I have been predicted by fitnlm. The program has been provided in the Appendix.

The values of the parameters, μ_{\max} , K_S and K_I of the Haldane model have been determined based on the statistical analysis of error by comparing the experimental values of μ and the predicted ones obtained using Method-I and Method-II at all values of C_S over the entire of substrate concentration regime.

Power Law Model

$$\mu = \mu_{without\ inhibition} \left(1 - \frac{C_S}{C_{S,crit}}\right)^n \quad (5.12)$$

Where, $C_{S,crit}$ is the concentration of substrate at which there is almost no growth.

5.1.7 Mathematical models for Algal growth

5.1.7.1 Dependence on CO₂ and NaNO₃

Monod type model has been attempted to explain the growth kinetics of the cyanobacteria with respect to NaNO₃. The validity of Monod model has been assessed by the verification of the linearity of the double reciprocal plot generated by graphing the inverse values of specific growth rate and substrate concentration (NaNO₃) as ordinate and abscissa respectively.

5.1.7.2 Dependence on Light Intensity

Three different models, namely, those recommended by Aiba, Steele and Bernard and Remond have been used to explain the dependence of growth on light intensity. The specific growth rate (μ), obtained from the experiments described in the sub-section **6.1.1.5 (Chapter 6)** at any particular value of light intensity ($1.45\text{kLux} \leq I \leq 3.2\text{kLux}$) has been normalized by that obtained at optimum light intensity. The regression analysis using all the three model equations have been conducted to correlate the normalized value of specific growth rate

$\mu_{Norm,I} \left(= \frac{\mu}{\mu_{Optimum,I}} \right)$ with light intensity. The fittest model has been chosen through the comparison between the simulated and experimental results using statistical analysis. For both Bernard and Remond model and Aiba model, the kinetic parameters have been determined by regression analysis using the "**fitnlm**" function of MATLAB software version R2016a. In case of Steele Model, the values of " μ " at different light intensities and the R^2 have been calculated from MATLAB software version R2016a.

The model equations used to correlate specific growth rate with light intensity are as follows:

Aiba model,

$$\mu_{Norm,I} = \frac{I}{K_{S,I} + I + \frac{I^2}{K_{I,I}}} \quad (5.13)$$

Steele model,

$$\mu_{Norm,I} = \frac{I}{I_{Optimum}} \exp\left(1 - \frac{I}{I_{Optimum}}\right) \quad (5.14)$$

Bernard and Remond model,

$$\mu_{Norm,I} = \frac{I}{I + \left(\frac{\mu_{max,I}}{\alpha}\right) \times \left(\frac{I}{I_{Optimum}} - 1\right)^2} \quad (5.15)$$

5.1.7.3 Multi-Variate (CO₂-NaNO₃-I) Kinetics

A kinetic model has also been developed to represent the growth rate as a function of concentrations of CO₂ and NaNO₃ and light intensity simultaneously. This has been performed by introducing two correction factors, namely f_{NaNO_3} and f_I in the original Monod equation using CO₂ as substrate. The parameters of the Monod equation have been determined using the growth data of experiments, described in sub-section 6.1.1.6 of chapter 6. The factors, f_{NaNO_3} and f_I account for the variation of NaNO₃ concentration (1-2.5 g/L) and light intensity (1.45 to 3.2 kLux) respectively. Therefore,

$$\mu = f(C_{CO_2}, C_{NaNO_3}, I) = \frac{\mu_{max,CO_2} C_{CO_2}}{k_{s,CO_2} + C_{CO_2}} * f_{NaNO_3} * f_I \quad (5.16)$$

At any particular CO₂ concentration and at the optimum value of light intensity (= $I_{Optimum}$), the experimental value of f_{NaNO_3} has been calculated by normalizing the specific growth rate at any particular value of NaNO₃ concentration ($1g/L \leq C_{NaNO_3} \leq 2.5g/L$) by that obtained at the optimum value of C_{NaNO_3} (= $C_{Optimum NaNO_3}$). The correction factor is a function of the concentration of C_{NaNO_3} . Analogous to the form of Monod equation, the Langmuir-Hinshelwood type functionality is chosen. Therefore, the correction factor for the variation of NaNO₃ is as follows:

$$f_{NaNO_3} = \frac{\alpha_1 \times C_{NaNO_3}}{\beta_1 + C_{NaNO_3}} \quad (5.17)$$

Similarly, at any particular CO₂ concentration and optimum value of C_{NaNO_3} , the experimental value of f_I has been calculated by normalizing the specific growth rate at any particular value of light intensity ($1.45kLux \leq I \leq 3.2kLux$) by that obtained at the optimum value of I

($I_{Optimum}$). Significance of f_I is analogous to that of $\mu_{Norm,I}$. The functionality, similar to the best suited model equation correlating $\mu_{Norm,I}$ with I , has been chosen to represent the dependence of f_I with I . Therefore, the correction factor equation for light intensity is as follows,

$$f_I = \frac{I}{I_{Optimum}} \times \exp\left(1 - \frac{I}{I_{Optimum}}\right) \quad (5.18)$$

Therefore, by incorporating the correction factors, namely, f_{NaNO_3} and f_I in terms of C_{NaNO_3} and I (Eq. s 5.17 and 5.18), the Equation 5.16, 5.17 and 5.18 reduces to the following form:

$$\mu = \frac{\mu_{max,CO_2} C_{CO_2}}{k_{s,CO_2} + C_{CO_2}} \times \frac{\alpha_1 \times C_{NaNO_3}}{\beta_1 + C_{NaNO_3}} \times \left(\frac{I}{I_{Optimum}} \times \exp\left(1 - \frac{I}{I_{Optimum}}\right)\right) \quad (5.19)$$

By regression analyses, the values of μ_{max,CO_2} , k_{s,CO_2} , $\mu_{max,NaNO_3}$, $k_{s,NaNO_3}$, $K_{S,I}$, $K_{I,I}$, $\mu_{max,I}$, α , α_1 and β_1 have been determined and have been provided in Table 6.18 of section 6.5.1.6 (Chapter 6).

5.1.7.4 Statistical analysis

To compare the experimental data with the simulated ones using different growth models, statistical parameters such as the root-mean-square error (RMSE), bias factor (BF) and standard error of prediction % SEP have been determined to select the best fitted model [3]. The statistical equations are mentioned below [3]:

Root mean square error (RMSE):

$$RMSE = \sqrt{\frac{\sum_{i=1}^n (pd_i - ob_i)^2}{n - k}} \quad (5.20)$$

Standard error of prediction (%SEP):

$$\%SEP = \frac{100}{mean(obs)} \sqrt{\frac{\sum (Obs - Pred)^2}{n}} \quad (5.21)$$

Bias factor (Bf):

$$B_f = 10 \sum_{i=1}^n \log(pd_i - ob_i) / n \quad (5.22)$$

Where,

p_{di} = predicted values,

o_{bi} = observed experimental values,

n = number of runs

5.1.8 Response surface methodology (RSM)

The aim of response surface methodology (RSM) is to optimize the output response and also to determine the optimum values of input variables [4]. Response surface design employs second-order model and is symmetrical. Box–Behnken design (BBD) of RSM represents second order design and is a mathematical technique to formulate different sets of experimental designs, develop 3-D models and evaluate the effect of input variables on output response variables. The maximum and minimum values of input variables are designated as +1 and –1 levels respectively. The design ensures spherical experimental domain. The number of design points increases at the same rate as the number of polynomial coefficients when the spherical arrangement of BBD levels is followed. The number of experiments (N) is defined as follows:

$$N = 2k(k - 1) + C_0 \quad (5.23)$$

Where, k = number of variables ; C_0 = number of centrepoints

Evaluation of fitness of predictive model with the experimental values of output responses is conducted by ANOVA (Analysis of variables).

Using Design Expert 13.0.5 software, BBD has been used to correlate the effects of input variables, namely, substrate concentrations (CO_2 , $NaNO_3$ as carbon and nitrogen source) and light intensity (I) with the output response, i.e. specific growth rate “ μ ”. Under this study, a second order polynomial response surface model have been attempted and the equation (5.24) is expressed below:

$$\mu = A_0 + A_1X_1 + A_2X_2 + A_3X_3 + A_{12}X_1X_2 + A_{13}X_1X_3 + A_{23}X_2X_3 + A_{11}X_1^2 + A_{11}X_1^2 + A_{22}X_2^2 + A_{33}X_3^2 \quad (5.24)$$

Where, $X_1 = C_{CO_2}$; $X_2 = C_{NaNO_3}$; $X_3 = I$

5.1.9 Determination of equivalent glycerol concentration against each gas phase concentration of CO₂

Growth medium for photoheterotrophic growth was prepared by supplementing M18 medium with glycerol instead of CO₂ as carbon source. The values of concentrations of glycerol were maintained at levels to supply equal number of gram atoms of carbon which was available in the aqueous phase corresponding to different gas phase concentration (5-20%) of CO₂, as used in photoheterotrophic growth. Equivalent glycerol concentration against each gas phase concentration of CO₂ has been calculated using the following equation

$$C_{gly} = \frac{p_{CO_2} \times H_{CO_2}^{CP} \times n_{C_{CO_2}}}{n_{C_{gly}}} \quad (5.25)$$

C_{gly} = Glycerol concentration, M

$n_{C_{gly}}$ = Number of g. atom of carbon in mol gly

$n_{C_{CO_2}}$ = Number of g. atom of carbon in mol CO₂

p_{CO_2} = Partial pressure of CO₂ in gas phase, kPa

$H_{CO_2}^{CP}$ = Henry's constant for CO₂, M/kPa

The values of C_{gly} was maintained for substitution of C , available at different gas phase concentration (5-20%) of CO₂ used under the present study. Volume of glycerol (V_{gly}) required for 1L photoheterotrophic solution (glycerol supplemented M-18) was as follows,

$$V_{gly} = C_{gly} \times \frac{MW_{gly}}{\rho_{gly}} \quad (5.26)$$

MW_{gly} = Molecular weight of glycerol

ρ_{gly} = Density of glycerol (g/mL)

5.1.9.1 Conversion of Glycerol

Conversion of glycerol at each culture time has been determined using the following equation:

$$X_{Gly} = \frac{(C_{Gly}(t) - C_{Gly0})}{C_{Gly0}} \quad (5.26)$$

Where,

X_{Gly} = conversion of glycerol,

$C_{Gly}(t)$ =glycerol concentration at any culture time, t;

C_{Gly0} = initial glycerol concentration

5.1.10 Carbon capture

The carbon capture (%) (CC) through biomass generation has been determined using the following equation:

$$CC = \frac{\text{g-atom of carbon present in algal mass produced at any time}}{\text{g-atom of carbon supplied through CO}_2 \text{ or glycerol}} * 100 \quad (5.27)$$

Or

$$CC = \frac{C_x(t)*(1-MC)*x_C*100}{AW_C*\text{g-atom of carbon supplied through CO}_2 \text{ or glycerol /L using Table 6.3}} \quad (5.28)$$

Where,

$C_x(t)$ = concentration of biomass (g) at time, t

MC = weight fraction of moisture in algal mass;

x_C = weight fraction of carbon in dry algal mass;

AW_C =atomic weight of carbon=12

5.1.11 Estimation of Lipid content

The lipid content of algal mass was determined using the following equation:

$$\text{Lipid content (\% w/w) (LC)} = \frac{L_f - L_i}{X} \times 100 \quad (5.29)$$

Where,

L_f is mass of empty beaker + extracted lipid (g),

L_i is mass of empty beaker (g),

X is weight of algal mass from which the lipid is extracted.

5.1.11.1 Lipid production rate (P_L) has been determined as follows:

$$P_L = \frac{P_x(t) \times (1 - MC) \times LC}{100} \quad (5.30)$$

5.1.12 Calculation of content of extracted Pigment

The following equations for the respective solvents have been used to determine the content(%w/w) of Chlorophyll a, Chlorophyll b and total carotenoid present in the sample [5,6]:

$$\text{Chlorophyll content, } P_{\text{Chl}} = \frac{C_{\text{Chl}}}{C_x} \times 100 \quad (5.31)$$

$$\text{Carotenoid content, } P_{\text{Carotenoid}} = \frac{C_{\text{Carotenoid}}}{C_x} \times 100 \quad (5.32)$$

Whereas,

P_{Chl} and $P_{\text{Carotenoid}}$ are pigment content of chlorophyll and carotenoid (% w/w)

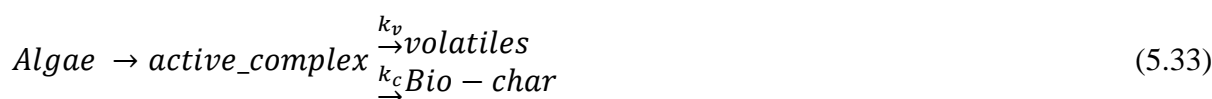
C_{Chla} is chlorophyll concentration ($\mu\text{g/mL}$)

$C_{\text{Carotenoid}}$ is carotenoid concentration ($\mu\text{g/mL}$) and

C_x is weight of biomass at time t

5.1.13 Lumped Kinetics Pyrolysis of Algal biomass

Under the present investigation, a parallel reaction model has been described to evaluate the parameters of pyrolysis kinetics of algae. It has been considered that homogeneous solid phase reaction occurs and products have been lumped as solid product (char) and volatiles (oil and gas).



$$\frac{dW}{dt} = -(k_c + k_v)W = -kW \quad (5.34)$$

$$\frac{dW_c}{dt} = k_c W \quad (5.35)$$

$$\frac{dW_v}{dt} = k_v W \quad (5.36)$$

Where, W , W_v , W_c are the values of dimensionless mass of pyrolysing algal mass, volatile v and W_c product and char, which can be described as follows:

$$W = \frac{\text{Actual mass of pyrolysing algal biomass}}{\text{Initial mass of algal biomass fed to the reactor}} \quad (5.37)$$

$$W_v = \frac{\text{Actual mass of volatile product of pyrolysis}}{\text{Initial mass of algal biomass fed to the reactor}} \quad (5.38)$$

$$W_c = \frac{\text{Actual mass of char from pyrolysis}}{\text{Initial mass of algal biomass fed to the reactor}} \quad (5.39)$$

$$k = k_c + k_v \quad (5.40)$$

Where k , k_v are the overall rate constant, rate constant of formation of volatiles and rate v k_c constant of formation of char respectively.

The values of rate constants k , k_v at different temperatures are determined using integral method of analysis. On integration from $t=0$ to t , the equations (5.34), (5.35) and (5.36), reduce to equations (5.43), (5.44) and (5.45) with the following boundary conditions:

$$\text{At } t = 0, \langle W_c = W_{c0} = 0 \rangle \quad (5.41)$$

$$\text{At } t = t, \langle W_c = W_c \rangle \quad (5.42)$$

$$(t) = \exp(-kt) \quad (5.43)$$

$$W_v(t) = \left(\frac{k_v}{k}\right)[1 - \exp(-kt)] \quad (5.44)$$

$$W_c(t) = \left(\frac{k_c}{k}\right)[1 - \exp(-kt)] \quad (5.45)$$

5.1.13.1 Determination of overall rate constants (k , k_v) at different temperatures

The validity of the first order rate kinetics of overall decomposition reaction has been checked by the linearity of graph($\ln(W)$ versus t (min)) in Figure 9.6. The overall rate constants (k) at different temperatures (300 °C; 500 °C and 700 °C) have been determined from the slope of the graph($\ln(W)$ versus t (min)), as shown in the Figure 9.5. The validity of the first order rate kinetics of volatile production has been checked by the linearity of graph(W_v) versus $t [1 - \exp(-kt)]$, plotted in in Figure 9.7. The rate constants of formation of volatiles (k_v) at different temperatures (300 °C; 500 °C and 700 °C) have been

determined from the slope. The Values of the rate constants of formation of volatiles (k_v) at 300°C; 500 °C and 700 °C have been reported in Table 9.7.

5.1.13.2 Activation energies and pre-exponential factors

Assumption:

The rate constants follow Arrhenius equation with respect to the dependence on temperature.

The Arrhenius equation is as follows:

$$k_i = k_o \exp\left(\frac{-E_i}{RT}\right) \quad (5.46)$$

k_i = rate constant ; k_o = pre – exponential factor ; E_A = Activation energy

The values of activation energies and pre-exponential factors, determined by plotting the natural logarithm of each rate constant, $\ln(k_i)$ against the inverse of temperature in kelvin, $\frac{1}{T}$, shown in the Figure 9.7 (where $k_i = k$ or k_v or k_c).

5.1.13.3 Determination of Pyrolysis Products

5.1.13.3.1 Volatiles

The mass of volatiles at any pyrolysis time has been obtained by subtracting the mass of solid residue from initial algal mass. The values of dimensionless mass of volatile products has been calculated using equation 5.38. Therefore, At any time t, using equations 5.34,5.35 and 5.36,

$$W_v(t) = W_o - W_R(t) \quad (5.47)$$

5.1.13.3.2 Pyro-oil

The mass of pyro-oil at any pyrolysis time has been determined from that of the condensed mass of volatiles, collected at that time. Thus the dimensionless mass of pyro oil, $W_1(t)$ can be obtained as follows:

$$W_1(t) = \frac{\text{Mass of condensable volatiles}}{\text{Initial mass of algal biomass fed to the reactor}} \quad (5.48)$$

5.1.13.3.3 Pyro-gas

The mass of pyro-gas at any pyrolysis time has been determined by subtracting the mass of pyro-oil from that of volatiles generated at that time. Thus the dimensionless mass of pyro gas,

$W_g(t)$ can be obtained as follows:

$$W_g(t) = \frac{\text{Mass of non-condensable volatiles, i.e pyro-gas}}{\text{Initial mass of algal biomass fed to the reactor}} \quad (5.49)$$

5.1.13.3.4 Pyro-char and unreacted algal mass

Actually, the residual solid left over after devolatilization during pyrolysis of biomass is a mixture of the unreacted feedstock and the char, formed as a pyro-product. As the char is inseparable from the unconverted biomass, the mass of char is indirectly calculated [7,8,9].

At any time, t , using equations 5.34, 5.35 and 5.36,

$$\frac{W_v(t)}{W_c(t)} = \frac{k_v}{k_c} \quad (5.50)$$

As the reaction can be assumed to go to completion at this time it can be defined as infinite time, $t \rightarrow \infty$. Therefore, the solid residue at $t \rightarrow \infty$. can be assumed to be formed of char only, i.e., $W_R(t \rightarrow \infty) = W_C(t \rightarrow \infty)$. Since equation (5.50) is valid at each time,

$$\frac{W_v(t \rightarrow \infty)}{W_R(t \rightarrow \infty)} = \frac{W_v(t \rightarrow \infty)}{W_C(t \rightarrow \infty)} = \frac{k_v}{k_c} = \frac{W_v(t)}{W_c(t)} \quad (5.51)$$

The value of $\frac{W_v(t \rightarrow \infty)}{W_c(t \rightarrow \infty)}$ has been determined using the experimental data obtained at different reaction temperature. At any time, t , the dimensionless mass of char is calculated using the following equation:

$$w_c(t) = \frac{w_R(t \rightarrow \infty)}{w_v(t \rightarrow \infty)} \times w_v(t) \quad (5.52)$$

where, $w_R(t \rightarrow \infty)$ is the dimensionless mass of solid residue left at a long pyrolysis time where there is no further change of mass of residue.

Table 5.1 The experimental values of $\frac{w_R(t \rightarrow \infty)}{w_v(t \rightarrow \infty)}$ at different reaction temperatures are as follows:

| T (°C) | 300 | 500 | 700 |
|---|------|-------|-------|
| $\frac{W_R(t \rightarrow \infty)}{W_V(t \rightarrow \infty)}$ | 0.42 | 0.149 | 0.077 |

Using the equation (5.52), the values of the dimensionless mass of char. The value of the dimensionless mass of unreacted alga (W) at any reaction time, t , was calculated as follows:

$$W(t) = W_R(t) - W_C(t) \quad (5.53)$$

To test the validity of the assumed first order kinetics, the linearity of the plot of $\ln(W)$ against t was verified. The value of the kinetic rate constant, k was determined from the slope of the straight line. Similarly, the linearity of the logarithmic plots of W_v each against $(1 - \exp(-kt))$ were verified and the value of k_v was determined.

References

1. Sander, R. (2015). Compilation of Henry's law constants (version 4.0) for water as solvent. *Atmospheric Chemistry and Physics*, 15(8), 4399-4981.
2. Kassim, M. A., & Meng, T. K. (2017). Carbon dioxide (CO₂) biofixation by microalgae and its potential for biorefinery and biofuel production. *Science of the total environment*, 584, 1121-1129.
3. Lacerda LMCF, M. I. Queiroz, L. T. Furlan, M. J. Lauro, K. Modenesi, E. Jacob-Lopes, T.T. Franco. 2011 "Improving refinery wastewater for microalgal biomass production and CO₂ biofixation: Predictive modeling and simulation". *Journal of petroleum science and engineering* 78.3-4: 679-686. <https://doi.org/10.1016/j.petrol.2011.07.003>
4. Verma, R., Kumari, K. K., Srivastava, A., & Kumar, A. (2020). Photoautotrophic, mixotrophic, and heterotrophic culture media optimization for enhanced microalgae production. *Journal of Environmental Chemical Engineering*, 8(5), 104149.
5. Sumanta, N., Haque, C. I., Nishika, J., & Suprakash, R. (2014). Spectrophotometric analysis of chlorophylls and carotenoids from commonly grown fern species by using various extracting solvents. *Res J Chem Sci*, 2231, 606X.
6. Porra, R. J., Thompson, W. A., & Kriedemann, P. E. (1989). Determination of accurate extinction coefficients and simultaneous equations for assaying chlorophylls a and b extracted with four different solvents: verification of the concentration of chlorophyll standards by atomic absorption spectroscopy. *Biochimica et Biophysica Acta (BBA)-Bioenergetics*, 975(3), 384-394.
7. Ghosh, S., Das, S., & Chowdhury, R. (2019). Effect of pre-pyrolysis biotreatment of banana pseudo-stem (BPS) using synergistic microbial consortium: role in deoxygenation and enhancement of yield of pyro-oil. *Energy Conversion and Management*, 195, 114-124.
8. Sarkar, A., & Chowdhury, R. (2016). Co-pyrolysis of paper waste and mustard press cake in a semi-batch pyrolyzer—optimization and bio-oil characterization. *International Journal of Green Energy*, 13(4), 373-382.
9. Poddar, S., De, S., & Chowdhury, R. (2015). Catalytic pyrolysis of lignocellulosic bio-packaging (jute) waste—kinetics using lumped and DAE (distributed activation energy) models and pyro-oil characterization. *RSC advances*, 5(120), 98934-98945.

Chapter 6

Growth Performance of isolated blue green alga under photoautotrophic (CO₂)-photoheterotrophic(Glycerol)-photo-mixotrophic(CO₂+Glycerol) conditions

Algae follow several mechanisms for production of biomass as well as lipid and can be grown under different metabolic modes: (i) photo-autotrophic (with light energy and inorganic carbon source e.g., CO₂, Na₂CO₃, NaHCO₃ etc.); (ii) photo-heterotrophic growth (with light energy and organic carbon source e.g., glucose, glycerol etc.) (iii) Mixotrophic mode (with light energy and carbon sources of both organic and inorganic ones) [1,2]. Heterotrophic growth of different algae has also been reported in absence of light under dark condition [3]. For the industrial application of any alga, it is important to understand its performance under these conditions. This chapter is focused on the investigation and analysis of the performance of the isolated blue green alga, under photoautotrophic, photoheterotrophic(Glycerol) and photo-mixotrophic (CO₂+Glycerol) conditions.

6.1 Growth under photoautotrophic condition

Under photoautotrophic condition, CO₂ was used as the carbon substrate for the isolated blue-green alga, *Leptolyngbya subtilis JUCHE1*. The following objectives, described under Aim 2 in Chapter 3, are addressed in this chapter:

- Determination of CO₂ fixation rate
- Determination of growth kinetics of isolated blue green alga by varying inlet-CO₂ concentrations
- Determination of growth kinetics of isolated blue green alga by varying initial concentrations of nitrogen source (NaNO₃)
- Determination of growth kinetics of isolated blue green alga by varying light intensity
- Determination of growth kinetics of isolated blue green alga by simultaneously varying inlet-CO₂ concentrations, initial concentrations of nitrogen source and light intensity

6.1.1 Experimental

6.1.1.1 Maintenance and Growth Culture medium

The CO₂- substituted maintenance medium was prepared by bubbling pure CO₂ into M18 medium for 10 h. The algal strain was maintained in this medium under constant illumination of 2.5 kLux at 37°C. Culture medium for experiments with varying CO₂ concentration was

prepared by bubbling M18 medium with CO₂-Air mixture having different partial pressure of CO₂ for 10 h. The values of equilibrium concentration of CO₂ in the aqueous phase were determined using Henry's law [4]. After the bubbling of air- CO₂ mixture (5-20% CO₂) through M18 medium for 20h, pH of the was measured. The values of pH after 20h of bubbling have been provided in Table 1 to investigate the effect of CO₂ bubbling on medium pH.

6.1.1.2 Experimental setup

All the experiments were conducted in small-scale bioreactors developed by attaching different accessories to 250 ml Erlenmeyer conical flasks. Conventionally, Photobioreactors have built-in arrangements made for the control of pH, temperature, gas flow rate and adjustment of light intensity. Under this study, individual bioreactor consisted of outlet channels at the bottom of the conical flask for withdrawal of liquid samples. To maintain the specific concentration of CO₂: Air ratio (v/v) at the head space of the bioreactor, two gas exchange tubes were used as inlet and outlets at the top. The pH was also monitored by making sampling arrangement from the flasks. After inoculation, the culture flasks were placed inside the incubator having light arrangements and temperature controllers.

6.1.1.3 Batch experiments for CO₂ as substrate under Photoautotrophic growth mode

Conical flasks of 250 ml capacity were used as algal bioreactors. The working volume was maintained at 150 ml for all the experiments. Each bioreactor was equipped with two glass tubes; one for transfer of inoculum and another for gas transfer. An outlet was also provided at the bottom of the conical flask as shown in Figure 6.1. At first, the bioreactors were filled to the brim with minimal salt medium (M18). Air-CO₂ mixture having different concentration of (5-20% v/v) CO₂ was subsequently introduced in the conical flask by displacement of M18 medium through the gas transfer tube. Algal mass weighing 1g (Equivalent to 0.1 g dry mass) was introduced into the inoculation tube and an injection vial containing M18 medium was held above it. Algal inoculum was ultimately transferred to the flask by pushing the M18 medium using the movement of the piston of the injection vial. Algal growth in culture medium having saturated liquid phase concentration of CO₂ against each gas phase concentration 5-20% (v/v) was conducted for different time periods up to 4 days. For each gas phase concentration (5-20%) of CO₂, four sets of experiments were conducted for 1,2,3, and 4 days. Constant illumination of 2.5 kLux and temperature of 37°C were maintained during all growth experiments. Each growth medium was analyzed for biomass concentration and the corresponding lipid content at 24h interval. The pigment content was also determined at the

condition where the biomass concentration reached the maximum. The protocols for the extraction of lipid and pigment have been described in Chapter 7. After respective interval of 24 hours the algal biomass was filtered using muslin cloth and was subsequently dried overnight at 100-105 °C inside the hot air oven as recommended in literature [5]. The algal biomass was dried overnight until the moisture was removed completely. Finally, the weight of the dry algal biomass was determined. The dry biomass was also analysed by CHNS analyser.



Figure 6.1. Small scale bioreactor set up for batch experiments under Photoautotrophic growth mode.

6.1.1.4 Batch studies for Growth kinetics on Nitrogen Substrate

The batch study to assess the influence of nitrogen substrate (NaNO_3) was conducted in 100 ml Erlenmeyer conical flasks with 60 ml working volume as shown in Figure 6.2. The batch experiments were performed by the variation of initial NaNO_3 concentrations from 1-2.5 g/L. Culture period was varied from 0-5 days. For each NaNO_3 concentration, separate flasks were used to allow different culture periods. The values of CO_2 concentration and the light intensity were maintained at 15% (v/v) and 2.5 kLux ($33.75 \mu\text{mol}/\text{m}^2/\text{s}$) as maximum productivity of biomass was obtained corresponding to these values during previous studies meant for the observation of influence of CO_2 on the growth of the cyanobacteria. At first, 0.4 g of wet cyanobacterial biomass was inoculated in the culture media and the headspace of the conical flasks was continuously sparged with 15% CO_2 -85% air mixture at a flowrate of 1 LPM. The batch reactors (Erlenmeyer flasks) were placed inside the incubator at 37 °C. The light intensity of 2.5 kLux ($33.75 \mu\text{mol}/\text{m}^2/\text{s}$) of light intensity was provided by white fluorescent lamps. After

an interval of 24 hours of batch culture, the algal biomass was determined. The protocol for the extraction of lipid has been described in Chapter 7.



Figure 6.2 Experimental set-up of the batch study for 0-5 days at different concentrations of NaNO_3 as nitrogen substrate

6.1.1.5 Determination of dependence of Growth kinetics on Light Intensity

The experiments were performed by varying light intensities in a range of 1.45 to 3.2 kLux ($19.57\text{-}43.2 \mu\text{mol}/\text{m}^2/\text{s}$). 1g of wet algal inoculum was introduced into 150 ml of culture media (M-18) as working volume. For the batch study 250 ml of Erlenmeyer conical flasks were used to conduct the experiment. For each light intensity, the flasks were purged at the beginning with 15% CO_2 -85% (v/v) air mixture. The initial concentration of NaNO_3 of 1.5 g/L was used for each experiment. The culture and analysis protocols were the same as those used in case of variation of carbon and nitrogen substrates. The protocol for the extraction of lipid has been described in Chapter 7.

6.1.1.6 Dependence of Growth simultaneously on CO_2 - NaNO_3 -I

For the determination of multi-parameter growth kinetics two sets of experiments were conducted at each gas phase inlet CO_2 concentration (v/v) i.e., 5%, 10%, 15% and 20%. According to Henry's law, the values of the equilibrium aqueous phase CO_2 concentrations corresponding to inlet gas phase CO_2 level of 5, 10, 12.5, 15 and 20%(v/v) are 0.5456, 0.10912, 0.13618, 0.16368 and 0.2178 g/L respectively. In one set of experiments, the values of NaNO_3 concentration were varied ($1\text{g}/\text{L} \leq C_{\text{NaNO}_3} \leq 2.5\text{g}/\text{L}$) maintaining the value of light intensity at optimum level (I_{Optimum}). In another one, the values of I was changed ($1.45\text{kLux} \leq I \leq 3.2\text{kLux}$) and the concentration of NaNO_3 was kept at the optimum value (

$C_{Optimum NaNO_3}$). The experimental data were used to calculate the correction factors, f_{NaNO_3} and f_I , as described in equations 5.16 and 5.17 with respect to the growth at the optimum values of $NaNO_3$ concentration and I respectively. Finally, the specific growth rate was correlated to CO_2 , $NaNO_3$ and I simultaneously using the correction factors (equation 5.18).

6.1.1.7 Experimental Design

Box–Behnken method of response surface methodology (RSM) in Design Expert 13.0.5 software has been used to determine the multi-variable functionality of the specific growth rate on the substrate concentrations (CO_2 , $NaNO_3$ as carbon and nitrogen source) and light intensities. Accordingly, a set of seventeen experiments were performed using three numerical factors such as A: CO_2 concentrations (g/L), B: $NaNO_3$ concentrations (g/L) and C: light intensities (kLux). As the present study investigates the dependence of the output response, i.e., specific growth rate μ (d^{-1}) on the coded input variables, A, B and C the values of these parameters have been varied to study the effect on algal growth rate, $\mu(d^{-1})$. However, to design the experiment the lower and the upper limits of values of these numerical factors are provided in Table 6.1. The values of 17 sets of coded variables of experiments which has been designed by Box-Behnken method are tabulated in Table 6.2.

Table 6.1 Lower and Upper limits of values of input variables (A: CO_2 concentrations (g/L), B: $NaNO_3$ concentrations (g/L) and C: light intensities (kLux).

| Parameters | Numerical factor | Unit | Lower limit | Upper limit |
|-----------------|------------------|------|-------------|-------------|
| CO_2 | A | g/L | 0.05 | 0.22 |
| $NaNO_3$ | B | g/L | 1 | 2.5 |
| Light intensity | C | kLux | 1.45 | 3.2 |

Table 6.2 The values of coded variables in the seventeen sets of experiments, designed using Box-Behnken method.

| Run | A (CO ₂ Concentrations (g/L) | B NaNO ₃ Concentrations (g/L) | C Light intensity (kLux) | X ₁ (g/L) | X ₂ (g/L) | X ₃ (kLux) |
|-----|--|---|-----------------------------------|-------------------------|-------------------------|--------------------------|
| 1 | 0.13618 | 2.5 | 3.2 | 0 | 1 | 1 |
| 2 | 0.2178 | 2.5 | 2.325 | 1 | 1 | 0 |
| 3 | 0.13618 | 1.75 | 2.325 | 0 | 0 | 0 |
| 4 | 0.05456 | 1.75 | 3.2 | -1 | 0 | 1 |
| 5 | 0.2178 | 1.75 | 1.45 | 1 | 0 | -1 |
| 6 | 0.2178 | 1 | 2.325 | 1 | -1 | 0 |
| 7 | 0.13618 | 1.75 | 2.325 | 0 | 0 | 0 |
| 8 | 0.05456 | 2.5 | 2.325 | -1 | 1 | 0 |
| 9 | 0.13618 | 1.75 | 2.325 | 0 | 0 | 0 |
| 10 | 0.13618 | 1 | 3.2 | 0 | -1 | 1 |
| 11 | 0.05456 | 1.75 | 1.45 | -1 | 0 | -1 |
| 12 | 0.13618 | 1 | 1.45 | 0 | -1 | -1 |
| 13 | 0.13618 | 1.75 | 2.325 | 0 | 0 | 0 |
| 14 | 0.05456 | 1 | 2.325 | -1 | -1 | 0 |
| 15 | 0.13618 | 2.5 | 1.45 | 0 | 1 | -1 |
| 16 | 0.13618 | 1.75 | 2.325 | 0 | 0 | 0 |
| 17 | 0.2178 | 1.75 | 3.2 | 1 | 0 | 1 |

Note: Factorial points: -1 (low level value), +1 (high level value); 0 (center point).

The regression analysis has been conducted by using analysis of variance (ANOVA), as reported in most of the literatures [6, 7]. The second order quadratic model equation has also been obtained to study the effect of carbon concentrations (CO_2), nitrogen concentrations (NaNO_3) and light intensities on response variable, μ (d^{-1}).

6.2 Growth under Photoheterotrophic condition

Under photoheterotrophic condition, glycerol was used as the carbon substrate for the isolated blue-green alga, *Leptolyngbya subtilis JUCHE1*. The following objective, described under Aim 3 in Chapter 3, is addressed in this chapter:

- Determination of growth kinetics using glycerol as organic carbon source

6.2.1 Experimental

6.2.1.1 Maintenance and Growth Culture medium

The glycerol substituted maintenance medium was prepared by adding an amount of glycerol which could substitute C-mole available from an aqueous M18 medium saturated with pure CO_2 . The algal strain was maintained in this medium under constant illumination of 2.5 kLux ($33.75 \mu\text{mol}/\text{m}^2/\text{s}$) at 37°C .

6.2.1.2 Batch experiments under Photoheterotrophic condition

The culture tubes of 60ml capacity were filled with 30 ml glycerol supplemented M-18 medium as shown in Figure 6.3. For batch studies, different initial amount of glycerol was added to M-18 medium so that C-equivalence with M-18 medium saturated with air- CO_2 mixture of different CO_2 concentration (5-20% v/v), used under photoautotrophic condition, could be maintained. The equation (5.25) has been used for the calculation of amount of glycerol for maintaining C-equivalence. The values of concentration of glycerol, C_{gly} used for different CO_2 concentration in inlet gas used under photoautotrophic condition (5-20% v/v) have been provided in Table 6.3. 0.2 g of wet algal biomass was inoculated in each of the tubes. The remaining headspace was sparged with argon to remove any trace of carbon dioxide and other gases present in the headspace. The tubes were closed using caps and sealed with parafilm. The tubes were then carefully placed as slants inside an incubator and incubated at 37°C for duration up to 4 days under illumination of 2.5 kLux ($33.75 \mu\text{mol}/\text{m}^2/\text{s}$). For each concentration of glycerol 4 sets of experiments varying time duration of 1, 2, 3 and 4 days were conducted. Each growth medium was analyzed for biomass concentration and the corresponding lipid content.

The glycerol in the culture medium (M18) after respective intervals of algal growth was quantified by analyzing its liquid part using a spectrophotometric method suggested by Bondioli et al. (2005)[8]. The detailed method is provided in the materials and method(chapter4).

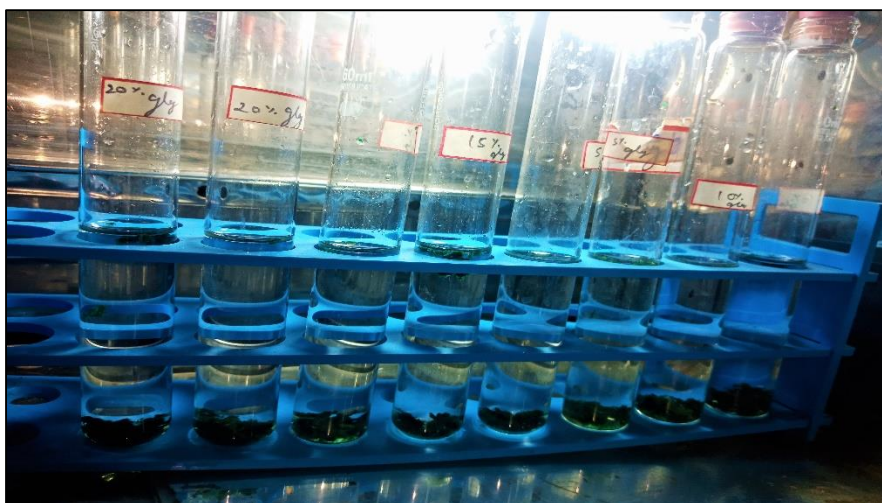


Figure 6.3. Culture tubes for the batch experiments under photoheterotrophic condition.

6.3 Growth under Photomixotrophic condition

Under photomixotrophic condition, glycerol and CO_2 were used simultaneously as the organic and inorganic carbon substrates respectively for the isolated blue-green alga, *Leptolyngbya subtilis JUCHE1*. The following objective, described under Aim 3 in Chapter 3, is addressed in this chapter:

- Determination of growth kinetics of *Leptolyngbya subtilis JUCHE1* based on integrated effect of organic and inorganic carbon substrates supplied by glycerol and CO_2 in 1:1 ratio.

6.3.1 Experimental

6.3.1.1 Maintenance and Growth Culture medium

The maintenance medium was prepared by dissolving 2mmol glycerol/L M18 medium saturated with pure CO_2 . The algal strain was maintained in this medium under constant illumination of 2.5kLux ($33.75 \mu\text{mol}/\text{m}^2/\text{s}$) at 37°C .

6.3.1.2 Batch experiments under mixotrophic condition

In the batch mode experiments separate runs were conducted using C-mole equivalent to 5-

20%v/v CO₂ concentration used under photoautotrophic condition. For each run half of the carbon source is organic, i.e. glycerol and half of it is CO₂. All the experiments were conducted in small-scale bioreactors, i.e., 250 ml Erlenmeyer conical flasks, as used in case of batch studies under photoautotrophic condition. For mixotrophic experiments with C-mole equivalent to 5%, 10%, 15% and 20% (v/v) CO₂, the flasks were first sparged with air-CO₂ mixture having CO₂ concentration of 2.5%, 5%, 7.5% and 10% (v/v). Afterwards glycerol equivalent to 2.5%, 5%, 7.5% and 10% (v/v) CO₂ was added to the flasks. The concentration of glycerol equivalent to 2.5%, 5%, 7.5% and 10% (v/v)CO₂, as calculated using equation (5.24) in chapter 5.

The values of aqueous phase concentrations of CO₂ (mM) and glycerol (C₃H₈O₃) (mM) in growth medium used for the heterotrophic and mixotrophic growth of *Leptolyngbya subtilis* JUCHE1 have been calculated using Equations (5.1) and (5.24) respectively and have been provided in Table 6.3.

Table 6.3 Calculated values of equilibrium concentration of CO₂ and glycerol (C₃H₈O₃) in aqueous phase corresponding to each gas phase concentration in CO₂-air mixture

| Serial no. | Gas phase inlet- CO ₂ concentration (%v/v) | C _{gly} , glycerol (C ₃ H ₈ O ₃) concentration, (g/L) | Aqueous phase inlet- CO ₂ concentration (g/L) | Equivalent concentrations of Carbon (mg-atom/L) | C _{gly} , glycerol (C ₃ H ₈ O ₃) concentration, (mg-atom/L) |
|------------|---|--|--|---|--|
| 1 | 2.5 | 0.01899 | 0.02728 | 0.62 | 0.206 |
| 2 | 5 | 0.03799 | 0.05456 | 1.24 | 0.413 |
| 3 | 7.5 | 0.05699 | 0.08184 | 1.86 | 0.619 |
| 4 | 10 | 0.07599 | 0.10912 | 2.48 | 0.826 |
| 5 | 15 | 0.11398 | 0.16368 | 3.72 | 1.289 |
| 6 | 20 | 0.15207 | 0.2178 | 4.95 | 1.653 |

6.5 Results and discussions

6.5.1 Morphological characterization of Power Plant Blue Green Alga

The FESEM micrographs of algal sample at 600x (figure a) and 5000x (figure b) magnification have been presented in Figures 6.4 A and B. The diameter of the *Leptolyngbya subtilis* JUCHE1 has been determined to be between 2.503 μm to 3.497 μm .

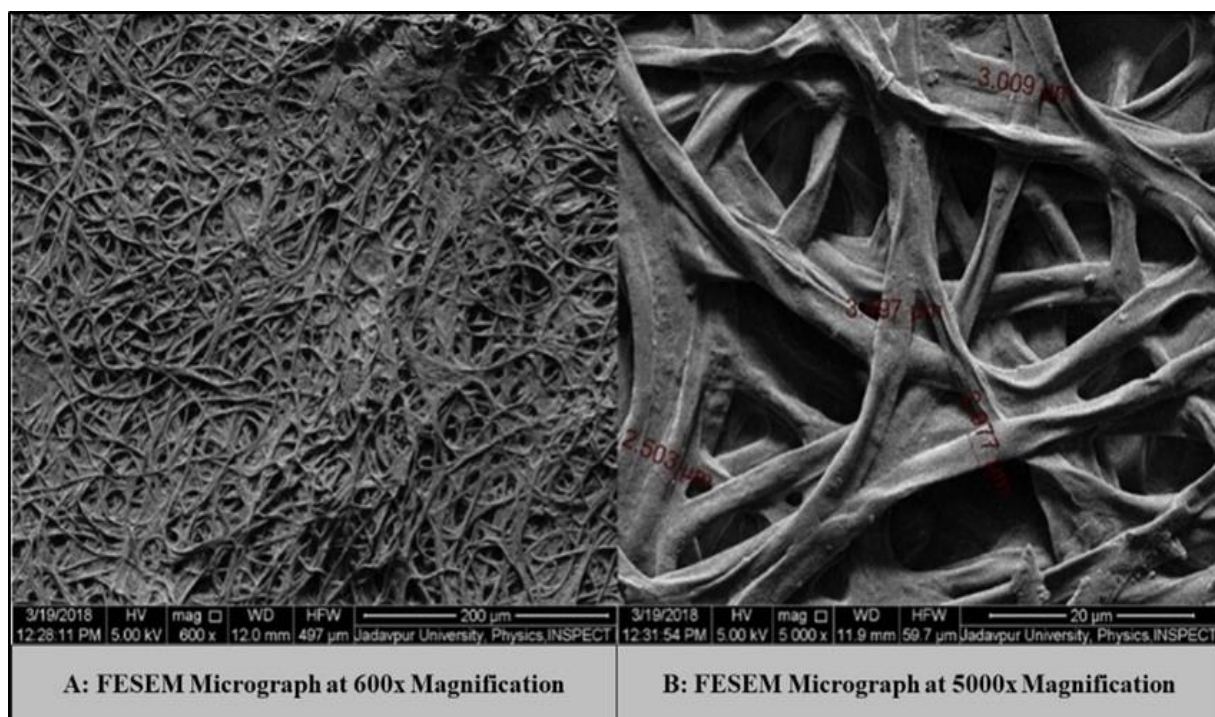


Figure 6.4 Micrographs of *Leptolyngbya subtilis* JUCHE1 with different magnifications as shown in: (A) 600x magnification and (B) 5000x magnification.

6.5.2 Effect of CO₂ bubbling on medium pH

The values of pH after 20h of bubbling have been provided in Table 6.4.

Table 6.4 Values of pH against CO₂ concentrations(%v/v) of bubbling gas

| CO ₂ Concentrations (% v/v) | pH |
|--|-----|
| 0 | 6.8 |
| 2.5 | 6.4 |
| 5 | 5.9 |
| 10 | 5.5 |
| 20 | 5.2 |

The drop in pH clearly indicates acidification. when CO₂ reacts with H₂O to form carbonic acid H₂CO₃, two protons are lost to form bicarbonate, HCO₃⁻, and carbonate, CO₃²⁻ as shown in the reaction given below.



Similar observation was reported by Ota et.al (2009) which showed that with the increase in inlet CO₂ concentrations there was a decrease in the values of pH [9]. Another research article reported that when CO₂ concentration was as low as 0.04%, pH increased with the increase in algal growth. However, when the same algal biomass was transferred to higher concentration of CO₂ i.e. 40%(v/v) the value of pH suddenly decreased to 6 within four hours and constantly varied between the range of 5.8- 6.4 in another culture period of 9 days [10].

6.5.3 Equilibrium aqueous phase concentration of CO₂

Following the method described in sections 5.1 and 5.8 in chapter 5, the equilibrium aqueous phase concentrations of CO₂ have been calculated against those in inlet CO₂-Air mixture and the values are provided in table 6.3.

6.5.4 Effect of inorganic carbon source (CO₂) on algal growth

In Figure 6.5, the biomass concentration has been plotted against culture time using gas phase inlet concentration of CO₂ (5-20% v/v) as a parameter. As evident from the growth curves of *L. subtilis* JUCHE1, in case of 5% and 10% inlet-CO₂ concentrations, there is a significantly increasing trend of biomass growth from 0-4 days which ultimately reaches the saturation on 5th day. Whereas, for 15 and 20%, it is clearly observed that the growth curves follow an increasing trend up to 3rd day beyond which a declining pattern appears. It may be due to the fact that at low inlet CO₂ concentration i.e. 5% and 10%, the capability of CO₂ uptake of *Leptolyngbya subtilis* JUCHE1 is very high due to its natural adaptation in an CO₂-rich atmosphere of thermal power plant. It is also noticed that the maximum value of biomass concentration increases with the increase of gas phase CO₂ concentration up to 15%(v/v) used for saturation of aqueous medium. Beyond 15% the maximum value decreases. The maximum value of biomass concentration of 0.7286 g/L is obtained for 15% CO₂ on 3rd day of cultivation as shown in table 6.5. Therefore, the optimum inlet CO₂ concentration is 15%. The comparison

of the initial growth rate data also indicates that inlet CO₂ concentration of 20% is inhibitory. All the observed values of biomass concentrations and productivities varying inlet-CO₂ concentrations from 5-20% v/v are provided in table 6.5.

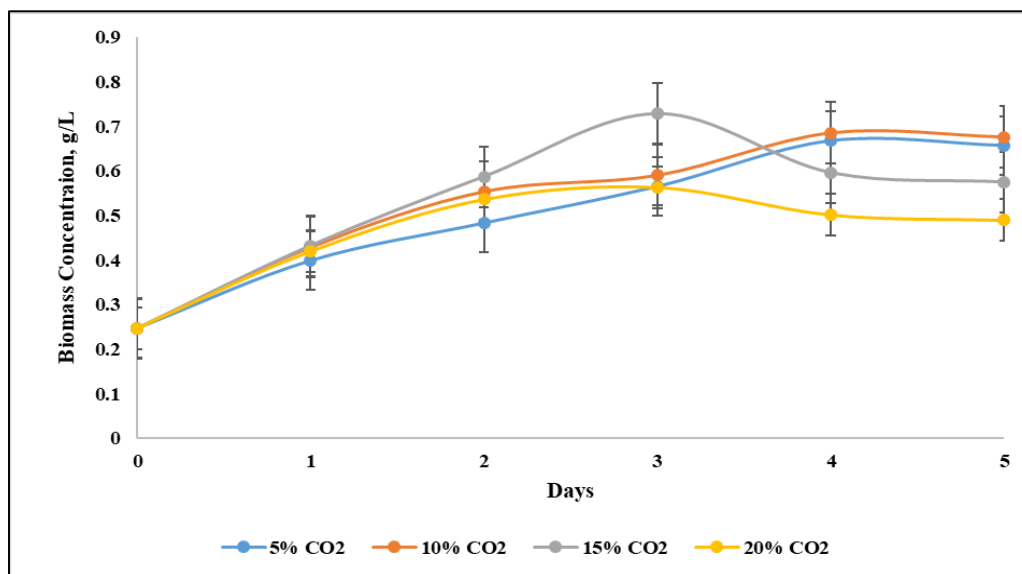


Figure 6.5 Growth curve of *Leptolyngbya subtilis* JUCHE1 under photoautotrophic condition varying inlet CO₂ concentrations from 5-20(%v/v).



Figure 6.6 Algal growth of *L.subtilis* JUCHE1 at 5th day varying different inlet-CO₂ concentrations from 5-20%v/v.

Table 6.5 Experimental values of biomass concentrations (g/L) and productivities (g/L/d) of *L.subtilis* JUCHE1 have been observed against each time intervals at different CO₂ concentrations(%v/v) under photo-autotrophic growth mode.

| Biomass concentrations g/L | | | | | Biomass productivity(g/L/d) | | | |
|----------------------------|---|---------|--------|--------|---|--------|--------|--------|
| Days | Inlet-CO ₂ concentrations(% v/v) | | | | Inlet-CO ₂ concentrations(% v/v) | | | |
| | 5 | 10 | 15 | 20 | 5 | 10 | 15 | 20 |
| 0 | 0.2473 | 0.2473 | 0.2473 | 0.2473 | 0 | 0 | 0 | 0 |
| 1 | 0.399 | 0.429 | 0.433 | 0.4201 | 0.1517 | 0.1817 | 0.1857 | 0.1728 |
| 2 | 0.4833 | 0.554 | 0.5877 | 0.5366 | 0.118 | 0.1533 | 0.1702 | 0.1446 |
| 3 | 0.5653 | 0.5906 | 0.7286 | 0.5634 | 0.106 | 0.1144 | 0.1604 | 0.1053 |
| 4 | 0.668 | 0.68595 | 0.596 | 0.5013 | 0.1051 | 0.1096 | 0.0871 | 0.0635 |
| 5 | 0.6571 | 0.6765 | 0.575 | 0.4895 | 0.0819 | 0.0858 | 0.0655 | 0.0484 |

Thus, the growth of *Leptolyngbya subtilis* JUCHE1 is inhibited beyond the optimum substrate concentration. Similar reports are also available in the literature where specific growth rate of algae has been observed to increase with increase in CO₂ concentration up to a certain level, beyond which there is a sudden decrease in growth rate. Taher et al. 2015, reported that the inhibition started from the input CO₂ concentration of 2%(v/v) during the research studies on fresh water algae, namely, *Chlorella sp.* and *Pseudochlorococcum sp.* and a marine alga, *Nannochloropsis sp* [5]. They explained that the inhibition of growth rate was due to increase in the release of oxygen at high CO₂ level which ultimately caused severe competition between the two (O₂ and CO₂) for 1,5-bisphosphate carboxylase/oxygenase (RuBisCO) enzyme [5]. To verify whether the concentration of oxygen generated through algal growth has also any effect in the present study, the values of the relative molar concentration(O_R) against culture have been provided in Table 6.6 using the inlet-CO₂ concentration as a parameter. O_R has been defined in equation (5.6) in chapter 5.

Table 6.6 Time histories of relative molar concentrations of oxygen (O_R) at different inlet- CO_2 concentrations (5-20% v/v).

| Relative molar concentration of oxygen (O_R) | | | | |
|--|-----------|------------|------------|------------|
| Days | 5% CO_2 | 10% CO_2 | 15% CO_2 | 20% CO_2 |
| 0 | 1 | 1 | 1 | 1 |
| 1 | 1.070 | 1.206 | 1.266 | 1.595 |
| 2 | 1.132 | 1.238 | 1.523 | 1.726 |
| 3 | 1.152 | 1.354 | 1.647 | 1.773 |
| 4 | 1.213 | 1.375 | 1.747 | 2.095 |

From the table 6.6, it is clearly observed that with the increase in inlet CO_2 concentrations the oxygen concentration also increases with time and the maximum relative concentration of oxygen is observed for 20% CO_2 concentration. In case of 20% CO_2 , the relative value reaches up to 2.095, i.e., an increase of 109.5% is attained through the release of O_2 through photosynthesis. This obviously leads to a competition between CO_2 and O_2 for RuBisCO enzyme at 20%. According to reported literature, the enzyme RuBisCO is responsible for the fixation of CO_2 by the blue green alga/ cyanobacteria [5]. The enzyme can act on two substrates, namely CO_2 and O_2 respectively as carboxylase and oxygenase[5]. While it fixes CO_2 , as carboxylase, it generates a toxic product 2-phosphoglycolate and decelerates the rate of CO_2 fixation during its action as oxygenase. Moreover, specificity of RuBisCO towards CO_2 is less than that for O_2 . Hence the fixation of CO_2 and in turn the production of biomass is affected at higher concentration of CO_2 which leads to inhibitory growth at 20%.

Although some of the *Chlorella sp.* can withstand CO_2 concentrations as high as 25%(v/v), most of the studies on algal research was conducted using inlet CO_2 concentration up to 2.5% [11,12,13]. Ho et al. 2012, reported a study using different strains of *Scenedesmus obliquus* (AS-6-1, CHW-1, FSP-3, ESP-5, ESP-7, CNW-N), cultivated using 2.5%(v/v) CO_2 [13]. The concentration ranges of CO_2 during the studies on another three algal species, namely, *Chlorella sp.*, *Pseudochlorococcum sp.* and *Nannochloropsis sp.* was also varied from 0.04-2%(v/v) [5]. Therefore, analyzing different studies on algal strains, it appears that *L. subtilis* JUCHE1 is a highly CO_2 -tolerant algal strain. This can be due to its adaptation to high- CO_2 -environment of power plants from where it was isolated.

6.5.4.1 Growth kinetic study on CO₂

The values of initial specific growth rates of *Leptolyngbya subtilis* JUCHE1 at the inlet CO₂ concentrations of 5-20% (v/v), i.e., the aqueous concentration of CO₂ of 0.05456 g/L to 0.2178 g/L as presented in Table 6.3, have been determined using the biomass concentrations over 0-1 day and have been plotted in Figure 6.7A. It has been observed that with increase in CO₂ concentration the specific growth rate, μ , increases up to a maximum point having inlet CO₂ concentration 15% (v/v), i.e., aqueous phase concentration of 0.1636 g/L, and beyond that there is a decreasing trend. This signifies that the growth rate gets inhibited at 20% (v/v), i.e., 0.2178 g/L. From the analysis of Figure 6.7A, the value of C_{Smax} , signifying the substrate concentration at which the highest value of μ is obtained experimentally, is 0.1636 g/L corresponding to inlet CO₂ concentration of 15% (v/v). Since the bell-shaped nature of the curve μ versus initial substrate concentration, C_S is observed, hence substrate inhibition is established and Haldane model, as described in Section 5.1.6 of Chapter 5, has been attempted. Both **methods I and II**, as described in Section 5.1.6 of Chapter 5, have been used to determine the values of μ_{max} , K_s and K_I .

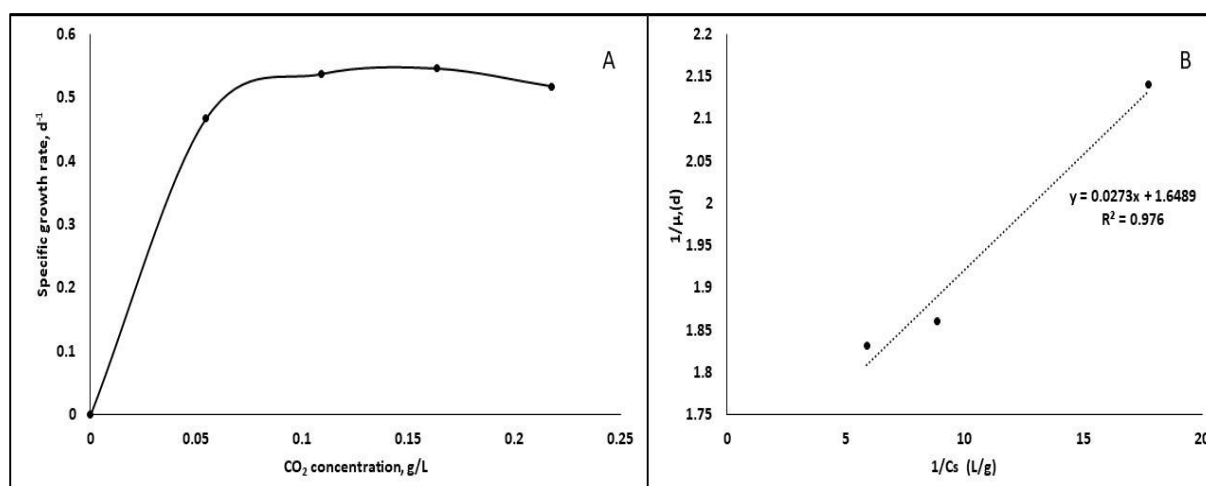


Figure 6.7 (A) Experimental growth curve of *Leptolyngbya subtilis* JUCHE1 with variation of CO₂ concentration (μ against Initial liquid phase CO₂ concentration);

Figure 6.7 (B) Double reciprocal plot ($1/\mu$ versus $1/C_{CO_2}$)

Method-I

The values of μ_{max} and K_s of $0.6064d^{-1}$, 0.0165 g/L respectively have been determined from the intercept and slope of the double reciprocal plot (Figure 6.7B), generated by graphing the inverse values of μ against inverse of initial substrate concentration in the uninhibited zone,

i.e. up to the substrate concentration of 0.1636 g/L (inlet CO₂ concentration =15%(v/v)). Using the values of $C_{Smax}=0.1636$ g/L and $K_s=0.0165$ g/L, the value of K_I has been determined to be 1.7429g/L from Equation 5.11($C_{Smax} = \sqrt{K_S K_I}$).

Method-II

From the Figure 6.7A, the highest experimental value of μ , i.e., μ'_{max} obtained at C_{Smax} has been determined to be 0.5459 d⁻¹. According to the Method-II, described in Section 5.1.6 of Chapter 5, all the values of μ have been normalized to obtain μ_{norm} , where, $\mu_{norm} = \frac{\mu}{\mu'_{max}}$.

The non-linear regression analysis of the dataset of μ_{norm} and C_S over the entire substrate concentration regime, spanning over uninhibited and inhibited growth regime (i.e., $C_S = 0$ to 0.2178g/L), has been done using "fitnlm" of MATLAB. The regression has been repeated by adjusting the value of μ'_{max} in a narrow range around the experimental μ'_{max} until the Root mean square error (RMSE), represented in Equation 5.1.7.3 is less than 0.02. The final value of μ'_{max} is considered as μ_{max} of the Haldane equation. Similarly, the values of K_S and K_I , predicted by fitnlm using the μ_{norm} values using the final value of μ'_{max} have been considered as the actual K_S and K_I of the Haldane model. The program has been provided in the Appendix. The values of μ_{norm} , K_S and K_I of 0.65 d⁻¹, 0.0162 g/L and 1.97 g/L.

Table 6.7 Experimental values of Specific growth rates at different substrate concentrations(g/L).

| Cco2 (g/L) | Specific growth rate, μ (d ⁻¹) | 1/ Cco2 | 1/ μ |
|------------|--|---------|----------|
| 0.05456 | 0.4694 | 17.7556 | 2.141 |
| 0.10912 | 0.5373 | 8.84329 | 1.861 |
| 0.16368 | 0.5459 | 5.88789 | 1.832 |
| 0.2178 | 0.5178 | 4.42282 | 1.931 |

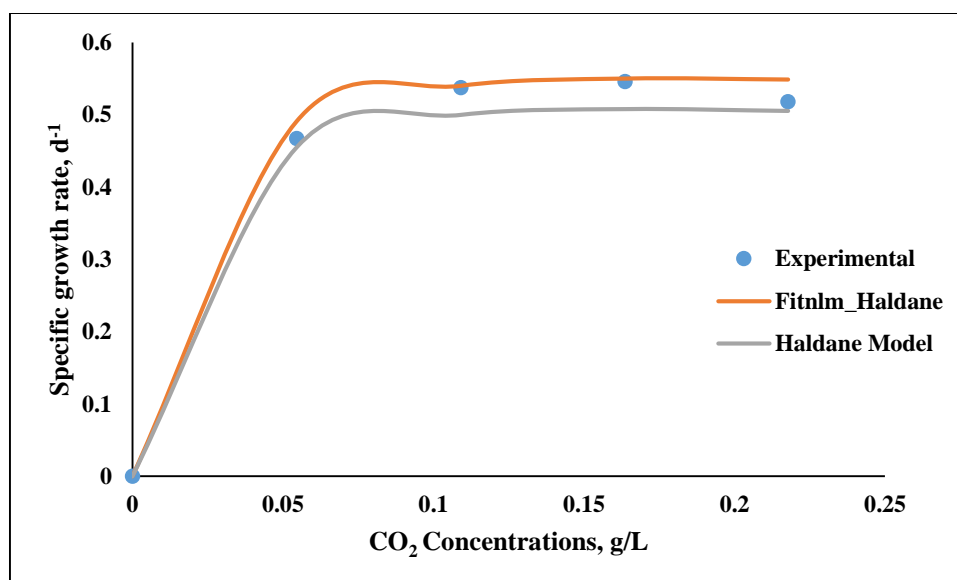


Figure 6.8 Simulated and experimental values of specific growth rate “μ” against Initial liquid phase CO₂ concentration

In Figure 6.8, the simulated values of specific growth rate “μ”, obtained using Method-I and Method-II have been plotted against Initial liquid phase CO₂ concentration. The corresponding experimental values have been superimposed on the same figure. It appears that the agreement between the experimental data and the predictions of Method –II is more. The parameters of statistical analysis have been represented in Table 6.9.

Table 6.8 Haldane model parameters using Method-I and Method-II along with RMSE values

| Method | μ_{\max} d ⁻¹ | K_S g/L | K_I g/L | RMSE |
|-----------|---------------------------------|--------------|--------------|--------|
| Method-I | 0.6064 | 0.0165 | 1.7429 | 0.0253 |
| Method-II | 0.65 | 0.0162 | 1.97 | 0.0174 |

From the analysis of Table 6.9, it is again established that the all the error parameters are acceptable in case of predictions following Method-II. Therefore, the parameters of Haldane model appear to be more appropriate. Thus, the changing pattern of μ against initial liquid phase CO₂ concentration can be represented by Haldane Model by the following equation:

$$\mu_{CO_2} = \frac{0.65 * C_{CO_2}}{0.0162 + C_{CO_2} + \frac{C_{CO_2}^2}{1.97}} \quad (6.4)$$

6.5.4.2 CO₂ fixation rate of *L. subtilis* JUCHE1

The CO₂ fixation rate has been calculated on the basis of the elemental C-H-N composition. The maximum CO₂ fixation rate for all the inlet CO₂ concentrations (5-20% v/v) has been observed between 0-1day. The values of CO₂ fixation rate, as calculated using Equation 5.5, for all the inlet-CO₂ concentrations are provided in Table 6.9. The analysis of the data reveals that the maximum CO₂ fixation rate of 0.2383 g/L/d is observed over 0-1day at 15% inlet gas phase CO₂ concentration. In Figure 6.9 the time history of CO₂ fixation rate has been depicted using inlet CO₂ concentration as a parameter. From the analysis of Figure 6.9, it can be inferred that the CO₂ fixation rate not only depends on the inlet CO₂ concentration but also on the incubation period of the algal specimen.

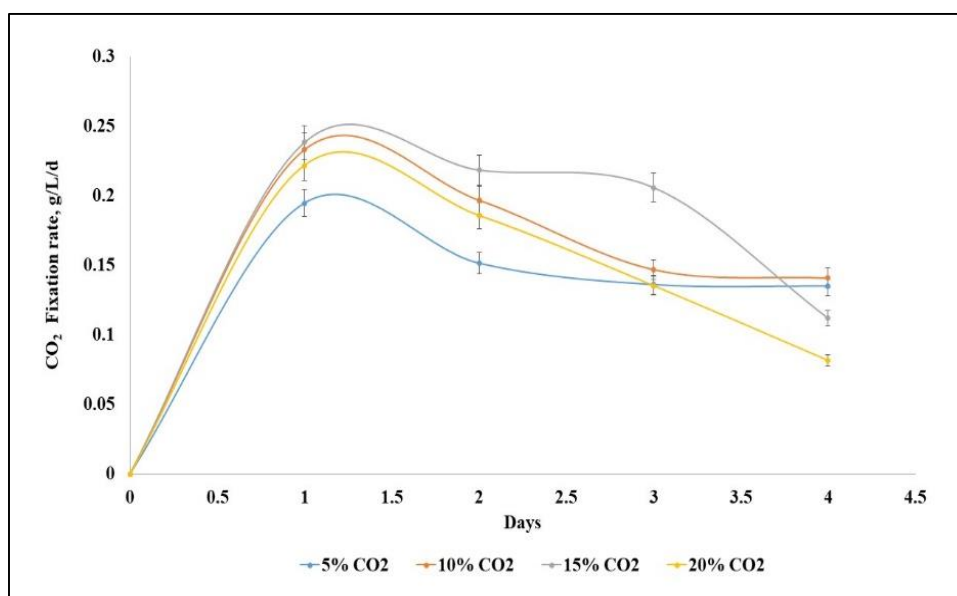


Figure 6.9 CO₂ fixation rate of *Leptolyngbya subtilis* JUCHE1 under photoautotrophic growth by varying inlet CO₂ concentrations.

The increase of CO₂ fixation rate with the increase of inlet CO₂ concentration up to 15% can be explained by the high CO₂-affinity of the specimen due to its adaption to CO₂-rich power plant environment. Similar observation has been reported by Pradhan et al.2018, during their studies on power plant algae [14]. The declining trend beyond 1st day may be explained by the hindrance in the light propagation path due to the increase in algal mass at each inlet CO₂ concentration. The % carbon capture (CC), as calculated using Equation 5.27, on the basis of the biomass data over 0-5 days for all inlet CO₂ concentration (5-20%v/v) have been provided in Table 6.10. It is evident that the value of CC is the maximum for the lowest inlet CO₂ concentration, i.e., 5% (v/v). This can again be explained by the hindrance in light

propagation path with the increase in biomass concentration. As the biomass concentration, obtained at 5%(v/v) lies at the lowest level among those obtained with all values, overall value of CC becomes maximum at that inlet value of CO₂ concentration.

Table 6.9 Calculated values of CO₂-Fixation rates(g/L/d) of *L.subtilis* JUCHE1 under photo-autotrophic condition.

| Days | CO ₂ -Fixation rates(g/L/d) | | | |
|------|--|--------|--------|--------|
| | Inlet-CO ₂ concentrations(%v/v) | | | |
| | 5 | 10 | 15 | 20 |
| 0 | 0 | 0 | 0 | 0 |
| 1 | 0.1946 | 0.2331 | 0.2383 | 0.2217 |
| 2 | 0.1514 | 0.1967 | 0.2184 | 0.1856 |
| 3 | 0.1360 | 0.1468 | 0.2058 | 0.1352 |
| 4 | 0.1349 | 0.1407 | 0.1118 | 0.0814 |

Table 6.10 Values of % carbon capture (CC) of *L.subtilis* JUCHE1 at maximum CO₂capture rate

| Inlet-Carbon concentrations %(v/v) | CC (%) |
|------------------------------------|--------|
| 5 | 98.94 |
| 10 | 51.59 |
| 15 | 27.33 |
| 20 | 14.97 |

As reported by Demoris et.al (2007), the algal strains, *Chlorella kessleri* and *Scenedesmus obliquus*, isolated from thermo-electric power plant, show fixation rates of 0.163 g/L/d and 0.142 g/L/d when inlet concentrations of CO₂ are fixed at 6 and 12% (v/v) respectively [15]. In Table 6.12, the fixation rate of CO₂ of *Leptolyngbya subtilis*JUCHE1 has been compared with that of other algal species[15, 16, 17, 18,19, 20]. From the analysis of the Table 6.11, it is clear that for most of the algal species, the CO₂ fixation rate increases up to a certain value of inlet CO₂ concentration beyond which there is a decreasing trend. As reported in the literature, pure culture of the microalga *Chlorella vulgaris*, when cultivated in a flat plate photobioreactor

using pure water and four different inlet CO₂ concentration (0.03%, 2%, 5% and 10%), exhibits an increasing trend of CO₂ fixation rate [17]. The fixation rate of 0.144 g/L/d is attained at 10% (v/v) inlet CO₂ concentration [17]. When artificial seawater is used as the medium, the carbon fixation rate of the same species increases from 0.041-0.055g/L/d as the inlet CO₂ concentration is increased from 0.03-10% (v/v) [17]. According to another report, the carbon fixation rate of *Chlorella vulgaris* decreases from 0.14g/L/d to 0.073g/L/d as the inlet CO₂ concentration is increased from 4-8%(v/v) [16]. *Nannochloropsis gaditana*, also shows a decreasing trend of CO₂ fixation rate from 0.112-0.1g/L/d as the inlet CO₂ concentration is raised from 4-8% [16]. In case of *Chorella sp.*, as the CO₂ concentration is varied from 0.04-30%, the CO₂ fixation rate increases from 0.0876g/L/d to a maximum value of 0.09687g/L/d at 10%(v/v) CO₂ concentration [18]. Beyond inlet CO₂ concentration of 10%, a decreasing trend in the CO₂ fixation rate is noticed [18]. Similarly, *Tetraselmis suecica* exhibits an increasing trend in the carbon fixation rate having a variation from 0.075-0.11126 g/L/d as the inlet CO₂ concentration increases from 0.04-5%. Beyond 5% a declining trend in the carbon fixation rate is observed up to the inlet CO₂ concentration of 30%(v/v)[18]. As reported in the literature, *Scenedesmus obliquus* SJTU-3 and *Chlorella pyrenoidosa* show a similar trend in the CO₂ fixation rate as the inlet CO₂ concentration is varied from 0.03-50%(v/v) [19]. The maximum CO₂ fixation rate of 0.29g/L/d and 0.26g/L/d are achieved respectively for *Scenedesmus obliquus* SJTU-3 and *Chlorella pyrenoidosa* at 10%(v/v) inlet CO₂ concentration [19]. The carbon fixation rate of *Spirulina platensis* also shows an increasing trend as the inlet CO₂ concentration is varied from 0.03-10%(v/v) [17]. At 10%(v/v) inlet CO₂ concentration, the carbon fixation rate as high as 0.41g/L/d is achieved [17]. In another report, the carbon fixation rate of *Spirulina* at 10%(v/v) CO₂ concentration has been reported to be 0.378g/L/d [20]. As analyzed from the literature data, the maximum carbon fixation rate of most of the algal strains lies within 0.15 g/L/d and has been achieved within 10%(v/v) [17]. Although the maximum carbon fixation rate of *Spirulina* seems to be the highest, it is achieved at 10%(v/v) [20]. The carbon fixation rate of the power plant algae *Chlorella kesslari* and *Scenedesmus obliquus* are comparable to that of *Leptolyngbya subtilis* JUCHE [15], the maximum CO₂ fixation rate for the latter being 0.2383 g/L/d. Unlike other algal strains showing high capacity of carbon fixation, the present strain shows the maximum at an inlet CO₂ concentration as high as 15%(v/v). Therefore, this species will be particularly suitable for an algal biorefinery having the potential to be integrated with a power plant with CO₂-rich environment.

Table 6.11 Comparison of the CO₂ fixation rate of *Leptolyngbya subtilis* JUCHE1 with other algal strains.

| Algal strains | Inlet CO ₂ concentrations (v/v)% | Maximum CO ₂ Fixation rate(g/L/d) | Ref. |
|---------------------------------|---|--|------|
| <i>Chlorella kessleri</i> | 6 | 0.163 ^a | 15 |
| <i>Scenedesmus obliquus</i> | 12 | 0.142 ^a | |
| <i>Chlorella vulgaris</i> | 4 | 0.14 | 16 |
| | 8 | 0.073 | |
| <i>Nannochloropsis gaditana</i> | 4 | 0.112 | |
| | 8 | 0.1 | |
| <i>Chlorella vulgaris</i> | 10 | 0.144 | 17 |
| <i>Chlorella vulgaris</i> | 0.03 | 0.041 | |
| | 2 | 0.045 | |
| | 5 | 0.049 | |
| | 10 | 0.055 | |
| <i>Spirulina platensis</i> | 0.03 | 0.31 | |
| | 2 | 0.37 | |
| | 5 | 0.394 | |
| | 10 | 0.419 | |
| <i>Chlorella sp.</i> | 0.04 | 0.08776 | 18 |
| | 5 | 0.09573 | |
| | 15 | 0.09687 | |
| | 30 | 0.00638 | |

| Algal strains | Inlet CO ₂ concentrations (v/v)% | Maximum CO ₂ Fixation rate(g/L/d) | Ref. |
|-------------------------------------|---|--|----------------------|
| <i>Tetraselmis suecica</i> | 0.04 | 0.07578 | 18 |
| | 5 | 0.11126 | |
| | 15 | 0.10412 | |
| | 30 | 0.00481 | |
| <i>Scenedesmus obliquus</i> SJTU-3 | 0.03 | 0.15 | 19 |
| | 5 | 0.28 | |
| | 10 | 0.29 | |
| | 20 | 0.248 | |
| | 30 | 0.152 | |
| | 50 | 0.11 | |
| <i>Chlorella pyrenoidosa</i> SJTU-2 | 0.03 | 0.115 | 19 |
| | 5 | 0.248 | |
| | 10 | 0.26 | |
| | 20 | 0.225 | |
| | 30 | 0.155 | |
| | 50 | 0.11 | |
| <i>Spirulina platensis</i> | 10 | 0.378 | 20 |
| <i>Leptolyngbya subtilis</i> JUCHE1 | 5 | 0.1946 | Present study |
| | 10 | 0.2331 | |
| | 15 | 0.2383 | |
| | 20 | 0.2217 | |

^aAccording to equation, CO₂ fixation rate has been calculated by using the values of biomass productivity, $(R_{CO_2}) = 1.88 \times \text{Biomass productivity } (B_P)$, and the equation is derived from the typical molecular formula of micro algal biomass, CO_{0.48}H_{1.83}N_{0.11}P_{0.01} as reported in Chisti et al. 2007 [21].

6.5.4.3 Effect of different nitrogen concentrations on algal growth

The experimental setup for batch study is represented in Figure 6.10. Generally, the plots of biomass concentration corresponding to any initial nitrate concentration lies above that obtained at lower value of NaNO_3 in the range of 1-2 g/L as shown in Figure 6.11. At all concentrations of nitrate in the range 1-2.5 g/L the time span of exponential phase of the growth is 0 - 4 days, beyond which concentration of biomass saturates. The maximum biomass concentration of 0.745g/L is observed at 2 g/L NaNO_3 concentrations on 4th day of cultivation. The maximum biomass productivities of 0.125,0.1515,0.176 and 0.1351 g/L/d respectively are obtained for nitrogen concentrations of 1, 1.5, 2 and 2.5 g/L of NaNO_3 . From the literature review, it is clear that the effect of variation of concentration of NaNO_3 has been studied for several algal strain namely, *Scenedesmus abundans*, *Chlorella minutissima* etc.[22,23] .While the studies of *Scenedesmus* were conducted using NaNO_3 concentration range of 0.16 to 0.4 g/L those on *Chlorella minutissima* was focused in the range of 0.075 to 0.225 g/L[22, 23]. All the observed values of biomass concentration and productivities are provided in table 6.12.

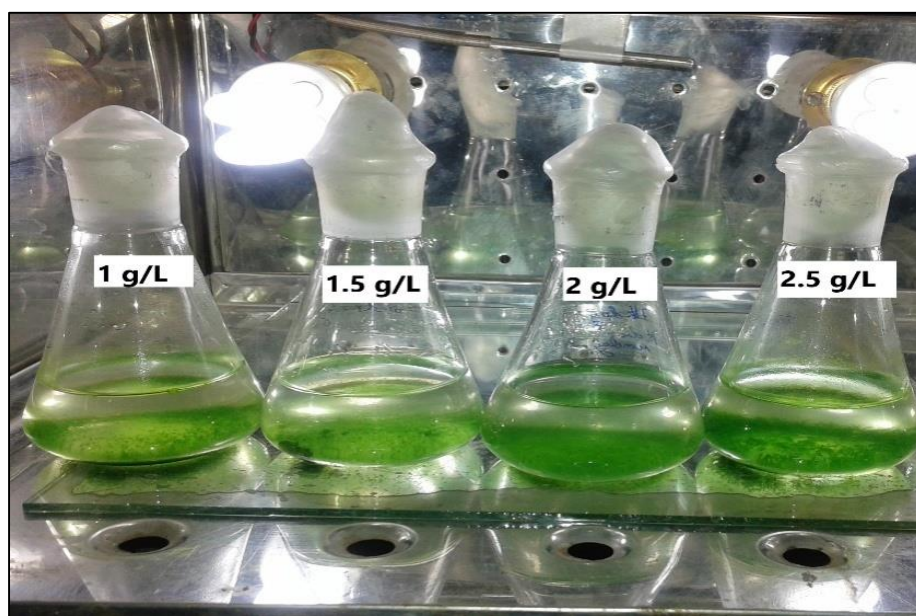


Figure 6.10 Experimental set up for batch study varying NaNO_3 concentrations from 1-2.5g/L as substrate.

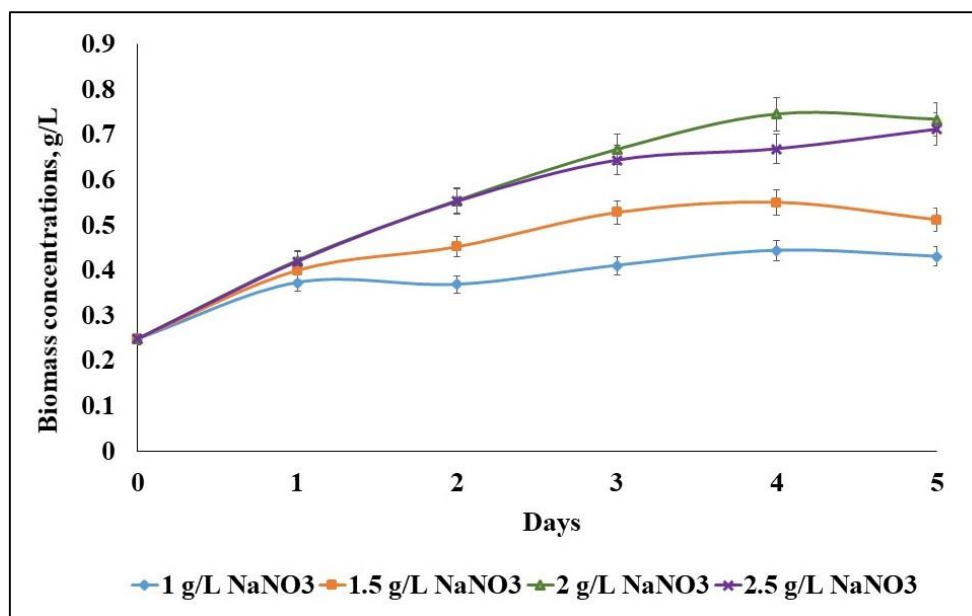


Figure 6.11 Effect of different NaNO₃ concentrations (1 - 2.5g/L of NaNO₃) on the cell growth of *Leptolyngbya subtilis* JUCHE1.

Table 6.12 Experimental values of biomass concentrations (g/L) and productivities (g/L/d) against each time intervals at individual NaNO₃ concentrations(g/L) as nitrogen source.

| Days | Biomass concentration (g/L) | | | | Biomass productivities (g/L/d) | | | |
|------|---------------------------------------|--------|--------|--------|---------------------------------------|--------|---------|--------|
| | NaNO ₃ Concentrations(g/L) | | | | NaNO ₃ Concentrations(g/L) | | | |
| | 1 | 1.5 | 2 | 2.5 | 1 | 1.5 | 2 | 2.5 |
| 0 | 0.2473 | 0.2473 | 0.2473 | 0.2473 | 0 | 0 | 0 | 0 |
| 1 | 0.3722 | 0.3987 | 0.4211 | 0.4189 | 0.1249 | 0.1514 | 0.1738 | 0.1716 |
| 2 | 0.386 | 0.4512 | 0.5538 | 0.552 | 0.0693 | 0.1019 | 0.15325 | 0.152 |
| 3 | 0.4102 | 0.5272 | 0.6667 | 0.6433 | 0.0543 | 0.0933 | 0.1398 | 0.132 |
| 4 | 0.4433 | 0.5495 | 0.745 | 0.6683 | 0.049 | 0.0755 | 0.1244 | 0.1052 |
| 5 | 0.43 | 0.5112 | 0.7333 | 0.7117 | 0.0365 | 0.0527 | 0.0972 | 0.0928 |

In Table 6.14 the productivities of *Scenedesmus abundans*, *Chlorella minutissima* and *L. subtilis*JUCHE1 have been provided. Comparison of the trends clearly reveals that, both for

Leptolyngbya subtilis JUCHE1 and *Scenedesmus abundans*, the productivity passes through a maximum as the NaNO₃ concentration is increased up to a critical value, beyond which the former shows a declining trend. This behaviour can be explained by inhibitory effect of NaNO₃, beyond a certain range. Similar observation has been reported in case of action of KNO₃ on *Scenedesmus abundans*[22]. In the reported range of NaNO₃ concentration (0.075 to 0.225 g/L), productivities of *Chlorella minutissima*, however shows ever increasing trend with the increase of NaNO₃ concentration [23].

Table 6.13 Comparison of effect of NaNO₃ concentration on biomass productivity of *Leptolyngbya subtilis* JUCHE1 with literature data on other algal strains.

| Algal strains | NaNO ₃ Concentrations(g/L) | Biomass productivity (g/L/d) | Reference |
|-------------------------------------|---------------------------------------|------------------------------|-----------|
| <i>Scenedesmus abundans</i> | 0.08 | 0.0523 | 22 |
| | 0.16 | 0.09386 | |
| | 0.24 | 0.1214 | |
| | 0.32 | 0.1672 | |
| | 0.4 | 0.14317 | |
| <i>C. minutissima</i> | 0.075 | 0.1 | 23 |
| | 0.15 | 0.138 | |
| | 0.225 | 0.188 | |
| <i>Monoraphidium sp. T4X</i> | 0.05 | 0.01 | 24 |
| | 0.1 | 0.011 | |
| | 0.5 | 0.013 | |
| | 1.0 | 0.013 | |
| | 1.5 | 0.0153 | |
| | 2.0 | 0.014 | |
| <i>Phaeodactylum tricornutum</i> | 0 | 0.00192 ± 0.00024 | 25 |
| | 0.016 | 0.00648 ± 0.00024 | |
| | 0.032 | 0.0084 ± 0.00096 | |
| | 0.064 | 0.00936 ± 0.00072 | |
| <i>Scenedesmus quadricauda</i> Sq19 | 0.2125 | 0.039 | 26 |
| | 0.425 | 0.037 | |
| | 0.6375 | 0.032 | |
| | 0.85 | 0.037 | |
| | 1.0625 | 0.026 | |
| | 1.5 | 0.043 | |

| Algal strains | NaNO ₃ Concentrations(g/L) | Biomass productivity (g/L/d) | Reference |
|---|---------------------------------------|------------------------------|----------------------|
| <i>Scenedesmus dimorphus</i> <i>Sd12</i> | 0.2125 | 0.052 | |
| | 0.425 | 0.055 | |
| | 0.6375 | 0.068 | |
| | 0.85 | 0.039 | |
| | 1.0625 | 0.049 | |
| | 1.5 | 0.044 | |
| <i>Chlorella sp Ch116</i> | 0.2125 | 0.0300 | |
| | 0.425 | 0.0193 | |
| | 0.6375 | 0.0170 | |
| | 0.85 | 0.0280 | |
| | 1.0625 | 0.0230 | |
| | 1.5 | 0.0265 | |
| <i>Nannochloropsis oceanica</i> <i>DUT01</i> | 0.0375 | 0.0166 | 27 |
| | 0.075 | 0.03125 | |
| | 0.3 | 0.025 | |
| | 0.75 | 0.0625 | |
| | 1.5 | 0.075 | |
| | 6 | 0.0708 | |
| <i>Leptolyngbya subtilis</i> JUCHE1 | 1 | 0.125 | Present study |
| | 1.5 | 0.1515 | |
| | 2 | 0.176 | |
| | 2.5 | 0.1351 | |

6.5.4.3.1 Growth kinetics

The values of initial specific growth rate (μ) determined through equation (5.7) as provided in chapter 5, using the biomass concentrations in the interval of 0-1 days, have been plotted against the corresponding value of initial NaNO₃ concentration C_{NaNO_3} in Figure 6.12(A). The double reciprocal plot by graphing $1/\mu$ against $1/C_{NaNO_3}$ is shown in Figure 6.12(B). For different values of initial NaNO₃ concentration, Table 6.15 provides the values of initial μ , $1/\mu$ and $\frac{1}{C_{NaNO_3}}$.

Figure 6.12 (A), showing μ versus C_{NaNO_3} , clearly indicates a rectangular hyperbola type pattern indicating the validity of Monod type kinetics. The linearity of the double reciprocal

plot with $R^2 = 0.9654$ again establishes the validity of Monod model. From the intercept and the slope of the double reciprocal plot the values of μ_{\max} and K_s have been determined to be 0.667 d^{-1} and 0.644 g/L respectively.

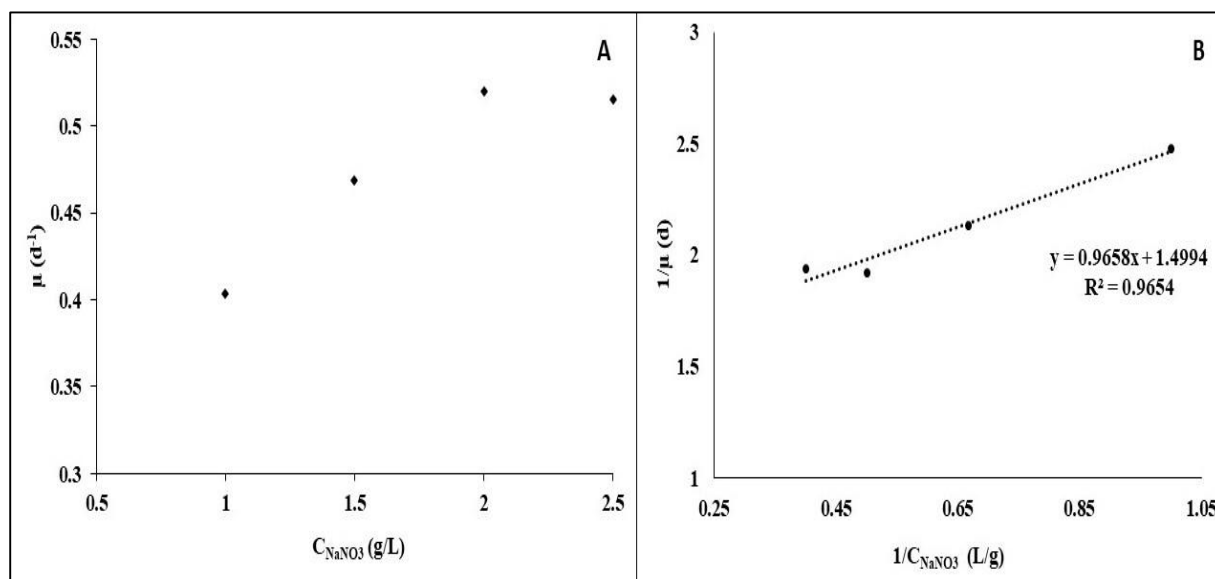


Figure 6.12(A) Specific growth rate against initial NaNO₃ concentrations (1-2.5 g/L) and **(B)** Double reciprocal plot of $1/\mu$ against $1/C_{\text{NaNO}_3}$.

Table 6.14 The values of initial μ , $1/\mu$ and $\frac{1}{C_{\text{NaNO}_3}}$ against different values of initial NaNO₃ concentration.

| NaNO ₃ concentrations (g/L) | Specific growth rate, μ (d ⁻¹) | $\frac{1}{C_{\text{NaNO}_3}}$ | $1/\mu$ |
|--|--|-------------------------------|---------|
| 1 | 0.40325 | 1 | 2.4798 |
| 1.5 | 0.4689 | 0.6666 | 2.1326 |
| 2 | 0.52004 | 0.5 | 1.9228 |
| 2.5 | 0.5151 | 0.4 | 1.9411 |

6.5.4.3.2 Effect of NaNO₃ concentration on CO₂ fixation rate of *L. subtilis* JUCHE1

From the bar of Figure 6.13, it has been observed that the CO₂ fixation rate of *L. subtilis* JUCHE1 increases with increase in NaNO₃ concentrations from 1-2 g/L at 15% v/v inlet CO₂ concentration. As the value of C_{NaNO_3} is increased from 2 to 2.5g/L no variation in the CO₂ fixation rate at each culture period except on 4th day. While the CO₂ fixation rate of 0.159g/L/d is obtained with C_{NaNO_3} value of 2g/L on 4th day, at 2.5g/L the value reduces to 0.1351 g/L/d. For all values of NaNO₃ concentration, the CO₂ fixation rate decreases from first day onwards. Overall, the highest CO₂ fixation rate of 0.2230 g/L/d has been obtained for 2 g/L of NaNO₃ concentrations on the first day as shown in Table 6.15. From the results of the study it is evident that the relationship of assimilation of nitrogen source with that of carbon source is synergistic up to a certain value, beyond which the synergism disappears. This may be due to the increase of nitrogen content of algal cells with the increase in nitrogen supply up to a certain level, as indicated by S. Li et al. 2020 during their studies on Cyanobacterial strain “*Spirulina platensis*” [28]. Similar observations have also be reported by other researchers [28, 29, 30].

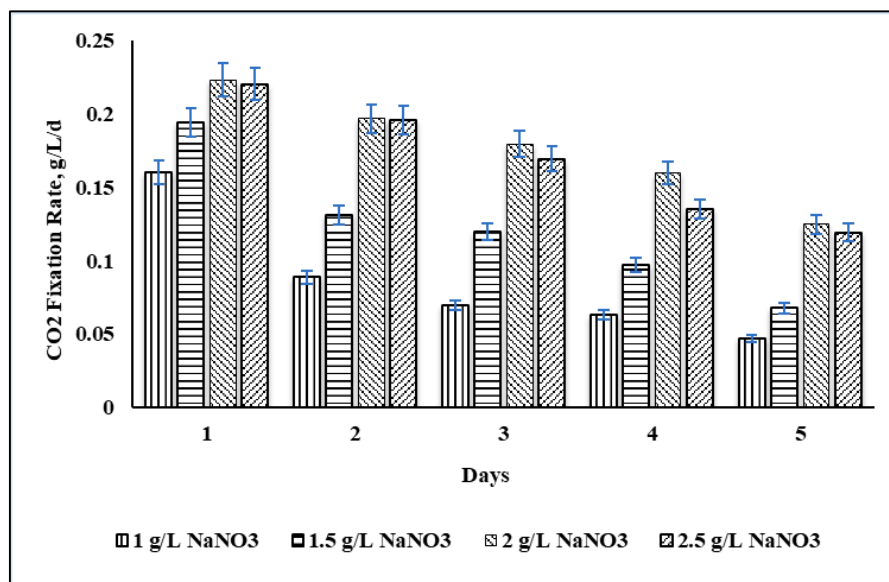


Figure 6.13 CO₂ fixation rate of *L. subtilis* JUHE1 with the variation of NaNO₃ concentration

Table 6.15 The values of CO₂ Fixation rate variation of NaNO₃ concentration

| Day | CO ₂ Fixation rate | | | |
|-----|---------------------------------------|--------|--------|--------|
| | NaNO ₃ concentration (g/L) | | | |
| | 1 | 1.5 | 2 | 2.5 |
| 1 | 0.1603 | 0.1943 | 0.2230 | 0.2202 |
| 2 | 0.0889 | 0.1308 | 0.1966 | 0.1955 |
| 3 | 0.0696 | 0.1197 | 0.1794 | 0.1694 |
| 4 | 0.0628 | 0.0969 | 0.1596 | 0.1351 |
| 5 | 0.0468 | 0.0677 | 0.1247 | 0.1191 |

6.5.4.4 Effect of light intensity on algal growth

Figure 6.14, represents the time histories of biomass concentration of *L. subtilis* JUCHE1 with respect to over 0-4 days using light intensity, in the range of 1.45-3.2 kLux, as a parameter. The Figure 6.14, reveals that the growth curve shows exponentially increasing trend upto 3rd days, followed by a declining trend under the light intensity of 1.45, 2.5 and 3.2 kLux. In case of 1.95 kLux the growth curve slows down and finally saturates on 4th days. The declining and saturating trends can be explained by the depletion of carbon source with time, as observed in case of experiments with the variation of inlet CO₂ concentration. The maximum biomass concentration of 0.7196 g/L is obtained at 3rd day for 2.5 kLux light intensity. The time history curves corresponding to a higher light intensity lies above that for a lower light intensity except that obtained at 3.2kLux. The growth curve at 3.2kLux lies below that at 2.5kLux. Thus, the biomass time history obtained at 2.5kLux lies above all other and hence it can be considered to be the optimum light intensity for the growth of *L.subtilis* JUCHE1. There are also reported data on photo-inhibition beyond certain light intensities for other algal strains [30, 31, 32].

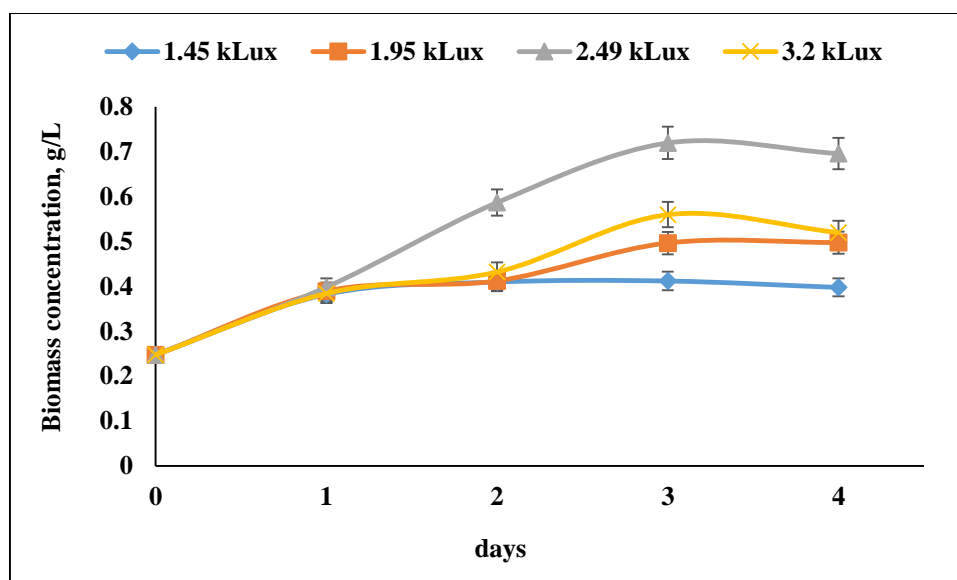


Figure 6.14 Growth curve of *L.subtilis* JUCHE1 varying light intensities from 1.45-3.2 kLux for 0-4 days under photoautotrophic growth.

All the experimental values of biomass concentrations and productivities at each time interval for all light intensities are also provided below in Table 6.16. The time trajectories of biomass productivities have been represented in Figure 6.15 using the light intensities (1.45-3.2 kLux) as a parameter. In case of light intensity of 1.45, 1.95 and 3.2 kLux, an increasing trend is observed up to 1st day beyond which there exist a decreasing trend. However, at 2.49 kLux, the biomass productivity increases up to 2nd days followed by a decreasing trend. The highest value of biomass productivity of 0.1696g/L/d is also obtained on the 2nd day at 2.5kLux. Pavlik et al. 2017, conducted the experiment in Pilot-scale algae photobioreactors (APBs) varying light intensities from 31-531 $\mu\text{mol m}^{-2} \text{s}^{-1}$ to observe their effect on the growth of algal strain, *Chlorella vulgaris* 395 [33]. They reported that the maximum biomass concentration and productivity of 1.30 g/ L and 0.40 g /L/d respectively were obtained at 531 $\mu\text{molm}^{-2} \text{s}^{-1}$ photosynthetic photon flux density (PPFD)[33]. In another article, the effect of variation of light intensity, in the range of 60–540 $\mu\text{molm}^{-2}\text{s}^{-1}$, on the growth and CO₂ fixation capability of *Scenedesmus obliquus* CNW-N was studied [34]. The article reported the highest values of biomass concentration, productivity, CO₂ fixation rate and lipid content of $2.10 \pm 0.08\text{g/L}$, $440.68 \pm 15.79\text{g/L/d}$, $744.75 \pm 26.69 \text{g/L/d}$ and 10.32% under culture conditions of 90% nitrogen source, at 140 $\mu\text{mol m}^{-2} \text{s}^{-1}$ light intensity, 2.5% CO₂ concentration [34].

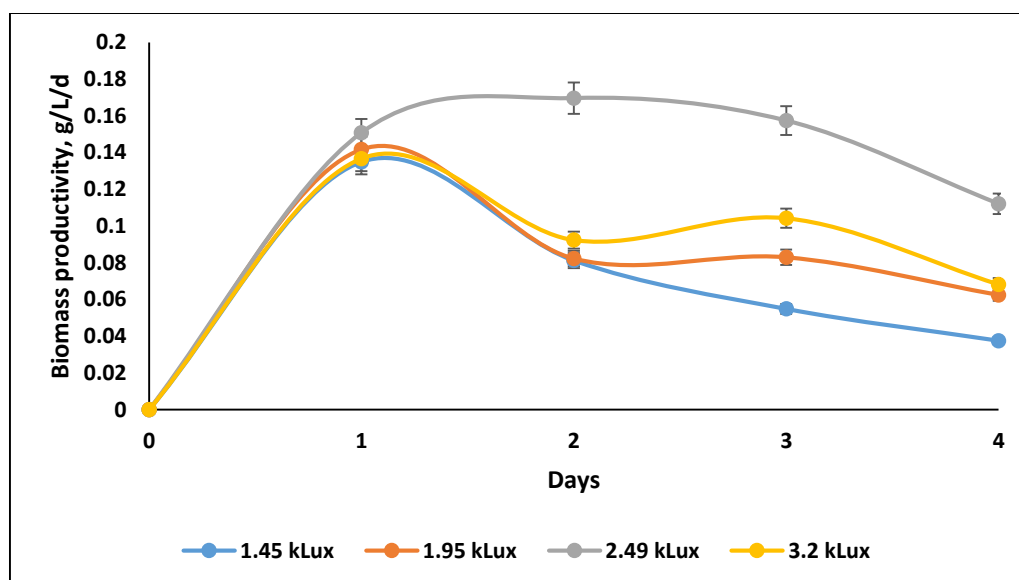


Figure 6.15 Biomass productivities (g/L/d) of *L. subtilis* JUCHE1 for all light intensities for 0-4 days.

Table 6.16 The experimental values of biomass concentrations and productivities at each time intervals under the irradiance of light intensities having range of 145-3.2kLux.

| Days | Biomass concentrations g/L | | | | Biomass productivities(g/L/d) | | | |
|----------|----------------------------|--------|--------|--------|-------------------------------|--------|--------|--------|
| | Light intensity (kLux) | | | | Light intensity (kLux) | | | |
| | 1.45 | 1.95 | 2.49 | 3.2 | 1.45 | 1.95 | 2.49 | 3.2 |
| 0 | 0.2473 | 0.2473 | 0.2473 | 0.2473 | 0 | 0 | 0 | 0 |
| 1 | 0.3822 | 0.389 | 0.3981 | 0.384 | 0.1349 | 0.1417 | 0.1508 | 0.1367 |
| 2 | 0.4097 | 0.4119 | 0.5866 | 0.432 | 0.0812 | 0.0823 | 0.1696 | 0.0924 |
| 3 | 0.412 | 0.4963 | 0.7196 | 0.56 | 0.0549 | 0.083 | 0.1574 | 0.1042 |
| 4 | 0.3976 | 0.4973 | 0.6959 | 0.5201 | 0.037575 | 0.0625 | 0.1122 | 0.0682 |

6.5.4.4.1 CO₂ fixation rate of *L. subtilis* JUCHE1 under different of light intensities

The bar plot of dynamics of CO₂ fixation rates for the variation of light intensity is represented in Figure 6.16. The figure reveals that the fixation dynamics has an upward tendency with increase in light intensity from 1.45-2.49kLux. However, beyond 2.5 kLux the CO₂ capture

rate decreased. The highest value of CO₂ fixation rate of 0.8176g/L/d was observed at 2.49kLux.

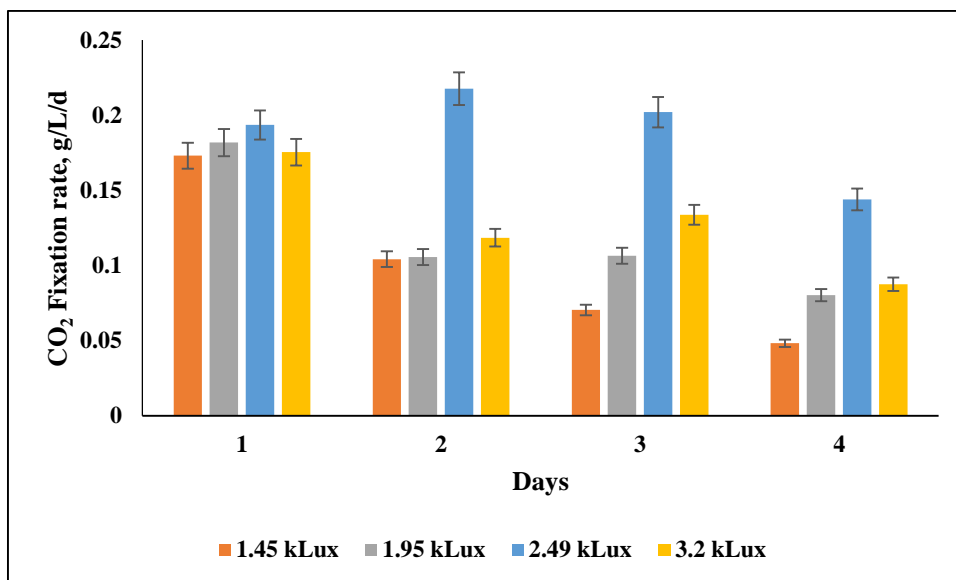


Figure 6.16 Time histories plot of CO₂ fixation rate of *L.subtilis* JUCHE1 varying light intensities from 1.45-3.2kLux

Table 6.17 Values of CO₂ fixation rate (g/L/d) at each time intervals under the irradiance of light intensities having range of 145-3.2kLux.

| Days | CO ₂ fixation rate (g/L/d) | | | |
|------|---------------------------------------|--------|--------|--------|
| | Light intensity(kLux) | | | |
| | 1.45 | 1.954 | 2.497 | 3.2 |
| 0 | 0 | 0 | 0 | 0 |
| 1 | 0.1731 | 0.1818 | 0.1935 | 0.1754 |
| 2 | 0.104 | 0.1056 | 0.2177 | 0.1185 |
| 3 | 0.0704 | 0.1065 | 0.2020 | 0.1337 |
| 4 | 0.0482 | 0.0802 | 0.1439 | 0.0875 |

6.5.4.5 Predictive modeling and simulation

6.5.4.5.1 Statistical validation of mathematical growth models

From the discussions in section 6.5.1.5.1 it is clear that while Monod model can explain the dependence of specific growth rate on NaNO_3 , Steele model can explain the functionality on I. The multivariable dependence of specific growth rate is however represented by Equation 5.15. The statistical analysis, as provided in Table 6.18, establishes the same due to the very low RMSE values, signifying the goodness of fit for all models. The same is established due to low values of % SEP for the models under consideration. The values of % SEP for Haldane model (Experimental), Haldane model (predicted), and Monod model are 6.123, 4.23 and 2.58 % respectively when used to represent the growth kinetics on CO_2 and NaNO_3 respectively. On the other hand, the values of % SEP for the three mathematical models, namely, Aiba, Steele and Bernard and Remond used for growth kinetics with respect to light intensity, lie in the range of 3.125-3.4787. As the % SEP values of all growth models lie below 10%, they can be approved as “best fitted models” for the respective cases [35]. The values of bias factor, B_f , another statistical parameter for the assessment of fitness of model, are provided in Table 6.16. In case of Haldane model (Experimental), Haldane model (predicted), Monod model are used for the growth kinetics with respect to CO_2 and NaNO_3 variation, the values of B_f are 0.9613, 1.024 and 1 respectively. Similarly, in case of Aiba, Steele and Bernard and Remond models, values of B_f lie between 0.9997-1.0117. Since it is known that the value of B_f in the range of 0.9- 1.05 represents good fitness of mathematical models, the validity of all models under consideration is thus re-confirmed [35]. In case of combined kinetic model, the predicted values of specific growth rate have been compared with the experimental ones at different set of input variables decided through design of experiment. Both the experimental and the simulated values have been represented in the Table 6.21. The values of parameters of statistical analysis have been provided in the Table 6.18. From the values of the parameters, it is confirmed that there is a perfect agreement between the experimental and simulated values.

Table 6.18 Statistical Analysis for the validation of predictive growth models

| Substrate/P arameter | Range | Growth Kinetic Model | Constant Parameters | Statistical Analysis values | | |
|---|--|--|---|-----------------------------|--------|----------------|
| | | | | RMSE | %SEP | B _f |
| CO ₂ | 5– 20% (v/v) | Haldane (Method-I) [described in section 5.1.6 in Chapter 5] | $\mu_{max,CO_2} =$ 0.6064 d ⁻¹ $k_{s,CO_2} = 0.0165$ g/L $k_{I,CO_2} = 1.7429$ g/L | 0.0253 | 6.123 | 0.9613 |
| | | Haldane (Method-II) [described in section 5.1.6 in Chapter 5] | $\mu_{max,CO_2} = 0.65$ d ⁻¹ $k_{s,CO_2} = 0.0162$ g/L $k_{I,CO_2} = 1.97$ g/L | 0.0174 | 4.23 | 1.024 |
| NaNO ₃ | 1 – 2.5 (g/L) | Monod | $\mu_{max,NaNO_3} =$ 0.667d ⁻¹ $k_{s,NaNO_3} = 0.644$ g/L | 0.0098 | 2.58 | 1 |
| Light intensity | 1.45-3.2 (kLux) | Aiba | $K_{S,I} = 0.092$ kLux $K_{I,I} = 217.390$ kLux | 0.026 | 3.478 | 1.000 |
| | | Steele | - | 0.0237 | 3.125 | 1.005 |
| | | Bernard & Remond | $\mu_{max,I} =$ 0.4673d ⁻¹ $\alpha = 0.49816$ | 0.026 | 3.479 | 1.012 |
| f_{NaNO_3} | | Monod | $\alpha_1 = 1.3919$ d ⁻¹ $\beta_1 = 0.798$ g/L | 0.164 | 22.35 | 0.847 |
| CO ₂ - NaNO ₃ -I | CO ₂ : 5– 20% NaNO ₃ : 1 – 2.5 (g/L) I: 1.45-3.2 (kLux) | $\mu = \frac{0.65 * C_{CO_2}}{0.0162 + C_{CO_2} + \frac{C_{CO_2}^2}{1.97}}$ $* \frac{\alpha_1 * C_{NaNO_3}}{\beta_1 + C_{NaNO_3}} * \left(\frac{I}{I_{Optimum}} \right)$ $* \exp\left(1 - \frac{I}{I_{Optimum}}\right)$ | $\mu_{max,CO_2} = 0.65$ d ⁻¹ $k_{s,CO_2} =$ 0.0162 g/L $k_{I,CO_2} = 1.97$ $\alpha_1 = 1.3919$ d ⁻¹ $\beta_1 = 0.798$ g/L | 0.0009 | 0.1814 | 0.9999 |

6.5.4.6 Effect of light intensity on algal growth

Figure 6.17, represents the dependence of specific growth rate with light intensity in the range of 1.45- 3.2 kLux. It is observed that the value of the specific growth rate passes through a maximum at $I=2.5$ kLux. Therefore, the optimum value of light intensity is 2.5 kLux. The observed, normalized and simulated values of specific growth rate at each light intensities are provided in table 6.18.

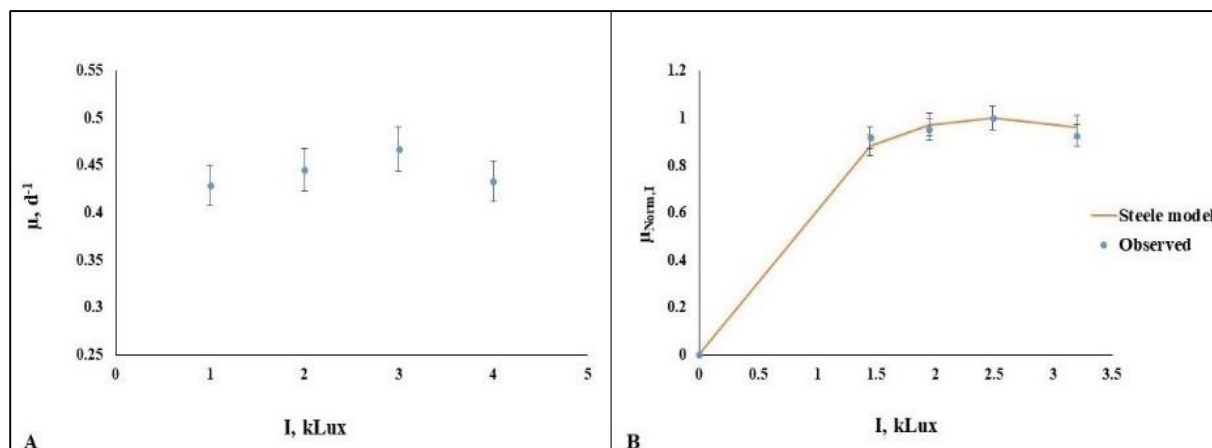


Figure 6.17 Graphical plots of : (A) Experimental variation of μ against light intensity and (B) Comparison of observed and simulated values of $\mu_{Norm,I}$ using Steele model against light intensity.

Table 6.19 Normalized experimental and calculated values of specific growth rates, $\mu_{Norm,I}$ for three different growth models such as Steele, Aiba and Bernard and Remond varying light intensities in the range of 1.45- 3.2 kLux.

| Light intensity (kLux) | Observed μ, d^{-1} | Normalized μ, d^{-1} | Steele model μ, d^{-1} | Bernard and remond | Aiba model |
|------------------------|------------------------|--------------------------|----------------------------|--------------------|------------|
| 1.45 | 0.4285 | 0.917 | 0.8842 | 0.8986 | 0.917 |
| 1.95 | 0.4453 | 0.953 | 0.9728 | 0.9779 | 0.953 |
| 2.49 | 0.4673 | 1 | 1 | 1 | 1 |
| 3.2 | 0.4330 | 0.9266 | 0.9633 | 0.9769 | 0.9266 |

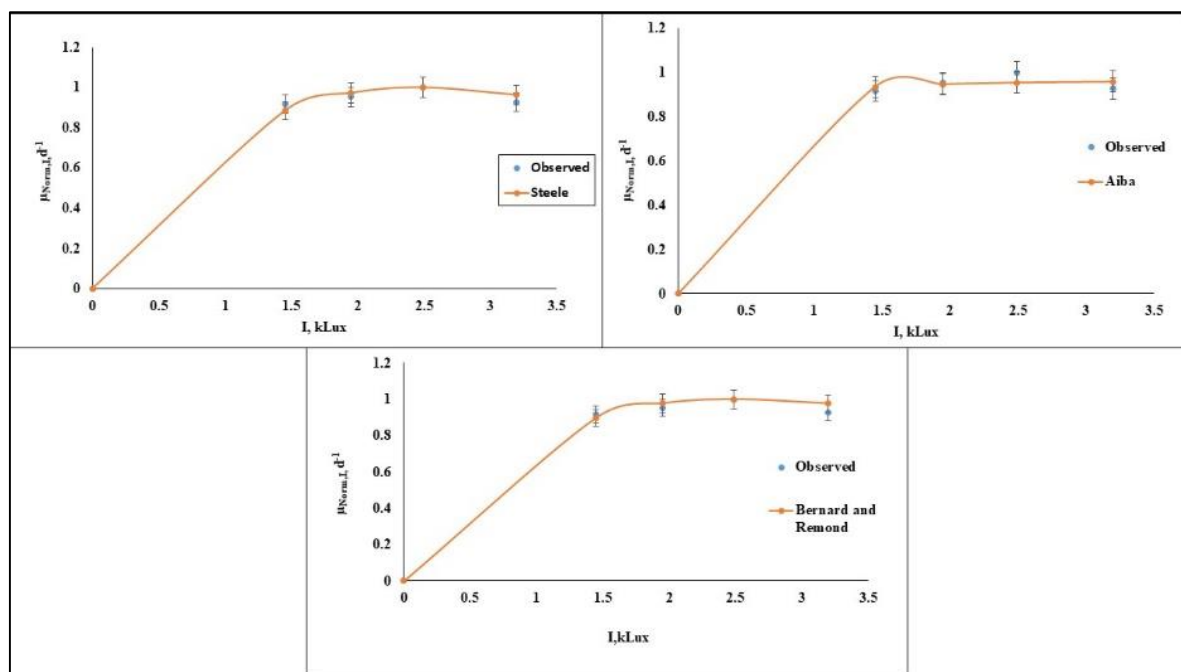


Figure 6.18 Growth curve of the normalized values of specific growth rate of experimental and simulated models of Steele, Aiba and Bernard and Remond have been compared.

In Figure 6.18, the normalized values of specific growth rate, simulated using Aiba, Steele and Bernard and Remond models have been compared with the experimental ones. The observed and simulated model values of specific growth rates were provided above in table 6.19. The close analysis reveals that although three models are in good agreement with the experimental observations, the Steele model is the fittest one. This is also established from the values of statistical assessment parameters provided in Table 6.18. The comparison of the experimental and simulated values of the normalized specific growth rate using Steele model ($\mu_{Norm,I} = \frac{\mu}{\mu_{Optimum,I}} = \frac{I}{2.5} * \exp(1 - \frac{I}{2.5})$) is represented in Figure 6.17(B).

6.5.4.7 Growth kinetics incorporating Combined effects of CO₂- NaNO₃-I

6.5.4.7.1 Correction factor for NaNO₃

The parameters, α_1 and β_1 , involved in the Eq. 6.5 defining f_{NaNO_3} have been determined by regression analysis of the functionality of $\frac{1}{f_{NaNO_3}}$ on $\frac{1}{C_{NaNO_3}}$. The plot of $\frac{1}{f_{NaNO_3}}$ against $\frac{1}{C_{NaNO_3}}$, represented in Figure 6.19 shows the linear relationship between them. From the regression equation, the values of α_1 and β_1 have been determined to be 1.3919 and 0.798g/L respectively. The normalized values of μ , (d^{-1}) with respect to each NaNO₃ concentrations from 1-2.5 g/L

are provided in Table 6.20. Thus, the functionality of f_{NaNO_3} on C_{NaNO_3} can be represented as follows:

$$f_{NaNO_3} = \frac{1.3919 \times C_{NaNO_3}}{0.798 + C_{NaNO_3}} \quad (6.5)$$

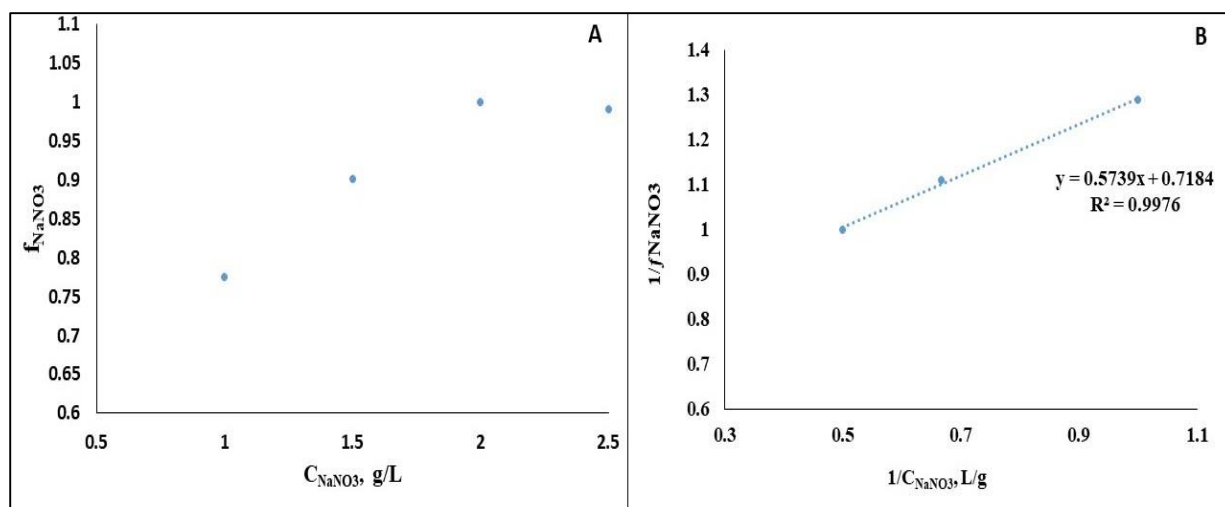


Figure 6.19 The growth kinetic plots: (A) f_{NaNO_3} versus each concentration of $NaNO_3$ (C_{NaNO_3}) and (B) Double reciprocal plot of $\frac{1}{f_{NaNO_3}}$ versus $\frac{1}{C_{NaNO_3}}$.

Table 6.20 Normalized values of μ , (d^{-1}) with respect to each $NaNO_3$ concentrations from 1-2.5 g/L.

| $NaNO_3$ Concentration s (g/L) | μ , (d^{-1}) | μ_{opt} (Optimum) | $f_{NaNO_3} = \mu/\mu_{opt}$ | $1/C_{NaNO_3}$ (L/g) | $1/f_{NaNO_3}$ (d) |
|--------------------------------------|----------------------|--------------------------|------------------------------|-------------------------|-----------------------|
| 0 | 0 | 0.52 | 0 | 0 | 0 |
| 1 | 0.4032 | | 0.7754 | 1 | 1.2896 |
| 1.5 | 0.4689 | | 0.9016 | 0.6666 | 1.1091 |
| 2 | 0.52 | | 1 | 0.5 | 1 |
| 2.5 | 0.5151 | | 0.9906 | 0.4 | 1.009 |

6.5.4.7.2 Correction factor for Light Intensity

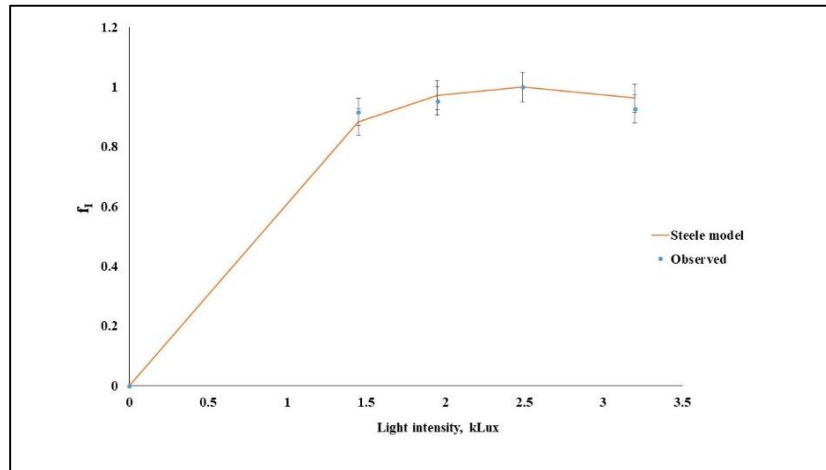


Figure 6.20 Comparison between experimental and simulated (Steele model) trend of f_I against light intensity.

As f_I and $\mu_{Norm,I}$ are analogous, the Steele model explains the relationship. Thus, the functionality of f_I on I can be represented as a function of I in Figure 6.20.

The functionality can be represented as follows:

$$f_I = \frac{I}{2.5} * \exp\left(1 - \frac{I}{2.5}\right) \quad (6.6)$$

By inserting the values of all parameters, the combined growth kinetic equation reduces to the following form:

$$\mu = \frac{0.65 * C_{CO_2}}{0.0162 + C_{CO_2} + \frac{C_{CO_2}^2}{1.97}} * \frac{1.3919 * C_{NaNO_3}}{0.798 + C_{NaNO_3}} * \left(\frac{I}{2.5} * \exp\left(1 - \frac{I}{2.5}\right)\right) \quad (6.7)$$

In Table 6.22 the predicted values of specific growth rate using Eq. (6.7) have been compared with the experimental values. The values of statistical parameters, namely, RMSE, %SEP, and B_f provided in Table 6.18 indicate that all the model equations are valid. The values of RMSE, %SEP, and B_f for the combined kinetic model are 0.0009, 0.1814 and 0.9999 respectively.

6.5.4.8 Response surface methodology (RSM)

A second-order polynomial equation (eq. 6.8) to correlate μ with different parameters, A, B and C, have been obtained.

$$\mu = 0.5157 + 0.0441 \times A + 0.0712 \times B + 0.0202 \times C + 0.0069 \times AB + 0.0019 \times AC + 0.0031 \times BC - 0.024 \times A^2 - 0.0219 \times B^2 - 0.0363 \times C^2 \quad (6.8)$$

Table 6.21 The ANOVA table for the quadratic model.

| Source | Sum of Squares | df | Mean Square | F-value | p-value | |
|---------------------------|----------------|----|-------------|----------|----------|--------------------|
| Model | 0.0708 | 9 | 0.0079 | 5252.47 | < 0.0001 | Significant |
| A-CO₂ | 0.0155 | 1 | 0.0155 | 10368.22 | < 0.0001 | |
| B-NaNO₃ | 0.0406 | 1 | 0.0406 | 27108.85 | < 0.0001 | |
| C-Light Intensity | 0.0033 | 1 | 0.0033 | 2188.47 | < 0.0001 | |
| AB | 0.0002 | 1 | 0.0002 | 126.31 | < 0.0001 | |
| AC | 0.0000 | 1 | 0.0000 | 9.89 | 0.0163 | |
| BC | 0.0000 | 1 | 0.0000 | 25.99 | 0.0014 | |
| A² | 0.0025 | 1 | 0.0025 | 1668.60 | < 0.0001 | |
| B² | 0.0020 | 1 | 0.0020 | 1344.70 | < 0.0001 | |
| C² | 0.0055 | 1 | 0.0055 | 3697.51 | < 0.0001 | |
| Residual | 0.0000 | 7 | 1.498E-06 | | | |
| Lack of Fit | 0.0000 | 3 | 3.495E-06 | | | |
| Pure Error | 0.0000 | 4 | 0.0000 | | | |
| Cor Total | 0.0708 | 16 | | | | |

Values greater than 0.1000 indicate that the model terms are not significant. Therefore, the following equation (Eq. 6.9) considering only the significant terms can be used to correlate the response factor, μ with the factors, A, B and C.

From the ANOVA table 6.21, it is observed that A, B, C, AB, BC, A², B², C² are significant model terms, the P-values being less than 0.0500. Therefore, the quadratic equation reduces to the following:

$$\mu = 0.5157 + 0.0441 \times A + 0.0712 \times B + 0.0202 \times C + 0.0069 \times AB + 0.0031 \times BC - 0.024 \times A^2 - 0.0219 \times B^2 - 0.0363 \times C^2 \quad (6.9)$$

Table 6.22 Fit statistics summary.

| | | | |
|------------------|--------|--------------------------------|----------|
| Std. Dev. | 0.0012 | R² | 0.9999 |
| Mean | 0.4769 | Adjusted R² | 0.9997 |
| C.V. % | 0.2566 | Predicted R² | 0.9976 |
| | | Adeq Precision | 245.6751 |

The **Predicted R²** of 0.9976 is in reasonable agreement with the **Adjusted R²** of 0.9997; i.e. the difference is less than 0.2. This signifies that similar to the combined model, based on actual growth kinetics, the quadratic model equation derived through statistical analysis is equally capable of predicting multi-variable dependence of specific growth rate on the most important input parameters (CO₂, NaNO₃ and I). Figure 6.21 represents the correlation plot of actual versus predicted values of specific growth rate, μ (d⁻¹), obtained using Eq.6.9 The figure clearly shows that the deviation level between the experimental and predicted values is almost negligible. The low level of deviation indicates the goodness of fit of the model equation.

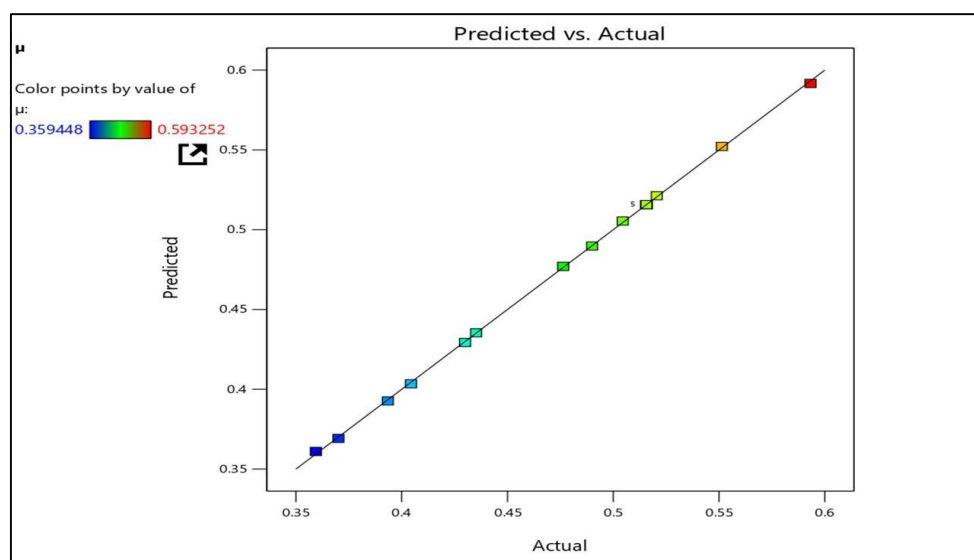


Figure 6.21 Predicted versus Actual plot of specific growth rate, μ (d⁻¹)

The fitness parameters of the statistical analysis in table 6.22. The correlation plot of actual versus predicted values of specific growth rate, μ (d⁻¹) has been represented in Figure 6.21. In Table 6.23, the experimental values of specific growth rate, μ (d⁻¹) have been compared with the predicted values using the quadratic model equation (Eq.6.8) at different combinations of input variables (CO₂, NaNO₃ and Light intensity) have been provided.

Table 6.23 The comparison of experimental values of set of “ μ ” with the prediction of Kinetic Model and the Quadratic Model Equation using Box–Behnken Design method

| Run | A (CO ₂ Concentrations (g/L)) | B NaNO ₃ Concentrations (g/L) | C Light intensity (kLux) | Output response μ , (d ⁻¹) | | |
|-----|--|---|-----------------------------------|---|--------------------|--------------------|
| | | | | μ_{Exp} | $\mu_{Sim(Eq.15)}$ | $\mu_{Sim(Eq.17)}$ |
| 1 | 0.13618 | 2.5 | 3.2 | 0.551313 | 0.551313 | 0.552172 |
| 2 | 0.2178 | 2.5 | 2.325 | 0.593252 | 0.593252 | 0.591651 |
| 3 | 0.13618 | 1.75 | 2.325 | 0.515707 | 0.515707 | 0.515707 |
| 4 | 0.05456 | 1.75 | 3.2 | 0.429966 | 0.429966 | 0.431259 |
| 5 | 0.2178 | 1.75 | 1.45 | 0.476339 | 0.476339 | 0.478893 |
| 6 | 0.2178 | 1 | 2.325 | 0.435183 | 0.435183 | 0.435411 |
| 7 | 0.13618 | 1.75 | 2.325 | 0.515707 | 0.515707 | 0.515706 |
| 8 | 0.05456 | 2.5 | 2.325 | 0.490007 | 0.490007 | 0.489779 |
| 9 | 0.13618 | 1.75 | 2.325 | 0.515707 | 0.515707 | 0.515707 |
| 10 | 0.13618 | 1 | 3.2 | 0.404419 | 0.404419 | 0.403449 |
| 11 | 0.05456 | 1.75 | 1.45 | 0.393441 | 0.393441 | 0.390775 |
| 12 | 0.13618 | 1 | 1.45 | 0.370064 | 0.370064 | 0.369204 |
| 13 | 0.13618 | 1.75 | 2.325 | 0.515707 | 0.515707 | 0.515707 |
| 14 | 0.05456 | 1 | 2.325 | 0.359448 | 0.359448 | 0.361049 |
| 15 | 0.13618 | 2.5 | 1.45 | 0.504479 | 0.504479 | 0.505449 |
| 16 | 0.13618 | 1.75 | 2.325 | 0.515707 | 0.515707 | 0.515707 |
| 17 | 0.2178 | 1.75 | 3.2 | 0.52056 | 0.52056 | 0.519377 |

6.5.4.8.1 Effect of the interaction of coded variables: (A) CO₂ Concentration, (B) NaNO₃ Concentration and (C) Light Intensity on the specific growth rate

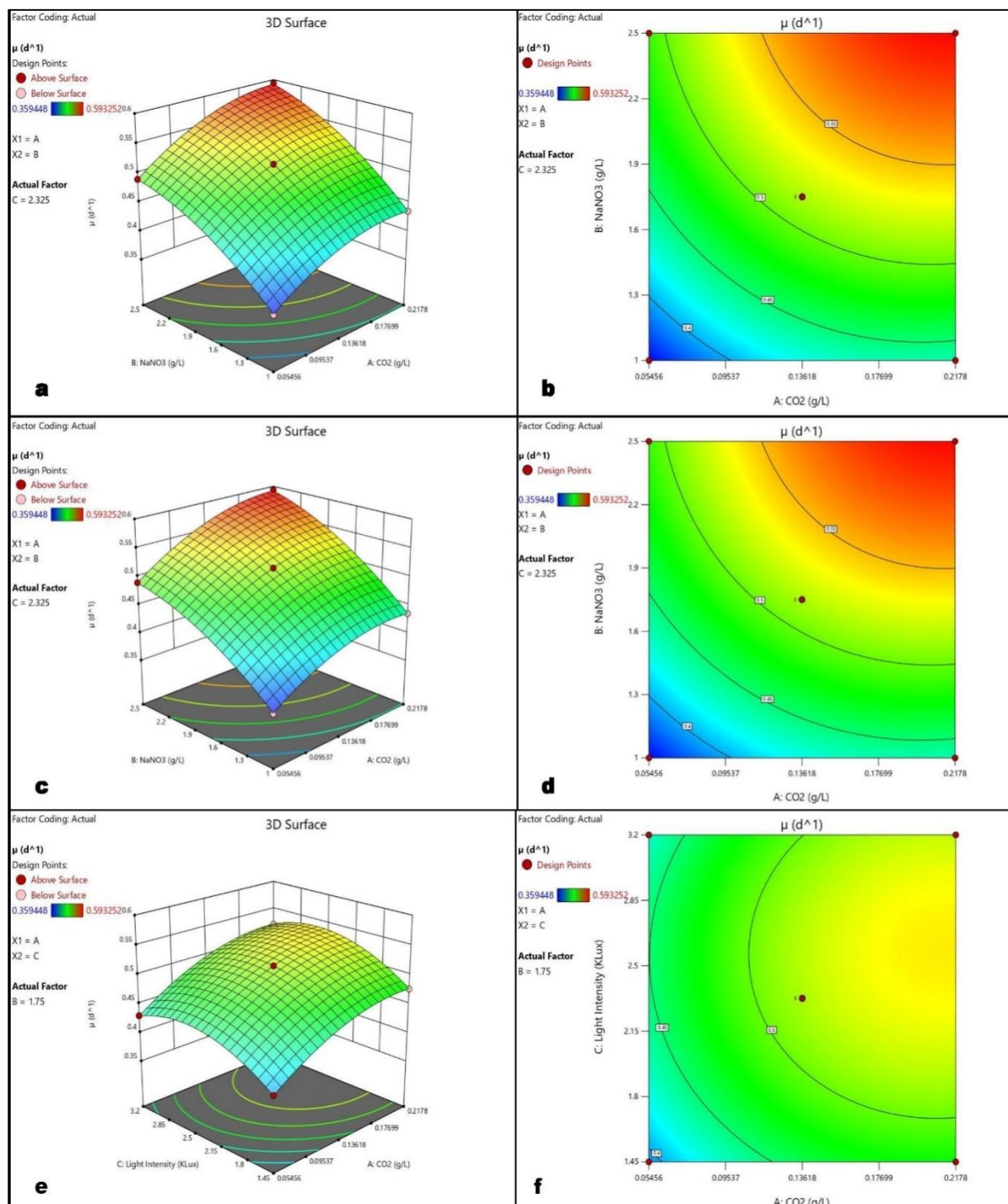


Figure 6.22 The change of μ according to AB: CO₂ concentration (g/L) and NaNO₃ concentrations (g/L) , BC: NaNO₃ concentrations (g/L) and Light intensities (kLux) and AC: CO₂ concentrations (g/L) and Light intensities (kLux) using Box–Behnken method (a, c, e) 3-D model graphs, (b, d, f) Contour Graphs.

The 3D and contour plots show the effect of three input variables (A) CO₂ Concentration, (B) NaNO₃ Concentration and (C) Light Intensity on the algal growth rate (μ) of *L. subtilis* JUCHE1. Figure 6.22, shows the dependence of the specific growth rate on A and B; A and C and B and C respectively. While considering two parameters affecting the growth rate, the third parameter was considered constant at the optimum value. The three-dimensional (3-D) plots along with the contour plot of AB in Figure 6.22 (a) and 4 (b) depicts that with the increase in (B) NaNO₃ concentrations (1-2.5 g/L) along with the (A) CO₂ concentrations (0.05456-0.2178 g/L) the growth curve of " μ " simultaneously increases. In similar manner, the 3D and contour plot of BC in Figure 6.22 (c) and 16 (d), clearly shows that the growth rate μ increases with increase in both the parameters i.e. (B) NaNO₃ concentrations and (C) Light intensity. Figure 6.22(e) and 16 (f) A clearly depicts that when both the parameter (A) CO₂ concentrations (0.05456- 0.2178 g/L) and (C) light intensity (1.45-3.2 kLux) increase, the growth rate of *L. subtilis* JUCHE1 also increases from 0.3593-0.5932 d⁻¹.

6.5.5 Effect of organic carbon source (Glycerol) on growth of algal biomass under photoheterotrophic condition

In Figure 6.23, the growth curves were constructed for photoheterotrophic growth using equivalent glycerol concentrations, as described in the materials and methods section, as a parameter. From the analysis of the Figure 6.23, it is clear that the span of exponential phase of photoheterotrophic growth for all C- concentrations were extends up to 4 days. The short length of lag phase ascertains that the blue-green alga *Leptolyngbya subtilis* JUCHE1 is well adapted to the medium of both photoautotrophic and photoheterotrophic growth. The batch experiments were conducted in 30 mL respectively as working volume during photoheterotrophic growth, in once-charged mode. Therefore, the nutrients got depleted due to their high rate of up-take, as evident from the sharply increasing trend of growth curve over two days and the appearance of plateau either on 4th day (96 h). Although in many cases a long period of growth is reported for algae, early saturation has been observed in case of growth of microalga *Chlorella sorokiniana*, cyanobacteria *Aphanizomenon flos-aquae* Naegeli, *Chlorococcum littorale* and so on [9, 36, 37, 38]. In photoheterotrophic growth with glycerol concentration equivalent to 15% CO₂ in the feed gas, the maximum biomass concentration and productivity are respectively 0.817 gL⁻¹ on 4th day and 0.2733 gL⁻¹d⁻¹ on the 1st day. From the literature review the maximum biomass productivity using treated waste glycerol at 5 gL⁻¹, 10 gL⁻¹ and 20 gL⁻¹ are 0.192±0.002 gL⁻¹d⁻¹, 0.196±0.009 and 0.198±0.009 gL⁻¹d⁻¹ respectively [39]. This clearly indicates that even at much higher concentrations of glycerol compared to

the present case, the biomass productivity of algal strain *Scenedesmus obliquus* is lower than that ($0.2733 \text{ gL}^{-1}\text{d}^{-1}$) of *Leptolyngbya subtilis* JUCHE1 under study [39]. One research study on different newly isolated strains of *Chlorella* using glycerol at 20 mM under constant illumination of 14 kLux indicates a variation of biomass concentration in the range of 0.4-0.8 g/L [36]. Therefore, the transformation of carbon to algal biomass is achieved more efficiently by *Leptolyngbya subtilis* JUCHE1 in comparison to other algal strains. In another study on *Chlorella minutissima* using $9.02\text{-}25.2 \text{ gL}^{-1} \text{ C}$, supplied from glycerin, i.e., $0.752\text{-}2.1 \text{ g-atom C/L}$ and hence 250-700 mM glycerol, the biomass concentration has been reported to vary from $5.31\text{-}7.28 \text{ g/L}$ [40]. Narayan et al. (2005), reported some observations on a cyanobacterium *Spirulina platensis* CFTRI grown on both bicarbonate and glycerol carbon sources[41]. In case of photo-heterotrophic growth mode, 2.5 mM of glycerol concentration was used for the production of biomass, lipid and pigments (chlorophyll, Phycocyaninetc.)[41]. It was reported that $0.1157 \pm 0.0049 \text{ g/L}$ of maximum biomass concentration was achieved [41]. Observed values of biomass concentration(g/L) and productivities (g/L/d) of *L.subtilis*JUCHE1 obtained at different CO_2 equivalent carbon concentrations of glycerol as parameter are provided in Table 6.24.

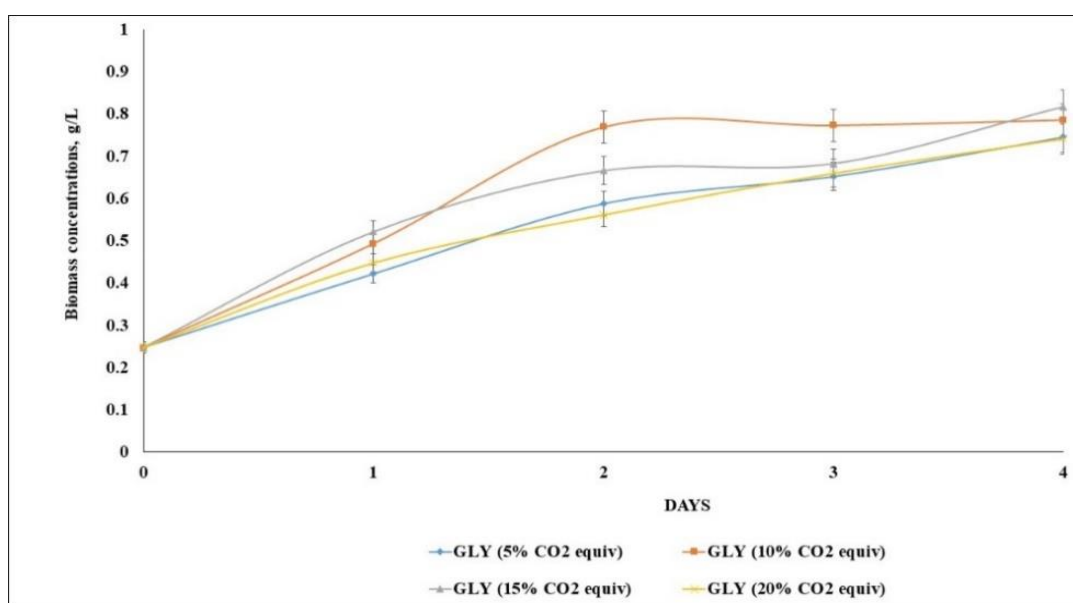


Figure 6.23 Biomass concentration time histories of *L.subtilis*JUCHE1 under photo-heterotrophic mode of growth.

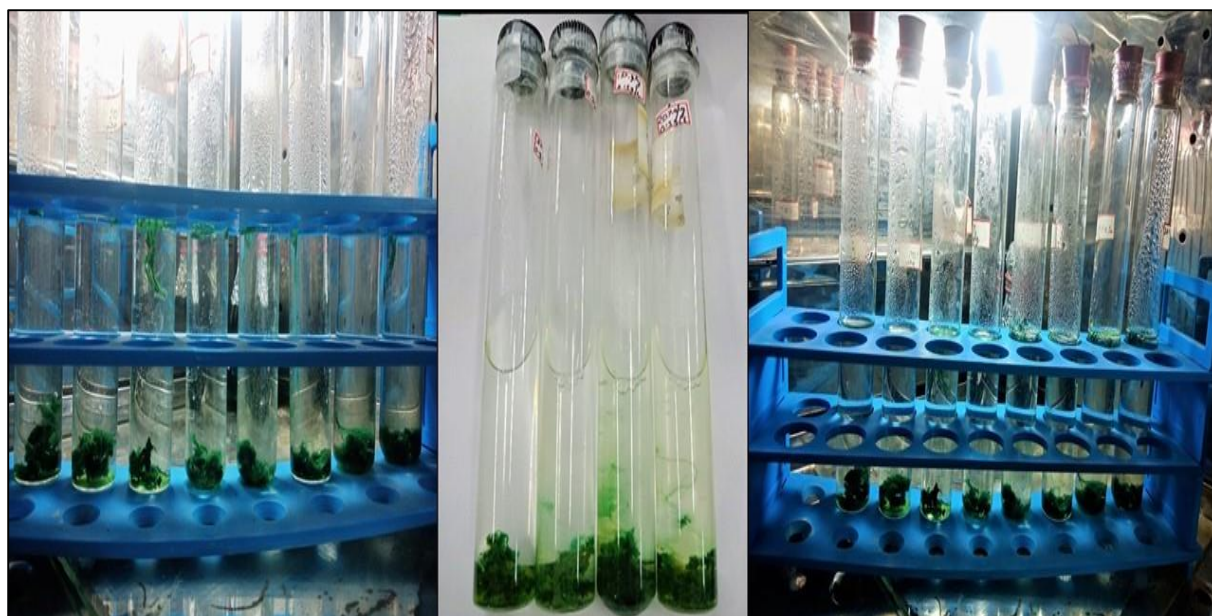


Figure 6.24 Algal growth at different CO₂ equivalent carbon concentrations of glycerol under photo heterotrophic growth.

Table 6.24 Experimental values of biomass concentrations (g/L) against each time intervals at different gas phase CO₂ equivalent glycerol concentrations under photoheterotrophic growth mode.

| Biomass concentrations g/L | | | | | Biomass productivities (g/L/d) | | | |
|----------------------------|---|--------|--------|--------|--------------------------------|--------|--------|--------|
| Days | Glycerol (C ₃ H ₈ O ₃) concentrations (g/L) | | | | | | | |
| | 0.0379 | 0.0759 | 0.1139 | 0.152 | 0.0379 | 0.0759 | 0.1139 | 0.152 |
| 0 | 0.2473 | 0.2473 | 0.2473 | 0.2473 | 0 | 0 | 0 | 0 |
| 1 | 0.422 | 0.493 | 0.5206 | 0.4473 | 0.1747 | 0.2457 | 0.2733 | 0.2 |
| 2 | 0.588 | 0.7688 | 0.6653 | 0.561 | 0.1703 | 0.2607 | 0.209 | 0.1568 |
| 3 | 0.6526 | 0.7727 | 0.6824 | 0.6595 | 0.1351 | 0.1751 | 0.1450 | 0.1374 |
| 4 | 0.746 | 0.7857 | 0.817 | 0.7413 | 0.1246 | 0.1346 | 0.1424 | 0.1235 |

It is also noticed that the maximum value of biomass concentration increases with the increase of gas phase CO₂ concentration up to 15%(v/v) used for saturation of aqueous medium and their glycerol equivalents. Beyond 15% CO₂ equivalent glycerol concentration the maximum value of biomass concentration decreases. The time history plot obtained at higher gas phase CO₂ equivalent concentration of glycerol lies above its counterpart obtained at lower concentration up to 15% with the exception of the plots obtained at 20% CO₂ equivalent glycerol concentration. The values of % carbon capture (CC) for each gas phase CO₂ equivalent

concentration of glycerol, respectively calculated using Equations 5.1 and 5.8 have been provided in Table 6.25

Table 6.25 Values of % carbon capture (CC) of *L.subtilis*JUCHE1 under photo-heterotrophic growth.

| Inlet-Carbon concentrations %(v/v) | CC (%) |
|------------------------------------|--------|
| 5 | 99.43 |
| 10 | 63.32 |
| 15 | 44.67 |
| 20 | 29.11 |

As compared to the previous study using CO₂ concentrations as inorganic carbon source, the values of carbon capture (CC) obtained for CO₂ equivalent glycerol concentration are higher for glycerol compared to its CO₂ equivalent regardless of the concentration. The carbon capture data shows that this strain of blue green alga *Leptolyngbya subtilis* JUCHE1 has a high potential of carbon sequestration. This may be due to the fact that this strain has been isolated from a water source of a power plant which environment is inherently rich in CO₂. The results also suggest that for *Leptolyngbya subtilis* JUCHE1 glycerol is a favorable carbon substrate besides CO₂ which is reflected in ultimate higher concentration of biomass obtained in the heterotrophic system. This can be because of the difference in the mechanisms of uptake of carbon under photoautotrophic and mixotrophic growth.

Cyanobacteria usually consists three bicarbonate transporters which are responsible for the trans-membrane passage of HCO₃⁻ into the cytoplasm. Cytoplasmic bicarbonate diffuses to carboxysome, containing carbonic anhydrase and enzyme 1,5 bisphosphate carboxylase (RubisCO). CO₂ is generated through the reaction catalyzed by carbonic anhydrase. OH⁻ ion is transported outside the cell and H⁺ is sequestered inside the thylakoid. CO₂ is assimilated in the photosynthetic system using RubisCO enzyme and biomass is formed [42, 43]. The higher biomass productivity under mixotrophic condition can be attributed to simultaneous assimilation of glycerol as carbon source and re-utilization of CO₂ liberated through photosynthesis [44]. The Literature review suggests that under photoheterotrophic /mixotrophic growth, there is a possibility of algal cell concentration and volumetric productivity [37, 45,46]. It was proposed that ATP formed in the photochemical reactions accelerated the anabolism using organic carbon source as glucose in the mixotrophic culture of *Euglena gracilis*[47].

6.5.5.1 Growth kinetics

The values of initial specific growth rate (μ , d^{-1}), using the data of $t=0$ and $t=1d$ are provided in table 6.26.

Table 6.26 The calculated values of Specific growth rate, $\mu(d^{-1})$ at each individual inlet- CO_2 equivalent glycerol concentrations under photo-heterotrophic growth condition.

| Inlet- CO_2 concentrations %(v/v) | Equivalent glycerol concentrations (g/L) | Specific growth rate, $\mu(d^{-1})$ |
|--|---|-------------------------------------|
| 5 | 0.0379 | 0.5220 |
| 10 | 0.0759 | 0.6638 |
| 15 | 0.1139 | 0.7119 |
| 20 | 0.1520 | 0.5759 |

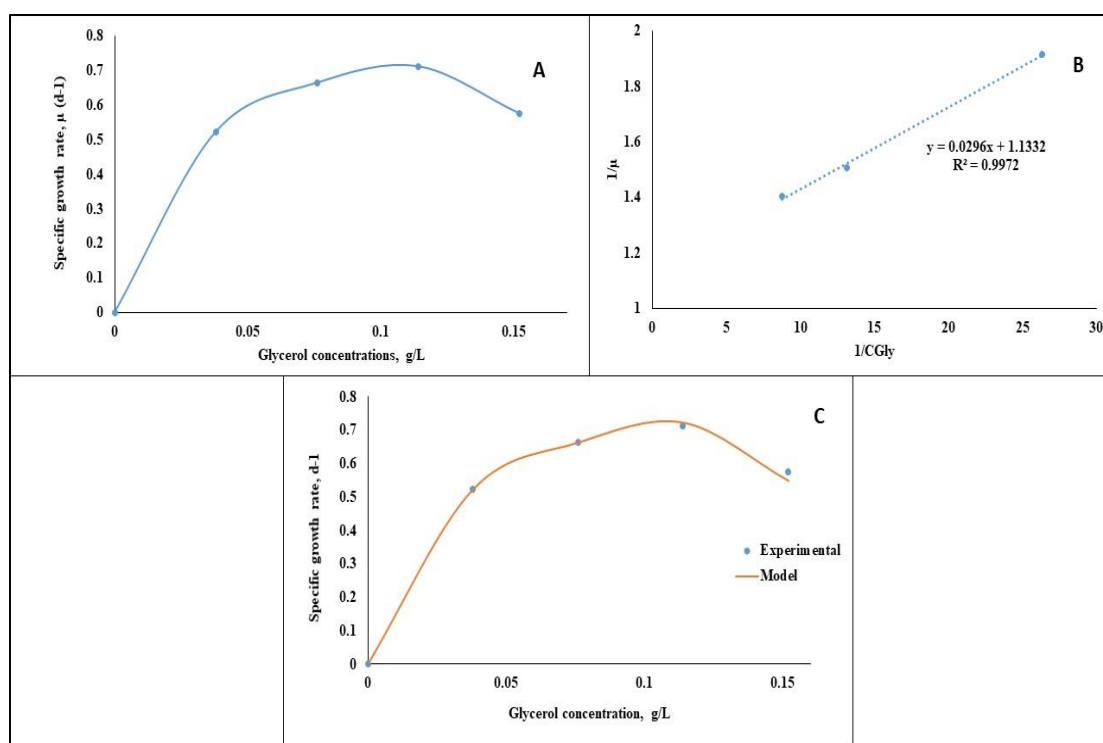


Figure 6.25 The growth kinetic plots (A, B and C) of *Leptolyngbya subtilis* JUCHE1 under photoheterotrophic growth using glycerol as organic carbon source: (A) Graphical representation of specific growth rates at different CO_2 equivalent glycerol concentrations (g/L), (B) Double reciprocal plot of $1/\mu$ versus $1/C_{gly}$, (C) Simulated and experimental values of specific growth rate “ μ ” against different CO_2 equivalent glycerol concentrations.

In Figure 6.25(A), the initial values of specific growth rates have been plotted against glycerol concentrations. It has been observed that the growth curve increases with increase in inlet-CO₂ equivalent concentration of glycerol i.e. up to 0.1139 g/L (15% inlet-CO₂) and beyond this inlet concentration the growth gets inhibited /declined. The values of specific growth rates for all glycerol concentrations have been calculated using the biomass concentrations over 0-1 day. The bell-shaped curve, depicted in Figure 6.25, clearly indicates the presence of substrate inhibition and hence the Haldane model, presented in equation 5.10 has been attempted. The value of regression coefficient, R² of 0.9972 of the double reciprocal plot, Figure 6.25 (B), obtained by plotting the inverse of μ against the inverse of glycerol concentration, establishes the validity of Monod model up to concentration of glycerol i.e. up to 0.1139 g/L, i.e., in the uninhibited zone of growth. The values of μ_{max} and K_s have been determined from the intercept and the slope of Figure 6.25 (B). As the value of $C_{S,max}$ corresponding to the maximum value of μ is 0.1139 g/L, hence the value of K_I have been determined by using the correlation, $C_{S,max} = \sqrt{K_s K_I}$ using Method-I, described in Section 5.1.6 of Section 5. The values of growth kinetic parameters, namely, μ_{max} , K_s , K_I have been determined to be 0.8824 d⁻¹, 0.0261 g/L and 0.4974 g/L, respectively. The RMSE value has been determined to be 0.06 and is high. The Method-II, described in Section 5.1.6 of Section 5 has also been applied. But it cannot be converged with the restriction of RMSE ≤ 0.02 with narrow adjustment of original μ'_{max} . Therefore, it appears that Haldane model is difficult to be valid in case of the heterotrophic growth on glycerol. Therefore, as described in Section 5.1.6 of Chapter 5, power law model, Equation 5.12 ($\mu = \mu_{without\ inhibition} \left(1 - \frac{C_S}{C_{S,crit}}\right)^n$) has been applied. Accordingly, $C_{S,crit}$, i.e., the glycerol concentration at which no growth is obtained, has been determined to be 0.25g/L. The value of $\mu_{without\ inhibition}$ at 0.152g/L has been determined using Monod model with already determined values of μ_{max} and K_s of 0.8824 d⁻¹, 0.0261 g/L respectively. Using the experimental value of μ and $\mu_{without\ inhibition}$ at 0.152g/L, the value of “n” has been determined to be 0.29. Figure 6.25 (C) shows the comparison of experimental and simulated trend of variation of specific growth rate “ μ ” against glycerol concentrations. The agreement is satisfactory and the RMSE value has been obtained to be 0.013.

Hence the growth kinetics on glycerol can be described as follows:

$$\text{For } 0 \leq C_S \leq \frac{0.1139g}{L}, \mu = \frac{0.8824C_{glycerol}}{0.0261+C_{glycerol}} \quad (6.10)$$

$$\text{For } C_S > 0.1139 \text{ g/L, } \mu = \left(\frac{0.8824 C_{\text{glycerol}}}{0.0261 + C_{\text{glycerol}}} \right) \left(1 - \frac{C_{\text{glycerol}}}{0.25} \right)^{0.29} \quad (6.11)$$

6.5.5.2 Glycerol Consumption

The time histories of conversion of glycerol have been plotted in Figure 6.26 using initial glycerol concentration as a parameter. As per expectation, the conversion of glycerol increases with time at all values of initial concentration. The trends are in agreement with those of time histories of biomass concentration under heterotrophic growth. Similar trend was observed by Abomohra et al. (2018), during their studies on *Scenedesmus obliquus* using glycerol as the carbon source [39]. All the experimental data's have been provided below in table 6.27.

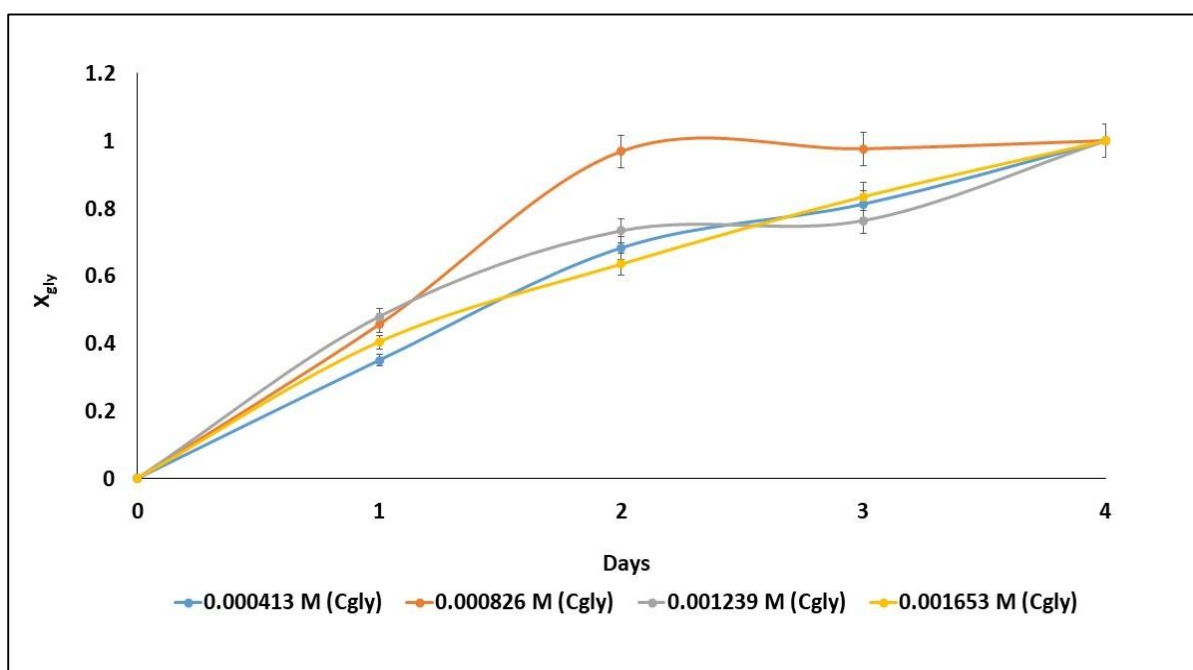


Figure 6.26 Glycerol consumption of *Leptolyngbya subtilis JUCHE1* at different time intervals under photo-heterotrophic growth.

Table 6.27 Values of glycerol consumption, X_{gly} against each time intervals at time (t) under photo-heterotrophic growth.

| Days | X_{gly} (t) | | | |
|------|---|-----------|-----------|-----------|
| | C_{gly} , Glycerol ($C_3H_8O_3$) concentrations (M) | | | |
| | 0.000413M | 0.000826M | 0.001239M | 0.001653M |
| 0 | 0 | 0 | 0 | 0 |
| 1 | 0.3503 | 0.4563 | 0.4797 | 0.4048 |
| 2 | 0.6831 | 0.9686 | 0.7337 | 0.635 |
| 3 | 0.8127 | 0.9758 | 0.7637 | 0.8344 |
| 4 | 1 | 1 | 1 | 1 |

6.5.6 Effect of mixture of inorganic + organic carbon source (CO_2 :Glycerol) in (1:1 ratio) on growth of algal biomass under mixotrophic condition

As mentioned previously the photo-autotrophic growth study was conducted by varying inorganic CO_2 concentrations from 5-20(%v/v). whereas, in photo-heterotrophic growth study the equivalent amount of carbon was supplied to the culture medium using glycerol as organic carbon source. In mixotrophic growth the batch study was conducted by using both the carbon sources ($CO_2 +$ Glycerol) in 1:1 ratio so that number of moles of supplied carbon lied equivalent to that supplied by 5-20(%v/v) CO_2 . The batch experiments were carried out for 0-5 days.

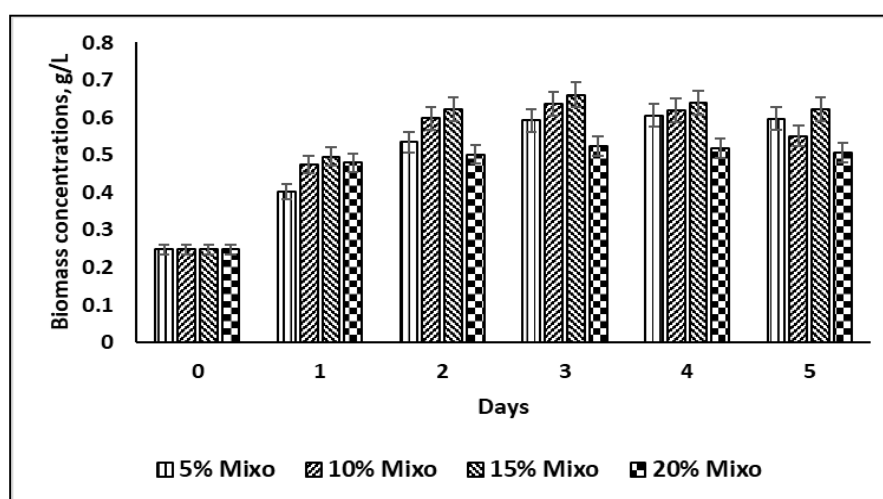


Figure 6.27 Biomass concentrations of *L. subtilis* JUCHE1 at each time intervals varying carbon concentrations under mixotrophic growth.

From the bar plot as shown in Figure 6.27 it has been found that the highest peak of biomass concentration is obtained for 15% mixture (CO₂:Glycerol::1:1) on 3rd day and the value is 0.6393 g/L. After analysing the trend of growth it has been revealed that in case of 10, 15 and 20% equivalent concentrations of carbon, the growth curve increases with increase in incubation time i.e. upto 0-3rd days and then decreases due to nutrient depletion in the growth medium. While in case of 5%, the growth curve shows increasing trend upto 0-4 days and then declined at 5th day. The mixotrophic growth is a combination of heterotrophic and autotrophic mode. In cases where inorganic and organic carbon has been supplied together, the system may shift between autotrophy and heterotrophy and due to complexity of mixotrophic mode, the growth efficiency of such a system is partially unpredictable [48]. All the experimental data of biomass concentrations and productivities were provided below in table 6.28

Table 6.28 Experimental values of biomass concentrations at each time interval under mixotrophic growth using CO₂ and glycerol as carbon sources.

| Equivalent moles of carbon using both the sources (CO ₂ and glycerol) in 1:1 ratio | | | | | | | | |
|---|------------------------------|--------|--------|--------|--------------------------------|--------|--------|--------|
| Days | Biomass concentrations (g/L) | | | | Biomass productivities (g/L/d) | | | |
| | 5 | 10 | 15 | 20 | 5 | 10 | 15 | 20 |
| 0 | 0.2473 | 0.2473 | 0.2473 | 0.2473 | 0 | 0 | 0 | 0 |
| 1 | 0.4012 | 0.4746 | 0.4953 | 0.4793 | 0.1539 | 0.2273 | 0.248 | 0.232 |
| 2 | 0.534 | 0.5973 | 0.6213 | 0.5013 | 0.1433 | 0.1750 | 0.187 | 0.127 |
| 3 | 0.5916 | 0.6366 | 0.66 | 0.5226 | 0.1147 | 0.1297 | 0.1375 | 0.0917 |
| 4 | 0.6048 | 0.6194 | 0.6393 | 0.5182 | 0.0893 | 0.093 | 0.098 | 0.0677 |
| 5 | 0.5966 | 0.5498 | 0.6219 | 0.5066 | 0.0698 | 0.0605 | 0.0749 | 0.0518 |

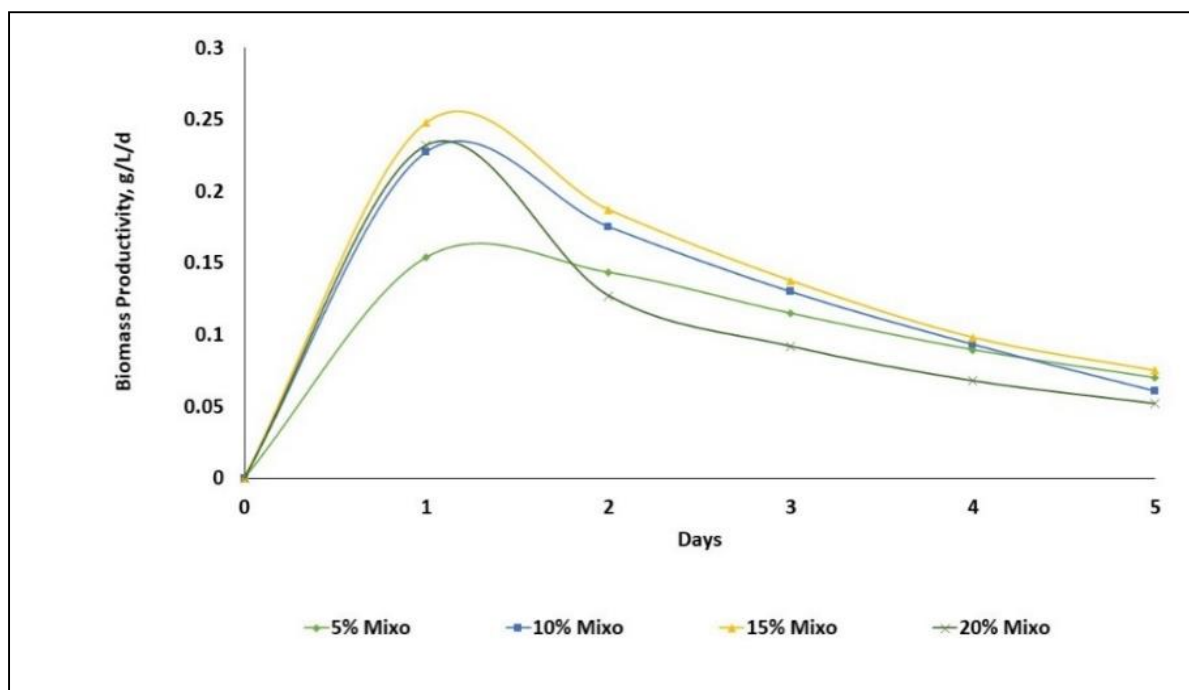


Figure 6.28 Biomass productivities (g/L/d) of *L.subtilis*JUCHE1 at each time intervals varying Carbon concentrations under mixotrophic growth.

From Figure 6.28, it has been observed that with increase in C-concentrations, the biomass production rate also increases from 5 to 15% C-concentration and the values of biomass productivity lies between 0.1539- 0.248g/L/d on 1st day. Beyond 15% the biomass productivity becomes inhibited at highest carbon concentration i.e. 20% and the value is found to be 0.232g/L/d on 1st day as shown in table 6.28.

The microalgae *Chlorella sp.* Y8-1 has been cultivated under mixotrophic condition using both organic carbon sources (Glucose, Glycerol, Fructose, Sucrose, Xylose)and inorganic carbon source (CO₂) as shown in table 6.29[49]. The experimental study has been performed using concentraion of 1g/L organic carbon sources and 10% v/v inlet-CO₂ concentration [49].

Table 6.29 Biomass concentration(g/L) of various algal strains under mixotrophic growth.

| Algal strain | Organic C-source | Organic C-conc. (g/L) | Inorganic C-source | Inorganic C-conc. (%v/v) | Biomass Conc. (g/L) | Ref. |
|--|------------------|-----------------------|--------------------|--------------------------|---------------------|------|
| <i>Chlorella sp.</i> Y8-1 | Fructose | 1g/L | CO ₂ | 10 | 0.32±0.03 | 49 |
| | Glucose | | | | 0.4±0.05 | |
| | Glycerol | | | | 0.45± 0.04 | |
| | Sucrose | 0.5 | | | 0.45 | |
| | Xylose | 1 | | | 0.24±0.01 | |
| <i>Chlorella protothecoides</i> (UTEX-256) | Glucose | 5 | CO ₂ | 5 | 4.39 ± 0.22 | 50 |
| | Acetic acid | | | | 4.25 ± 0.22 | |
| | Glycerol | | | | 2.87 ± 0.12 | |
| Freshwater <i>Chlorella sp.</i> | Glucose | 2 | AIR | 0.04 | 1.4±0.2 | 51 |
| <i>Chlorella sp.</i> | | | | | | |
| Marine | | | | | 1.45±0.05 | |
| <i>Nannochloropsis sp.</i> | | | | | 1.1±0.1 | |
| <i>Cheatoceros sp.</i> | | | | | 0.25±0.05 | |
| <i>Chlorella vulgaris</i> (KMMCC-355) | Crude glycerol | 5 | CO ₂ | - | 1.91 | 52 |
| <i>B. braunii</i> (KMMCC-1681) | Crude glycerol | | | | 2.32 | |

| Algal strain | Organic C-source | Organic C-conc. (g/L) | Inorganic C-source | Inorganic C-conc. (%v/v) | Biomass Conc. (g/L) | Ref. |
|--|----------------------------|-----------------------|--------------------|--------------------------|---------------------|----------------------|
| <i>Scenedesmus sp.</i> (KMMCC-1235) | Crude glycerol | | | | 1.92 | |
| <i>Chlorella vulgaris</i> | Glucose | 10 | Air | 0.04 | 1.696 | 47 |
| | Glycerol | 10 | | | 0.722±0.012 | |
| | | 20 | | | 0.656±0.015 | |
| <i>Chlorella protothecoides</i> | Glycerol | 20.4 | Air | 0.04 | 2.33±0.93 | 46 |
| | Glucose | 15 | | | 4.07±0.23 | |
| <i>Chlamydomonas sp.</i> BTA 9032 | Cheese whey permeate (CWP) | - | Air | 0.04 | 1.15 | 53 |
| <i>Chlorella sp.</i> | | | | | 1.62 | |
| <i>Chlorella sp.</i> BTA 9031 | Molasses | 5 | | | 1.55 | |
| <i>Chlorella vulgaris</i> ESP-31 | Glucose | 10 | CO ₂ | 2 | 3 | 54 |
| <i>N. oleoabundans</i> UTEX 1185 | Glucose | 2.5 | Air | 0.04 | 1.8 | 55 |
| <i>L.subtilis</i> JUCHE1 | Glycerol | 0.0569 | CO ₂ | 7.5 | 0.6393 | Present study |

6.5.7 Algal growth rate under three different modes of cultivation (Photo-autotrophic, Photo-heterotrophic and Photo-mixotrophic)

From Figure 6.29, it has been observed that growth rate curve against carbon concentrations for photoautotrophic, photoheterotrophic and photomixotrophic follows similar increasing trend along with increase in carbon concentrations from 1.24-3.72 mM. Beyond 3.72 mM the growth is inhibited at higher carbon concentration at 4.95 mM (equivalent to 20% v/v inlet- CO_2). It has also been observed from table 6.30 that the highest values of specific growth rate, μ (d^{-1}) i.e. 0.7119 d^{-1} is obtained for photoheterotrophic growth at 3.72 mM carbon concentration. It is also revealed that the biomass production rate of *L.subtilis*JUCHE1 is higher under photoheterotrophic condition utilizing glycerol as organic carbon source as compared to photoautotrophic and mixotrophic growth.

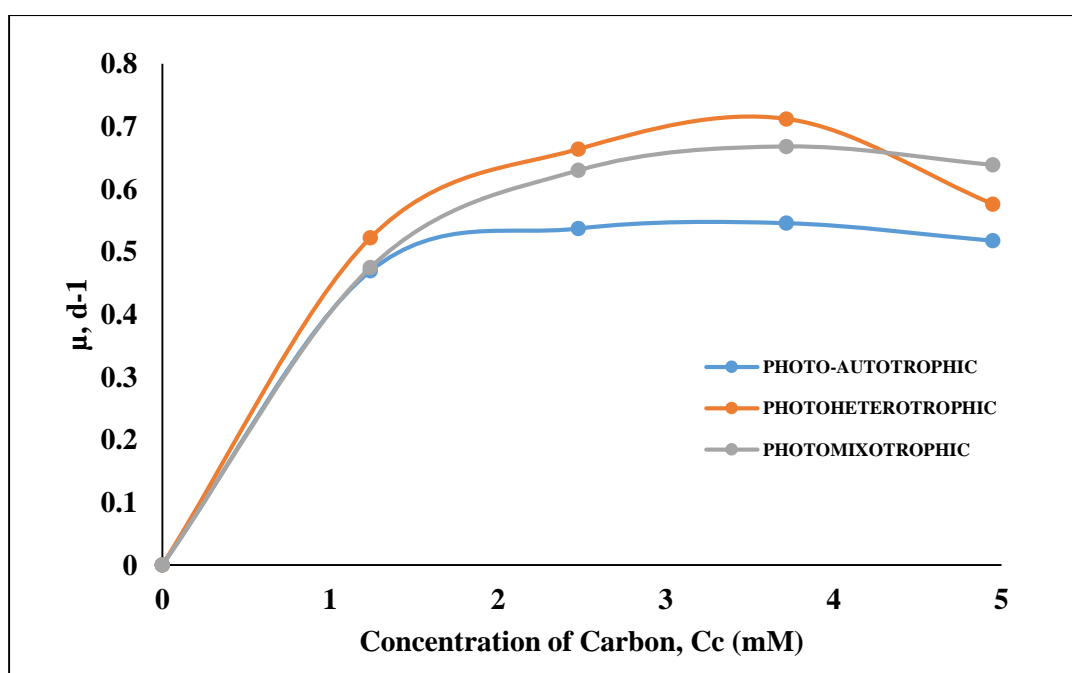


Figure 6.29 Specific growth rates of *L.subtilis* JUCHE1 against each equivalent Carbon concentrations under three growth modes (photoautotrophic, photoheterotrophic and mixotrophic).

Table 6.30 Calculated values of specific growth rates at each equivalent carbon concentrations (mg-atom/L) for three growth modes (photoautotrophic, photoheterotrophic and mixotrophic).

| Equivalent-Carbon concentrations (mg-atom/L) | specific growth rate , μ (d ⁻¹) | | |
|--|--|----------------------------|--------------------------|
| | Photo-autotrophic growth | Photo-heterotrophic growth | Photo-mixotrophic growth |
| 0 | 0 | 0 | 0 |
| 1.24 | 0.4694 | 0.5220 | 0.4747 |
| 2.48 | 0.5373 | 0.6638 | 0.6298 |
| 3.72 | 0.5459 | 0.7119 | 0.6679 |
| 4.95 | 0.5178 | 0.5759 | 0.6386 |

References

1. Chen, C. Y., & Yeh, K. L. Aisyah et al (2011) Cultivation, photobioreactor design and harvesting of microalgae for biodiesel production: a critical review. *Biores Technol*, 102(1), 71-81.
2. Kim, S., Park, J. E., Cho, Y. B., & Hwang, S. J. (2013). Growth rate, organic carbon and nutrient removal rates of *Chlorella sorokiniana* in autotrophic, heterotrophic and mixotrophic conditions. *Bioresource technology*, 144, 8-13.
3. Sachdeva, N., Kumar, G. D., Gupta, R. P., Mathur, A. S., Manikandan, B., Basu, B., & Tuli, D. K. (2016). Kinetic modeling of growth and lipid body induction in *Chlorella pyrenoidosa* under heterotrophic conditions. *Bioresource Technology*, 218, 934-943.
4. Sander, R. (2015). Compilation of Henry's law constants (version 4.0) for water as solvent. *Atmospheric Chemistry and Physics*, 15(8), 4399-4981.
5. Taher, H., Al-Zuhair, S., Al-Marzouqi, A., Haik, Y., & Farid, M. (2015). Growth of microalgae using CO₂ enriched air for biodiesel production in supercritical CO₂. *Renewable Energy*, 82, 61-70.
6. Li, Z., Yuan, H., Yang, J., & Li, B. (2011). Optimization of the biomass production of oil algae *Chlorella minutissima* UTEX2341. *Bioresource technology*, 102(19), 9128-9134.
7. Garg, A., & Jain, S. (2020). Process parameter optimization of biodiesel production from algal oil by response surface methodology and artificial neural networks. *Fuel*, 277, 118254.
8. Bondioli, P., & Della Bella, L. (2005). An alternative spectrophotometric method for the determination of free glycerol in biodiesel. *European journal of lipid science and technology*, 107(3), 153-157.
9. Ota, M., Kato, Y., Watanabe, H., Watanabe, M., Sato, Y., Smith Jr, R. L., & Inomata, H. (2009). Effect of inorganic carbon on photoautotrophic growth of microalga *Chlorococcum littorale*. *Biotechnology progress*, 25(2), 492-498.
10. Li, J., Tang, X., Pan, K., Zhu, B., Li, Y., Ma, X., & Zhao, Y. (2020). The regulating mechanisms of CO₂ fixation and carbon allocations of two *Chlorella sp.* strains in response to high CO₂ levels. *Chemosphere*, 247, 125814.

11. Hariz, H. B., Takriff, M. S., Ba-Abbad, M. M., Mohd Yasin, N. H., & Mohd Hakim, N. I. N. (2018). CO₂ fixation capability of *Chlorella sp.* and its use in treating agricultural wastewater. *Journal of applied phycology*, 30, 3017-3027.
12. Sung, K. D., Lee, J. S., Shin, C. S., Park, S. C., & Choi, M. J. (1999). CO₂ fixation by *Chlorella sp.* KR-1 and its cultural characteristics. *Bioresource technology*, 68(3), 269-273.
13. Ho, S. H., Chen, C. Y., & Chang, J. S. (2012). Effect of light intensity and nitrogen starvation on CO₂ fixation and lipid/carbohydrate production of an indigenous microalga *Scenedesmus obliquus* CNW-N. *Bioresource technology*, 113, 244-252.
14. Pradhan L, Bhattacharjee V, Mitra R, Bhattacharya I, Chowdhury R et al. Biosequestration of CO₂ using power plant algae (*Rhizoclonium hieroglyphicum* JUCHE2) in a Flat Plate Photobio-Bubble-Reactor–Experimental and modeling. *Chemical Engineering Journal*.2015; 275; 381-390.
15. de Morais, M. G., & Costa, J. A. V. (2007). Isolation and selection of microalgae from coal fired thermoelectric power plant for biofixation of carbon dioxide. *Energy Conversion and management*, 48(7), 2169-2173.
16. Adamczyk, M., Lasek, J., & Skawińska, A. (2016). CO₂ biofixation and growth kinetics of *Chlorella vulgaris* and *Nannochloropsis gaditana*. *Applied biochemistry and biotechnology*, 179, 1248-1261.
17. Shabani, M. (2016). CO₂ bio-sequestration by *Chlorella vulgaris* and *Spirulina platensis* in response to different levels of salinity and CO₂. *Proceedings of the International Academy of Ecology and Environmental Sciences*, 6(2), 53.
18. Kassim, M. A., & Meng, T. K. (2017). Carbon dioxide (CO₂) biofixation by microalgae and its potential for biorefinery and biofuel production. *Science of the total environment*, 584, 1121-1129.
19. Tang, D., Han, W., Li, P., Miao, X., & Zhong, J. (2011). CO₂ biofixation and fatty acid composition of *Scenedesmus obliquus* and *Chlorella pyrenoidosa* in response to different CO₂ levels. *Bioresource technology*, 102(3), 3071-3076.
20. Almomani F, Judd S, Bhosale RR, Shurair M, Aljaml K, Khraisheh M. Intergraded wastewater treatment and carbon bio-fixation from flue gases using *Spirulina platensis* and mixed algal culture. *Process Saf. Environ. Prot.* 2019; 124: 240-250.

21. Ho SH, Chen CY, Lee DJ, Chang JS. Perspectives on microalgal CO₂-emission mitigation systems—a review. *Biotechnol. Adv.* 2011; 29(2): 189-198. <https://doi.org/10.1016/j.biotechadv.2010.11.001>
22. Mandotra, S.K., Kumar, P., Suseela, M.R. and Ramteke, P.W., 2014. Fresh water green microalga *Scenedesmus abundans*: a potential feedstock for high quality biodiesel production. *Bioresource technology*, 156, pp.42-47.
23. Tagliaferro, G.V., Izário Filho, H.J., Chandel, A.K., da Silva, S.S., Silva, M.B. and dos Santos, J.C., 2019. Continuous cultivation of *Chlorella minutissima* 26a in a tube-cylinder internal-loop airlift photobioreactor to support 3G biorefineries. *Renewable Energy*, 130, pp.439-445.
24. Dhup, S. and Dhawan, V., 2014. Effect of nitrogen concentration on lipid productivity and fatty acid composition of *Monoraphidium sp.* *Bioresource technology*, 152, pp.572-575.
25. Yodsuwan, N., Sawayama, S. and Sirisansaneeyakul, S., 2017. Effect of nitrogen concentration on growth, lipid production and fatty acid profiles of the marine diatom *Phaeodactylum tricornutum*. *Agriculture and Natural Resources*, 51(3), pp.190-197.
26. Gour, R. S., Bairagi, M., Garlapati, V. K., & Kant, A. (2018). Enhanced microalgal lipid production with media engineering of potassium nitrate as a nitrogen source. *Bioengineered*, 9(1), 98-107.
27. Wan, C., Bai, F. W., & Zhao, X. Q. (2013). Effects of nitrogen concentration and media replacement on cell growth and lipid production of oleaginous marine microalga *Nannochloropsis oceanica* DUT01. *Biochemical engineering journal*, 78, 32-38.
28. Li, S., Song, C., Li, M., Chen, Y., Lei, Z., & Zhang, Z. (2020). Effect of different nitrogen ratio on the performance of CO₂ absorption and microalgae conversion (CAMC) hybrid system. *Bioresource technology*, 306, 123126.
29. Farooq, W., Naqvi, S. R., Sajid, M., Shrivastav, A., & Kumar, K. (2022). Monitoring lipids profile, CO₂ fixation, and water recyclability for the economic viability of microalgae *Chlorella vulgaris* cultivation at different initial nitrogen. *Journal of Biotechnology*.
30. Kong, W., Kong, J., Ma, J., Lyu, H., Feng, S., Wang, Z., ... & Shen, B. (2021). *Chlorella vulgaris* cultivation in simulated wastewater for the biomass production, nutrients

- removal and CO₂ fixation simultaneously. *Journal of Environmental Management*, 284, 112070.
31. Schipper, K., Das, P., Al Muraikhi, M., AbdulQuadir, M., Thaher, M. I., Al Jabri, H. M. S., & Barbosa, M. J. (2021). Outdoor scale-up of *Leptolyngbya* sp.: Effect of light intensity and inoculum volume on photo inhibition and-oxidation. *Biotechnology and Bioengineering*, 118(6), 2368-2379.
 32. Farahdiba, A. U., Cahyonugroho, O., Nindhita, S. N., & Hidayah, E. N. (2020, July). Photo inhibition of algal photobioreactor by intense light. In *Journal of Physics: Conference Series* (Vol. 1569, No. 4, p. 042095). IOP Publishing.
 33. Pavlik, D., Zhong, Y., Daiek, C., Liao, W., Morgan, R., Clary, W., & Liu, Y. (2017). Microalgae cultivation for carbon dioxide sequestration and protein production using a high-efficiency photobioreactor system. *Algal research*, 25, 413-420.
 34. Ho, S. H., Chen, C. Y., & Chang, J. S. (2012). Effect of light intensity and nitrogen starvation on CO₂ fixation and lipid/carbohydrate production of an indigenous microalga *Scenedesmus obliquus* CNW-N. *Bioresource technology*, 113, 244-252.
 35. Lacerda LMCF, M. I. Queiroz, L. T. Furlan, M. J. Lauro, K. Modenesi, E. Jacob-Lopes, T.T. Franco.2011 “Improving refinery wastewater for microalgal biomass production and CO₂ biofixation: Predictive modeling and simulation”. *Journal of petroleum science and engineering* 78.3-4: 679-686. <https://doi.org/10.1016/j.petrol.2011.07.003>
 36. Leite GB, Paranjape K, Abdelaziz AE, Hallenbeck PC (2015) Utilization of biodiesel-derived glycerol or xylose for increased growth and lipid production by indigenous microalgae. *Bioresour Technol* 184:123–130.
 37. Li T, Zheng Y, Yu L, Chen S (2014) Mixotrophic cultivation of a *Chlorella sorokiniana* strain for enhanced biomass and lipid production. *Biomass Bioenergy* 66:204–213.
 38. Jacob-Lopes E, Lacerda LMCF, Franco TT (2008) Biomass production and carbon dioxide fixation by *Aphanothece microscopica* Nägeli in a bubble column photobioreactor. *Biochem Eng J* 40(1):27–34.
 39. Abomohra AEF, Eladel H, El-Esawi M, Wang S, Wang Q, He Z, Hanelt D (2018) Effect of lipid-free microalgal biomass and waste glycerol on growth and lipid production of *Scenedesmus obliquus*: innovative waste recycling for extraordinary lipid production. *BioresourTechnol* 249:992–999.

40. Yang J, Rasa E, Tantayotai P, Scow KM, Yuan H, Hristova KR (2011) Mathematical model of *Chlorella minutissima* UTEX2341 growth and lipid production under photoheterotrophic fermentation conditions. *Bioresour Technol* 102(3):3077–3082.
41. Narayan MS, Manoj GP, Vatchravelu K, Bhagyalakshmi N, Mahadevaswamy M (2005) Utilization of glycerol as carbon source on the growth, pigment and lipid production in *Spirulina platensis*. *Int J Food Sci Nutr* 56(7):521–528.
42. Zeebe RE, Wolf-Gladrow D (2001). CO₂ in seawater: equilibrium, kinetics, isotopes (No. 65). Gulf Professional Publishing. http://geosci.uchicago.edu/~kite/doc/Zeebe_CO2_In_Seawater_Ch_1.pdf
43. Badger MR, Price GD, Long BM, Woodger FJ (2006) The environmental plasticity and ecological genomics of the cyanobacterial CO₂ concentrating mechanism. *J Exp Bot* 57(2):249–265. <https://doi.org/10.1093/jxb/eri286>.
44. Aubert, S., Gout, E., Bligny, R., & Douce, R. (1994). Multiple effects of glycerol on plant cell metabolism. Phosphorus-31 nuclear magnetic resonance studies. *Journal of Biological Chemistry*, 269(34), 21420-21427.
45. Wang, Y. Z., Hallenbeck, P. C., Leite, G. B., Paranjape, K., & Huo, D. Q. (2016). Growth and lipid accumulation of indigenous algal strains under photoautotrophic and mixotrophic modes at low temperature. *Algal Research*, 16, 195-200.
46. Heredia-Arroyo T, Wei W, Ruan R, Hu B (2011) Mixotrophic cultivation of *Chlorella vulgaris* and its potential application for the oil accumulation from non-sugar materials. *Biomass Bioenergy* 35(5): 2245–2253. <https://doi.org/10.1016/j.biombioe.2011.02.036>
47. Yamane YI, Utsunomiya T, Watanabe M, Sasaki K (2001) Biomass production in mixotrophic culture of *Euglena gracilis* under acidic condition and its growth energetics. *Biotechnol Lett* 23(15):1223–1228. <https://doi.org/10.1023/A:1010573218863>
48. Park, J. E., Zhang, S., Han, T. H., & Hwang, S. J. (2021). The contribution ratio of autotrophic and heterotrophic metabolism during a mixotrophic culture of *Chlorella sorokiniana*. *International Journal of Environmental Research and Public Health*, 18(3), 1353.

49. Lin, T. S., & Wu, J. Y. (2015). Effect of carbon sources on growth and lipid accumulation of newly isolated microalgae cultured under mixotrophic condition. *Bioresource technology*, 184, 100-107.
50. Patel, A. K., Joun, J. M., Hong, M. E., & Sim, S. J. (2019). Effect of light conditions on mixotrophic cultivation of green microalgae. *Bioresource technology*, 282, 245-253.
51. Cheirsilp, B., & Torpee, S. (2012). Enhanced growth and lipid production of microalgae under mixotrophic culture condition: effect of light intensity, glucose concentration and fed-batch cultivation. *Bioresource technology*, 110, 510-516.
52. Choi, H. J., & Yu, S. W. (2015). Influence of crude glycerol on the biomass and lipid content of microalgae. *Biotechnology & Biotechnological Equipment*, 29(3), 506-513.
53. Mondal, M., Ghosh, A., Sharma, A. S., Tiwari, O. N., Gayen, K., Mandal, M. K., & Halder, G. N. (2016). Mixotrophic cultivation of *Chlorella* sp. BTA 9031 and *Chlamydomonas* sp. BTA 9032 isolated from coal field using various carbon sources for biodiesel production. *Energy Conversion and Management*, 124, 297-304.
54. Yeh, K. L., & Chang, J. S. (2012). Effects of cultivation conditions and media composition on cell growth and lipid productivity of indigenous microalga *Chlorella vulgaris* ESP-31. *Bioresource technology*, 105, 120-127.
55. Baldisserotto, C., Popovich, C., Giovanardi, M., Sabia, A., Ferroni, L., Constenla, D., ... & Pancaldi, S. (2016). Photosynthetic aspects and lipid profiles in the mixotrophic alga *Neochloris oleoabundans* as useful parameters for biodiesel production. *Algal Research*, 16, 255-265.

Chapter 7

Studies on lipid and pigments (Chlorophyll and Carotenoid) production by alga under Photoautotrophic, Photoheterotrophic and Photomixotrophic conditions using white light

This chapter focuses on the assessment of capability of lipid production of Power plant alga “*L.subtilis* JUCHE1” under photoautotrophic, photoheterotrophic and photomixotrophic conditions using respectively CO₂, Glycerol and mixture of CO₂, Glycerol as carbon sources. In all growth conditions, the effect of variation of concentration of inlet carbon source/s on the lipid content and productivity was assessed. In photo-autotrophic growth, the effects of variation of concentration of nitrogen, source, namely NaNO₃ and light intensities were assessed with respect to lipid content and productivity. Chapter also focuses on the assessment of production of pigment under different growth modes (photoautotrophic, photoheterotrophic and photomixotrophic). Studies have been conducted according to the following objectives, as described under Aim 4 and Aim 5 in Chapter 3:

- **Determination of Lipid content and productivity under Photoautotrophic, Photoheterotrophic and Photomixotrophic conditions using white light’**
- **Comparison of lipid production**
- **Characterization of lipid under Photoautotrophic, Photoheterotrophic and Photomixotrophic conditions using white light**
- **Determination of chlorophyll and carotenoid content under Photoautotrophic, Photoheterotrophic and Photomixotrophic**
- **Comparison of chlorophyll and carotenoid content under photoautotrophic, photoheterotrophic and photomixotrophic conditions using white light**

7.1 Materials and Methods

7.1.1 Chemicals

The lipid was extracted from dry algal biomass followed by solvent extraction process. NaOH procured from Merck, India. and Acetone, Chloroform and Methanol, procured from CDH (Central Drug House Pvt. Limited), India were used in the experiment.

7.1.2 Lipid extraction

The depigmented algal biomass was used for lipid extraction. For depigmentation process the dry biomass was treated with a 20ml mixture of 1% NaOH and acetone in a 3:4 ratio (%v/v) and placed inside the hot air oven at 60° C for around 1 hour as followed from the protocol reported by Li et al., (2016)[1]. The dry and de-pigmented algal biomass was added to solvent mixture of chloroform - methanol (2:1 v/v) and homogenized for 10 minutes for rupturing the algal cell mass (Mandotra et al. 2014)[2]. After homogenization, the heterogeneous mixture was centrifuged at 10,000 rpm for 15 minutes to separate supernatant containing the lipids and the pellet containing the algal debris. The supernatant was collected in a beaker and the solvent part was removed inside a hot air oven at 60°C. The lipid part was left in the beaker. The lipid content(%w/w) of algal biomass was determined using eq. (5.29) and (5.30) provided in chapter 5. The overall lipid extraction process has been represented in figure 7.1.

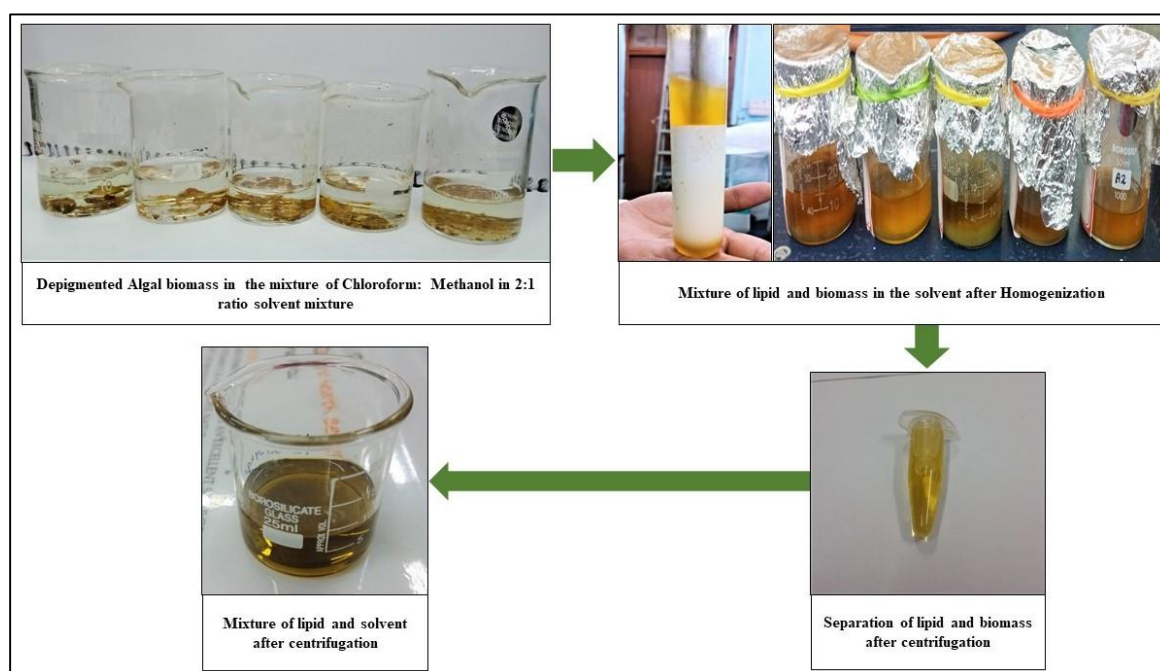


Figure 7.1 Overall flow diagram of lipid extraction process from algal biomass.

7.1.3 Pigment extraction

Photosynthetic pigments like Chlorophyll a, Chlorophyll b and carotenoids are reported to be extracted through solvent extraction process [3]. In this study, 80% Acetone as extraction solvent was used to extract the pigments from the dry algal biomass collected on 3rd, 4th and 5th days of culture period under three different growth modes (photoautotrophic, photoheterotrophic and photomixotrophic conditions). The different steps of solvent extraction

process of algal pigment have been schematically described in Figure 7.2. The pigment concentrations($\mu\text{g/mL}$) in the extract of solvent extraction process and mass fraction (%w/w.) in dry algal biomass have been calculated by using equations 4.1, 4.2, 4.3 (section 4.3.3.2) and 5.31, 5.32 of section 5.1.12.

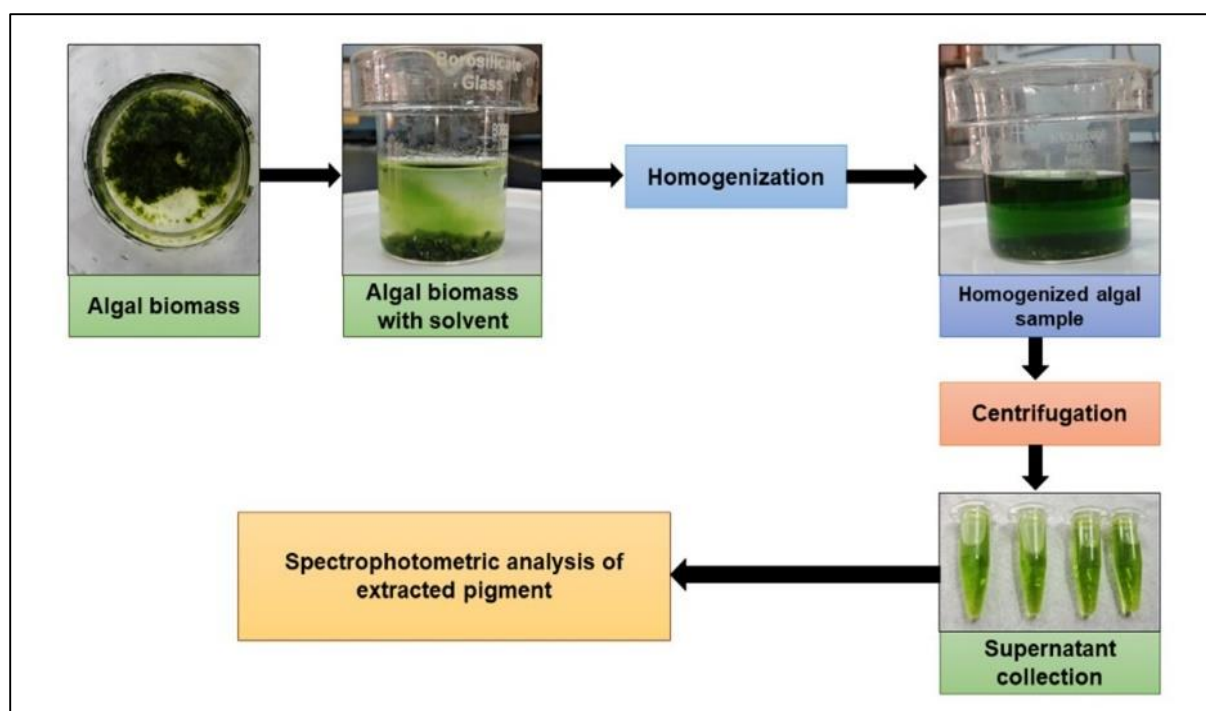


Figure 7.2 Overall solvent extraction process for pigment extraction from algal biomass of *L.subtilis* JUCHE1.

7.1.4 Characterization of Lipid

The extracted lipid from the algal biomass of *L. subtilis* JUCHE was characterized through GC-MS analysis, described in Section 4.3.3 of Chapter 4.

7.2 Experimental conditions

7.2.1 Lipid

The lipid contents of algal biomass obtained during the batch experiments, as described in Sections 6.1.1.3, 6.2.1.2 and 6.3.1.2. of Chapter 6, were determined and consequently were used to reveal the effects of variation of concentration of carbon sources on the capability of algal oil production during photoautotrophic, photoheterotrophic and photomixotrophic growth conditions. Similarly, the lipid content of algal mass produced during the batch experiments, described in Section 6.1.1.4 with the variation of concentration of nitrogen, source, namely NaNO_3 and light intensities, as described in Section 6.1.1.5, was determined. The experimental

data have been used to elucidate the effects of variation of C: N ratio and light intensity on lipid production during autotrophic growth. Lipid contents of *L.subtilis* JUCHE1 have been compared with other algal strains, as reported in available literature, in similar growth modes.

7.2.2 Pigment

As described in Chapter 6, the pigment content was also determined at the condition where the biomass concentration reached the maximum. As described in section 6.5.4, under photoautotrophic condition, the maximum biomass concentration was obtained on 3rd day when the algal cultivation was conducted with inlet gas phase CO₂ concentration of 15% (v/v). Similarly, under photoheterotrophic condition, the maximum biomass concentration was obtained on 4th day when the algal cultivation was conducted with inlet glycerol concentration equivalent to 15% (v/v)CO₂ as described in section 6.5.5. Under mixotrophic condition, the maximum biomass concentration was obtained on 5th day when the algal cultivation was conducted at inlet carbon moles, equivalent to those from 15% (v/v)CO₂, of which 50% contribution was from CO₂ and glycerol each. The pigment concentrations at the above conditions were determined following the protocol described in 7.1.3.

7.3 Results and Discussion

7.3.1 Lipid accumulation of *L.subtilis* JUCHE1 under Photoautotrophic growth

7.3.1.1 Lipid production varying inlet-CO₂ concentrations (%v/v) under photoautotrophic mode of cultivation

Figure 7.2 represents the variation of lipid content (%w/w) of *Leptolyngbya subtilis* JUCHE1 with culture period using the inlet concentration of CO₂ as a parameter. It has been observed that similar to the pattern of change of biomass concentration, the lipid accumulation increases with the increase in inlet CO₂ concentrations from 5-15%, and beyond that the lipid content decreases. It is also clearly observed that in case of 5, 10 and 20 % CO₂ inlet concentration, the maximum values of lipid content (%w/w) of 5.34, 6.97 and 5.712 respectively are obtained on 2nd day. However, for 15% CO₂ concentration, the value of lipid content of 12.5% is the highest among all and is obtained on 3rd day.

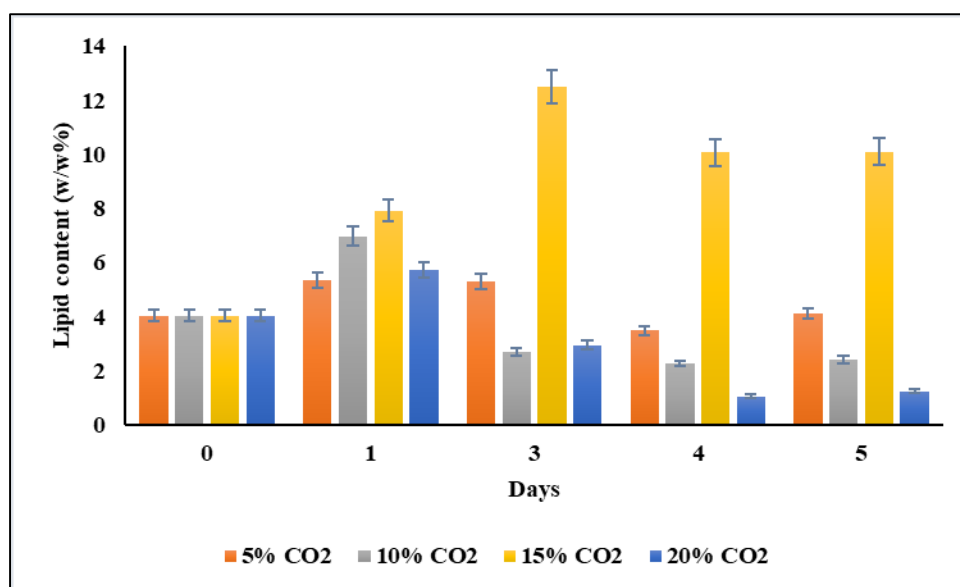


Figure 7.3 Effect of inlet-CO₂ concentrations (5-20%v/v) on time history of Lipid content under photoautotrophic growth

From some of the literatures it was also noticed that in case of biomass growth or lipid accumulation, algae do not follow any particular pattern during cultivation [4, 5]. More studies have to be done to unwind the exact reason behind this observation. It is clear that *Leptolyngbya subtilis* JUCHE1 uptakes CO₂ very efficiently in the presences of light to produce energy for metabolic needs using Photo System I. In this metabolic pathway, the excess amount of carbon is stored as lipid in the cells [6]. Taher et al. 2015, also focused on the lipid production under photoautotrophic growth mode of three algal strains, namely, *Chlorella sp.*, *Pseudochlorococcum sp.*, and *Nannochloropsis sp.* varying inlet CO₂ concentrations in the range of 0.04 to 2% (v/v). For all the three strains, the optimum CO₂ concentration for growth as well as lipid production was determined to be 1% (v/v) [7]. The values of lipid content of *Chlorella sp.*, *Pseudochlorococcum sp.*, and *Nannochloropsis sp.* were determined to be 13, 2.9 and 14%(w/w) respectively. Except *Pseudochlorococcum sp.*, the lipid content of the algal strains are comparable to that of *L. subtilis* JUCHE1, obtained at the optimum CO₂ concentration [7]. In another study, lipid content of *Scenedesmus obliquus* AS-6-1 was reported to be 11.71%(w/w)[8]. In addition to Figures 7.3 and 7.4, the experimental values of lipid content(%w/w) for all the inlet concentrations of CO₂ in gas phase are also provided in table 7.1.

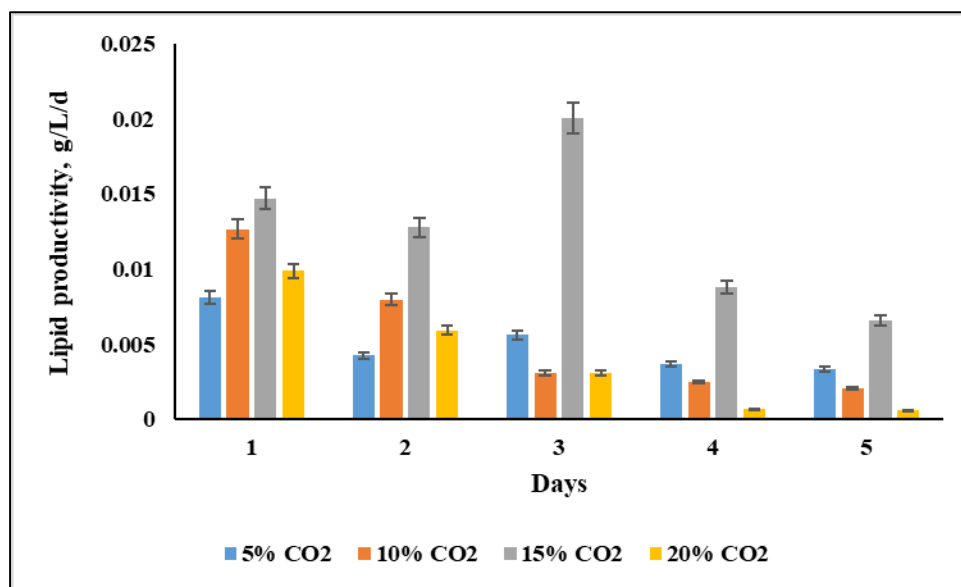


Figure 7.4 Effect of inlet CO₂ concentrations (5-20%v/v) on time history of Lipid productivity under photo- autotrophic growth

Table 7.1 Time history of Lipid content and productivity under photo- autotrophic growth mode with the variation of inlet gas-phase CO₂ concentrations

| Lipid content (%w/w) | | | | | Lipid productivities (g/L/d) | | | |
|----------------------|---------------------------------------|--------|---------|--------|------------------------------|---------|---------|---------|
| Time | CO ₂ concentrations (%v/v) | | | | | | | |
| Days | 5 | 10 | 15 | 20 | 5 | 10 | 15 | 20 |
| 0 | 4.0436 | 4.0436 | 4.0436 | 4.0436 | 0 | 0 | 0 | 0 |
| 1 | 5.3467 | 6.9774 | 7.9291 | 5.7129 | 0.0081 | 0.01267 | 0.01472 | 0.00987 |
| 2 | 4.6278 | 5.1985 | 8.02 | 4.0998 | 0.0042 | 0.00797 | 0.01277 | 0.00593 |
| 3 | 5.3069 | 2.6865 | 12.4988 | 2.9582 | 0.0056 | 0.00307 | 0.02005 | 0.0031 |
| 4 | 3.493 | 2.2742 | 10.0671 | 1.0639 | 0.0036 | 0.00249 | 0.0087 | 0.00067 |
| 5 | 4.12 | 2.416 | 10.1 | 1.25 | 0.0033 | 0.00207 | 0.0066 | 0.0006 |

7.3.1.2 Characterization of Lipid

Qualitative analysis of the extracted lipid was performed using GC-MS analyzer (**Thermo-Scientific**). By following the methodology, described in Chapter 4, the lipid was extracted,

filtered and injected for analysis. The process has been carried out using TR-Wax column. Finally, the compounds were identified from the MS library. The following compounds are as shown below in table 7.2.

C16 fatty acids were also detected to be predominant in the lipid produced by the cyanobacteria *Spirulina platensis*. The production of C15-C19 fatty acids by cyanobacteria *Nostocmuscorum*, *Trichodesmiumerythaeum* and C15-C-C18 alcohols in case of mutant strains of cyanobacteria, *Synechocystis* PCC6803, *Synechococcus elongatus* PCC7942 and *Anabaena sp.* PCC7120 having overexpression of Acetyl CoA Carboxylase (Accase) for inhibiting fatty acid biosynthesis also prove the same chain length pattern of cyanobacteria [9]. In the photoautotrophic mode, the algae utilize CO₂ in presences of light to produce energy for metabolic needs using Photo System I. The excess of carbon is stored as lipid in the cells. As suggested by Choi et al. (2014), DHA was extracted using Acid-catalyzed hot-water extraction treatment process [10]. The algal biomass was initially treated with different concentrations of H₂SO₄ in the range of 0.05- 3.00% w/w. The reaction temperatures were 80, 100 and 120 °C. After that the lipid was extracted from the acid treated biomass, using solvent extraction method using a mixture of methanol and hexane in 7:3 ratios (v/v) and chloroform, methanol solution in 2:1 ratio (v/v) respectively [10]. In this lipid sample, DHA and other poly unsaturated fatty acids were qualitatively detected using GC-MS. The chromatograms of algal oil samples are represented in Figure 7.5 and 7.6

Table 7.2: Fatty acid profile of *Leptolyngbya subtilis* JUCHE1.

| Serial no. | Fatty acids | Type of Fatty acid | Chemical formula | Retention time |
|------------|---------------------|--------------------|--|----------------|
| 1. | Palmitic acid | SFA | C ₁₇ H ₃₄ O ₂ | 19.36 |
| 2. | Heptanoic acid | SFA | C ₇ H ₁₄ O ₂ | 4.93 |
| 3. | Stearic acid | SFA | C ₁₉ H ₃₈ O ₂ | 21.28 |
| 4. | Oleic acid | SFA | C ₂₄ H ₄₆ O ₂ | 19.55 |
| 5. | Hexadecanoic acid | SFA | C ₁₆ H ₃₂ O ₂ | 20.88 |
| 6. | Octanoic acid | SFA | C ₈ H ₁₆ O ₂ | 4.85 |
| 7. | Dodecanoic acid | SFA | C ₁₂ H ₂₄ O ₂ | 19.61 |
| 8. | Undecanoic acid | SFA | C ₁₁ H ₂₂ O ₂ | 4.87 |
| 9. | Nonanoic acid | SFA | C ₉ H ₁₈ O ₂ | 10.47 |
| 10. | Docosahexanoic acid | Omega-3 FA | C ₂₂ H ₃₂ O ₂ | 3.59 |

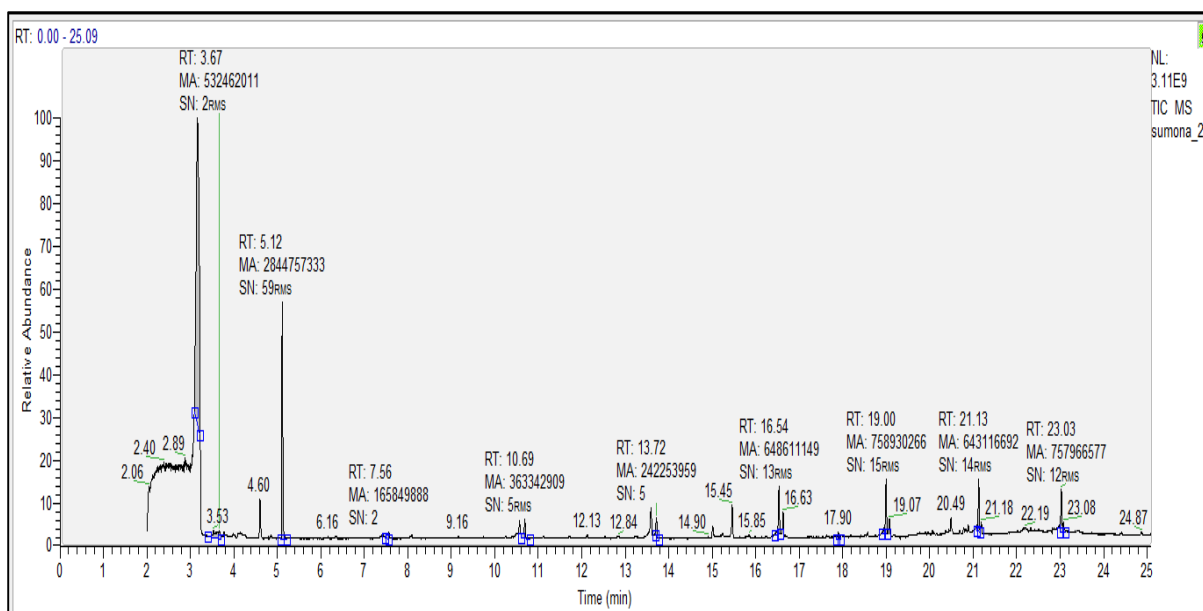


Figure 7.5 GC-MS chromatogram of extracted lipid of *L. subtilis*JUCHE1

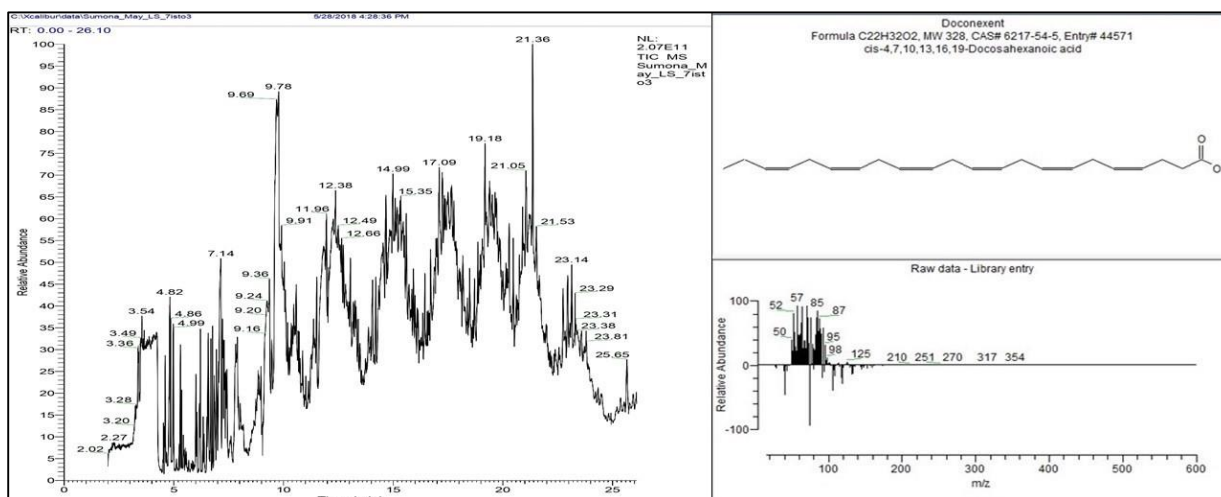


Figure 7.6 GC-MS chromatogram of identified DHA from the extracted lipid of *L. subtilis*JUCHE1

7.3.1.3. Effect of Sodium nitrate concentrations(NaNO_3) on lipid accumulation

Figure 7.7, shows a bar-plot of time histories of lipid content of *Leptolyngbya subtilis* JUCHE1 over 5 days of culture period using initial NaNO_3 concentration as a parameter. The Figure 7.7 reveals that as the value of N:C decreases, the content of lipid in the algal strain increases. This is very much in agreement with the increase of algal lipid content under nitrogen stress. Hence, the maximum value of lipid content of 53.87% (w/w) has been achieved on 5th day using initial NaNO_3 concentration of 1g/L. This is almost twice the lipid content (28.68 %) obtained on 2nd day using 2.5 g/L of NaNO_3 concentration. Similarly, a bar-plot has been depicted in

Figure 6, showing the dependence of time histories of lipid productivity on initial concentration of NaNO_3 over a culture period of 5 days. The maximum productivity of lipid has been achieved on 5th day using initial NaNO_3 concentration of 2 g/L although lipid content is maximum for 1g/L at the same culture time. This signifies that although minimum value of N:C at 1g/L NaNO_3 favours the accumulation of lipid in the culture, it simultaneously reduces the biomass production as nitrogen is an essential substrate to sustain algal growth. The Figure 7.8 represents the dependence of time history of lipid productivity of *Leptolyngbya subtilis* JUCHE1 on NaNO_3 concentration (1-2.5g/L). Lipid productivity, as defined in Equation (5.30) of chapter 5, is a function of both lipid content and biomass productivity. Hence, it is influenced by the changing patterns of both of them with the variation of NaNO_3 concentration. The maximum productivity of lipid for *Leptolyngbya subtilis* JUCHE1 is thus attained at a condition (Initial NaNO_3 concentration = 2g/L) which also ensures the maximum biomass production and the value is 0.04228g/L/d obtained on 3rd day of culture period. Thus for this strain a strategy recommending 2-stage operation of algal growth, the first under N-sufficient condition producing sufficient quantity of algal mass, followed by another one under N-stressed condition, can be useful to enhance the overall production of lipid. For *Leptolyngbya subtilis*JUCHE1, the first stage can be operated at initial NaNO_3 concentration of 2g/L, followed by another stage using NaNO_3 concentration of 1g/L.

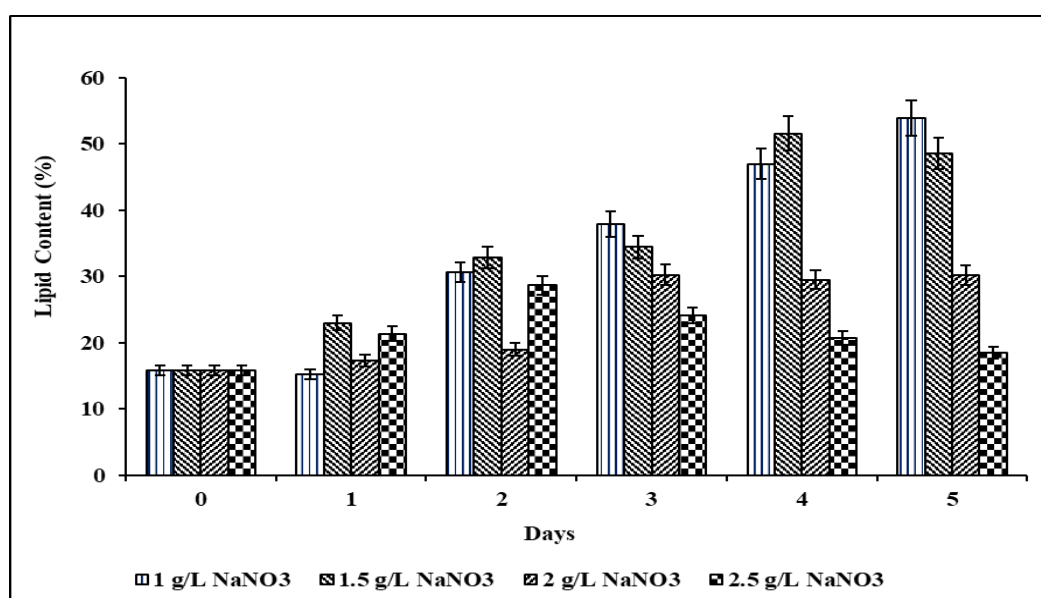


Figure 7.7 Dependence of time history of lipid content of *Leptolyngbya subtilis* JUCHE1 on NaNO_3 concentration (1-2.5g/L)

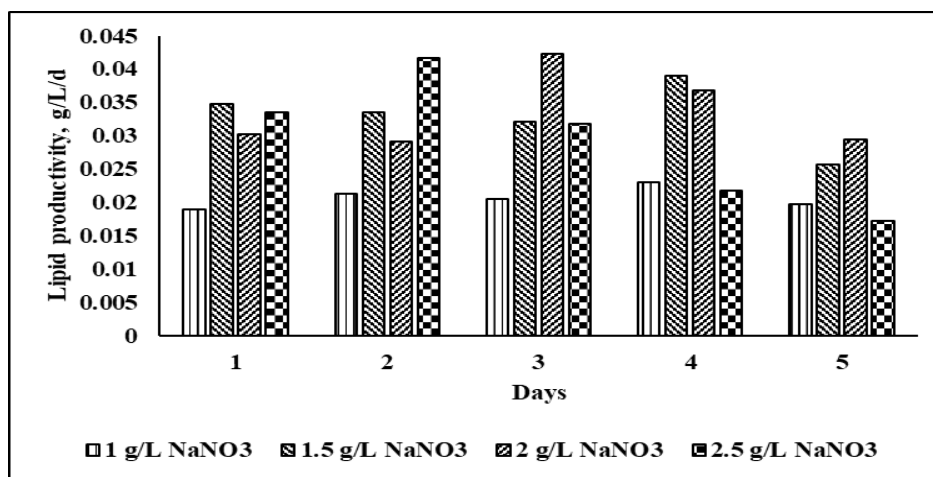


Figure 7.8 Dependence of time history of Lipid productivity of *Leptolyngbya subtilis* JUCHE1 on NaNO₃ concentration (1-2.5g/L)

Table 7.3 Experimental values of Lipid content and productivity of *Leptolyngbya subtilis* JUCHE1 varying concentrations of NaNO₃ from 1-2.5g/L at each time intervals.

| Day | Lipid content (%w/w) | | | | Lipid productivity(g/L/d) | | | |
|----------|---------------------------------------|-------|-------|-------|---------------------------------------|---------|--------|--------|
| | NaNO ₃ concentration (g/L) | | | | NaNO ₃ concentration (g/L) | | | |
| | 1 | 1.5 | 2 | 2.5 | 1 | 1.5 | 2 | 2.5 |
| 0 | 15.83 | 15.83 | 15.83 | 15.83 | 0 | 0 | 0 | 0 |
| 1 | 15.22 | 22.98 | 17.32 | 21.35 | 0.019 | 0.0348 | 0.0303 | 0.0335 |
| 2 | 30.66 | 32.87 | 18.95 | 28.68 | 0.0213 | 0.0335 | 0.0291 | 0.0417 |
| 3 | 37.90 | 34.45 | 30.24 | 24.09 | 0.0206 | 0.0322 | 0.0423 | 0.0318 |
| 4 | 46.99 | 51.56 | 29.53 | 20.69 | 0.023 | 0.0389 | 0.0367 | 0.0218 |
| 5 | 53.87 | 48.57 | 30.22 | 18.50 | 0.0197 | 0.02564 | 0.0294 | 0.0172 |

In Table 7.4, the influence of variation of concentration of nitrogen source, NaNO₃, on lipid production performance of *Leptolyngbya subtilis* JUCHE1 has been compared with the reported data of other algal strains. In a study on the effect of NaNO₃ concentration (0.057-0.225 g/L) on the content and productivity of lipid of *Monoraphidium contortum*, *Tetraselmis suecica* and *Chlorella minutissima*, it was observed that the highest values of of $36.6 \pm 0.66\%$ wt. and 0.00935 ± 0.00016 g/L/d respectively were obtained from *Chlorella minutissima* at the nitrate

concentration of 0.113 g/L [11]. Another literature reported the highest lipid content of $53.04 \pm 3.26\%$ wt. for *Phaeodactylum tricorutum* sp under nitrogen stressed condition [12]. Ra, C. H et al. 2015, conducted the batch experiments using different algal strains, namely, *Isochrysis galbana*, *Nanochloropsis oculata*, *Dunaliella tertiolecta*, *Dunaliellas alinato* investigate the effect of different NaNO_3 concentrations (0.018 and 0.024 g/L)[13]. The cultures were continuously aerated by supplying sterile air (0.04% CO_2) at a flow rate of 2.5 L/min using 0.2 μm PTFE membrane as Carbon source[13].The study reported that among the three algal strains the lipid accumulation of *Isochrysis galbana* was the highest and lipid content of 24%wt. was obtained [13].R. S. Gour et al., 2018 reported the maximum lipid content of 23.170% w/w for *Chlorella* sp *Chl16* at 0.2125g/L NaNO_3 during their study with the variation of NaNO_3 concentrations in the range of 0.2125-1.5 g/L [15]. It has been observed that in comparison o other algal strains under consideration, the content and productivity of lipid of *Leptolyngbya subtilis* JUCHE1is high.

Table 7.4 Comparison of the influence of variation of NaNO_3 concentration on the performance of algal strains with respect to lipid production.

| Strain | NaNO_3 Conc. (g/L) | Carbon source and concentration | Light Intensity (kLux) | Lipid Content (%) | Lipid Productivity (g/L/d) | Ref. |
|--------------------------------|-----------------------------|---------------------------------|------------------------|-------------------|----------------------------|------|
| <i>Monoraphidium contortum</i> | 0.057 | Air (0.04% CO_2) | 5.92 | 32.6 ± 1.11 | 0.00489 ± 0.00016 | 11 |
| | 0.113 | | | 28.2 ± 0.96 | 0.00479 ± 0.0001 | |
| | 0.225 | | | 9.6 ± 1.21 | 0.00278 ± 0.00035 | |
| <i>Tetraselmis suecica</i> | 0.057 | | | 8.0 ± 0.23 | 0.0017 ± 0.00004 | |
| | 0.113 | | | 6.38 ± 0.15 | 0.00192 ± 0.00004 | |
| | 0.225 | | | 17.15 ± 0.49 | 0.00704 ± 0.0002 | |
| <i>Chlorella minutissima</i> | 0.057 | | | 22.7 ± 0.92 | 0.00296 ± 0.00012 | |
| | 0.113 | | | 36.6 ± 0.66 | 0.00935 ± 0.00016 | |
| | 0.225 | | | 36 ± 0.88 | 0.01379 ± 0.00034 | |

| Strain | NaNO ₃ Conc. (g/L) | Carbon source and concentration | Light Intensity (kLux) | Lipid Content (%) | Lipid Productivity (g/L/d) | Ref. |
|-------------------------------------|-------------------------------|---------------------------------|------------------------|-------------------|----------------------------|---------------|
| <i>Phaeodactylumtricornutum</i> | 0 | - | 5.92 – 7.4 | 53.04 ± 3.26 | 0.00168 ± 0.00* | 12 |
| | 0.01645 | | | 23.02 ± 1.25 | 0.00192 ± 0.00024* | |
| | 0.03209 | | | 9.61 ± 3.89 | 0.00096 ± 0.00048* | |
| | 0.06429 | | | 2.79 ± 0.35 | 0.00024 ± 0.00* | |
| <i>Isochrysisgalbana</i> | 0.024 | Air (0.04% CO ₂) | 8.058 | 24 | 0.0156* | 13 |
| <i>Nanochloropsisoculata</i> | 0.024 | | | 17 | 0.00646* | |
| <i>Dunaliellatertiolecta</i> | 0.024 | | | 23 | 0.00575* | |
| <i>Dunaliellasalina</i> | 0.018 | | | 22 | 0.00506* | |
| <i>Monoraphidium sp. T4X</i> | 0.05 | - | - | 18.42 ± 0.4 | 0.18 | 14 |
| | 0.1 | | | 15.57 ± 0.8 | 0.16 | |
| | 0.5 | | | 14.30 ± 0.5 | 0.19 | |
| | 1.0 | | | 11.85 ± 0.1 | 0.15 | |
| | 1.5 | | | 11.57 ± 0.6 | 0.17 | |
| | 2.0 | | | 10 ± 0.7 | 0.14 | |
| <i>Chlorella sp Ch116</i> | 0.2125 | Air (0.04% CO ₂) | - | 23.170 | 0.007 | 15 |
| | 0.425 | | | 19.983 | 0.0039 | |
| | 0.6375 | | | 15.770 | 0.0028 | |
| | 0.85 | | | 15.770 | 0.0044 | |
| | 1.0625 | | | 15.607 | 0.0036 | |
| | 1.5 | | | 14.65 | 0.0038 | |
| <i>Leptolyngbya subtilis JUCHE1</i> | 1 | 15 % CO ₂ | 2.5 | 53.87 | 0.0197 | Present study |
| | 1.5 | | | 51.56 | 0.03895 | |
| | 2 | | | 30.24 | 0.04228 | |
| | 2.5 | | | 28.68 | 0.04198 | |

*Biomass concentration data were used for calculation of lipid productivity using the equation (5.30) [1, 7].

7.3.1.4 Effect of different light intensities on *L. subtilis*JUCHE1 for lipid production

The bar plot (Figure 7.9) represents the time history of lipid content of *L. subtilis*JUCHE1 using light intensity as a parameter (1.45, 1.95, 2.49 and 3.2kLux). From figure 7.9, it is revealed that the lipid content quantitatively increases with the increase in light intensities from 1.45-2.49 kLux, above which a decreasing trend is observed. While the maximum lipid content of is obtained on 4th day at 1.45 and 1.95kLux, the maximum value of lipid content of 13.35%w/w is reached on 3rd day with light intensity of 2.49kLux. This is caused due to photo-inhibition. The time history of contents and productivities of lipid at all the light intensities(1.45-3.2kLux) are provided in table 7.5. For light intensities of 1.4with the variation of light intensities 5 and 1.95 kLux, the lipid productivity initially increases up to 1st day and afterwards there is a decreasing trend up to 4th day. As expected, the trend is similar to that of the biomass productivity. The lipid productivity of *L.subtilis* JUCHE lies in the range of 0.0032-0.021g/L/d for the light intensity within 1.45-3.2kLux. The highest value of lipid productivity of 0.021g/L/d is observed on 3rd day under the illumination of 2.5kLux. During the study on *Chlorella vulgaris* (ESP-6) in a cubical airlift Photobioreactor using inorganic carbon sources (NaHCO₃, 600 mg/L and 10% CO₂) and light intensities of 11.04, 23, 40.94 and 52.44 $\mu\text{mol m}^{-2} \text{s}^{-1}$, [15] Xia Hu. et al. 2016 observed the increase in both the lipid content as well as productivity with the increase in light intensity [15]. As reported by the researchers, the highest values of lipid content and productivity of 30%w/w and 135 mg/L/d respectively were achieved under the illumination of 52.44 $\mu\text{mol m}^{-2} \text{s}^{-1}$ [15]. During the studies on *Desmodesmus sp.*, *Scenedesmus obliquus.*, *C. vulgaris*, *E. pseudoalveolaris* using waste water as carbon source with the variation of light intensities from 50-300 $\mu\text{mol m}^{-2} \text{s}^{-1}$, it was observed that the highest value of lipid content was obtained for *Scenedesmusobliquus*.i.e. 11.6% under the light intensity of 300 $\mu\text{mol m}^{-2} \text{s}^{-1}$ [16]. The maximum values of lipid contents for *Desmodesmus sp.*, *C. vulgaris*, *E. pseudoalveolaris* were, however, observed to be 7, 4.5 and 3%w/w respectively under the illumination of 300, 50 and 150 $\mu\text{mol m}^{-2} \text{s}^{-1}$ [16]. When the effect of variation of light intensity (260, 530, 770 and 1000 $\mu\text{mol m}^{-2} \text{s}^{-1}$) on the lipid content of the microalgal strain, *Ettlia sp.* YC001 was studied, it was also reported that the lipid content followed an increasing trend with the increase of light intensity [17]. According to the report, the lipid content of *Ettlia sp.* YC001 increased from 17%w/w to 23 %w/w as the light intensity was increased from 260 to 1000 $\mu\text{mol m}^{-2} \text{s}^{-1}$ [17]. Through the comparison of the lipid production data of *L. subtilis*JUCHE1 with the reported literature data it can be inferred that the effect of light intensity on the lipid production is similar [15, 16, 17]. It can also be claimed that the

capability of lipid accumulation of *L. subtilis*JUCHE1 is higher than the algal strained reported in the literature and can be considered as an oleaginous species.

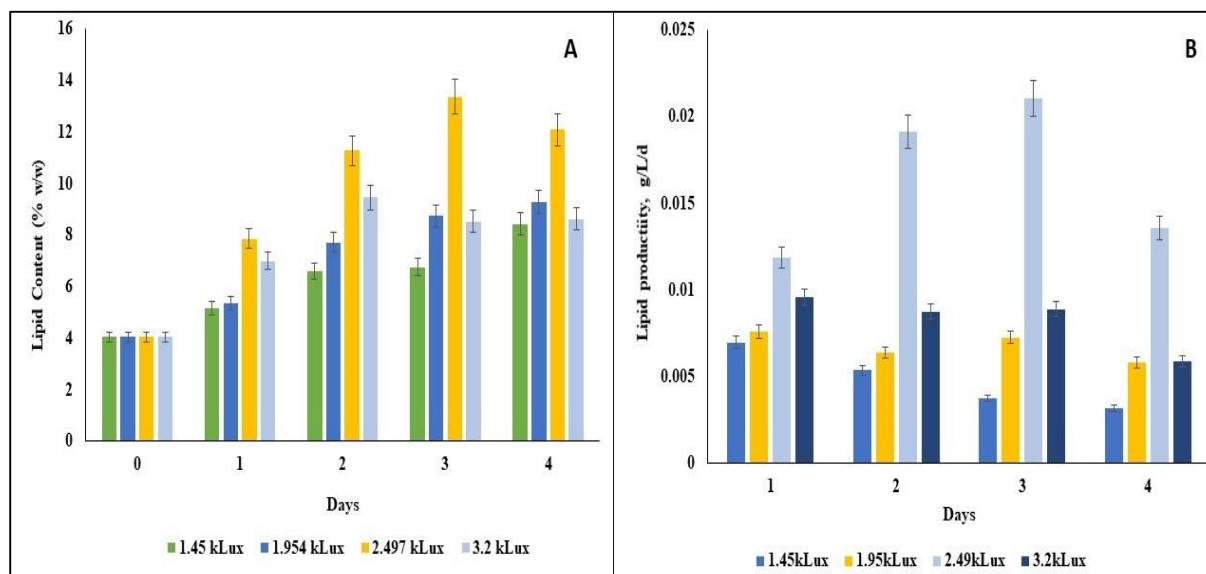


Figure 7.9 Bar plot of (A)Lipid content(%w/w) and (B) Lipid productivity of *L.subtilis* JUCHE1 at each time intervals i.e. 0-4th days for different light intensities having range of 1.45-3.2kLux.

Table 7.5 Experimental values of lipid content at each time intervals varying light intensities from (1.45-3.2kLux).

| Days | Lipid content(%w/w) | | | | Lipid productivity (g/L/d) | | | |
|------|------------------------|------|-------|------|----------------------------|---------|--------|--------|
| | Light intensity (kLux) | | | | Light intensity (kLux) | | | |
| | 1.45 | 1.95 | 2.5 | 3.2 | 1.45 | 1.95 | 2.5 | 3.2 |
| 0 | 4.04 | 4.04 | 4.04 | 4.04 | 0 | 0 | 0 | 0 |
| 1 | 5.16 | 5.34 | 7.85 | 6.99 | 0.0069 | 0.0076 | 0.0118 | 0.0095 |
| 2 | 6.59 | 7.71 | 11.27 | 9.45 | 0.0054 | 0.0063 | 0.0191 | 0.0087 |
| 3 | 6.75 | 8.74 | 13.35 | 8.53 | 0.0037 | 0.0073 | 0.021 | 0.0089 |
| 4 | 8.43 | 9.27 | 12.08 | 8.61 | 0.0032 | 0.00579 | 0.0135 | 0.0058 |

7.3.2 Lipid accumulation of *L.subtilis* JUCHE1 under Photoheterotrophic growth

7.3.2.1 Lipid production varying CO₂ equivalent glycerol concentrations under photoheterotrophic mode of cultivation

As revealed from Figure 7.10, the cultivation of *L. subtilis* JUCHE1 under photoheterotrophic condition using equivalent glycerol concentrations shows a reverse trend from photoautotrophic condition. Here in this Figure 7.10 it is clear that with increase in equivalent glycerol concentrations the lipid accumulation of *L. subtilis* JUCHE1 get decreased. Finally, the maximum lipid content of 56.34% (w/w) has been observed at the minimum glycerol concentration equivalent to 5% (v/v). Since glycerol is easily available to the cells, the majority of carbon assimilated is stored in form of lipids (Jajesniak et al. 2014; Khanra et al. 2017)[18, 19]. Therefore, lipid content of algal strains in photoheterotrophic mode is much higher as compared to the photoautotrophic mode.

Moreover, the CO₂ produced during glycerol assimilation is assimilated through photosynthesis, as shown in Figure 7. 12[20]. The calculated values of lipid contents and productivities against each time interval for photo-heterotrophic growth have been provided below in table 7.6. From table 7.6, it has been found that the maximum lipid productivity was also obtained at 5% equivalent concentration of glycerol i.e. 0.070248 g/L/d on 4th day. G. H. Gim et al.2016, reported that under photoheterotrophic condition three different strains of microalgae such as *Isochrysis galbana* LB987, *Nannochloropsis oculata* CCAP849/1, and *Dunaliella salina* are cultivated using organic carbon (Glucose) under constant illumination [21]. In this study the glucose concentrations for *Isochrysis galbana* LB987, *Nannochloropsis oculata* CCAP849/1 is 0.02 M and 0.05 M for *Dunaliella salina* and also the experiments were conducted through variation of light intensities in the range 0 to 200 $\mu\text{mol}/\text{m}^2/\text{s}$ [21]. the article reported that the maximum values of lipid contents for *Isochrysis galbana* LB987, *Nannochloropsis oculata* CCAP849/1, and *Dunaliella salina*, are 35, 38 and 33% w/w approximately obtained under the illumination of 150 $\mu\text{mol m}^{-2} \text{s}^{-1}$ [21].

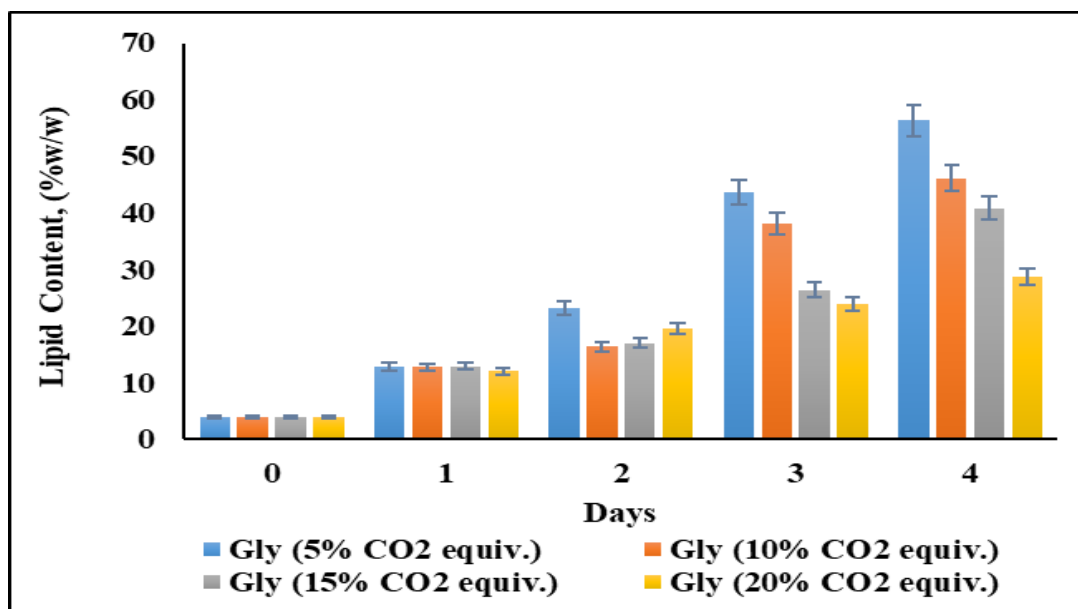


Figure 7.10 Lipid content(%w/w) of *Leptolyngbya subtilis* JUCHE1 varying different equivalent glycerol concentrations.

Table 7.6 Experimental values of Lipid content(%w/w) and lipid productivities (g/L/d) with respect to time under photo-heterotrophic growth.

| Days | Lipid content (%w/w) | | | | Lipid productivities(g/L/d) | | | |
|------|----------------------|-----------|-----------|-----------|-----------------------------|-----------|-----------|-----------|
| | 5% equiv. | 10% equiv | 15% equiv | 20% equiv | 5% equiv. | 10% equiv | 15% equiv | 20% equiv |
| 0 | 3.88 | 3.88 | 3.88 | 3.88 | 0 | 0 | 0 | 0 |
| 1 | 12.79 | 12.69 | 12.84 | 12.07 | 0.0223 | 0.0315 | 0.0347 | 0.0241 |
| 2 | 23.18 | 16.33 | 16.9 | 19.6 | 0.0394 | 0.0440 | 0.0341 | 0.0307 |
| 3 | 43.62 | 38.1 | 26.39 | 23.8 | 0.0589 | 0.0462 | 0.0552 | 0.0327 |
| 4 | 56.34 | 46.1 | 40.76 | 28.77 | 0.07024 | 0.0548 | 0.0656 | 0.0355 |

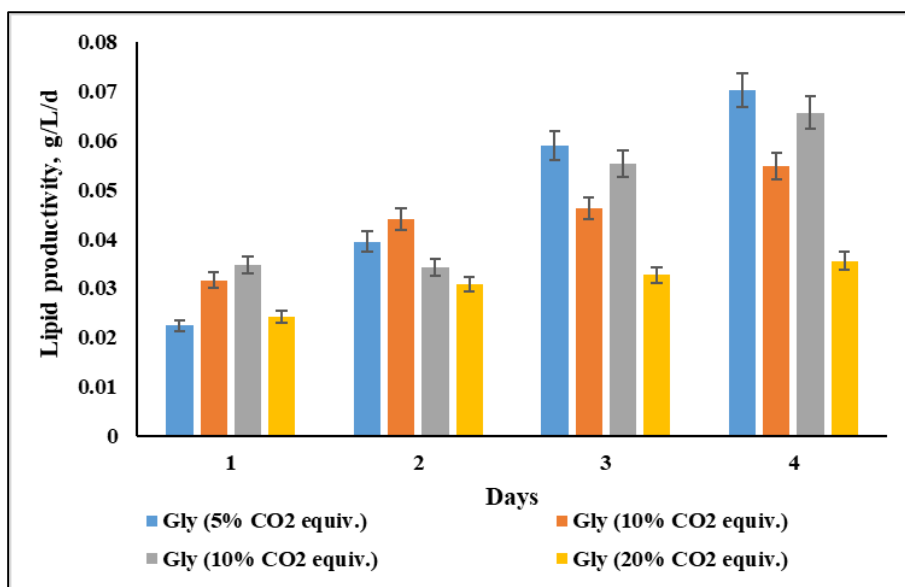


Figure 7.11 Lipid productivities(g/L/d) of *Leptolyngbya subtilis* JUCHE1 varying different equivalent glycerol concentrations.

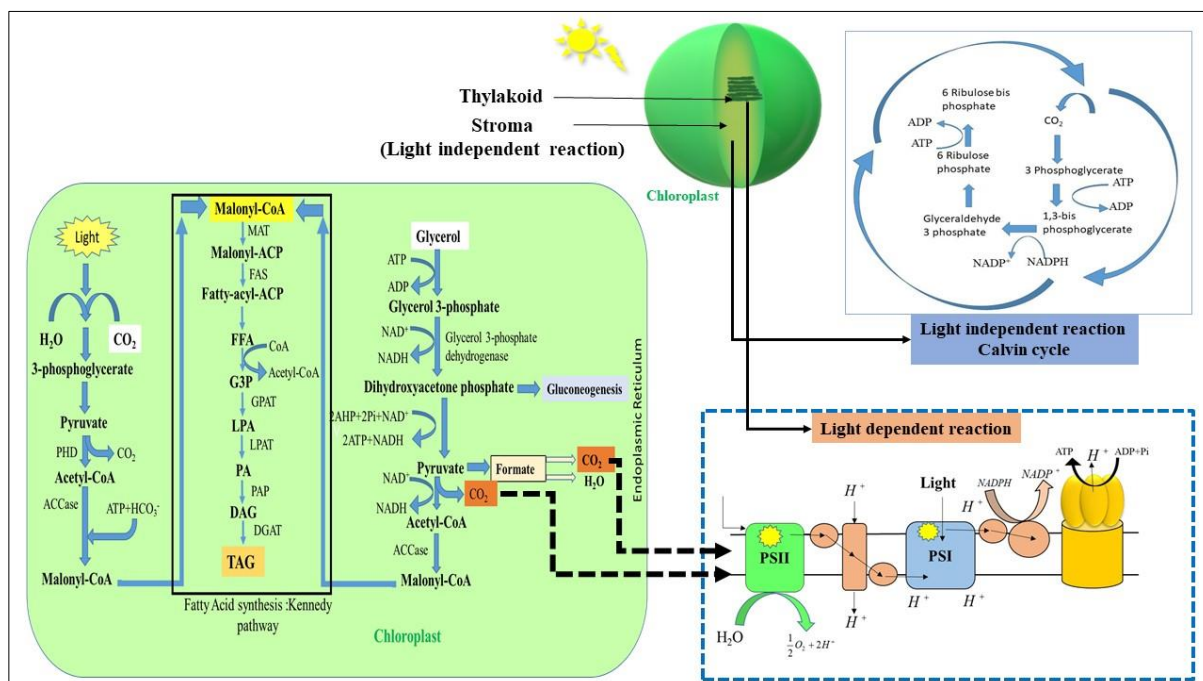


Figure 7.12 Reaction pathway for fatty acid synthesis under mixotrophic growth of algae using CO₂ and glycerol.

7.3.2.2 Characterization of Lipid

Figure 7.13 represents the chromatogram of GC-MS analysis of lipid sample extracted from the algal biomass which has been cultivated under photoheterotrophic condition using glycerol as organic carbon source. In Table 7.7, the fatty acid profiles have been identified from MS-Library. Other than fatty acids, alcohol group i.e. “Glycidol” also identified which is an organic compound mainly used for synthesis of glycerol, glycidyl ethers, esters etc. Some other compounds also identified d-Gala-1-ido-octonicamide (Amine group), 2-Myristinoyl pantetheine (Amide group), N-(N-Glycyl-L-leucyl)glycine (Amino acids).

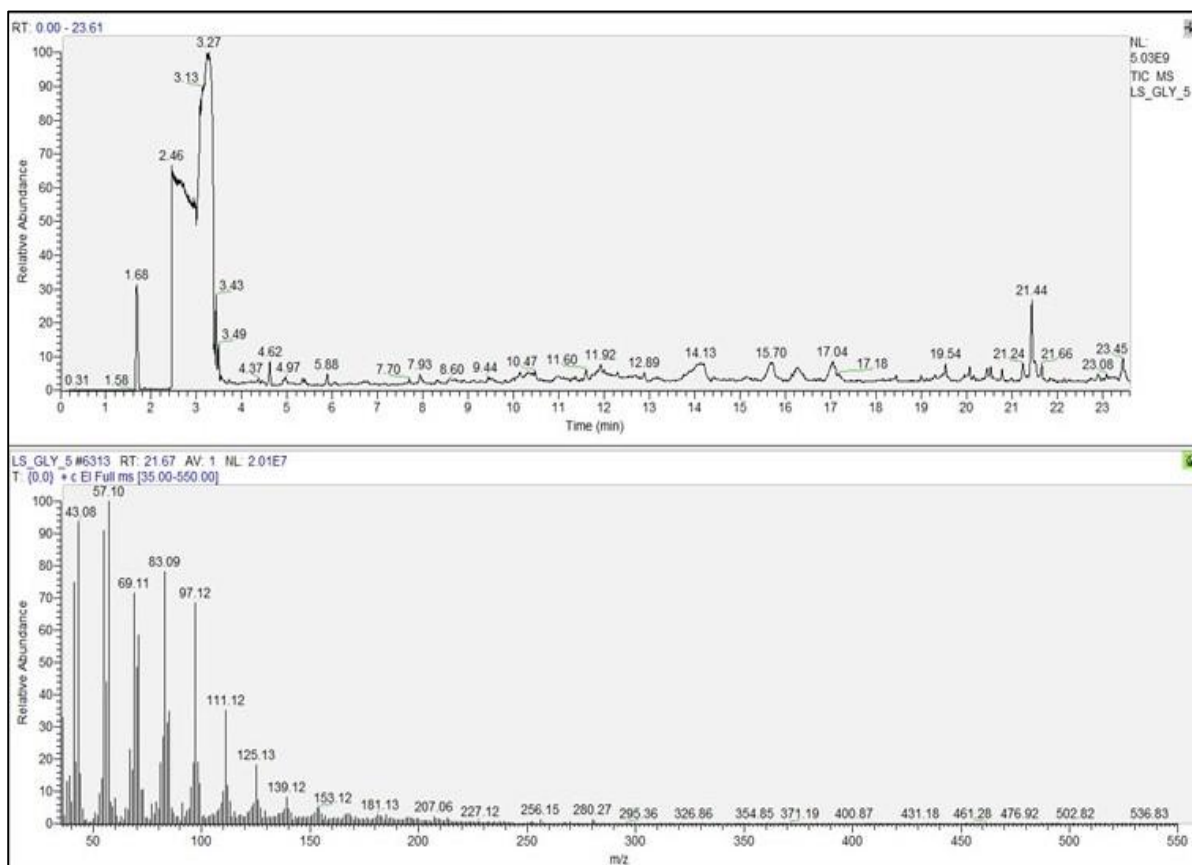


Figure 7.13 Chromatogram of extracted lipid under photoheterotrophic growth using glycerol as organic carbon source.

Table 7.7 Identified compounds from extracted lipid of *L.subtilis* JUCHE1 under photo-heterotrophic growth using glycerol (as carbon source)

| Serial no. | Identified compounds | Molecular formula | Retention time |
|------------|--|--|----------------|
| 1 | Phosphorochloridic acid, heptylpentyl ester | C ₁₂ H ₂₆ ClO ₃ P | 3.48 |
| 2 | 2-Propenoic acid, 3-phenyl-, methyl ester | C ₁₀ H ₁₀ O ₂ | 4.64 |
| 3 | Glycidol | C ₃ H ₆ O ₂ | 4.94 |
| 4 | Oxalic acid, isohexylpentyl ester | C ₁₃ H ₂₄ O ₄ | 4.97 |
| 5 | 4-Hexenoic acid, 6-hydroxy-4-methyl-, methyl ester, (Z)- | C ₈ H ₁₄ O ₃ | 5.87 |
| 6 | Cyclooctaneacetic acid | C ₁₀ H ₁₆ O ₃ | 5.91 |
| 7 | Carbamic acid, phenyl ester | C ₇ H ₇ NO ₂ | 7.95 |
| 8 | 11,14-Eicosadienoic acid, methyl ester | C ₂₁ H ₃₈ O ₂ | 10.45 |
| 9 | Benzenepropanoic acid | C ₁₀ H ₁₂ O ₂ | 10.47 |
| 10 | 3-Hydroxydodecanoic acid | C ₁₂ H ₂₄ O ₃ | 11.60 |
| 11 | 1,3,5-Pentanetricarboxylic acid | C ₈ H ₁₂ O ₆ | 14.16 |
| 12 | 2,4-Diaminobutyric acid | C ₄ H ₁₀ N ₂ O ₂ | 15.66 |
| 13 | 2-Hydroxytetradecanoic acid | C ₁₄ H ₂₈ O ₃ | 18.47 |
| 14 | 9-Hexadecenoic acid | C ₁₆ H ₃₀ O ₂ | 19.57 |
| 15 | 3-Hydroxydodecanoic acid | C ₁₂ H ₂₄ O ₃ | 20.05 |
| 16 | Oleic acid | C ₁₈ H ₃₄ O ₂ | 20.51 |
| 17 | Palmitoleic acid | C ₁₆ H ₃₀ O ₂ | 21.22 |
| 18 | cis-11-Eicosenoic acid | C ₂₀ H ₃₈ O ₂ | 21.67 |

7.3.3 Comparison of lipid production of *L. subtilis* JUCHE1 under both photo-auto and heterotrophic growth condition

From the analysis of the table 7.8, it is revealed that similar to the observation with the present cyanobacteria, the lipid accumulation is also favored for photoheterotrophic/mixotrophic growth of different algae using glycerol as the carbon source. Wang et al reported a study where the lipid content obtained under mixotrophic condition is many fold higher than that obtained under autotrophic condition[22]. Similar observation has been reported by Li et al. 2014, during their studies on *Chlorella sokinianana* using glucose under mixotrophic condition [20]. Besides refixation of CO₂ through photosynthesis, the light dependent non-cyclic electron flow through PSI and PSII responsible for the formation of ATP and NADPH have been identified as some of the key factors responsible for enhanced lipid production during mixotrophic[20]. However, the exact mechanism behind the enhanced lipid content needs more focused studies in this area.

Table 7.8 Lipid content and lipid productivities of algal strains in both autotrophic and heterotrophic conditions.

| Sl. No. | Algal strain | Culture cultivation process | Light intensity (kLux) | Carbon source | Lipid content %(w/w) | Lipid productivity (g/L/d) | Ref. |
|---------|--------------------------------|-----------------------------|------------------------|-----------------|----------------------|----------------------------|------|
| 1. | <i>S. obliquus</i> AS-6-1 | Photo-autotrophic | 10.36* | CO ₂ | 11.7 | 0.04436 ± 0.00473 | 8 |
| 2. | <i>S. obliquus</i> CNW-1 | Photo-autotrophic | 10.36* | CO ₂ | 9.2 | 0.03615 ± 0.00386 | |
| 3. | <i>S. obliquus</i> ESP-5 | Photo-autotrophic | 10.36* | CO ₂ | 8.3 | 0.03121 ± 0.00157 | |
| 4. | <i>Pseudochlorococcum</i> sp. | Photo-autotrophic | 1.36 | CO ₂ | 3 | 0.0235 ± 0.00324 | 7 |
| 5. | <i>Synechococcus</i> spp. | Photo-autotrophic | 0.199* | CO ₂ | 11.78 | 0.0696 | 20 |
| 6. | <i>Desmodesmus</i> sp. (PCH19) | Photo-autotrophic | 4.76* | CO ₂ | 20.7 | - | 21 |
| 7. | <i>Scenedesmus obliquus</i> | Photo-heterotrophic | 7.4* | Glycerol | 24.39±0.781 | 0.04008 ± 0.00189 | 22 |

| Sl. No. | Algal strain | Culture cultivation process | Light intensity (kLux) | Carbon source | Lipid content %(w/w) | Lipid productivity (g/L/d) | Ref. |
|---------|-------------------------------------|-----------------------------|------------------------|-----------------|----------------------|----------------------------|----------------------|
| 8. | <i>Desmodesmus sp. (PCH19)</i> | Photo-heterotrophic | 4.76* | Glycerol | 28.3 | - | 21 |
| 9. | <i>Chlorella sp.PCH37</i> | Photo-heterotrophic | 4.76* | Glycerol | 31 | - | 21 |
| 10. | <i>Chlorella sp.LB1H09</i> | Photo-heterotrophic | 14.06* | Glycerol | 16.5 approx. | - | 23 |
| 11. | <i>Spirulina platensis CFTRI</i> | Photo-heterotrophic | 16.98* | Glycerol | 8.29± 0.54 | - | 24 |
| 12. | <i>Leptolyngbya subtilis JUCHE1</i> | Photoautotrophic | 2.5 | CO ₂ | 12.5 | 0.02005 | Present study |
| 13. | <i>Leptolyngbya subtilis JUCHE1</i> | Photo-heterotrophic | 2.5 | Glycerol | 56 | 0.070248 | |

*The light intensities were converted from $\mu\text{mol m}^{-2} \text{s}^{-1}$ to kLux using the correlation reported in Thimijan et al. 1983[25].

7.3.4 Lipid accumulation of *L.subtilis*JUCHE1 under mixotrophic growth

7.3.4.1 Lipid production of *L.subtilis*JUCHE1 under mixotrophic condition

Figure 7.14 represents the experimental data of time historis of lipid content(%w/w) of the blue-green alga using C-concentrations, equivalent to 5-20%(v/v) inlet gas phase CO₂ concentration, as supplied by mixture of glycerol and CO₂ (CO₂:Glycerol::1:1), as parameter. For all C-concentration, except that equivalent to 20%(v/v) inlet gas phase CO₂ concentration, the time history of lipid concentration follows an increasing trend up to 5th day. For C-concentration equivalent to 20%(v/v) inlet gas phase CO₂ concentration, increasing trend is shown up to 4th day, beyond which there exists a decreasing trend. The maximum lipid content of 26.71% w/w has been observed for C-concentration equivalent to 15%(v/v) inlet gas phase CO₂ concentration on 5th day. Figure7.15, represents the time history curves of lipid productivity of the blue-green alga using C-concentrations, equivalent to 5-20%(v/v) inlet gas phase CO₂ concentration, as supplied by mixture of glycerol and CO₂ (CO₂:Glycerol::1:1), as parameter. From the analysis of the figure, it is clear that the highest lipid productivity of

0.0272g/L/d is observed on 3rd day at 15% C-concentration. All the experimental values of both lipid content and productivities are provided in table 7.9. As discussed in sections 7.2.1.1 and 7.2.2, time histories of lipid concentration generally have increasing trends similar to the heterotrophic one. As discussed in sections 7.2.1.1 and 7.2.2, the highest values of lipid contents of 12.5%w/w on 3rd day and 56.34%w/w on 4th day have been obtained with inlet gas phase CO₂ concentration of 15%(v/v) and glycerol concentration equivalent to 5%(v/v) inlet gas phase CO₂ concentration for photoautotrophic and photoheterotrophic conditions respectively. From the comparison with the lipid content data of photoautotrophic and photoheterotrophic ones, it appears that the highest lipid content is enhanced in comparison to the former and is lower than that obtained for the latter one. In comparison to other trophic conditions, there is a time lag (*Mixo:5days > Hetero:4days > Auto:3days*)for the achievement of the highest lipid content under mixotrophic conditions. The enhancement in lipid content with respect to photoautotrophic condition can be explained by the incorporation of heterotrophic pathway for lipid generation due to the co-feeding of glycerol with CO₂. Availability of CO₂ in presence of light supposedly increases the activity of the Calvin cycle wherein lipid precursors are synthesised thus leading to increased lipid concentration in the cell (Shene et al. 2016)[26]. More studies in the direction of metabolic engineering should be conducted to unwind the underlying reasons behind the time lag. Figure 7.15, represents the time history curves of lipid productivity of the blue-green alga using C-concentrations, equivalent to 5-20%(v/v) inlet gas phase CO₂ concentration, as supplied by mixture of glycerol and CO₂ (CO₂:Glycerol::1:1), as parameter. From the analysis of the figure, it is clear that the highest lipid productivity of 0.0272g/L/d is observed on 3rd day at 15% C-concentration. In case of photoautotrophic and heterotrophic conditions, as discussed in Sections 7.2.1.1 and 7.2.2, the highest lipid productivities of 0.02g/L/d and 0.07g/L/d have been obtained on 3rd day and on 4th day with inlet gas phase CO₂ concentration of 15%(v/v) and glycerol concentration equivalent to 5%(v/v) inlet gas phase CO₂ concentration respectively. When the highest lipid productivities under three trophic conditions are compared, it is clearly observed that although the value for mixotrophic condition is slightly higher than that obtained under autotrophic condition, it is much lower than that obtained under heterotrophic condition. The time lag is exactly same as that observed in case of lipid content. Figure 7.16 represents a comparative bar plot for the maximum values of content and productivity of lipid under three trophic conditions. Table 7.10 represents the literature data on the lipid content of different algal strains using CO₂/Air and glycerol as carbon sources, gas phase CO₂ concentration ranging from 0.04-10%v/v and glycerol concentration ranging from 1-20.4g/L[27-30]. From the analysis of the

data it appears that the lipid content lies in the range of 15-34% w/w, while in the present case the highest lipid content of 26.71% using 7.5% CO₂ and 0.0569g/L glycerol (equivalent to 7.5% CO₂) is achieved and is comparable to others.

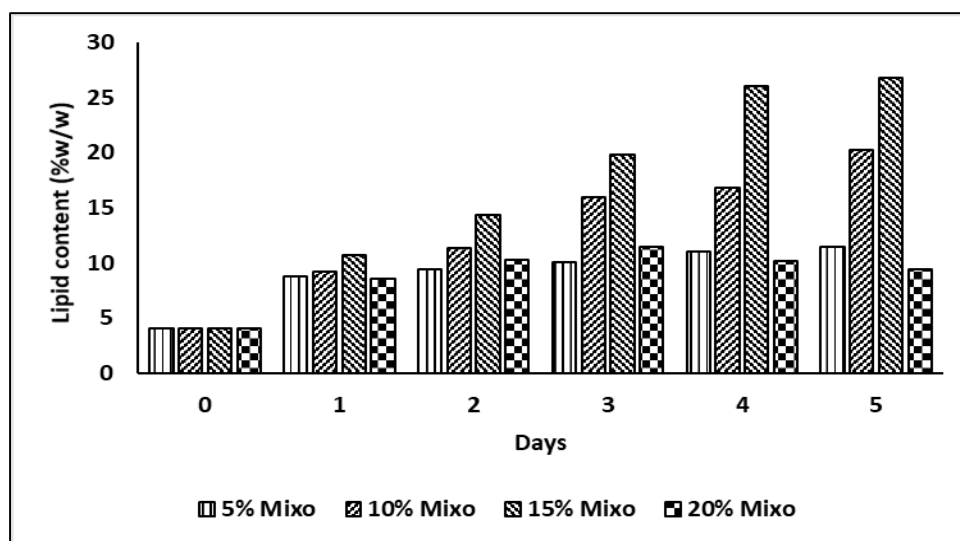


Figure 7.14 Lipid production (g/L) by *L.subtilis*JUCHE1 varying C-concentrations under mixotrophic growth.

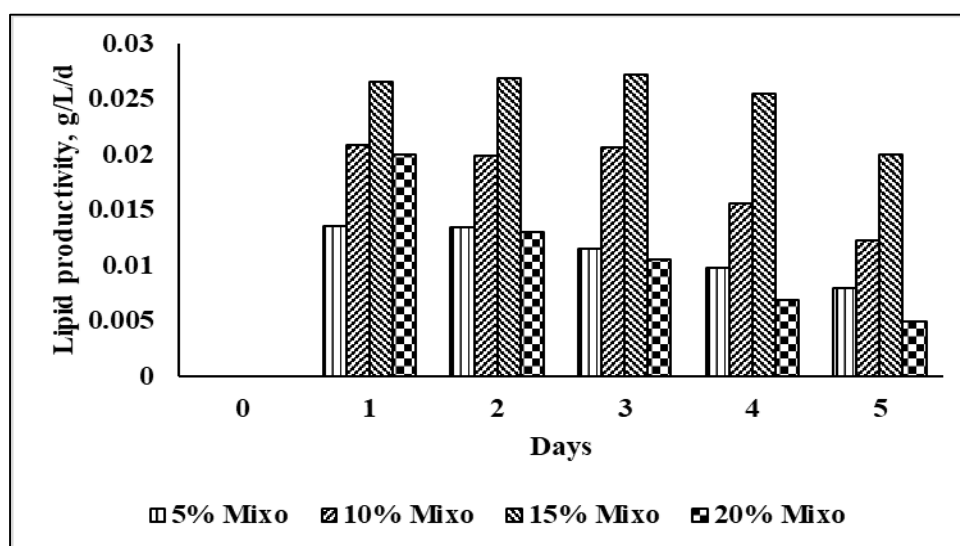


Figure 7.15 Lipid productivities (g/L/d) against each time intervals varying different C-concentrations under mixotrophic growth.

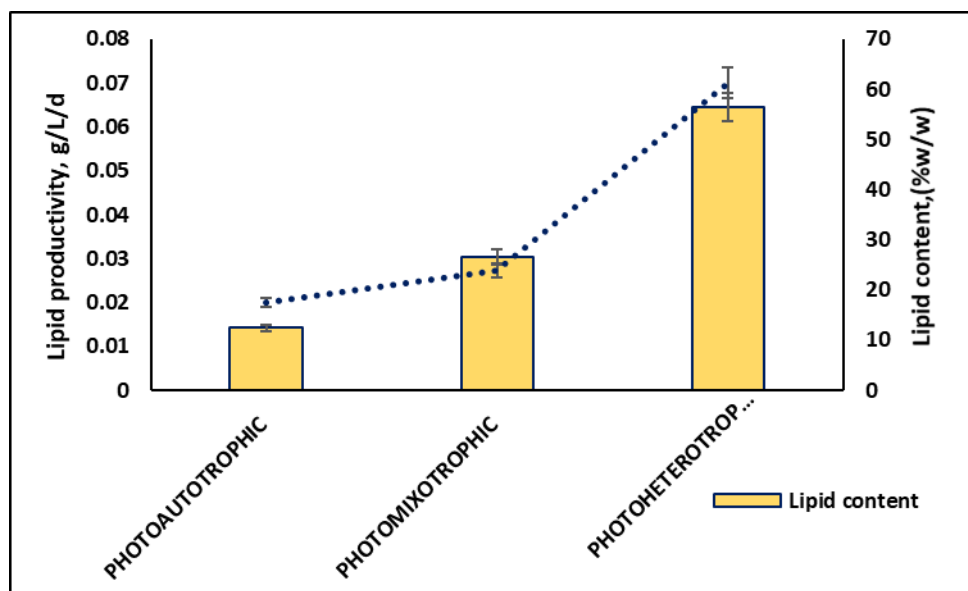


Figure 7.16 Maximum values of Lipid content (%w/w) and productivity (g/L/d) under photoautotrophic, photomixotrophic and photoheterotrophic growth.

Table 7.9 Experimental values of lipid content and productivities at different Carbon concentrations CO₂:Glycerol (1:1 ratio) under mixotrophic growth.

| Days | Lipid content(%w/w) | | | | Lipid productivities (g/L/d) | | | |
|------|---------------------|-------|-------|-------|------------------------------|--------|--------|--------|
| | 5 | 10 | 15 | 20 | 5 | 10 | 15 | 20 |
| 0 | 4.04 | 4.04 | 4.04 | 4.04 | 0 | 0 | 0 | 0 |
| 1 | 8.82 | 9.15 | 10.69 | 8.61 | 0.0136 | 0.0208 | 0.0265 | 0.0199 |
| 2 | 9.36 | 11.38 | 14.37 | 10.25 | 0.0134 | 0.0199 | 0.0269 | 0.013 |
| 3 | 10.05 | 15.91 | 19.79 | 11.42 | 0.0115 | 0.0206 | 0.0272 | 0.0104 |
| 4 | 11 | 16.79 | 26 | 10.19 | 0.0098 | 0.0156 | 0.0254 | 0.0069 |
| 5 | 11.39 | 20.24 | 26.71 | 9.44 | 0.0079 | 0.0123 | 0.02 | 0.0049 |

Table 7.10 The values of Lipid content (%w/w) of various algal strains under mixotrophic growth.

| Algal strain | Organic C-source | Organic C-conc. (g/L) | Inorganic C-source | Inorganic C-conc. (%v/v) | Lipid Content (%w/w) | Ref. |
|---------------------------------------|------------------|-----------------------|--------------------|--------------------------|----------------------|---------------|
| <i>Chlorella sp. Y8-1</i> | Glycerol | 1 | CO ₂ | 10 | 15±2.75 | 27 |
| <i>Chlorella vulgaris</i> (KMMCC-355) | Crude glycerol | 5 | CO ₂ | - | 15.91±0.78 | 28 |
| <i>B. braunii</i> (KMMCC-1681) | Crude glycerol | 5 | CO ₂ | - | 16.41±0.92 | |
| <i>Scenedesmus sp.</i> (KMMCC-1235) | Crude glycerol | 5 | CO ₂ | - | 16.24±0.84 | |
| <i>Chlorella vulgaris</i> | Glycerol | 10 | Air | 0.04 | 22±4 | 29 |
| <i>Chlorella protothecoides</i> | Glycerol | 20.4 | Air | 0.04 | 17.50±4.98 | 30 |
| <i>L.subtilis</i> JUCHE1 | Glycerol | 7.5% | CO ₂ | 7.5% | 26.71 | Present study |

7.4.5 Effect of organic and inorganic carbon source on pigments (Chlorophyll and Carotenoid) synthesis of *L.subtilis* JUCHE1 under different growth modes (Photoautotrophic, photoheterotrophic and photomixotrophic)

Figure 7.17 represents the bar plot depicting the chlorophyll (a+b) and carotenoid contents (%w/w), of *L.subtilis* JUCHE1 under different mode of growth (photoautotrophic, photoheterotrophic and photomixotrophic). From the close analysis of Figure 7.13, it is observed that as compared to photomixotrophic and photoheterotrophic growth, the highest value of chlorophyll (a+b) content of *L. subtilis* JUCHE1 was obtained under photoautotrophic growth i.e. 0.289 (%w/w). This has been extracted from the maximum biomass concentration achieved on 3rd day at 15 (%v/v) inlet CO₂ concentrations as described in section 6.5.4 (chapter 6).

Whereas, the chlorophyll (a+b) content of 0.227 is achieved from the maximum biomass concentration under mixotrophic growth which has been obtained on 5th day from inlet mixed carbon sources (CO₂ and glycerol) equivalent to 15% (v/v) CO₂. Lowest chlorophyll (a+b) content of 0.186 % w/w is achieved under photoheterotrophic growth from the biomass obtained on 4th day at 0.11398g/L of glycerol concentration which is equivalent to 15% (v/v) CO₂.

In similar manner, the highest value of carotenoid content i.e. 0.116 %w/w is achieved under photoautotrophic growth as compared to photomixotrophic (0.114%) and photoheterotrophic (0.087%) growth. The Chlorophyll (a+b) and Carotenoid contents (%w/w) of other algal strains have been compared with the values obtained for *L. subtilis* JUCHE1, as provided below in Table 7.8.

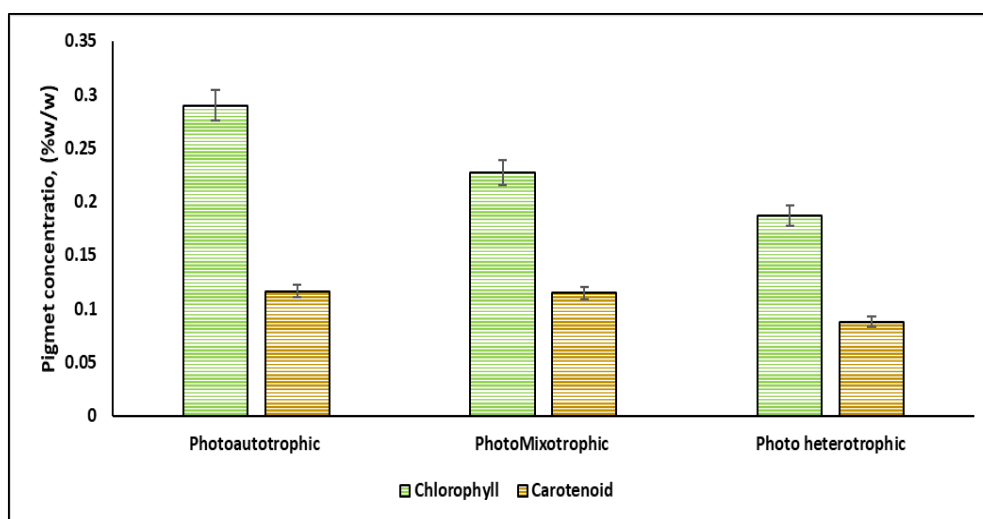


Figure 7. 17 Bar plot of Chlorophyll (a+b) and Carotenoid contents (%w/w) of *L.subtilis* JUCHE1 observed under different growth condition (Photoautotrophic, Photoheterotrophic and Photomixotrophic) on 4-5th day of culture period.

Table 7.11 is representing the pigment contents (% wt.) of different algal strains obtained under different modes of growth such as photoautotrophic, photoheterotrophic and photomixotrophic. In one article it has been reported that the experimental study on growth has been conducted by using four different algal strains: *Chlorella sp*, *Marine Chlorella sp.*, *Nannochloropsis sp.* and *Cheatoceros sp.* and cultivated under different modes of growth (Photoautotrophic, Photoheterotrophic and Photomixotrophic) using both inorganic carbon source (Na₂CO₃) and glucose as organic carbon sources [31]. From this study it has been revealed that the highest chlorophyll contents of 2.21, 2.41, 2.71 and 2.36 (%wt).have been achieved respectively for *Chlorella sp* (Fresh water), *Chlorella sp.*(Marine), *Nannochloropsis*

sp. and Cheatocerossp under photoautotrophic growth [31]. As provided in table 7.8, the lowest values of chlorophyll contents in the range of 0.3-0.415% w/w for all the algal strains have been achieved under photoheterotrophic growth [31]. Another study reported that under mixotrophic growth using both the organic as well as inorganic carbon sources such as NaHCO_3 and Glucose, the highest chlorophyll content of 1.4% has been achieved for the microalga *C. sorokiniana* [32]. Under mixotrophic growth, the chlorophyll contents of 2.83 and 2.91% have been found by supplying glycerol and glycerin as organic carbon sources and 0.04% CO_2 (Air) as inorganic carbon for algal cultivation [33]. Another study also conducted the experiments on algal growth cultivated under three different modes (Photoautotrophic, Photoheterotrophic and Photomixotrophic) by using different strains of microalgae namely *Isochrysis galbana* LB987, *Nannochloropsis oculata* CCAP849/1, *Dunaliellasalina* [34]. It was found that the highest values of chlorophyll content for all the algal strains were achieved under photoautotrophic conditions using NaHCO_3 as inorganic carbon source [34]. The values of chlorophyll contents i.e., 3.23, 4.19 and 3.85 %wt. were respectively obtained for *Isochrysis galbana* LB987, *Nannochloropsis oculata* CCAP849/1 and *Dunaliella salina* [34]. In heterotrophic and mixotrophic growth the range of chlorophyll contents varied from 0.026-0.041% w/w and 0.29-0.35% w/w respectively for the algal strains [34]. The study reported that the maximum chlorophyll and carotenoid contents of 1.9% and 0.24% for *N. oleoabundans* have been obtained respectively under mixotrophic growth [35].

From the literature study it has been revealed that the pigment synthesis in algal strains is higher under photoautotrophic condition as compared to photoheterotrophic and photomixotrophic growth [31, 32, 33, 34, 35]. The Chlorophyll (a+b) and Carotenoid production trends of *L. subtilis* JUCHE1 is similar with other algal strains i.e. the maximum values of pigment content is observed under photoautotrophic growth. Most of the study used Na_2CO_3 or NaHCO_3 as inorganic carbon source for conducting photoautotrophic growth of respective algae [31, 32, 34]. Under photoheterotrophic growth the pigment content is generally low for all the algal strains as shown in table 7.8 [31, 34].

Table 7.11 Pigment contents (%wt.) of different algal strains under different growth conditions (Photoautotrophic, Photoheterotrophic and Photomixotrophic).

| Growth condition | Algal strain | Inorganic Carbon source | Organic carbon source | Pigment content (%) | | Reference |
|---------------------|---|---|-----------------------|---------------------|------------|-----------|
| | | | | Chlorophyll | Carotenoid | |
| Photoautotrophic | <i>Chlorella sp.</i> | Na ₂ CO ₃ 0.02 | - | 2.21 | - | 31 |
| | <i>Marine Chlorella sp.</i> | | | 2.41 | - | |
| | <i>Nannochloropsis sp.</i> | | | 2.71 | - | |
| | <i>Cheatoceros sp.</i> | | | 2.36 | - | |
| Photo heterotrophic | Fresh water <i>Chlorella sp.</i> | - | Glucose | 0.388 | - | |
| | <i>Marine Chlorella sp.</i> | | | 0.415 | - | |
| | <i>Nannochloropsis sp.</i> | | | 0.3 | -- | |
| | <i>Cheatoceros sp.</i> | | | 0.33 | - | |
| Photomixotrophic | Fresh water <i>Chlorella sp.</i> | Na ₂ CO ₃ | Glucose | 1.88 | - | |
| | <i>Marine Chlorella sp.</i> | | | 2.29 | - | |
| | <i>Nannochloropsis sp.</i> | | | 2.25 | - | |
| | <i>Cheatoceros sp.</i> | | | 1.55 | - | |
| Photomixotrophic | <i>C. sorokiniana</i> | NaHCO ₃ | Glucose | 1.4 | - | 32 |
| Photomixotrophic | <i>P. tricornutum</i> | Air (0.04% CO ₂) | Glycerol | 2.83 | 0.59 | 33 |
| | | | Starch | 3.32 | 1.04 | |
| | | | Glycine | 2.97 | 0.02 | |
| | | | Glucose | 0.71 | 0.49 | |
| | | | Lactate | 3.79 | 0.64 | |
| Photoautotrophic | <i>Isochrysisgalbana LB987</i> | NaHCO ₃ | - | 3.23 | - | 34 |
| | <i>Nannochloropsisoculata CCAP849/1</i> | | - | 4.19 | - | |
| | <i>Dunaliellasalina,</i> | | - | 3.85 | - | |
| Photoheterotrophic | <i>Isochrysisgalbana LB987</i> | - | Glucose | 0.041 | - | |
| | <i>Nannochloropsisoculata CCAP849/1</i> | | Glucose | 0.037 | | |
| | <i>Dunaliellasalina,</i> | | Glucose | 0.026 | | |
| Photomixotrophic | <i>Isochrysisgalbana LB987</i> | NaHCO ₃ | Glucose | 0.29 | | |
| | <i>Nannochloropsisoculata CCAP849/1</i> | | Glucose | 0.39 | | |

References

1. Li, T., Xu, J., Wu, H., Wang, G., Dai, S., Fan, J., ... & Xiang, W. (2016). A saponification method for chlorophyll removal from microalgae biomass as oil feedstock. *Marine drugs*, 14(9), 162.
2. Mandotra, S. K., Kumar, P., Suseela, M. R., & Ramteke, P. W. (2014). Fresh water green microalga *Scenedesmus abundans*: a potential feedstock for high quality biodiesel production. *Bioresource Technology*, 156, 42-47.
3. Sumanta, N., Haque, C. I., Nishika, J., & Suprakash, R. (2014). Spectrophotometric analysis of chlorophylls and carotenoids from commonly grown fern species by using various extracting solvents. *Res J Chem Sci*, 2231, 606X
4. Li, J., Tang, X., Pan, K., Zhu, B., Li, Y., Ma, X., & Zhao, Y. (2020). The regulating mechanisms of CO₂ fixation and carbon allocations of two *Chlorella* sp. strains in response to high CO₂ levels. *Chemosphere*, 247, 125814.
5. Yang, J., Rasa, E., Tantayotai, P., Scow, K. M., Yuan, H., & Hristova, K. R. (2011). Mathematical model of *Chlorella minutissima* UTEX2341 growth and lipid production under photoheterotrophic fermentation conditions. *Bioresource Technology*, 102(3), 3077-3082.
6. Khanra, A., Vasistha, S., & Rai, M. P. (2017). Glycerol on lipid enhancement and fame characterization in algae for raw material of biodiesel. *International Journal of Renewable Energy Research (IJRER)*, 7(4), 1970-1978.
7. Taher, H., Al-Zuhair, S., Al-Marzouqi, A., Haik, Y., & Farid, M. (2015). Growth of microalgae using CO₂ enriched air for biodiesel production in supercritical CO₂. *Renewable Energy*, 82, 61-70.
8. Ho, S. H., Chen, C. Y., & Chang, J. S. (2012). Effect of light intensity and nitrogen starvation on CO₂ fixation and lipid/carbohydrate production of an indigenous microalga *Scenedesmus obliquus* CNW-N. *Bioresource technology*, 113, 244-252.
9. Tan, X., Yao, L., Gao, Q., Wang, W., Qi, F., & Lu, X. (2011). Photosynthesis driven conversion of carbon dioxide to fatty alcohols and hydrocarbons in cyanobacteria. *Metabolic engineering*, 13(2), 169-176.

10. Choi, S. A., Jung, J. Y., Kim, K., Lee, J. S., Kwon, J. H., Kim, S. W., ... & Park, J. Y. (2014). Acid-catalyzed hot-water extraction of docosahexaenoic acid (DHA)-rich lipids from *Aurantiochytrium sp.* KRS101. *Bioresource technology*, 161, 469-472.
11. Tagliaferro, G.V., Izário Filho, H.J., Chandel, A.K., da Silva, S.S., Silva, M.B. and dos Santos, J.C., 2019. Continuous cultivation of *Chlorella minutissima* 26a in a tube-cylinder internal-loop airlift photobioreactor to support 3G biorefineries. *Renewable Energy*, 130, pp.439-445.
12. Sánchez-García, D., Resendiz-Isidro, A., Villegas-Garrido, T. L., Flores-Ortiz, C. M., Chávez-Gómez, B., & Cristiani-Urbina, E. (2013). Effect of nitrate on lipid production by *T. suecica*, *M. contortum*, and *C. minutissima*. *Central European Journal of Biology*, 8, 578-590.
13. Yodsuwan, N., Sawayama, S., & Sirisansaneeyakul, S. (2017). Effect of nitrogen concentration on growth, lipid production and fatty acid profiles of the marine diatom *Phaeodactylum tricorutum*. *Agriculture and Natural Resources*, 51(3), 190-197.
14. Ra, C. H., Kang, C. H., Kim, N. K., Lee, C. G., & Kim, S. K. (2015). Cultivation of four microalgae for biomass and oil production using a two-stage culture strategy with salt stress. *Renewable Energy*, 80, 117-122.
15. Dhup, S., & Dhawan, V. (2014). Effect of nitrogen concentration on lipid productivity and fatty acid composition of *Monoraphidium sp.* *Bioresource technology*, 152, 572-575.
16. Gour, R. S., Bairagi, M., Garlapati, V. K., & Kant, A. (2018). Enhanced microalgal lipid production with media engineering of potassium nitrate as a nitrogen source. *Bioengineered*, 9(1), 98-107.
17. Jajesniak, P., & HEMO A, W. T. (2014). Carbon dioxide capture and utilization using biological systems: opportunities and challenges. *J Bioprocess Biotech* 4 (155): 2.
18. Li, T., Zheng, Y., Yu, L., & Chen, S. (2014). Mixotrophic cultivation of a *Chlorella sorokiniana* strain for enhanced biomass and lipid production. *Biomass and Bioenergy*, 66, 204-213.
19. Ho, S. H., Chen, C. Y., & Chang, J. S. (2012). Effect of light intensity and nitrogen starvation on CO₂ fixation and lipid/carbohydrate production of an indigenous microalga *Scenedesmus obliquus* CNW-N. *Bioresource technology*, 113, 244-252.

20. Eloka-Eboka, A. C., & Inambao, F. L. (2017). Effects of CO₂ sequestration on lipid and biomass productivity in microalgal biomass production. *Applied Energy*, 195, 1100-1111.
21. Wang, Y. Z., Hallenbeck, P. C., Leite, G. B., Paranjape, K., & Huo, D. Q. (2016). Growth and lipid accumulation of indigenous algal strains under photoautotrophic and mixotrophic modes at low temperature. *Algal Research*, 16, 195-200.
22. Abomohra, A. E. F., Eladel, H., El-Esawi, M., Wang, S., Wang, Q., He, Z., ... & Hanelt, D. (2018). Effect of lipid-free microalgal biomass and waste glycerol on growth and lipid production of *Scenedesmus obliquus*: Innovative waste recycling for extraordinary lipid production. *Bioresource technology*, 249, 992-999.
23. Leite, G. B., Paranjape, K., Abdelaziz, A. E., & Hallenbeck, P. C. (2015). Utilization of biodiesel-derived glycerol or xylose for increased growth and lipid production by indigenous microalgae. *Bioresource technology*, 184, 123-130.
24. Narayan, M. S., Manoj, G. P., Vatchravelu, K., Bhagyalakshmi, N., & Mahadevaswamy, M. (2005). Utilization of glycerol as carbon source on the growth, pigment and lipid production in *Spirulina platensis*. *International journal of food sciences and nutrition*, 56(7), 521-528.
25. Thimijan RW, Heins RD (1983) Photometric, radiometric, and quantum light units of measure: a review of procedures for interconversion. *HortScience* 18(6):818–822
https://www.plantgrower.org/uploads/6/5/5/4/65545169/light_conversion_paper_thimijan_1983_ocr.pdf
26. Shene, C., Chisti, Y., Vergara, D., Burgos-Díaz, C., Rubilar, M., & Bustamante, M. (2016). Production of eicosapentaenoic acid by *Nannochloropsis oculata*: effects of carbon dioxide and glycerol. *Journal of Biotechnology*, 239, 47-56.
27. Lin, T. S., & Wu, J. Y. (2015). Effect of carbon sources on growth and lipid accumulation of newly isolated microalgae cultured under mixotrophic condition. *Bioresource technology*, 184, 100-107.
28. Choi, H. J., & Yu, S. W. (2015). Influence of crude glycerol on the biomass and lipid content of microalgae. *Biotechnology & Biotechnological Equipment*, 29(3), 506-513.

29. Liang, Y., Sarkany, N., & Cui, Y. (2009). Biomass and lipid productivities of *Chlorella vulgaris* under autotrophic, heterotrophic and mixotrophic growth conditions. *Biotechnology letters*, 31, 1043-1049.
30. Heredia-Arroyo, T., Wei, W., & Hu, B. (2010). Oil accumulation via heterotrophic/mixotrophic *Chlorella protothecoides*. *Applied biochemistry and biotechnology*, 162, 1978-1995.
31. Cheirsilp, B., & Torpee, S. (2012). Enhanced growth and lipid production of microalgae under mixotrophic culture condition: effect of light intensity, glucose concentration and fed-batch cultivation. *Bioresource technology*, 110, 510-516.
32. Park, J. E., Zhang, S., Han, T. H., & Hwang, S. J. (2021). The contribution ratio of autotrophic and heterotrophic metabolism during a mixotrophic culture of *Chlorella sorokiniana*. *International Journal of Environmental Research and Public Health*, 18(3), 1353.
33. Garcia, M. C., Mirón, A. S., Sevilla, J. F., Grima, E. M., & Camacho, F. G. (2005). Mixotrophic growth of the microalga *Phaeodactylum tricornutum*: influence of different nitrogen and organic carbon sources on productivity and biomass composition. *Process Biochemistry*, 40(1), 297-305.
34. Gim, G. H., Ryu, J., Kim, M. J., Kim, P. I., & Kim, S. W. (2016). Effects of carbon source and light intensity on the growth and total lipid production of three microalgae under different culture conditions. *Journal of Industrial Microbiology and Biotechnology*, 43(5), 605-616.
35. Baldisserotto, C., Popovich, C., Giovanardi, M., Sabia, A., Ferroni, L., Constenla, D., ... & Pancaldi, S. (2016). Photosynthetic aspects and lipid profiles in the mixotrophic alga *Neochloris oleoabundans* as useful parameters for biodiesel production. *Algal Research*, 16, 255-265.

Chapter 8

Study the effect of different light wavelengths on algal growth and lipid accumulation by Blue-Green Alga *L.subtilis* JUCHE

From literature review, it has been observed that photoautotrophic algae can grow in different wavelengths of lights such as yellow, green, blue, red etc. [1, 2,3,4]. It has also been reported that the biomass growth as well as lipid accumulation of some algae are more in case of different wavelengths, compared to those obtained under fluorescent white light [1,4]. To systematically investigate the effect of variation of wavelength of light on the photoautotrophic growth of blue-green alga *L.subtilis* JUCHE, studies have been conducted according to the following objectives, as described under Aim 6 in Chapter 3:

- Determination of biomass growth by varying different wavelengths of light
- Determination of lipid content of alga
- Determination of Chlorophyll and Carotenoid content under different wavelength of light
- Study on the performance of Photobioreactor using the most suitable wavelength with respect to Biomass and lipid

8.1 Materials and methods

8.1.1 Nutrient medium

Similar to the experiments conducted under photoautotrophic growth of *L. subtilis* JUCHE1 using white light early adaptation and enrichment of the algae were conducted in Modified-18 (M-18) minimal salt medium. The composition of M-18 medium without carbon source has been provided in Chapter 4. After autoclaving, the carbon-free M-18 medium was supplemented with the carbon source, CO₂, by sparging with air-CO₂ gas stream. Corresponding fall of pH due to production of carbonic acid from solubilization of CO₂ in medium was adjusted to pH 7 using 1M NaOH solution. After enrichment with carbon source and pH adjustment, the nutritionally complete M-18 medium was used for cultivation of *L. subtilis* JUCHE1. Cultures were maintained under constant values of 2.5 kLux (33.75 μmol/m²/s) illumination and 37°C incubation temperature.

8.1.2 Batch mode cultivation of *L. subtilis* JUCHE1 with the variation of light wavelength

Under the present investigation, batch mode cultivation of *L. subtilis* JUCHE1 was studied using four different wavelengths of colored light namely, blue (465nm), green (520nm), yellow (640nm) and red (660 nm). For these experiments, 250mL conical flasks equipped with two glass tubes were used as small-scale PBRs, as shown in Figure 8.1. Each culture flask was inoculated with 1g active biomass of *L. subtilis* JUCHE1 obtained through stock culture under white light illumination. Working volume of the reactors was kept at 150 mL by replacing the remaining volume (headspace) by the gas mixture of CO₂ and air. The concentration of CO₂ in the inlet gas and the liquid phase concentration of NaNO₃ and the light intensity were maintained at the optimum values, obtained during the algal growth under white light, i.e., 15% CO₂; 1.5 g/L NaNO₃ and 2.5 kLux (33.75 μmol/m²/s). Protocols for inoculation was described in Chapter 6, dedicated to the experiments using white light LEDs. Lighting strips having LED panels commercially available for decorative home lighting were used for providing the illumination to the flask. Using transparent adhesive tapes, the lighting strips were wrapped around the external glass walls of the conical flask by inward facing the LEDs towards the interior of the flasks. The batch growth studies were performed by using four different set-ups varying the wavelength of light, i.e., blue (465 nm), green (510 nm), yellow (590 nm) and red (630–675 nm). Growth of *L. subtilis* JUCHE1 under different wavelength of light was conducted and monitored for 0-6 days. All flasks were incubated at 37°C and the initial pH was maintained at 7.0. Samples on each day was collected from individual flask illuminated with light of different wavelength. The concentrations of biomass and lipid were also measured.



Figure 8.1. Small scale bioreactor set up for batch experiments varying different wavelengths of light.

8.1.3 Semi-Continuous Operation of mode of Gas-lift Photobioreactor

Based on the results obtained from the batch studies performed in the small-scale PBRs using four different colour of lights, blue (465 nm), green (510 nm), yellow (590 nm) and red (630–675 nm). The Yellow color wavelength causing the maximum production of biomass was identified. The experiments in semi-batch mode were conducted in an internally-externally illuminated gas-lift Photobioreactor (IEIGPBR) using light of that wavelength. The indigenously designed and custom-made IEIGPBR was fabricated using polymethyl methacrylate (PMMA). PMMA was chosen as the material of construction due to its high transparency to light, inertness towards reaction with medium components/products and good mechanical strength besides being light in weight. The IEIGPBR was constructed following the principle of internal-loop air-lift bioreactors [5]. The reactor consisted of three concentric cylindrical bodies made up of PMMA. The 200mm diameter and 360mm high outermost cylinder was supported on a mirror at the base. The middle cylinder, i.e., the riser, was placed in a way so that it was extended downward from the upper portion of the bioreactor. The top of the riser was 100 mm below the top cover of the bioreactor and its bottom was 30mm above the base on which the outermost cylinder was placed. In the lower part, the riser was held in position with the aid of four cross-wisely placed PMMA plates creating a clearance of 30mm from the floor of the IEIGPBR. The innermost cylinder was placed from top-cover of the reactor and was extended downward up to a level 60mm above the base of the reactor. The innermost cylinder was provided for the insertion of a LED light for internal illumination, to be provided for algal growth within the riser. The bottom side of the innermost cylinder was also closed to restrict entry of liquid medium and the top side was open to fit in the internal lighting system. The lighting arrangement of the IEIGPBR was done in a manner to create a maximally luminous environment through simultaneous internal and external illumination system along with mirror reflection from the bottom. A long LED strip was spirally wound around the external surface of the outermost tube of the IEIGPBR covering the entire length from the base towards the top, so that the mini-LED bulbs face the downcomer in an inward manner. Therefore, the overall lighting arrangement ensured continuous external (from the outermost wall of the reactor towards the growth space in the downcomer) and internal (through the LED lighting in the innermost cylinder facing the riser) illumination, suitable for algal growth. The wavelength or color of the light provided through LEDs were changeable. However, the fixed wavelength corresponding to the colour, which provided the maximum algal growth in the previous batch study, was used for this study. The lighting arrangement of

the IEIGPBR and two-way radial illumination pattern are schematically depicted in Figure 8.2. The downcomer and the annular middle space between the central lighting chamber and riser tube were used for cultivation of the algae. The CO₂ (15% v/v) -Air (85% v/v) gas mixture, established to give the maximum growth of *L. subtilis* JUCHE1, was sparged from the bottom of the riser. The M-18 medium was fed intermittently from the side wall of the outermost cylinder near the base. Similar to the principle of air lift bioreactor, due to an increase in gas hold-up and decrease in fluid density, the liquid moved upward through the riser. There was disengagement of gas at the top and the bubble free liquid moved downward through the annular space, i.e., the downcomer, between the riser and the outermost cylinder. The gas was withdrawn continuously through the outlet, placed on the top cover. The liquid effluent was withdrawn intermittently through the liquid outlet, placed near the topmost level of the riser. To maximize the distribution of gas mixture, bubbling through the entire working volume, the main gas supply line of the IEIGPBR was divided into three outlets, situated at 120° angle to each other. The flowrates of CO₂ and air were controlled by rotameters (make) and the two individual supply lines were connected through a T-joiner and the resultant gas stream was introduced to the IEIGPBR through the main supply line and distributed via three ports, as depicted in Figure 8.2. The IEIGPBR was bubbled with the CO₂ – air mixture at every 24hrs for one hour. Except this period, ambient air was sparged continuously. During the operation, the IEIGPBR was closed with the lid. Other than the central lighting chamber (innermost concentric cylinder), two sensors for the measurement of pH and temperature were also provided through the lid of the IEIGPBR. The temperature of the reactor medium was maintained at 37°C. Temperature was controlled by circulating water from a constant temperature water bath through a coiled, hollow copper pipe inserted throughout the riser. pH was constantly measured with the help of a pH probe immersed in the reactor medium. The pH of the reaction medium was maintained at 6.8-7.0 at an interval of 24hrs. The IEIGPBR was inoculated with 50g wet biomass of *L. subtilis*JUCHE1 grown under the most suitable light and operated under semi-continuous mode for 14 days. Algal biomass was harvested from the IEIGPBR at 2nd, 4th, 6th, 8th, 10th, 12th and 14th days. and was analyzed for biomass growth, lipid accumulation and CO₂ fixation.

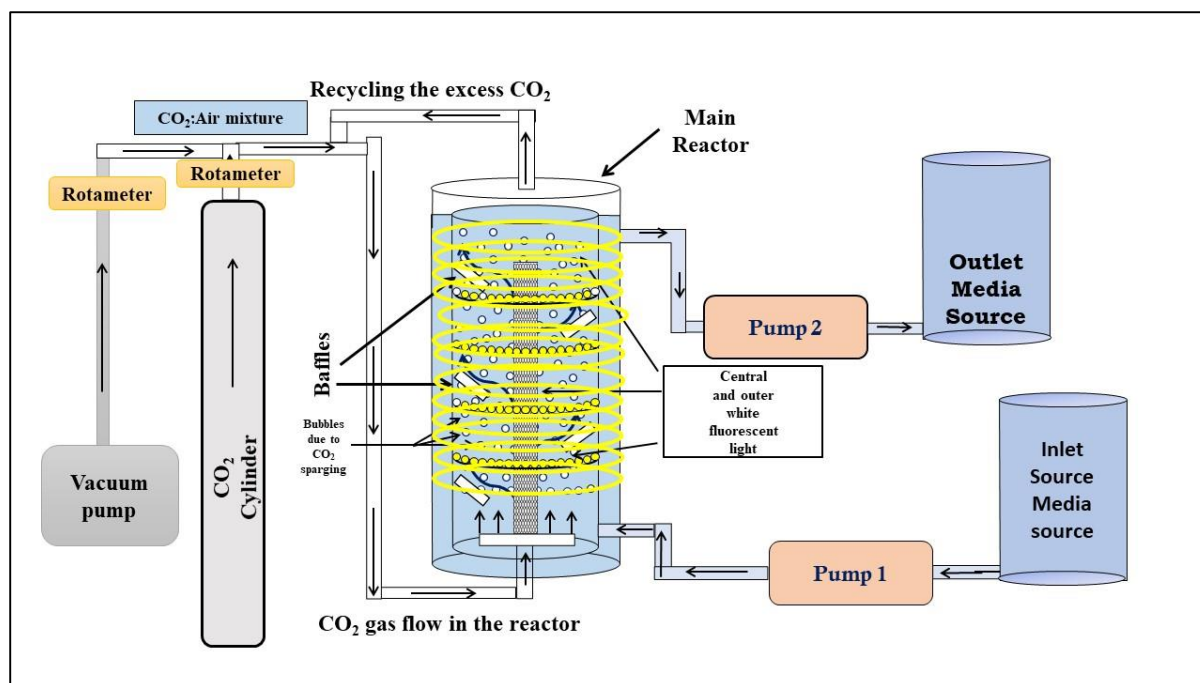


Figure 8.2. The schematic diagram of Internally-Externally Illuminated Gas lift Photobioreactor (IEIGPBR) using yellow wavelength for algal cultivation.

8.2 Results and discussion

8.2.1 Batch mode cultivation of *L. subtilis* JUCHE1

8.2.1.1 Growth of *L. subtilis* JUCHE1 under variation of wavelength of light

Time histories of biomass concentration obtained from the different batch cultures of *L. subtilis* JUCHE1 for 0-6 days under four different wavelengths of light provided by colored LEDs have been provided in Figure 8.3. Time trends for biomass, provided in Figure 8.3, evidently shows that *L. subtilis* JUCHE1 is able to grow under the irradiation of all four wavelengths used i.e., blue (465nm), green (510nm), yellow (590nm) and red (630–675 nm) and at fixed concentration of 15% CO₂. No lag phase is observed in any of the sets, indicating the quick adaptation of the viable algal cells of the seed culture, grown under white light, to the environments under the illumination of different wavelengths. However, it is also evident from the Figure 3, that the effect of each wavelength on the growth phases of *L. subtilis* JUCHE1 varies distinctly, which is also comparable with the data obtained through similar studies with other algal strains [1,2,4,6,7,8]. Comparison of the four different time trends over the time span of 0-6 days indicates that the algae have slowest growth under the irradiation of blue light with continuous increasing trend till day 3, reaching a maximum biomass concentration value of 0.77 g/L. The trend of growth during 4-6 days resembles a stationary phase with slight decline

in the value of biomass concentration. For red light, the exponential growth phase spans from 0-4 days and the biomass concentration passes through a peak (0.7998 g/L) at day 4 with a very distinct difference in value obtained at day 2 (0.6796 g/L). Afterwards, biomass concentration follows a clearly decreasing trend. *L. subtilis* JUCHE1 exhibits similar trends of biomass growth under the irradiation of green and yellow lights. In case of green light, the algal strain passes through the exponential growth during the span of 0-3 days, as reflected through the steep increase in biomass concentration in Figure 8.3. In case of yellow light, the growth curve shows increasing trend upto 6 days. For yellow and green lights, the maximum biomass concentration of 1.22 g/L and 0.98 g/L are obtained on 6th day and 3rd day respectively. These values of biomass concentration, obtained for yellow and green lights, are significantly higher in comparison to the maximum biomass produced under irradiation of red and blue lights. Day 3 onwards the growth phases show different patterns for yellow and green lights. While for yellow light an increasing trend prevails up to day 5, followed by a stationary phase within 5-6 days, a declining trend is observed for green light from 4-6 days. As the concentration of the carbon source was kept same for all four batches, it is confirmed that the wavelength of light influences the biomass growth of *L. subtilis* JUCHE1 and the yellow light (590 nm.) is the most suitable one. In accordance with the trends of biomass production, as represented in Figure 8.3, the corresponding specific growth rate (μ , d⁻¹) and biomass productivity (g/L/d) reach the highest values with respect to the growth maximum under yellow light.

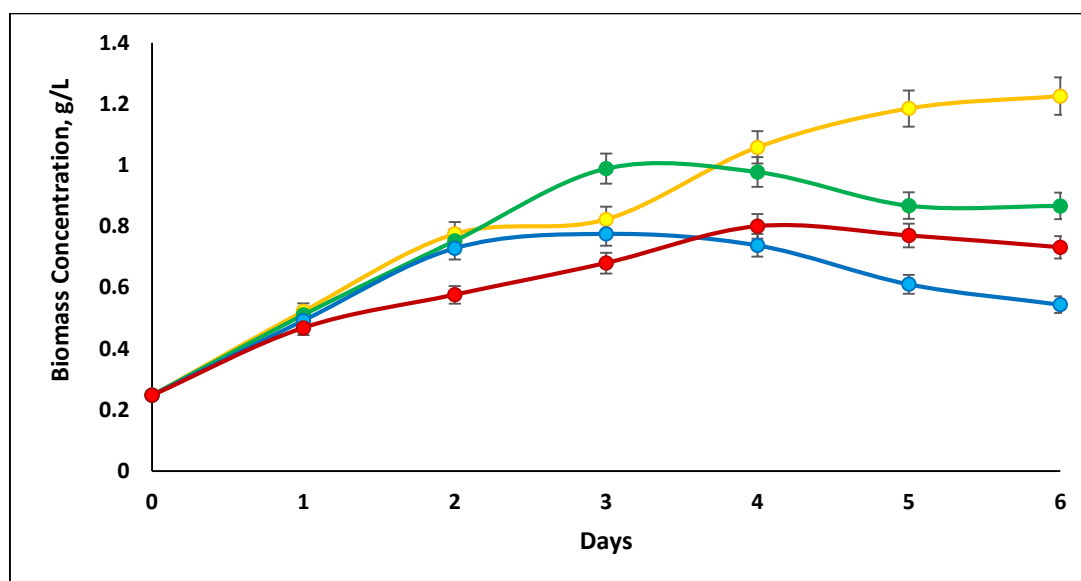


Figure 8.3 Time histories of photoautotrophic biomass growth of *L. subtilis* JUCHE1 under irradiation of varying wavelength of light (Blue, Green, Yellow and Red).

Maximum values of biomass concentration, biomass productivity and specific growth rates under the wavelengths of yellow, green, red and blue lights are presented in Table 8.2. Comparison of the values affirms that among all wavelength of light under study, that corresponding to yellow light is the optimum for illuminating cultures of *L. subtilis* JUCHE1 for enhanced biomass production.

Table 8.1. Observed values of biomass concentration and productivities of *L.subtilis* JUCHE1 at each time interval under different wavelengths of light (yellow, green, red and blue).

| Days | Biomass Concentration (g/L) | | | | Biomass productivity (g/L/d) | | | |
|------|-----------------------------|--------|--------|--------|------------------------------|--------|--------|--------|
| | Yellow | Green | Red | Blue | Yellow | Green | Red | Blue |
| 0 | 0.2473 | 0.2473 | 0.2473 | 0.2473 | 0 | 0 | 0 | 0 |
| 1 | 0.5216 | 0.5102 | 0.4678 | 0.4918 | 0.2743 | 0.2629 | 0.2205 | 0.2445 |
| 2 | 0.7745 | 0.752 | 0.5762 | 0.7281 | 0.2636 | 0.2523 | 0.1644 | 0.2404 |
| 3 | 0.8224 | 0.9882 | 0.6796 | 0.7753 | 0.1917 | 0.2469 | 0.1442 | 0.1760 |
| 4 | 1.0577 | 0.9772 | 0.7998 | 0.7376 | 0.2026 | 0.1824 | 0.1381 | 0.1225 |
| 5 | 1.1846 | 0.867 | 0.7696 | 0.6104 | 0.18746 | 0.1240 | 0.1044 | 0.0726 |
| 6 | 1.2251 | 0.8664 | 0.731 | 0.5437 | 0.162967 | 0.1031 | 0.0806 | 0.0494 |

Table 8.2. Values of maximum biomass concentration, biomass productivity and specific growth rate of *L. subtilis* JUCHE1 obtained for different wavelengths of light.

| | Unit | Yellow | Green | Red | Blue |
|---|-----------------|--------|--------|--------|--------|
| Maximum biomass productivity | g/L/d | 0.2743 | 0.2629 | 0.2205 | 0.2445 |
| Maximum Specific growth rate, “ μ ” | d ⁻¹ | 0.7134 | 0.7596 | 0.6168 | 0.6616 |

In Table 8.3, Since the maximum value of biomass concentration has been obtained on 6th day using the yellow light, the same has been compared with the literature data available on 6th day biomass concentration for different algal species. According to Table 8.3, Hwang and Maier, 2019 reported that due to the narrow emission spectra of LED diodes, the rate of photosynthesis as well as bio-metabolism of algal cells were improved which ultimately led to the enhancement of biomass and lipid production [7]. The study was performed by varying intensities of lights corresponding to white and red wavelengths for production of biomass and lipids in *Neochlorisoleo abundans* [7]. While the biomass concentration on 6th day was found to be 1 ± 0.03 g/ L at intensity of $404\mu\text{Em}^{-2} \text{ s}^{-1}$ for red LEDs, much lesser amount of biomass

(0.66 ± 0.02 g/ L) was formed using white LEDs at $323\mu\text{Em}^{-2} \text{ s}^{-1}$ light intensity [7]. E.R. Mattos et al.2015 reported that the biomass growth of *Scenedesmus bijuga* on 6th day was highest under green light i.e. 0.18 g L^{-1} compared to other wavelengths (white, red and blue) of lights [2]. Mohsenpour et al., 2013, used five different wavelengths namely; red, blue, yellow, green and orange to study their impact on the growth of two different algal strains namely; *Chlorella vulgaris* and *Gloeothecece mbranacea* [1]. For both algae the highest biomass concentration on 6th day was obtained under illumination by red light in comparison to the other ones, as represented in Table 8.3[1]. Ra et al, 2016, used six different wavelengths of lights such as red, purple, green, yellow, blue and fluorescent white light (as control) to investigate the effect on growth of the alga *Picochlorum atomus* [8]. The biomass concentration of *P. atomus* was obtained under illumination by red LEDs i.e. 0.11 g/L on 6th day among others, Table 8.3 [8]. *Scenedesmus quadricauda* produced higher amount of biomass on 6th day i.e., 0.26 g/L under illumination of blue light in comparison to lower biomass produced under yellow, red and green lights, Table 8.3 [4]. Analysis of the information provided in Table 8.3 indicates that different algal strains have variable preference towards wavelength of light and corresponding color regarding growth and biomass production. Similarly, in the present study, *L.subtilis* JUCHE1 exhibits preferential behavior to a particular colour of light, namely yellow with respect to biomass concentration. However, in most of the studies, red and blue colour appear to be the most preferred ones [1,4, 6, 7, 8]. Some researchers have also reported green colour to be the most preferred one [2]. It has been reported in the literature that red and blue are the strongly absorbed wavelength by chlorophylls (a and b) causing enhancement in photosynthetic activity at low cell density conditions [2,9]. However, with the increase of cell density, the penetration of these lights suffer compared to the less absorbed and higher scattering wavelengths, e.g., yellow, green etc. [2, 10]. According to Terashima et al., this phenomenon is known as the “detour effect” [2,11]. Moreover, with the increase of cell density the penetration of most absorbed light through the chloroplast decreases, known as “package or sieve effect”, which can lead to apparently less yield of biomass compared .to that obtained using less absorbed wavelength [2, 11, 12, 13]. Additionally, due to less penetration of light, there is a possibility of conversion of light energy to heat at the surface when highly absorbed wavelength of light is used [14]. Due to the avoidance of heat loss at the surface, the algal growth using less absorbed light (yellow, green etc.) appears to be more energy efficient.

Table 8.3. Comparison of biomass concentration under different wavelength at 6th day with literature data.

| Algal strain | Reactor Volume L | Carbon source | Concentration of carbon source (g/L) | CO ₂ Conc. %(v/v) | Light Intensity $\mu\text{mol/m}^2/\text{s}$ | Wavelengths of light | Most preferred Wavelength | Biomass concentrations on 6 th day, g/L | Ref. |
|---|------------------|----------------------------------|--------------------------------------|------------------------------|--|----------------------|---------------------------|--|------|
| <i>Chlorella ellipsoidea</i> | 1 | - | - | 0.04 (Air) | 200 | White | Blue | 0.002 | 6 |
| | | | | | | Green | | 0.008 | |
| | | | | | | Blue | | 0.015 | |
| | | | | | | Red | | 0.003 | |
| <i>Neochlorisoleo abundans</i> | 1 | TOC* | 0.0089 \pm 0.0001 | 0.04 (Air) | 323 | White | Red | 0.66 | 7 |
| | | TIC* | 0.0042 \pm 0.0001 | | 404 | Red | | 1 | |
| <i>Scenedesmus quadricauda</i> | 2 | - | - | 0.04 (Air) | 70 | Blue | Blue | 0.26 | 4 |
| | | | | | | Yellow | | 0.16 | |
| | | | | | | Red | | 0.155 | |
| | | | | | | Green | | 0.1 | |
| <i>Scenedesmus bijuga</i> | 0.5 | Na ₂ C O ₃ | 0.02 | 5% | 300 | Green | Green | 0.18 \pm 0.02 | 2 |
| | | | | | | Red | | 0.1 \pm 0.02 | |
| | | | | | | White | | 0.14 \pm 0.01 | |
| | | | | | | Blue | | 0.05 \pm 0.02 | |
| <i>Chlorella Vulgaris</i> (low density seed culture) | 0.45 | Na ₂ C O ₃ | 2 | 0.04 (Air) | 250 | Red | Red | 1 | 1 |
| | | | | | | Blue | | 0.85 | |
| | | | | | | Yellow | | 0.91 | |
| | | | | | | Green | | 0.9 | |
| | | | | | | Orange | 0.9 | Red | |
| | | | | | | Red | 1.45 | | |
| | | | | | | Blue | 1.3 | | |
| | | | | | | Yellow | 1.35 | | |
| <i>Chlorella Vulgaris</i> (high density seed culture) | | | | | | Green | 1.31 | | |
| | | | | | | Orange | 1.25 | | |

| Algal strain | Reactor Volume L | Carbon source | Concentration of carbon source (g/L) | CO ₂ Conc. %(v/v) | Light Intensity $\mu\text{mol/m}^2/\text{s}$ | Wavelengths of light | Most preferred Wavelength | Biomass concentrations on 6 th day, g/L | Ref. |
|--|------------------|----------------------------------|--------------------------------------|------------------------------|--|----------------------|---------------------------|--|---------------|
| <i>Gloeothecella mbranacea</i> (Low density seed culture) | 0.45 | Na ₂ C O ₃ | 2 | 0.04 (Air) | 250 | Red | Red | 1.3 | |
| | | | | | | Blue | | 1.1 | |
| | | | | | | Yellow | | 1.1 | |
| | | | | | | Green | | 0.9 | |
| | | | | | | Orange | | 0.9 | |
| <i>Gloeothecella mbranacea</i> (high density seed culture) | | | | | | Red | Red | 1.7 | |
| | | | | | | Blue | | 1.55 | |
| | | | | | | Yellow | | 1.5 | |
| | | | | | | Green | | 1.3 | |
| | | | | | | Orange | | 1.51 | |
| <i>Picochlorumatum</i> | 2 | - | - | 0.04 (Air) | 100 | Red | Red | 0.11 | 8 |
| | | | | | | Purple | | 0.06 | |
| | | | | | | Green | | 0.04 | |
| | | | | | | Yellow | | 0.05 | |
| | | | | | | Blue | | 0.085 | |
| | | | | | | White | | 0.06 | |
| <i>L. subtilis</i> JUCHE1 | 0.25 | CO ₂ | 0.638 | 15% | 33.75 | White | Yellow | 0.7286 | Present study |
| | | | | | | Yellow | | 1.2251 | |
| | | | | | | Green | | 0.9882 | |
| | | | | | | Red | | 0.7998 | |
| | | | | | | Blue | | 0.7753 | |

8.2.1.2 Effect of four different spectrums of light on lipid accumulation of *L. subtilis* JUCHE1

In Figure 8.4 the lipid contents of *L. subtilis* JUCHE1 biomass obtained at different wavelengths of light have been represented. From the comparative analysis of the plots, it has been observed that similar to the pattern of biomass production, the lipid production and accumulation of *L. subtilis* JUCHE1 is maximum under the irradiation by yellow light as

compared to other wavelengths during the growth period of 0-6 days. Maximum lipid content of 22.15% (w/w) is obtained on 6th day of growth under yellow light. Lipid production under wavelength of blue and red lights show similar trends of increase of lipid content over time. Maximum values of lipid contents for blue and red light were observed to be 19% (w/w) and 17.51 (%w/w), respectively. Whereas, the lowest lipid production of 11.4% (w/w) was obtained for green light on 6th day of culture period. From the trends represented in Figure 8.4 it is evident that lipid production by *L. subtilis* JUCHE1 has a lag phase of 0-2 days for all four wavelengths of light used for growth. While for blue and red lights, lipid content increases from second day onwards, increasing trend is observed right from the starting point using yellow light. Under irradiation of green light, lipid production is much slower in comparison to all other wavelengths and starts to increase only after 4th day of growth. Observations clearly indicated that yellow light is the most suitable one for the lipid production by *L. subtilis* JUCHE1 during photoautotrophic growth.

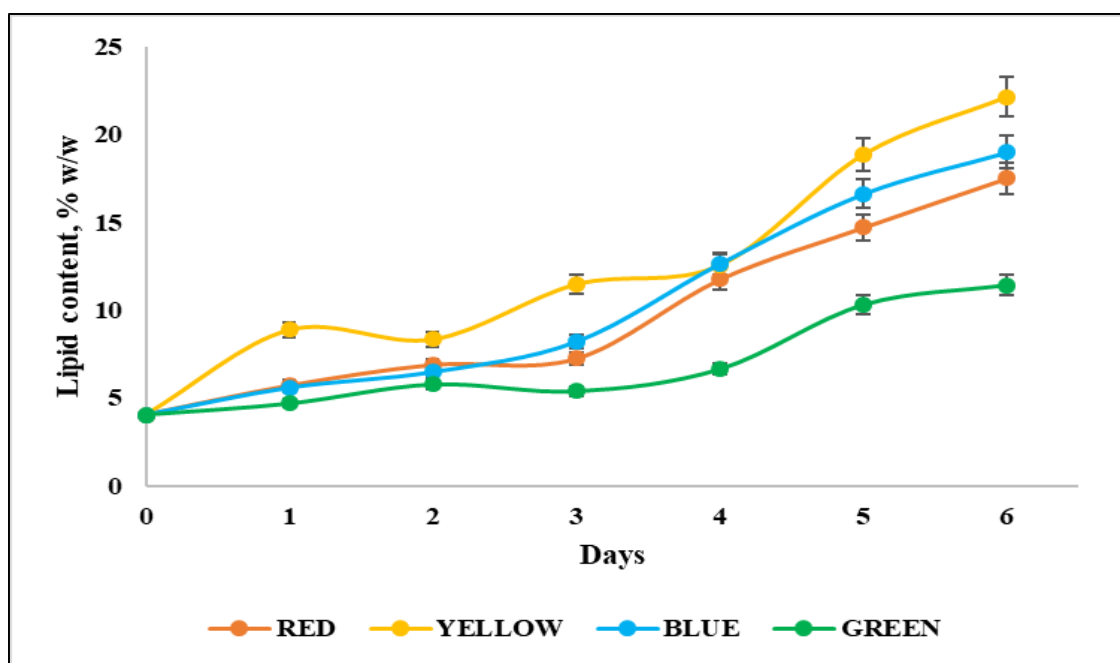


Figure 8.4 Time histories of lipid accumulation by *L. subtilis* JUCHE1 under irradiation of varying wavelength of light (blue, green, yellow and red).

Table 8.4. Experimental values of lipid content(%w/w) and productivities (g/L/d) under irradiance of varying different wavelengths of light

| Days | Lipid content (%w/w) | | | | Lipid productivity (g/L/d) | | | |
|------|----------------------|-------|-------|-------|----------------------------|--------|--------|--------|
| | Yellow | Blue | Red | Green | Yellow | Blue | Red | Green |
| 0 | 4.04 | 4.04 | 4.04 | 4.04 | 0 | 0 | 0 | 0 |
| 1 | 8.87 | 5.58 | 5.7 | 4.67 | 0.0243 | 0.0136 | 0.0125 | 0.0122 |
| 2 | 8.33 | 6.48 | 6.88 | 5.76 | 0.0219 | 0.0155 | 0.0113 | 0.0145 |
| 3 | 11.47 | 8.21 | 7.24 | 5.37 | 0.0219 | 0.0144 | 0.0104 | 0.0132 |
| 4 | 12.56 | 12.65 | 11.75 | 6.63 | 0.0254 | 0.0155 | 0.0162 | 0.0121 |
| 5 | 18.87 | 16.63 | 14.71 | 10.29 | 0.0353 | 0.0120 | 0.0153 | 0.0127 |
| 6 | 22.15 | 19 | 17.51 | 11.41 | 0.0361 | 0.0093 | 0.0141 | 0.0117 |

In Table 8.5, the pattern of lipid production by *L. subtilis* JUCHE1 has been compared with the data, reported in the literature. From the analysis of the table, it is clear that while some of the researchers have reported red light to be most suitable one for lipid production blue and green light has the best performance for some others. It appears that due to the same reason as discussed in case of algal biomass, lipid production is enhanced for wavelengths (blue and red), best suited for absorption by chlorophyll. Again, due to the avoidance of package effect in presence of less absorbed wavelengths corresponding to the colors like yellow, green etc. the lipid production is favoured by the use of green light and yellow in the present case [2,13,14]. As no literature data is available regarding lipid content for batch mode algal growth, the absolute values of present lipid data cannot be directly comparable with the reported ones. It has been observed that highest lipid contents have been reported to lie in the range of 11.1-60.8%(w/w) at the cultivation times ranging from 10-28 days [7, 8, 15, 16,17, 18].

Table 8.5. Lipid content(%w/w) of algal strains in different spectrums of light.

| Algal strains | Reactor vol. (L) | C-source | C-Conc. g/L | CO ₂ Conc. (%v/v) | Light intensity ($\mu\text{mol}/\text{m}^2/\text{s}$) | Color spectrums | Max. Lipid content (%w/w) | Culture period (Days) | Ref. |
|----------------------------|------------------|---------------------------------|-------------|------------------------------|---|-----------------|---------------------------|-----------------------|------|
| <i>Nannochloropsis sp.</i> | 1 | Na ₂ CO ₃ | 30 | 0.04 (air) | 100 | Blue | 60 | 28 | 15 |
| | | | | | | Blue-green | 50 | | |

| Algal strains | Reactor vol. (L) | C-source | C-Conc. g/L | CO ₂ Conc. (%v/v) | Light intensity ($\mu\text{mol}/\text{m}^2/\text{s}$) | Color spectrum | Max. Lipid content (%w/w) | Culture period (Days) | Ref. |
|-------------------------------------|------------------|-----------------|-----------------|------------------------------|---|----------------|---------------------------|-----------------------|---------------|
| | | | | | | Red | 48 | | |
| | | | | | | White | 52 | | |
| | | | | | | Pink | 51 | | |
| <i>Chlorella sp.</i> | 0.05 | - | - | - | 27.75 ^a | White | 29.3 | 20 | 16 |
| | | | | | 8.5 ^a | Red-Blue | 32.1 | | |
| | | | | | 3.74 ^a | Red | 60.8 | | |
| <i>Chlorella pyrenoidosa</i> | - | - | - | - | 200 | White | 16.22 | 13 | 17 |
| | | | | | | Purple | 13.54 | | |
| | | | | | | Blue | 17.48 | | |
| | | | | | | Green | 19.75 | | |
| | | | | | | Yellow | 14.16 | | |
| | | | | | | Red | 14.82 | | |
| <i>Picochlorum atomus</i> | - | - | - | 0.04% (Air) | 100 | Green | 50.3% | 20 | 8 |
| | | | | | | Red | 45 | | |
| | | | | | | Blue | 37 | | |
| <i>Neoclorisoleo abundans</i> | 1 | TOC* | 0.0089 ± 0.0001 | 0.04 (Air) | 323 | White | 25.2 ± 0.2 | 18 | 7 |
| | | | TIC* | | | | | | |
| <i>C. vulgaris</i> UTEX #236 | 0.25 | - | - | 0.04% | 110–120 | Red | 11.1 ± 1.8 | 10 | 18 |
| | | | | | | Blue | 10.8 ± 1.2 | | |
| <i>Leptolyngbya subtilis</i> JUCHE1 | 0.25 | CO ₂ | 0.638 | 15% | 33.75 ^a | White | 12.5 | 4 | Present study |
| | | | | | | Yellow | 22.15 | 6 | |
| | | | | | | Blue | 19 | | |
| | | | | | | Red | 17.5 | | |
| | | | | | | Green | 11.4 | | |

8.2.1.3 CO₂ fixation rate of *L. subtilis* JUCHE1 under variation of wavelength of light

As described in section 8.2.3, fixed optimum inlet-CO₂ concentration of 15% (v/v) was used for growing *L. subtilis* JUCHE1 under irradiation of different wavelength of light. The values of CO₂ fixation rates (R_{CO_2}) per day have been determined using Equation (5.5), provided in Section 5.1.3 per day and the impact of variation of wavelength of light on R_{CO_2} has been assessed. The values of R_{CO_2} , obtained at each different wavelength (and color) per day of batch growth have been plotted for the duration of 1-6 days, as represented in Figure 8.5. From Figure 8.5, it can be inferred that the maximum CO₂ fixation rate of 0.35201 g/L/d is achieved for yellow light on 0-1 day. The 2nd highest value of CO₂ fixation rate of 0.3373 g/L/d is observed for green light on 0-1 day of growth. As discussed in Chapter 6 (Section 6.5.1.4), the maximum CO₂ fixation rate of 0.2383 g/L/d is obtained for white light during 0-1 day of growth, which is notably lesser than the R_{CO_2} values obtained for yellow and green lights. Approximately, the values of R_{CO_2} are respectively 1.47-fold and 1.18-fold higher for yellow and green lights compared to the white light. Figure 8.5 indicates that maximum values of R_{CO_2} for red (0.2830 g/L/d) and blue (0.3137 g/L/d) lights are also higher compared to white light for this algal strain. In case of white light, the CO₂ fixation rate started to decline after 1 day which is also a different trend of R_{CO_2} by *L. subtilis* JUCHE1 from the other wavelengths of light used in the present study. Esteves et al.2020, reported the effect of variation of wavelength of light on R_{CO_2} of *Chlorella vulgaris*, *Tetradismus obliquus* and *Neochloris oleoabundans* using white, red and blue light for 12 days [19]. The article reported that the maximum CO₂ fixation rate of 11.4 mg/L/d, 7.5 mg/L/d, 7 mg/L/d was obtained for *C. vulgaris* using white, red and blue lights. According to the same report, maximum R_{CO_2} values of 7.4 mg/L/d, 5 mg/L/d, 6 mg/L/d using white, red and blue lights respectively for *Tetradismus obliquus*. Similarly, the values of R_{CO_2} of 9.2 mg/L/d, 6 mg/L/d respectively using white, red light have been reported for *Neochloris oleoabundans*[19]. Unlike in the present study the maximum R_{CO_2} values using white light exceed those obtained with other colours for all the algal strains investigated by Esteves et al.. The results of the present study are not directly comparable with the literature data as the main carbon source in the reported study was 50mg/L NaHCO₃ and air, filtered through cellulose acetate membrane, unlike CO₂ in the present case[19].

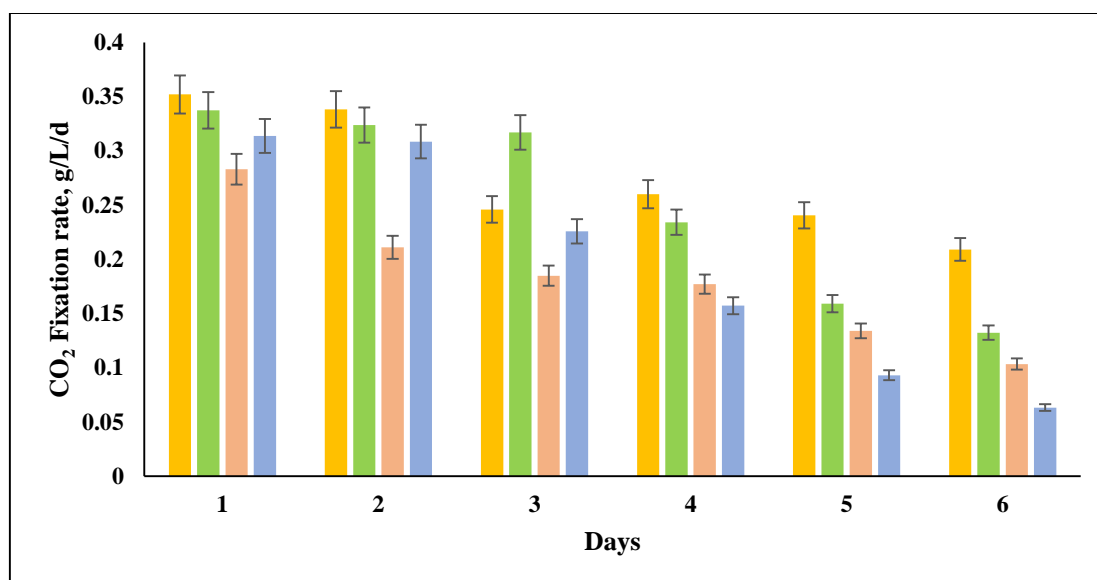


Figure 8.5. Values of CO₂ fixation rate of *L. subtilis* JUCHE1 under irradiation of varying wavelength of light (blue, green, yellow and red).

Table 8.6. Values of CO₂ Fixation Rate (g/L/d) at each time intervals for all the wavelengths of light.

| Days | CO ₂ Fixation Rate (g/L/d) | | | |
|------|---------------------------------------|--------|--------|--------|
| | Yellow | Green | Red | Blue |
| 0 | 0 | 0 | 0 | 0 |
| 1 | 0.3520 | 0.3373 | 0.2830 | 0.3137 |
| 2 | 0.3382 | 0.3238 | 0.2110 | 0.3085 |
| 3 | 0.2460 | 0.3169 | 0.1849 | 0.2258 |
| 4 | 0.26 | 0.2341 | 0.1772 | 0.1573 |
| 5 | 0.2405 | 0.1591 | 0.1340 | 0.0931 |
| 6 | 0.2091 | 0.1324 | 0.1034 | 0.0634 |

8.2.1.4 Effect of different spectrum of lights on photosynthetic activity for pigment production of *L.subtilis* JUCHE1

As reported in most of the literature, chlorophyll is the primary pigment present in plants, mainly responsible for light absorption, whereas the other pigment like carotenoid plays important role in light-harvesting as well as protecting the protein–pigment complexes present in chloroplast from excessive light [20,21, 22]. In Figure 8.6, the chlorophyll content of algal biomass grown in the batch reactor have been plotted against culture time using the colour of light as a parameter. It has been observed from the figure that the content of chlorophyll

increases from the initial value of 0.28% to 0.52% on 1st day and then reduces to 0.39 on 2nd day and remains almost constant up to 3rd day, followed by a decreasing trend. Under blue light, chlorophyll content increases from the start with an exception during 1st day to 2nd day period when the value decreases from 0.58% to 0.49%. On 6th day, the chlorophyll content reaches the maximum value of 0.93%. In case of green light, the chlorophyll content maximizes at 0.48% on the 1st day. Beyond 1st day, there is a decreasing trend up to 3rd day (0.29%), and then there is an increasing trend up to 5th day (0.45%), followed by saturation up to 6th day (0.46%). Under red light, the chlorophyll content increases up to 0.58% on 2nd day, followed by almost saturation up to 3rd day (0.59%), after which it reduces to 0.49% on 4th day, followed by saturation up to 5th day (0.5%). Finally, there is an increasing trend up to 0.68% on 6th day. Overall, the order of values of highest chlorophyll content under this study, as presented in Figure 8.7 is 0.93%, 0.68%, 0.52% and 0.48% for blue, red, yellow and green. While the highest values of chlorophyll content are obtained on 6th day for blue and red light, those for yellow and green light are attained on 1st day. The analysis of Figures 8.6 and 8.7 reveals that both red and blue light favours the formation of chlorophyll. This is because of the fact that the red and blue lights are the high absorbing wavelength to which the chlorophylls are very sensitive. Except yellow light, the chlorophyll content shows fluctuations within the culture period. This may be temporary hindrance in the penetration of light particularly under highly absorbing light. When compared to the literature data, it is clear that the chlorophyll content obtained in this case is very much in the range reported by previous researchers [6,15,23, 24,25]. The positive influence of red and blue light on the chlorophyll generation has also been reported in the literature [6,15, 23, 24,25].

In Figure 8.8, the carotenoid content of algal biomass grown in the batch reactor have been plotted against culture time using the colour of light as a parameter. The figure shows that the maximum value of carotenoid content of 0.2% is achieved on the 1st day under yellow light. For blue light, carotenoid content maximizes at 0.27.0% on 6th day . Under green light, the carotenoid content becomes maximum on 1st at 0.15% followed by a decreasing trend up to 0.11% on 3rd day. Beyond 3rd day, the content remains almost constant up to 4th day, followed by a decrease up to 0.09% on 5th day and there is saturation up to 6th day. Under the influence of red light, there is an increase in the carotenoid content up to 0.25% on 1st day, followed by a decreasing trend up to 6th day. Overall, the order of values of highest carotenoid content under this study, as presented in Figure 8.7 is 0.27%, 0.25%, 0.2%, 0.15% for blue, red, yellow and green. While the highest values of carotenoid content are obtained on 6th day for blue light,

those for red, yellow and green light are attained on 1st day. Similar to the trend of chlorophyll, the analysis of Figures 8.6, 8.7 and 8.8 indicates that even the formation of carotenoid is favoured by blue and red light. Sensitivity of pigments towards the high absorbing wavelengths (red, blue etc.) can be the underlying reason for the observation related to the carotenoid content of algal biomass.

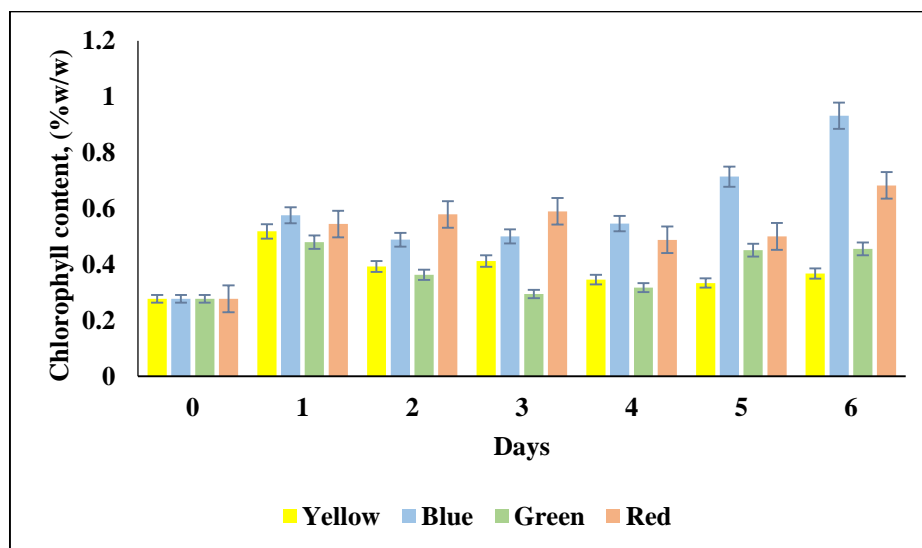


Figure 8.6 Bar plot of Chlorophyll contents (%w/w) of *L.subtilis* JUCHE1 against each time intervals from 0-6 days under the irradiation of different wavelengths of light (Yellow, Blue, Green and Red).

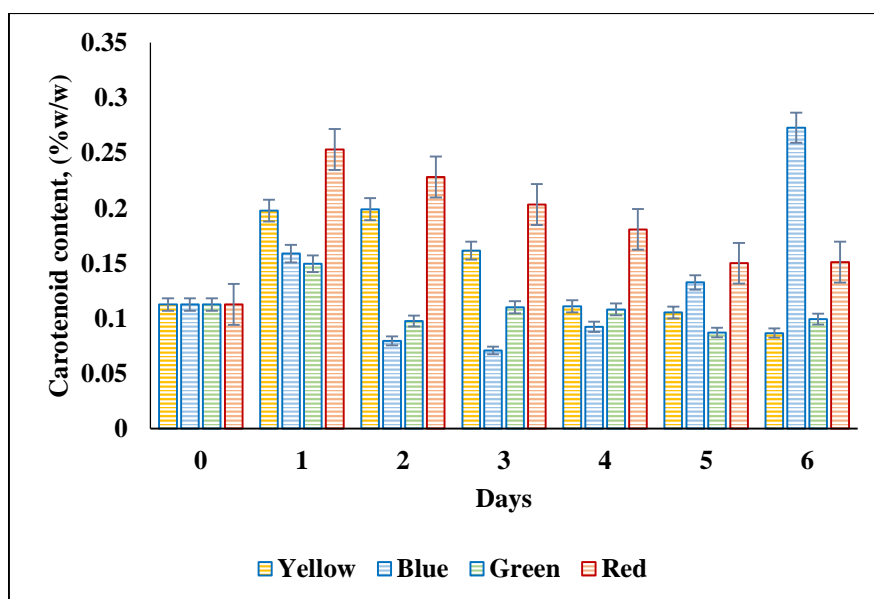


Figure 8.7 Bar plot of Carotenoid contents (%w/w) of *L.subtilis* JUCHE1 against each time intervals from 0-6 days under the irradiation of different wavelengths of light (Yellow, Blue, Green and Red).

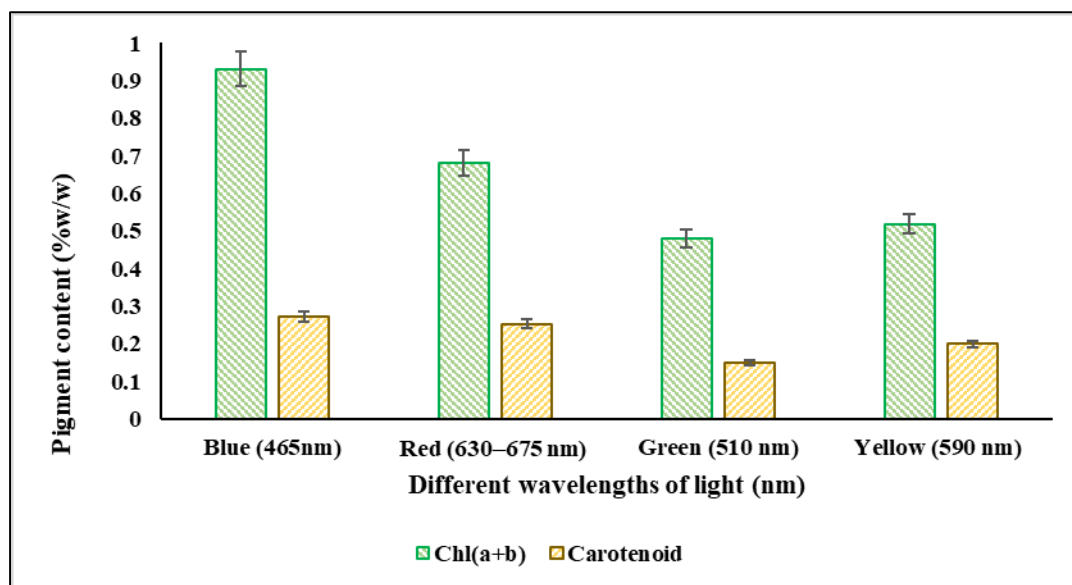


Figure 8.8 Maximum value of Chlorophyll(a+b) and Carotenoid content(%w/w) under the irradiation of different wavelengths of light (Yellow, Blue, Green and Red).

Table 8.7 The values of Chlorophyll (a+b) and Carotenoid content (%w/w) of *L.subtilis* JUCHE1 at each time intervals from 0-6 days under the irradiation of different wavelengths of light (Yellow, Blue, Green and Red)

| Days | Chlorophyll (a+b) content (%w/w) | | | | Carotenoid content (%w/w) | | | |
|------|----------------------------------|--------|--------|--------|---------------------------|--------|--------|--------|
| | Yellow | Blue | Red | Green | Yellow | Blue | Red | Green |
| 0 | 0.2773 | 0.2773 | 0.2773 | 0.2773 | 0.1126 | 0.1126 | 0.1126 | 0.1126 |
| 1 | 0.5185 | 0.5756 | 0.5445 | 0.4800 | 0.1976 | 0.1587 | 0.2531 | 0.1495 |
| 2 | 0.3929 | 0.4888 | 0.5790 | 0.3629 | 0.1989 | 0.0796 | 0.2282 | 0.0976 |
| 3 | 0.4125 | 0.5006 | 0.5902 | 0.2944 | 0.1614 | 0.0709 | 0.2032 | 0.1100 |
| 4 | 0.3458 | 0.5463 | 0.4883 | 0.3172 | 0.1108 | 0.0924 | 0.1807 | 0.1081 |
| 5 | 0.3335 | 0.7139 | 0.5005 | 0.4510 | 0.1053 | 0.1325 | 0.1499 | 0.0870 |
| 6 | 0.3680 | 0.9317 | 0.6827 | 0.4557 | 0.0867 | 0.2728 | 0.1510 | 0.0992 |

8.2.2 Semi-Continuous mode of Operation in Gas-lift Photobioreactor

As discussed in Section 8.3.1, it is confirmed that biomass growth, lipid production and CO₂-biosequestration performance of *L. subtilis* JUCHE1 is the best when grown under the irradiation of yellow light. Hence, the semi-continuous experiments using the IEIGPBR were conducted under yellow light (590 nm).

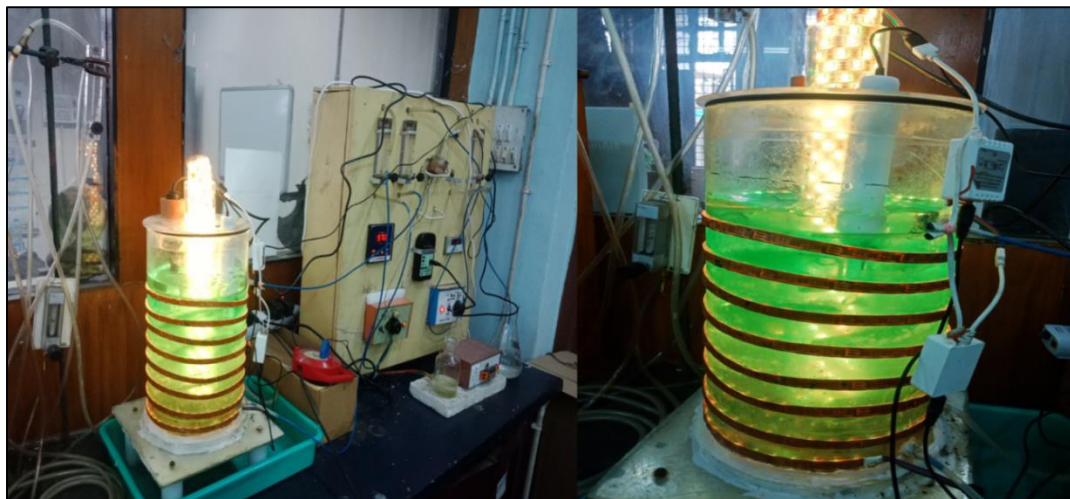


Figure 8.9. Photograph of IEIGPBR under operation

8.2.2.1 Visual appearance of IEIGPBR in operating condition

The photograph of the IEIGPBR (Figure 8.9) clearly shows a uniform distribution of algal suspension and illumination all over the reactor. After ascertaining the uniformity of reaction mass and illumination, the time histories of R_{CO_2} and concentrations of biomass and lipid have been analyzed.

8.2.2.2 Time history of Algal biomass in IEIGPBR

The time history of algal biomass obtained during the semi-continuous IEIGPBR operation under irradiation of yellow light and intermittent feeding of 15% (v/v) CO_2 for 14 days is plotted in Figure 8.10.

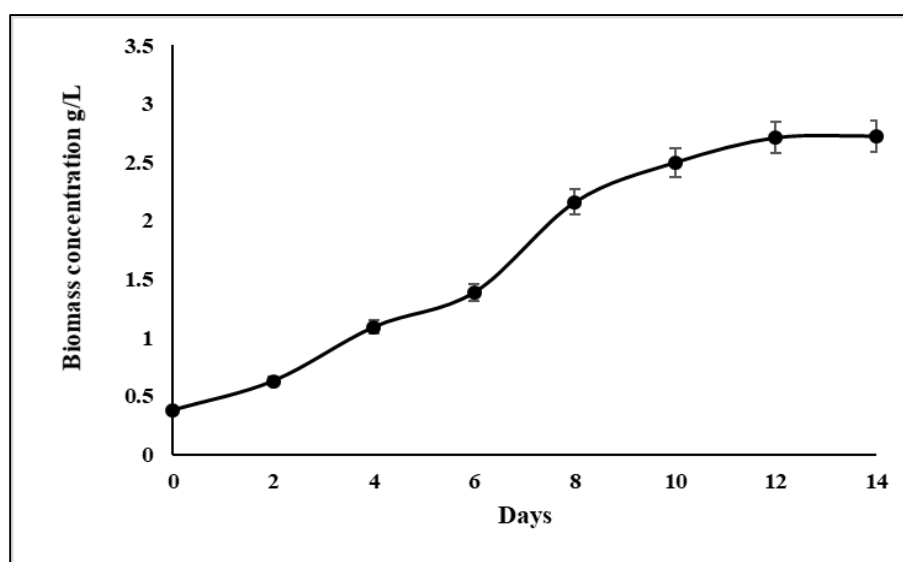


Figure 8.10. Time history of Algal biomass concentration in IEIGPBR

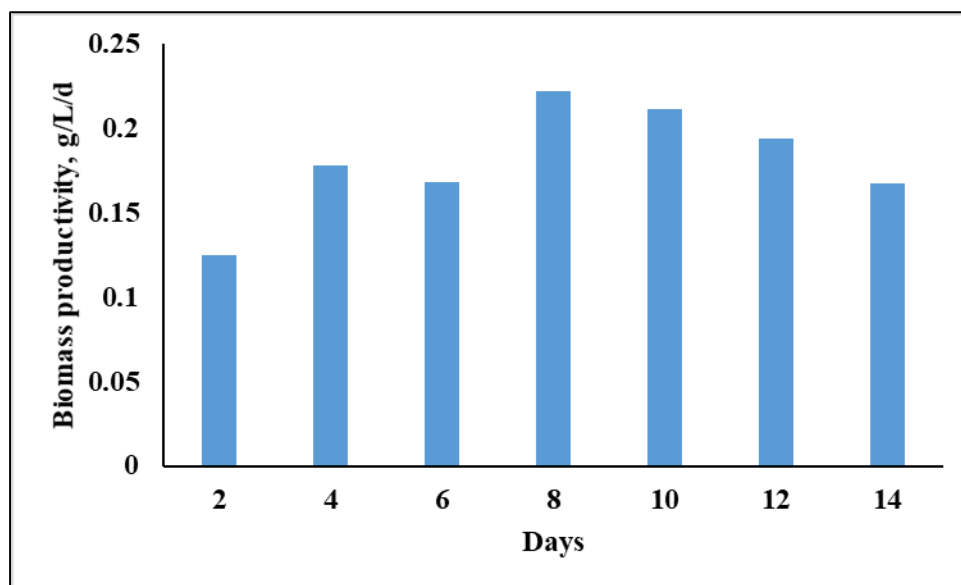


Figure 8.11 Time history of Algal biomass productivity(g/L/d) in IEIGPBR

From the depiction of Figure 8.10, it has been observed that when cultivated in the IEIGPBR under semi-continuous mode with intermittent feeding of CO₂, the growth of *L. subtilis* JUCHE1 exhibited consistent increase over 10 days. For the duration of 2-6 days the rate of growth seems to be bit slower than the growth phase of 6-12days. The figure reveals that the biomass concentration increases till 12th day (2.7g/L) and peaks at 14th day with negligible increase during 12-14 days (2.72 g/L). Therefore, beyond 12th day, the biomass growth has reaches a stationary phase. The IEIGPBR was constantly illuminated for 14 days with 1.5 kLux intensity of light supplied by yellow LED panels. Although in case of batch mode of operation, the growth was saturated day 6the growth was sustained up to 12th day under semi-continuous mode of operation.

Table 8.8 Observed values of biomass concentrations at each time interval under yellow light using IEIGPBR in the semi-continuous mode.

| Days | Biomass concentration, g/L | Biomass productivity , g/L/d |
|------|----------------------------|------------------------------|
| 0 | 0.38 | 0 |
| 2 | 0.63 | 0.1250 |
| 4 | 1.09 | 0.1779 |
| 6 | 1.38 | 0.1680 |
| 8 | 2.15 | 0.2224 |
| 10 | 2.49 | 0.2118 |
| 12 | 2.7 | 0.1941 |
| 14 | 2.72 | 0.1673 |

Hence, the semi-continuous IEIGPBR operation is confirmed as an effective mode of cultivation of *L. subtilis* JUCHE1 with respect to maximal production of biomass. The calculated value of maximum specific growth rate (μ) is 1.07 d^{-1} for the semi-continuous ALPBR. Mohsenpour et. al 2013, reported that for low density inoculum, the maximum specific growth rate of *C. vulgaris* has been found to be 0.51 d^{-1} (under green light). Whereas, the growth rate of 0.36 d^{-1} has been reported for the same algae under yellow light, which is comparatively lesser than the obtained value of *L. subtilis* JUCHE1 [1].

8.2.2.3 Time histories of lipid content and the productivity in IEIGPBR

In Figure 8.12, the time histories of lipid content and the productivity in the IEIGPBR have been plotted. From the Figure 8.12, of lipid content and productivity graph it has been observed that the lipid accumulation of *L. subtilis* JUCHE1 increases monotonically over the entire operating period till 14th day. Naturally the lipid productivity graph exhibits the similar trend. The maximum lipid content and productivity of 58.86(% w/w) and 0.1043 g/L/d respectively are observed for yellow wavelength of light on 14th day and 12th day. The maximum values are much higher than that obtained with yellow light under batch condition (22.15%, 0.0361 g/L/d). This is because of the fact that the reactor is operated with semi-continuous supply of CO_2 , while for batch runs CO_2 is sparged only during initiation. The finding also establishes the effectiveness of internal and external irradiation.

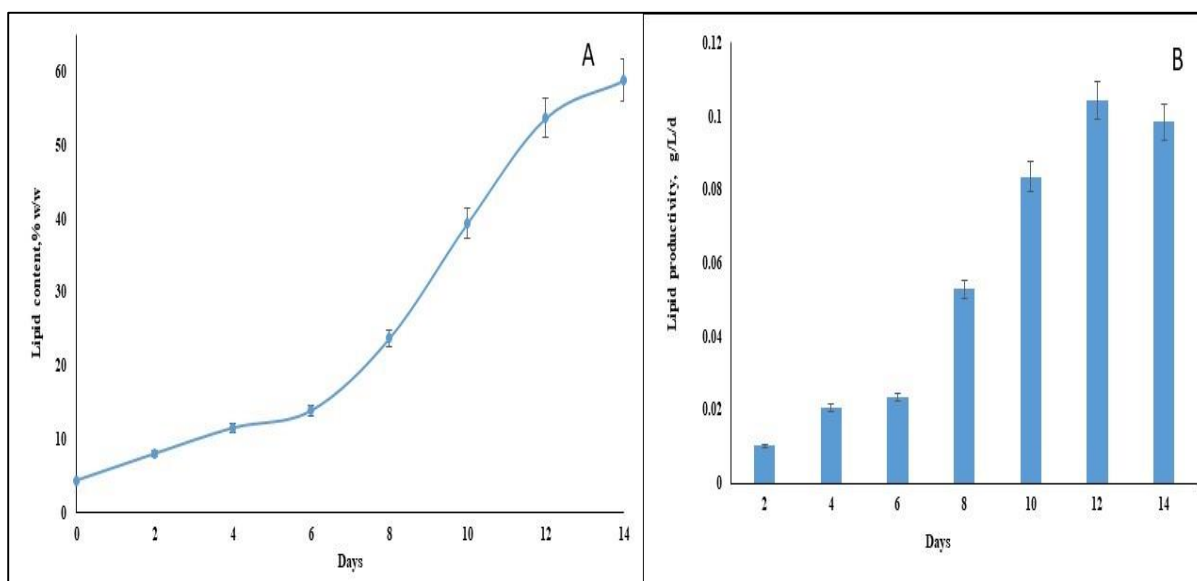


Figure 8.12 Time histories of lipid content and the productivity in IEIGPBR

Table 8.9 Values of Lipid content (%w/w) and Lipid productivity g/L/d at each time intervals under yellow light using IEIGPBR in the semi-continuous mode.

| Days | Lipid content (%w/w) | Lipid productivity g/L/d |
|------|----------------------|--------------------------|
| 0 | 4.4215 | 0 |
| 2 | 8.0761 | 0.0101 |
| 4 | 11.5822 | 0.0206 |
| 6 | 13.9213 | 0.0233 |
| 8 | 23.7300 | 0.0527 |
| 10 | 39.4149 | 0.0835 |
| 12 | 53.7531 | 0.1043 |
| 14 | 58.8685 | 0.0985 |

8.2.2.4 Time history of CO₂ Fixation rate of *L. subtilis* JUCHE1 in IEIGPBR

The time history of CO₂ fixation rate of *L. subtilis* JUCHE1 in the IEIGPBR over 14 days has been plotted in Figure 8.12. As represented in above Figure 8.12, the CO₂ fixation rate increases with increase in time and it has been observed that the maximum value is obtained at 8th days and the value is 0.2855g/L/d. Similar to the trend of biomass concentration trend, during the start-up, the CO₂ capture rate is slightly slow up to 6th day and after that the curve exponentially increases from 6-8th days and then slightly decreased from 10-14days. It can be explained by the fact that the production of algal biomass is directly related to the assimilation of CO₂.

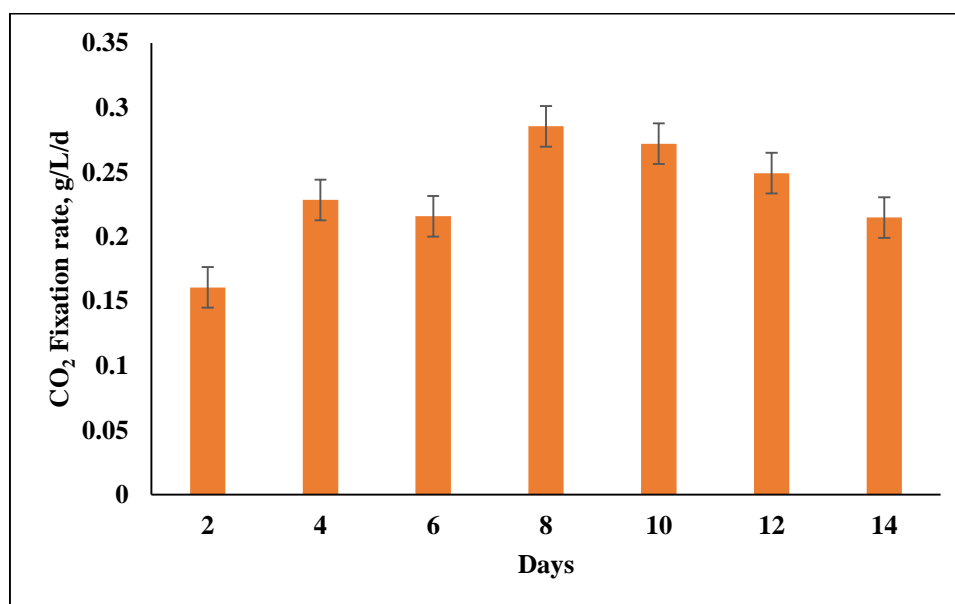


Figure 8.12. Time history of CO₂ Fixation rate of *L. subtilis* JUCHE1 in IEIGPBR

Table 8.10 Values of CO₂ Fixation rate of *L. subtilis* JUCHE1 at each time interval under yellow light using IEIGPBR in the semi-continuous mode.

| Days | CO₂ Fixation rate (g/L/d) |
|-------------|---|
| 0 | 0 |
| 2 | 0.1605 |
| 4 | 0.2283 |
| 6 | 0.2157 |
| 8 | 0.2855 |
| 10 | 0.2719 |
| 12 | 0.2491 |
| 14 | 0.2147 |

References

1. Mohsenpour, S. F., & Willoughby, N. (2013). Luminescent photobioreactor design for improved algal growth and photosynthetic pigment production through spectral conversion of light. *Bioresource technology*, 142, 147-153.
2. Mattos, E. R., Singh, M., Cabrera, M. L., & Das, K. C. (2015). Enhancement of biomass production in *Scenedesmus bijuga* high-density culture using weakly absorbed green light. *Biomass and Bioenergy*, 81, 473-478.
3. Niizawa, I., Heinrich, J. M., & Irazoqui, H. A. (2014). Modeling of the influence of light quality on the growth of microalgae in a laboratory scale photo-bio-reactor irradiated by arrangements of blue and red LEDs. *Biochemical engineering journal*, 90, 214-223.
4. Niizawa, I., Leonardi, R. J., Irazoqui, H. A., & Heinrich, J. M. (2017). Light wavelength distribution effects on the growth rate of *Scenedesmus quadricauda*. *Biochemical Engineering Journal*, 126, 126-134.
5. Doran, P. M. (1995). *Bioprocess engineering principles*. Elsevier.
6. Baidya, A., Akter, T., Islam, M. R., Shah, A. A., Hossain, M. A., Salam, M. A., & Paul, S. I. (2021). Effect of different wavelengths of LED light on the growth, chlorophyll, β -carotene content and proximate composition of *Chlorella ellipsoidea*. *Heliyon*, 7(12), e08525.
7. Hwang, J. H., & Maier, N. (2019). Effects of LED-controlled spatially-averaged light intensity and wavelength on *Neochloris oleoabundans* growth and lipid composition. *Algal Research*, 41, 101573.
8. Ra, C. H., Kang, C. H., Jung, J. H., Jeong, G. T., & Kim, S. K. (2016). Enhanced biomass production and lipid accumulation of *Picochlorum atomus* using light-emitting diodes (LEDs). *Bioresource technology*, 218, 1279-1283.
9. Lee, C. G., & Palsson, B. Ø. (1995). Light emitting diode-based algal photobioreactor with external gas exchange. *Journal of fermentation and bioengineering*, 79(3), 257-263.
10. Suh, I. S., & Lee, S. B. (2003). A light distribution model for an internally radiating photobioreactor. *Biotechnology and Bioengineering*, 82(2), 180-189.

11. Terashima, I., Fujita, T., Inoue, T., Chow, W. S., & Oguchi, R. (2009). Green light drives leaf photosynthesis more efficiently than red light in strong white light: revisiting the enigmatic question of why leaves are green. *Plant and cell physiology*, 50(4), 684-697.
12. Kim, N. J., & Lee, C. G. (2001). A theoretical consideration on oxygen production rate in microalgal cultures. *Biotechnology and Bioprocess Engineering*, 6, 352-358.
13. Morel, A., & Bricaud, A. (1981). Theoretical results concerning light absorption in a discrete medium, and application to specific absorption of phytoplankton. *Deep Sea Research Part A. Oceanographic Research Papers*, 28(11), 1375-1393.
14. de Mooij, T., de Vries, G., Latsos, C., Wijffels, R. H., & Janssen, M. (2016). Impact of light color on photobioreactor productivity. *Algal research*, 15, 32-42.
15. Vadiveloo, A., Moheimani, N. R., Cosgrove, J. J., Bahri, P. A., & Parlevliet, D. (2015). Effect of different light spectra on the growth and productivity of acclimated *Nannochloropsis* sp. (Eustigmatophyceae). *Algal research*, 8, 121-127.
16. Severes, A., Hegde, S., D'Souza, L., & Hegde, S. (2017). Use of light emitting diodes (LEDs) for enhanced lipid production in micro-algae based biofuels. *Journal of Photochemistry and Photobiology B: Biology*, 170, 235-240.
17. Chu, B., Zhao, J., Zheng, H., Gong, J., Chen, K., Zhang, S., ... & He, Y. (2021). Performance of LED with mixed wavelengths or two-phase culture on the growth and lipid accumulation of *Chlorella pyrenoidosa*. *International Journal of Agricultural and Biological Engineering*, 14(1), 90-96.
18. Michael, C., Del Ninno, M., Gross, M., & Wen, Z. (2015). Use of wavelength-selective optical light filters for enhanced microalgal growth in different algal cultivation systems. *Bioresource Technology*, 179, 473-482.
19. Esteves, A. F., Soares, O. S., Vilar, V. J., Pires, J. C., & Gonçalves, A. L. (2020). The effect of light wavelength on CO₂ capture, biomass production and nutrient uptake by green microalgae: a step forward on process integration and optimisation. *Energies*, 13(2), 333.
20. Ma, R., Thomas-Hall, S. R., Chua, E. T., Eltanahy, E., Netzel, M. E., Netzel, G., ... & Schenk, P. M. (2018). LED power efficiency of biomass, fatty acid, and carotenoid production in *Nannochloropsis* microalgae. *Bioresource technology*, 252, 118-126.

21. Kandilian, R., Lee, E., &Pilon, L. (2013). Radiation and optical properties of Nannochloropsisoculata grown under different irradiances and spectra. *Bioresource technology*, 137, 63-73.
22. Siefermann-Harms, D. (1987). The light-harvesting and protective functions of carotenoids in photosynthetic membranes. *Physiologia Plantarum*, 69(3), 561-568.
23. Mohsenpour, S. F., Richards, B., & Willoughby, N. (2012). Spectral conversion of light for enhanced microalgae growth rates and photosynthetic pigment production. *Bioresource technology*, 125, 75-81.
24. Nwoba, E. G., Rohani, T., Raeisossadati, M., Vadiveloo, A., Bahri, P. A., & Moheimani, N. R. (2021). Monochromatic light filters to enhance biomass and carotenoid productivities of *Dunaliella salina* in raceway ponds. *Bioresource Technology*, 340, 125689.
25. Maltsev, Y., Maltseva, K., Kulikovskiy, M., & Maltseva, S. (2021). Influence of light conditions on microalgae growth and content of lipids, carotenoids, and fatty acid composition. *Biology*, 10(10), 1060.
26. Thimijan, R. W., &Heins, R. D. (1983). Photometric, radiometric, and quantum light units of measure: a review of procedures for interconversion. *HortScience*, 18(6), 818-822.

Chapter 9

Studies on Power plant blue-green alga *Leptolyngbya subtilis* JUCHE1 for production of Biochar through slow pyrolysis.

Thermochemical processes like pyrolysis, gasification, hydrothermal liquefaction are the techniques used for conversion of biomass into bio-char [1,2]. Depending on individual thermochemical process the composition of char may differ after the decomposition of biomass. From the literature review, it is evident that production of bio-char from algal biomass using pyrolysis is very attractive because of easy operability and cost effectiveness [3]. Pyrolysis is a biomass conversion technique which is carried out at high temperature in the absence of air to produce solid, liquid and gaseous substances [4]. Due to porous nature of bio-char, it improves the nutritional values and water-retention capacity of soil [5]. Bio-char can also be used as an adsorbent for waste water treatment processes [5] In addition, pyro-oil and pyro-gas can be used as fuel after upgradation.

Under the present investigation the pyrolysis characteristics of the dry algal biomass was studied from the perspective of production of bio-char and oil. The following objectives, described under Aim 7 in Chapter 3, are addressed in this chapter:

- **Pyrolysis of algal biomass**
- **Characterization of char and oil**

9.1 Materials and methods

9.1.1 Pyrolysis of Algal biomass

A semi-batch pyrolyser of 50 mm diameter and 640 mm length, equipped with a continuous weighing arrangement, was used [1, 6]. Dry algal biomass weighing 20g, as shown in Figure 9.1, was used for each experimental run. The pyrolysis process was performed in the semi-batch reactor under isothermal condition in the temperature range of 300-700°C. Inert atmosphere was created by the flow of nitrogen and throughout the experiment the flow rate was maintained at 5LPM during pyrolysis. The mass of char at each temperature and reaction time was determined using the methodologies described in Chapter 5. The pyrolysis was carried out at different temperatures i.e. 300°C, 500°C and 700°C. The reaction time was varied from 0-60 minutes with 5 minutes of intervals and the weight loss of biomass were recorded.



Figure 9.1 Dry algal biomass of *L.subtilis* JUCHE1.

In this manner the process was repeated for all other temperatures. After deducting the mass of solid residue from that of initial biomass, the mass of volatiles was determined with respect to time at various temperatures. This is represented in Equation 5.41. Although the mass of volatiles could be determined directly, the mass of char was determined indirectly as the pyrolysis residue was a mixture of char and unreacted algal biomass. The detailed method has been described in section of Chapter 5. At any time, t , the dimensionless mass of char was calculated using the equation 5.46, i.e., $W_C(t) = \frac{w_R(t \rightarrow \infty)}{w_v(t \rightarrow \infty)} \times w_v(t)$, where, where, $w_R(t \rightarrow \infty)$ and $w_v(t \rightarrow \infty)$ are the values of the dimensionless mass of solid residue left and volatiles evolved at a long pyrolysis time where there is no further change of mass of residue. For each temperature, the time, $(t \rightarrow \infty)$, corresponding to the constancy of mass of solid residue, was determined. The value of the dimensionless mass of unreacted alga, $W(t)$ at any reaction time, t , was calculated using the equation 5.47, i.e., $W(t) = W_R(t) - W_C(t)$, where, $W_R(t)$ and $W_C(t)$ are the dimensionless mass of solid residue obtained through experiment and that of char, calculated using equation 5.43. The actual mass of char and unreacted algal mass were determined by multiplying the dimensionless $W_C(t)$ and $W(t)$ by the initial mass of algal biomass fed for pyrolysis. Similarly, the mass of pyro-oil at any pyrolysis time was determined from that of the condensed mass of volatiles, collected at that time. The mass of pyro-gas at any pyrolysis time was determined by subtracting the mass of pyro-oil from that of volatiles generated at that time.

To test the validity of the assumed first order kinetics, (Equation), the linearity of the plot of $\ln(W)$ against t has been verified. The value of the kinetic rate constant, k has been determined from the slope of the straight line. Similarly, the linearity of the logarithmic plots of W_v against

$(1 - \exp(-kt))$ has been verified and the values of k_v has been determined. The values of the pre-exponential factors, k_0, k_{v0} and the activation energies have also been determined by plotting $\ln k$ and $\ln k_v$ against the inverse of temperature (in K).

The behavior of thermal decomposition of dry algal biomass and char was also investigated through thermo-gravimetric analysis (TGA). The details of TGA is provided in chapter 4.

The pyro-oil was analyzed using GC-MS. The details of GC-MS is provided in chapter 4.

9.2. Results and discussion

9.2.1 Pyrolysis of algal biomass *L. subtilis* JUCHE1

Figure 9.2 (A) and (B) represent the time history curves for weight of residual biomass (W_R) and the weight of volatile matter (W_v) respectively at all reaction temperatures (300, 500, 700°C). From Figure 9.2A, it is clearly evident that for all pyrolysis temperatures (300, 500, 700°C) the time history of solid residue. Over sixty minutes the maximum weight loss was obtained at 700 °C. The time history plot of residual solid at a higher temperature lies below that obtained at lower temperature. While final weight loss of 92%w/w has been obtained at 700°C, the value of %weight loss at 300°C is 70.41 %w/w. Just the opposite results are obtained in case of volatiles. As per expectation, Figure 9.2 B depicts an increasing trend, in contrary to the trend of residual solid mass. The time history curve of volatiles at higher temperature always lies above that obtained data a lower one. All the obtained values of W_R and W_v at each time intervals for all the reaction temperatures (300, 500, 700°C) are provided in table 9.1.

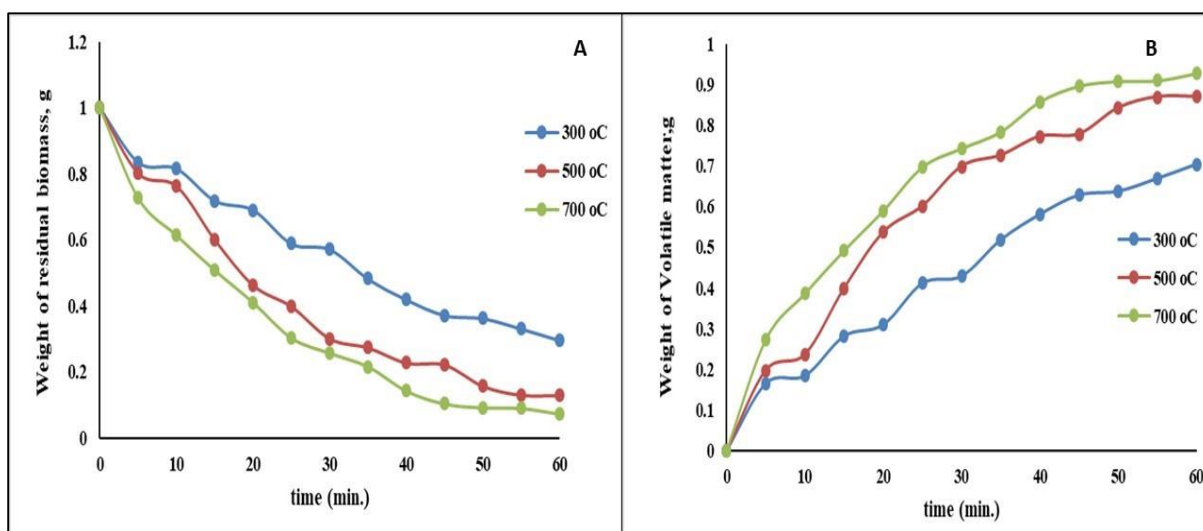


Figure 9.2. Graphical representation of weight of residue W_R and W_v with respect to reaction time by variation of temperature from 700°C to 300°C.

Table 9.1 Observed values of Weight of residual biomass (W_R , g) and Weight of volatile matter (W_V , g) at each time intervals varying reaction temperatures (300, 500, 700°C).

| Time (min) | Weight of residual biomass(W_R , g) | | | Weight of volatile matter (W_V , g) | | |
|---------------|--|----------|----------|--|----------|----------|
| | 300 | 500 | 700 | 300 | 500 | 700 |
| 0 | 1 | 1 | 1 | 0 | 0 | 0 |
| 5 | 0.83527 | 0.802519 | 0.726876 | 0.16473 | 0.197481 | 0.273124 |
| 10 | 0.816278 | 0.763379 | 0.613853 | 0.183722 | 0.236621 | 0.386147 |
| 15 | 0.718924 | 0.600496 | 0.508139 | 0.281076 | 0.399504 | 0.491861 |
| 20 | 0.690734 | 0.463013 | 0.410243 | 0.309266 | 0.536987 | 0.589757 |
| 25 | 0.588605 | 0.398519 | 0.302704 | 0.411395 | 0.601481 | 0.697296 |
| 30 | 0.571209 | 0.301194 | 0.257007 | 0.428791 | 0.698806 | 0.742993 |
| 35 | 0.481909 | 0.273898 | 0.215887 | 0.518091 | 0.726102 | 0.784113 |
| 40 | 0.418952 | 0.227638 | 0.14199 | 0.581048 | 0.772362 | 0.85801 |
| 45 | 0.371577 | 0.221685 | 0.103209 | 0.628423 | 0.778315 | 0.896791 |
| 50 | 0.362402 | 0.157237 | 0.09163 | 0.637598 | 0.842763 | 0.90837 |
| 55 | 0.330714 | 0.130419 | 0.089905 | 0.669286 | 0.869581 | 0.910095 |
| 60 | 0.295821 | 0.129769 | 0.072223 | 0.704179 | 0.870231 | 0.927777 |

From the experimental results, depicted in Figure 9.2A it appears that at each temperature the reaction time of 60 minutes can be considered to be $t \rightarrow \infty$ as no more decomposition occurred beyond that. The data of W_R and W_V , obtained at this reaction time have been used to calculate the values of W_C using Eq. 5.51. The values of $\frac{W_R(t \rightarrow \infty)}{W_V(t \rightarrow \infty)}$ at different temperature have been provided in Table 9.2.

Table 9.2. The experimental values of $\frac{W_R(t \rightarrow \infty)}{w_V(t \rightarrow \infty)}$ at different reaction temperatures are as follows:

| T (°C) | 300 | 500 | 700 |
|---|------|-------|-------|
| $\frac{W_R(t \rightarrow \infty)}{w_V(t \rightarrow \infty)}$ | 0.42 | 0.149 | 0.077 |

At different temperature, the values of normalized weight of char, W_c have been plotted against time in Figure 9.3. The trends are similar to those for solid residue. The experimental values of W_c have also been provided in Table 9.3

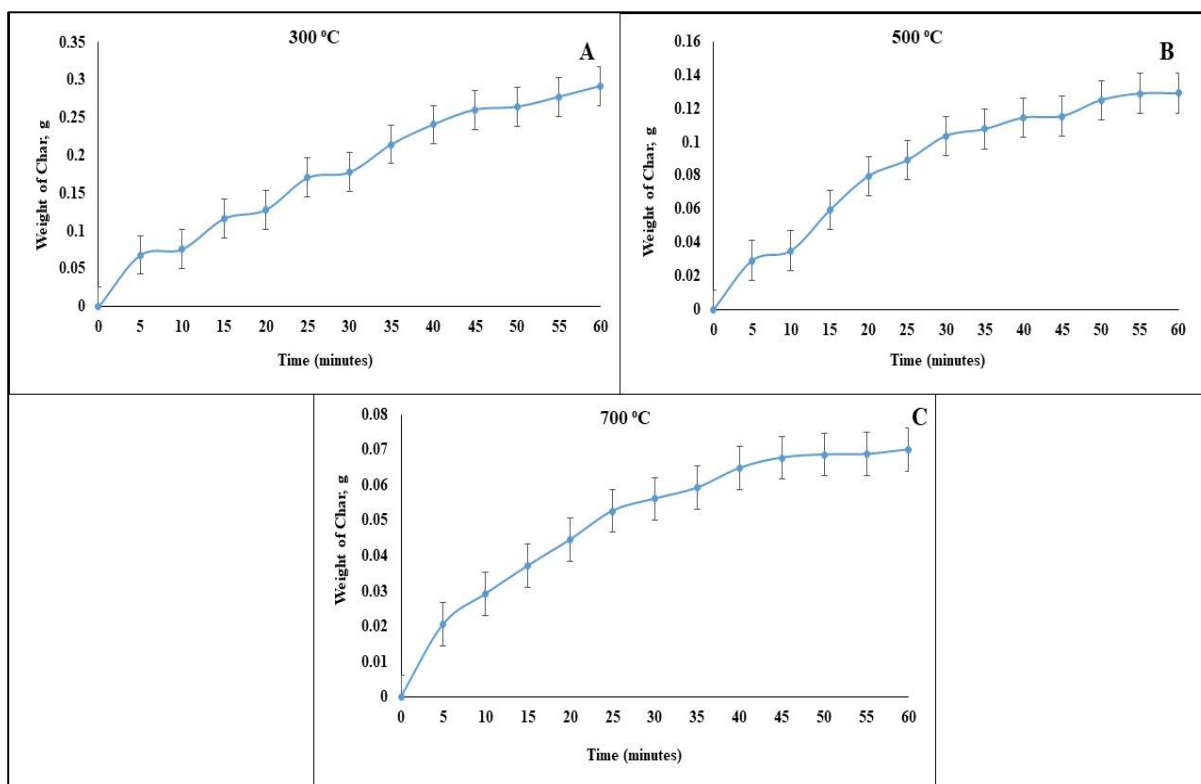


Figure 9.3 Graphical representation of weight of char (W_c) of *L. subtilis* JUCHE1 at different temperatures (300°C, 500°C and 700°C) in respective reaction time.

Table 9.3 Experimental values of W_c with respect to individual time intervals at different temperatures 300 °C, 500 °C and 700 °C.

| Time (minutes) | Weight of char(W_c , g) | | |
|----------------|----------------------------|----------|----------|
| | 300 °C | 500 °C | 700 °C |
| 0 | 0 | 0 | 0 |
| 5 | 0.068245 | 0.029282 | 0.020624 |
| 10 | 0.076113 | 0.035085 | 0.029159 |
| 15 | 0.116446 | 0.059237 | 0.037142 |
| 20 | 0.128124 | 0.079622 | 0.044534 |
| 25 | 0.170435 | 0.089185 | 0.052655 |
| 30 | 0.177642 | 0.103616 | 0.056105 |
| 35 | 0.214638 | 0.107663 | 0.05921 |
| 40 | 0.24072 | 0.114523 | 0.06479 |
| 45 | 0.260347 | 0.115405 | 0.067719 |
| 50 | 0.264148 | 0.124961 | 0.068593 |
| 55 | 0.277275 | 0.128938 | 0.068723 |
| 60 | 0.291731 | 0.129034 | 0.070059 |



Figure 9.4. Photographs of Pyro char of *Leptolyngbya subtilis* JUCHE1 at different pyrolysis temperatures (A) Dry algal biomass, (B) 300°C , (C)500°C, (D) 700°C.

Figure 9.4 represents the photographs of char at different temperature. From the photographs as shown in Figure 9.4, it is clear that as the temperature increases the solid residue becomes darker in appearance and also becomes more brittle. Figure 9.5 represents the maximum yields of Biochar, Oil and Gas obtained at different reaction temperatures (300 °C, 500 °C and 700 °C). From the bar plot it is clear that the highest value of biochar, i.e 29% (w/w) is obtained at 300 °C, whereas the maximum yield of oil and gas of 23.65% and 69.12% respectively are obtained at 700 °C. The range of Bio-oil lies between 9.55-23.65% with increase in pyrolysis temperature from 300-700 °C. The yield of pyro-gas lies in between the range of 60.86-69.12% (300-700 °C) which are high.

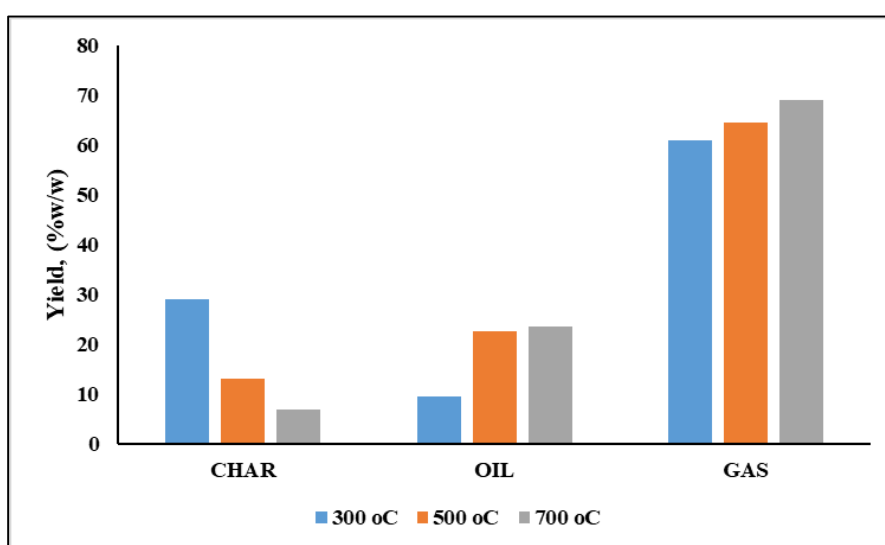


Figure 9.5. Yields of Bio-char, oil and gas of *Leptolyngbya subtilis* JUCHE1 at each time intervals and different reaction temperatures (300°C to 700°C).

Table 9.5 provides the yields (%) of pyro-char, pyro-oil and pyro-gas of different algal strains for the comparison with the data of *Leptolyngbya subtilis* JUCHE1 obtained at different reaction temperature. A research article on *Chlorella vulgaris* reported the maximum yield of Biochar, pyro-oil and pyro gas of 43.46%, 32.69% and 58.29 % respectively were obtained at 300, 500 and 900 °C [8]. In a study on *Chlorella vulgaris* char yield was reported to vary from 900-300°C [8]. In case of fluidized bed pyrolysis of *Chlorella vulgaris*, Biochar, pyro-oil and pyro-gas yield of 31%, 53%, 10 % respectively were obtained at 500 °C [9]. In a comparative analysis of algae and lignocellulosic biomass for biochar production, it was observed that three different species of algae namely *Spirulina sp.*, *Spirogyra sp.* and *Cladophora sp.* produces more amount of biochar in comparison to lignocellulosic feedstocks [4]. At 550 °C of pyrolysis temperature, the values of biochar of *Spirulina sp.*, *Spirogyra sp.* and *Cladophora sp.* were observed to be 31%, 28%, 31% respectively [4]. Kim et al. 2013, conducted the pyrolysis experiment using the dry biomass of microalga "*Scenedesmus sp.*" in fluidized bed pyrolyzer at 440 °C as reaction temperature [10]. From the article it was found that the maximum yields of pyro-char, oil and gas i.e. to be 26, 41.54 and 21.8% respectively [10]. Another literature reported that the experiments conducted using two different strains of blue green algae namely *Spirulina sp.* and *Spirogyrasp*[11]. Both type of pyrolysis such as slow as well as fast were conducted at a reaction temperature of 500 °C in stainless steel reactor system having nitrogen flow rate was maintained at 1LPM [11]. For *Spirulina sp* the yield of pyro char i.e. 31% was obtained under both slow and fast pyrolysis [11]. However, pyro-oil and gas yields of 29 and 40% respectively were obtained under fast pyrolysis condition [11]. Similarly in case of *Spirogyrasp*. the highest pyro-char and gas of 32% and 55% were obtained under fast pyrolysis and the maximum yields of oil was obtained to be 16% under slow pyrolysis process [11]. On the basis of comparison with reported data on pyrolysis of other algal strains, it can be inferred that the yield of bio-char from *L. subtilis*JUCHE1 is comparatively higher than many of them [4, 8, 9, 10, 11, 12]. In case of pyro-oil the yield value was comparatively higher than other blue green algal strains (*Spirulina sp.* and *Spirogyra sp.*) under slow pyrolysis at 500 °C as reported in the literature[11].

Table 9.4 Maximum yields values of Pyro-char (% wt.), Pyro-oil(%wt.) and Pyro-Gas (%wt.) of different Algae at different reaction temperatures.

| Algal strain | Type of pyrolysis | Temperature (°C) | Pyro-char (%wt.) | Pyro-oil (%wt.) | Pyro-Gas (%wt.) | Reference |
|---------------------------|---------------------|------------------|------------------|-----------------|-----------------|-----------|
| <i>Spirulina</i> | Slow pyrolysis | 550 | 31 | 46 | 23 | 4 |
| <i>Spirogyra</i> | | | 28 | 43 | 29 | |
| <i>Cladophora</i> | | | 31 | 39 | 30 | |
| <i>Chlorella vulgaris</i> | Fixed bed pyrolysis | 300 | 43.05 | 20.64 | 35.92 | 8 |
| | | 400 | 43.46 | 16.38 | 37.7 | |
| | | 500 | 29.28 | 32.69 | 34.25 | |
| | | 600 | 22.33 | 28.5 | 43.71 | |
| | | 700 | 23.73 | 27.25 | 46.8 | |
| | | 800 | 21.58 | 26.55 | 50.83 | |
| | | 900 | 19.3 | 2.04 | 58.29 | |
| <i>C. vulgaris</i> | Fast pyrolysis | 500 | 31 | 53 | 10 | 9 |
| <i>Scenedesmus sp.</i> | pyrolysis | 440 | 26 | 41.54 | 21.8 | 10 |
| <i>Spirulina sp.</i> | Slow | 500 | 31 | 20 | 23 | 11 |
| | Fast | | 31 | 29 | 40 | |

| Algal strain | Type of pyrolysis | Temperature (°C) | Pyro-char (%wt.) | Pyro-oil (%wt.) | Pyro-Gas (%wt.) | Reference |
|---|--|------------------|------------------|-----------------|-----------------|----------------------|
| <i>Spirogyra sp.</i> | Slow | 500 | 27 | 16 | 44 | |
| | Fast | | 32 | 13 | 55 | |
| <i>K. alvarezii</i> | (Microwave-assisted pyrolysis) Fast pyrolysis | 340 | 22.1 | 32.4 | 45.6 | 12 |
| <i>S. wightii</i> | | 320 | 33.3 | 25.9 | 40.9 | |
| <i>T. ornata</i> | | 280 | 30.9 | 27 | 42.1 | |
| <i>Leptolyngbya subtilis</i> JUCHE1 | Slow pyrolysis | 300 | 29 | 9.55 | 60.86 | Present study |
| | | 500 | 13 | 22.5 | 64.52 | |
| | | 700 | 7 | 23.65 | 69.12 | |

9.2.2 Rate constants

9.2.2.1 Determination of overall rate constants (k) at different temperatures

The overall rate constants (k) at different temperatures (300, 500 and 700 °C) have been determined from the slope of the graph ($\ln \left(\frac{W_t}{W_0} \right)$ versus t (min)), shown in the Figure 9.6. All the values of W(t) at each time intervals of 5 minutes for different reaction temperatures (300, 500 and 700 °C) are provided in table 9.5. The Values of the overall rate constants (k) at 300, 500 and 700 °C have been provided in Table 9.6.

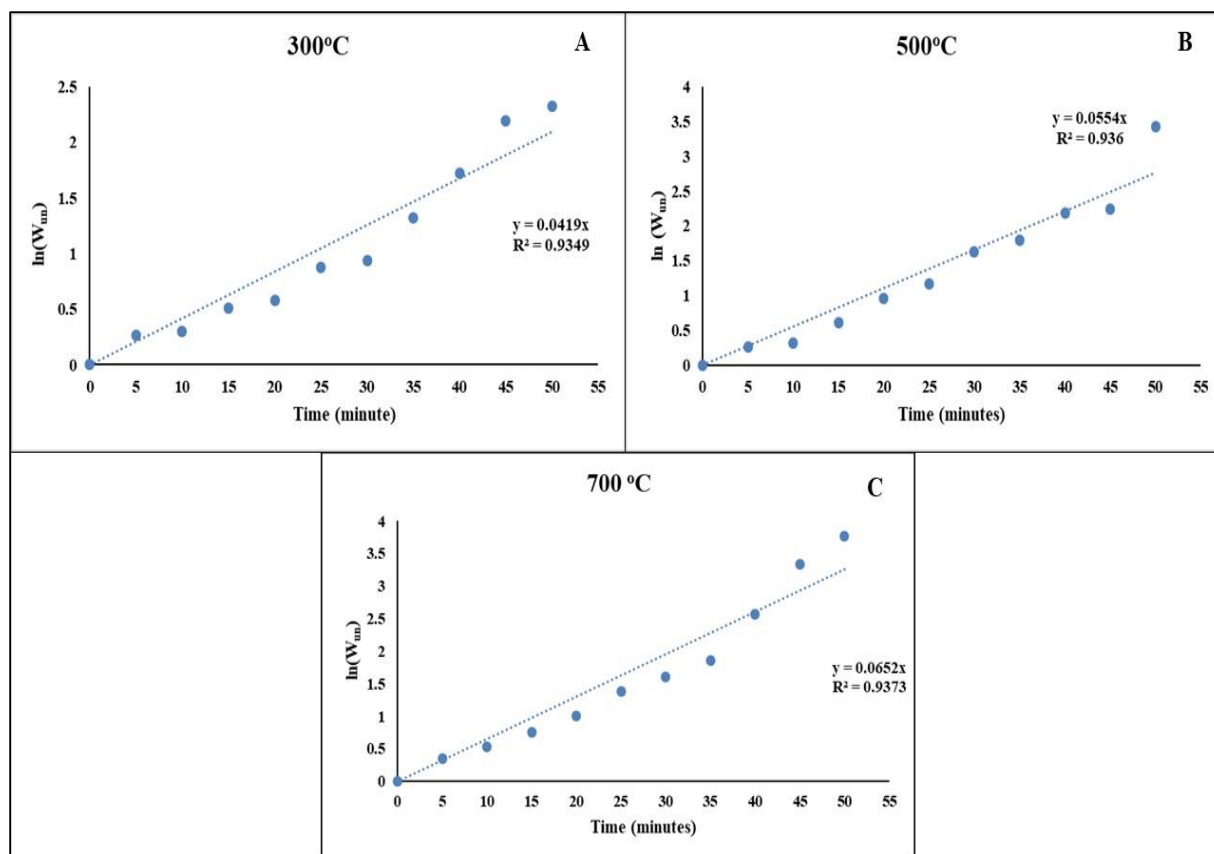


Figure 9.6 Graphical representation of the plot of $\ln W_{un}$ with respect to each to intervals at different reaction temperatures: (A) 300, (B) 500 and (C) 700 °C.

Table 9.5 Calculated values of $\ln W_{un}$ at each reaction time varying different temperatures.

| Time (minutes) | $\ln W_{un}$ | | |
|-------------------|--------------|----------|----------|
| | 300 °C | 500 °C | 700 °C |
| 0 | 0 | 0 | 0 |
| 5 | 0.265236 | 0.25717 | 0.347784 |
| 10 | 0.300882 | 0.31705 | 0.536667 |
| 15 | 0.506704 | 0.613858 | 0.752902 |
| 20 | 0.575169 | 0.9587 | 1.005916 |
| 25 | 0.871868 | 1.173334 | 1.386097 |

| Time (minutes) | ln W _{un} | | |
|-------------------|--------------------|----------|----------|
| | 300 °C | 500 °C | 700 °C |
| 30 | 0.932504 | 1.621621 | 1.60494 |
| 35 | 1.319491 | 1.794356 | 1.85357 |
| 40 | 1.724672 | 2.17935 | 2.561364 |
| 45 | 2.196156 | 2.241686 | 3.338502 |
| 50 | 2.320191 | 3.433438 | 3.770677 |
| 55 | 2.929215 | 6.514655 | 3.854618 |

Table 9.6 Values of rate constants at different temperatures

| Overall rate constant (min ⁻¹) | Temperature (°C) | | |
|---|------------------|--------|--------|
| | 300 | 500 | 700 |
| k | 0.0419 | 0.0554 | 0.0652 |
| R ² Value | 0.9349 | 0.936 | 0.9373 |

9.2.2.2 Determination of rate constants of formation of volatiles (k_v) at different temperatures

The rate constants of formation of volatiles (k_v) at different temperatures (300, 500 and 700 °C) have been determined from the slope ($W_0 \frac{k_v}{k}$) of the graph (W_v versus $[1 - \exp(-kt)]$), shown in the Figure 9.7 (where, $W_0 = 1$). The Values of the rate constants of formation of volatiles (k_v) at 300, 500 and 700 °C have been reported in Table 9.7. All the obtained values of W_v at different temperatures (300, 500 and 700 °C) are provided below in Table 9.1.

Table 9.7 Values of the rate constants of formation of volatiles at different temperatures

| k_v determination | Temperature (°C) | | |
|-----------------------------|------------------|--------|--------|
| | 300 | 500 | 700 |
| Slope | 0.6953 | 0.8526 | 0.9012 |
| k_v (min^{-1}) | 0.029 | 0.0471 | 0.0587 |
| R^2 Value | 0.9524 | 0.9665 | 0.9785 |

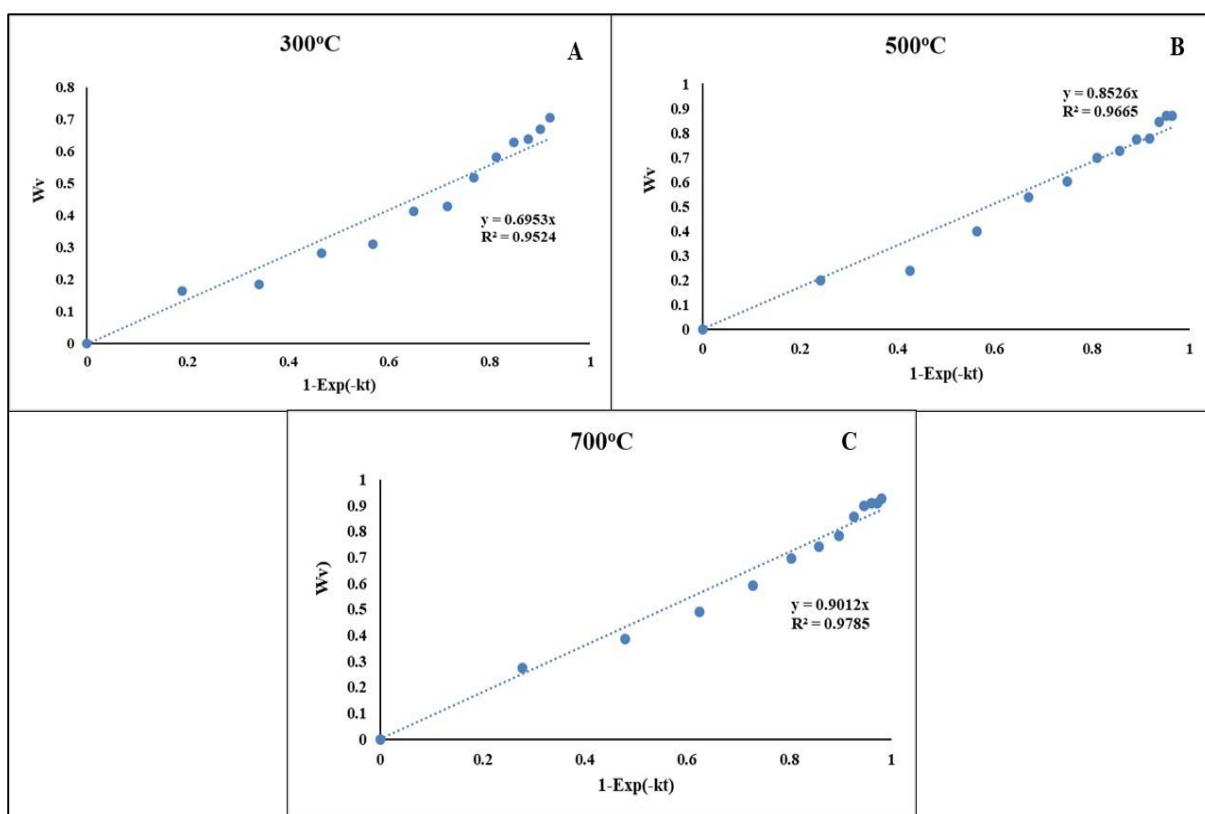
Figure 9.7 Graphical representation of the plot of $(1-\text{Exp}(-kt))$ vs W_v at different reaction temperatures (A)300, (B) 500 and (C) 700 °C.

Table 9.8. Calculated values of weight of volatile matters and (1-Exp(-kt)) at different temperatures and time intervals.

| Time (mins.) | (1-Exp(-kt)) | | |
|-----------------|--------------|---------|---------|
| | 300 °C | 500 °C | 700 °C |
| 0 | 0 | 0 | 0 |
| 5 | 0.18901 | 0.24194 | 0.27819 |
| 10 | 0.34229 | 0.42535 | 0.47899 |
| 15 | 0.46660 | 0.56438 | 0.62393 |
| 20 | 0.56742 | 0.66978 | 0.72855 |
| 25 | 0.64918 | 0.74967 | 0.80407 |
| 30 | 0.71549 | 0.81024 | 0.85857 |
| 35 | 0.76926 | 0.85615 | 0.89792 |
| 40 | 0.81287 | 0.89095 | 0.92631 |
| 45 | 0.84824 | 0.91733 | 0.94681 |
| 50 | 0.87692 | 0.93733 | 0.96161 |
| 55 | 0.90019 | 0.95249 | 0.97229 |
| 60 | 0.91905 | 0.96399 | 0.97999 |

9.2.2.3 Determination of activation energies and pre-exponential factors

Arrhenius equation has been used to represent the functionality of all rate constants on temperature. This is as follows:

$$k_i = k_o \exp\left(\frac{-E_i}{RT}\right) \quad (9.1)$$

k_i = rate constant ; k_o = pre – exponential factor ; E_A = Activation energy

The values of activation energies and pre-exponential factors, determined by plotting the natural logarithm of each rate constant, $\ln(k_i)$ against the inverse of temperature in kelvin, $\frac{1}{T}$, shown in the Figure 9.8 (where $k_i = k$ or k_v).

Table 9.9 Values of k , k_v , k_c , $\ln(k)$, $\ln(k_v)$ at different temperatures (300, 500 and 700 °C).

| T (K) | k (min^{-1}) | k_v (min^{-1}) | $1/T$ | $(-\ln k)$ | $(-\ln k_v)$ |
|-------|---------------------------|-----------------------------|----------|------------|--------------|
| 573 | 0.0419 | 0.029 | 0.001745 | 3.172469 | 3.540459 |
| 773 | 0.0554 | 0.0471 | 0.001294 | 2.893176 | 3.055482 |
| 973 | 0.0652 | 0.0587 | 0.001028 | 2.730296 | 2.835316 |

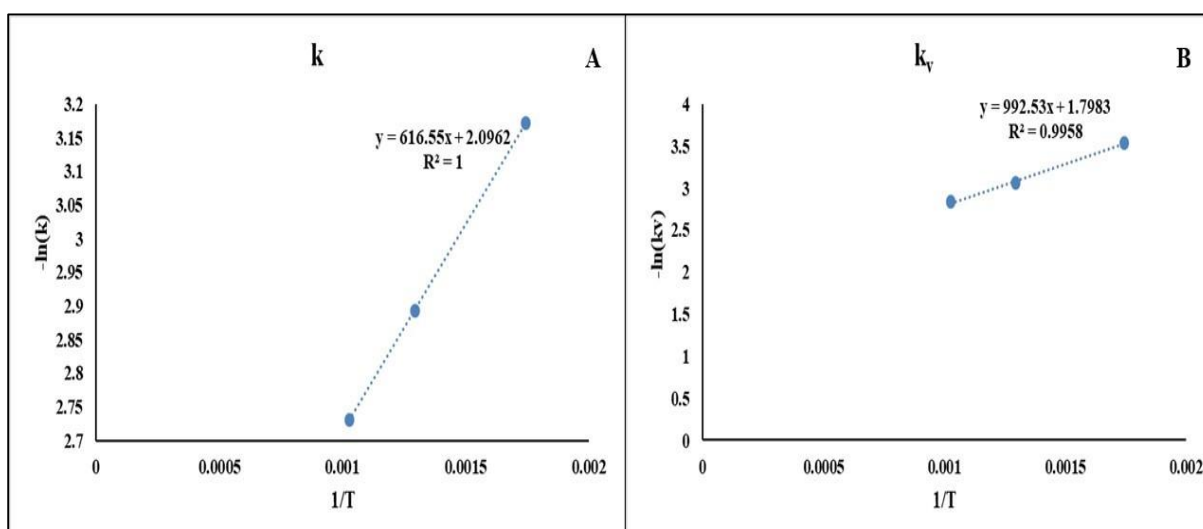


Figure 9.8 Determination of activation energies and pre-exponential factors (A: for k ; B: for k_v)

The values of activation energies and pre-exponential factors have been reported in Table 9.10.

Table 9.10 Values of activation energies and pre-exponential factors

| Rate constant (min^{-1}) | Slope | Activation energy (kJ/mol) | Intercept | Pre-exponential factor (min^{-1}) | R^2 Value |
|--|--------|-------------------------------|-----------|---|----------------|
| k | 616.55 | 5.125997 | 2.0962 | 8.135197 | 1 |
| k_v | 992.53 | 8.25189 | 1.7983 | 6.039372 | 0.9958 |

9.2.3 Thermo-gravimetric analysis (TGA)

In Figure 9.9, the mass trajectory of algal biomass has been plotted against temperature at heating rates of 10, 15, 20, 25 and 30 °C/min. From the graph it has been observed that the decomposition profile of dry algal biomass is steep S-shaped curve for all the heating rates. It has also been observed that under adiabatic condition, the decomposition process can be divided into four distinct temperature zones: I: 50-275°C, II: 275-380 °C, III: 380-570 °C and IV: 570-900 °C. This indicates that the pyrolysis is expected to occur mostly from 275-570°C. Beyond this temperature zone the mass-temperature profile is almost flat. The profiles obtained at different heating rates are almost overlapping, indicating that the pyrolysis is nearly independent of this parameter.

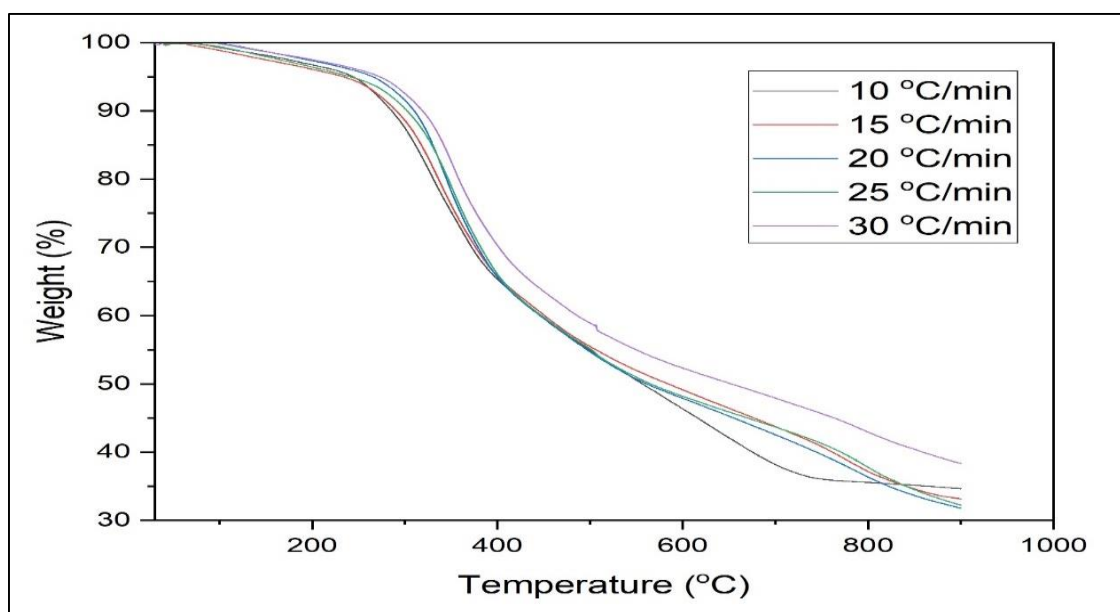


Figure 9.9 Thermo-Gravimetric Analysis (TGA) of Dry Algal biomass at different heating rate 10, 15, 20, 25 and 30 °C/min.

In Figures 9.10 and 9.11, mass-temperature plots, i.e., temperature dependence of thermal decomposition of biochar samples, obtained at 500 and 700 °C have been represented at the heating rate, set at 10 °C/min. In both the cases the thermal decomposition profile of pyro char depicts similar pattern. In both the cases the thermal decomposition curve can be divided into three distinctive zones. For 500 °C char sample, the temperature range of these zones are: (1) 50-425 °C, (2) 425-620 °C, and (3) 620-900 °C, while for 700 °C char sample ranges are: zone1: 50-400°C, zone2: 400-640 °C, zone 3: 640-900 °C.

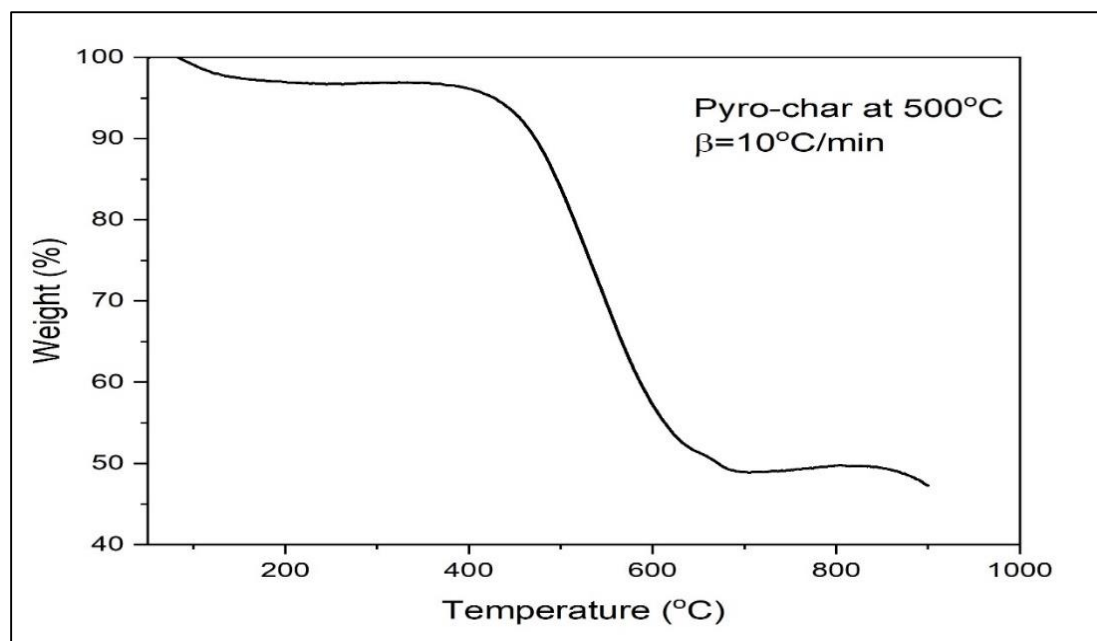


Figure 9.10 Thermogravimetric Analysis (TGA) of Pyro-char at 500 °C .

Similar patterns of TGA plots indicates the similarity in the constituents of pyro-char obtained at 500 and 700°C. While the mass-temperature profiles are almost flat in the 1st and the 3rd zones, the maximum decomposition of pyro-char occurred in the second zone for both the pyrolysis temperature 500°C and 700°C.

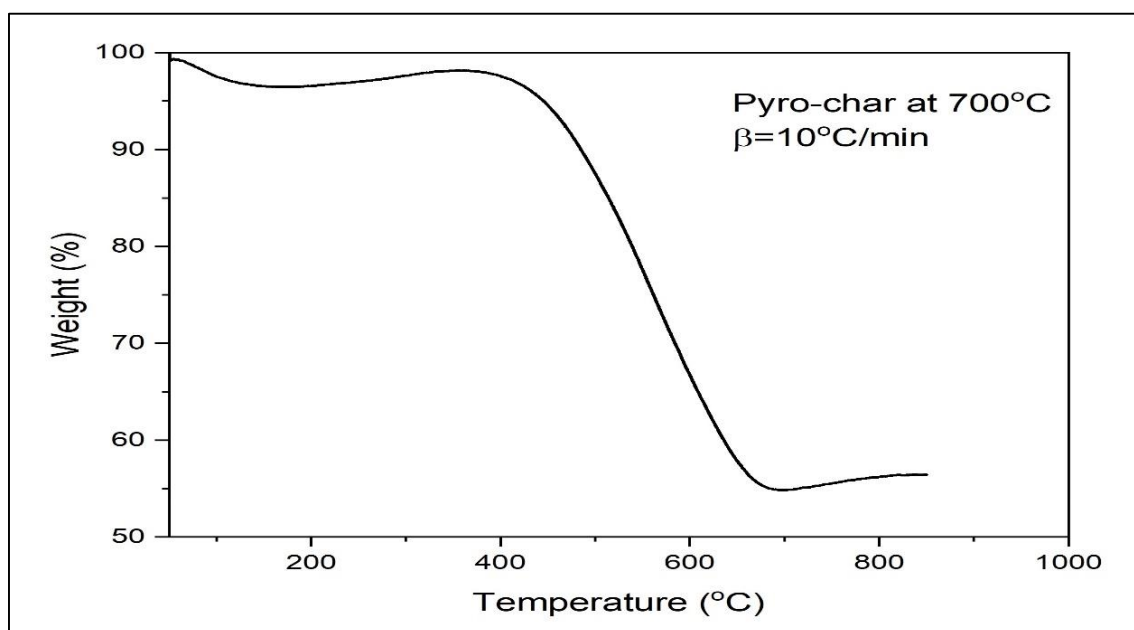


Figure 9.11 Thermogravimetric Analysis (TGA) of Pyro-char at 700 °C.

9.2.4 GC-MS analysis of Pyro-Oil

The chromatogram, obtained through the GC-MS analysis of pyro-oil, obtained through pyrolysis at 500°C, has been depicted in Figure 9.12. The chromatogram, obtained through the GC-MS analysis of pyro-oil of 500°C pyrolysis has been depicted in Figure 9.8. From the GC-MS analysis of pyro-oil, it is found that most of the identified organic compounds in the oil are mostly fatty acids (saturated, unsaturated, polyunsaturated, volatile fatty acids), esters and amino acids. As provided in Table 9.13. other than fatty acids some phytochemicals, namely, desulphosinigrin having antimicrobial properties are also identified. As reported in R. Gautamet al. 2017, at low reaction temperature the pyrolysis of lipid results in formation of long and short-chain carboxylic acids whereas at high temperature aliphatic hydrocarbon are expected to be formed due to decarboxylation [12].

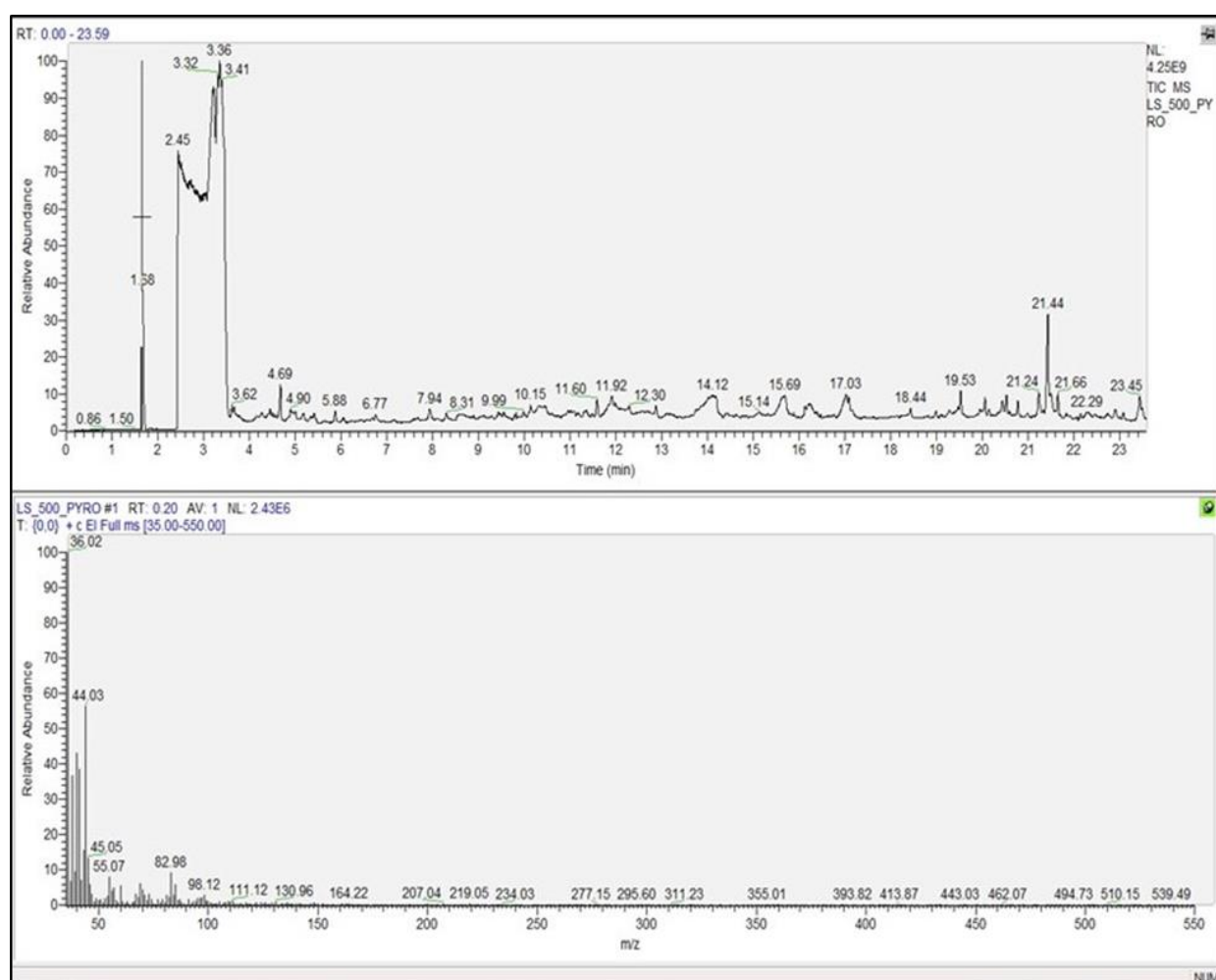


Figure 9.12 Chromatogram of Pyro-oil obtained at 500°C.

Table 9.11 Characterization of pyro-oil using GC-MS analysis.

| Name of the Identified compounds | Molecular formula | Retention time |
|--|---|----------------|
| 2-propenoic acid 3-(phenylmethyl)sulfonyl- methyl ester | C ₁₀ H ₁₀ O ₂ | 4.69 |
| 6-Nonynoic acid | C ₉ H ₁₄ O ₂ | 4.44 |
| 2-Propenoic acid, 1-methylpropyl ester | C ₁₅ H ₂₈ O ₂ | 5.57 |
| 4-Hexenoic acid, 6-hydroxy-4-methyl-, methyl ester, | C ₈ H ₁₄ O ₃ | 5.88 |
| 4-Pentenoic acid, 2-methylene-, methyl ester | C ₇ H ₁₀ O ₂ | 6.79 |
| Carbamic acid, phenyl ester | C ₇ H ₇ NO ₂ | 7.96 |
| 11,14-Eicosadienoic acid, methyl ester | C ₂₁ H ₃₈ O ₂ | 8.80 |
| 1,2-Cyclobutanedicarboxylic acid, 1-cyano-, dimethyl ester, trans- | C ₉ H ₁₁ NO ₄ | 8.35 |
| Linolenic Acid | C ₁₈ H ₃₀ O ₂ | 9.40 |
| Octanal, 7-hydroxy-3,7-dimethyl- | C ₁₀ H ₂₀ O ₂ | 10.17 |
| Dodecanoic acid, 3-hydroxy- | C ₁₂ H ₂₄ O ₃ | 11.61 |
| 11,11-Dimethylbicyclo[8.2.0]dodecane | C ₁₄ H ₂₆ | 11.90 |
| 8 11-octadecadienoic acid methyl ester | C ₁₉ H ₃₄ O ₂ | 12.30 |
| Phosphinic acid, dipropyl-, isopropyl ester | C ₉ H ₁₈ NO ₄ P | 14.07 |
| 2-Myristynoyl pantetheine | C ₂₅ H ₄₄ N ₂ O ₅ S | 15.11 |
| 3-Methyl-2-butenic acid, 4-hexadecyl ester | C ₂₁ H ₄₀ O ₂ | 15.67 |
| α -D-Glucopyranoside | C ₆ H ₁₁ O ₆ | 16.17 |
| Undecanoic acid, 10-methyl-, methyl ester | C ₁₃ H ₂₆ O ₂ | 17.3 |
| 2-Hydroxytetradecanoic acid | C ₁₄ H ₂₈ O ₃ | 18.46 |
| Decanoic acid | C ₁₀ H ₂₀ O ₂ | 19 |
| 13-Eicosenoic acid | C ₂₀ H ₃₈ O ₂ | 19.55 |
| cis-10-Nonadecenoic Acid | C ₁₉ H ₃₆ O ₂ | 20.07 |
| 9,12,15-Octadecatrienoic acid 2,3-bis(acetyloxy)propyl ester | C ₂₅ H ₄₀ O ₆ | 20.55 |
| 6-Octadecenoic acid, (Z)- | C ₁₈ H ₃₄ O ₂ | 20.79 |
| Oleic acid | C ₁₈ H ₃₄ O ₂ | 21.23 |
| Isopropyl palmitate | C ₁₉ H ₃₈ O ₂ | 21.44 |
| 9-Hexadecenoic acid | C ₁₆ H ₃₀ O ₂ | 23.46 |

References

1. Ghosh S, Das S, Chowdhury R ., Effect of pre-pyrolysis biotreatment of banana pseudo-stem (BPS) using synergistic microbial consortium: Role in deoxygenation and enhancement of yield of pyro-oil. *Energy Conversion and Management*.2019; 195; 114-124
2. Leng, LJ, Yuan XZ, Huang HJ, Wang H, Wu ZB, Fu LH, Zeng GM et al. Characterization and application of bio-chars from liquefaction of microalgae, lignocellulosic biomass and sewage sludge. *Fuel Processing Technology*.2015; 129; 8-14
3. Laird DA, Brown RC, Amonette JE, Lehmann J., Review of the pyrolysis platform for coproducing bio-oil and biochar. *Biofuels, bioproducts and biorefining*.2009; 3(5); 547-562.
4. Chaiwong K, Kiatsiriroat T, Vorayos N, Thararax C et al. Biochar production from freshwater algae by slow pyrolysis. *Maejo International Journal of Science and Technology*.2012; 6(2); 186.
5. Tan X, Liu Y, Zeng G, Wang X, Hu X, Gu Y, Yang Z. et al. Application of biochar for the removal of pollutants from aqueous solutions. *Chemosphere*.2015; 125; 70-85.
6. Mandotra SK, Kumar P, Suseela MR, Ramteke PW et al. Fresh water green microalga *Scenedesmus abundans*: a potential feedstock for high quality biodiesel production. *Bioresource technology*.2014;156; 42-47.
7. Poddar S, De S, Chowdhury R et al. Catalytic pyrolysis of lignocellulosic bio-packaging (jute) waste–kinetics using lumped and DAE (distributed activation energy) models and pyro-oil characterization. *RSC Advances*.2015; 5(120); 98934-98945.
8. Yuan T, Tahmasebi A, Yu J et al. Comparative study on pyrolysis of lignocellulosic and algal biomass using a thermogravimetric and a fixed-bed reactor. *Bioresource technology*. 2015;175; 333-341.
9. Wang K, Brown RC, Homsy S, Martinez L, Sidhu SS et al. Fast pyrolysis of microalgae remnants in a fluidized bed reactor for bio-oil and biochar production. *Bioresource technology*. 2013; 127; 494-499.
10. Kim, S. W., Koo, B. S., & Lee, D. H. (2014). A comparative study of bio-oils from pyrolysis of microalgae and oil seed waste in a fluidized bed. *Bioresource technology*, 162, 96-102.
11. Chaiwong, K., &Kiatsiriroat, T. (2015). Characterizations of bio-oil and bio-char products from algae with slow and fast pyrolysis. *Int J Environ Bioenergy*, 10, 65-76.
12. Gautam, R., Shyam, S., Reddy, B. R., Govindaraju, K., &Vinu, R. (2019). Microwave-assisted pyrolysis and analytical fast pyrolysis of macroalgae: product analysis and effect of heating mechanism. *Sustainable Energy & Fuels*, 3(11), 3009-3020.

Chapter 10

Conclusion

Under the present research study, the assessment of CO₂ Capture, assimilation of organic carbon source, glycerol and mixture of inorganic (CO₂) and organic carbon source (glycerol) and production of Oil, Pigments, Biochar and pyro-oil using Power Plant Blue Green Algal strain, *Leptolyngbya subtilis*JUCHE1 have been carried out. The experiments have been conducted under three different modes of growth conditions: (I) Photoautotrophic, (II) Photoheterotrophic and (III) Photomixotrophic ones using inorganic (CO₂) organic (Glycerol) and mixed carbon sources, namely CO₂ and Glycerol.

The foregoing chapters on the present research work revealed that the “*L. subtilis* JUCHE1”, the power plant algal strain isolated during the study is very versatile in nature and can be grown on either CO₂ or glycerol or on the mixture of the two. It can withstand CO₂ to a high level and hence can be used safely for the capture of CO₂ from the flue gas generated from coal-based power plants. The blue green alga/ cyanobacterium can also be utilized for the treatment of by-product, i.e., glycerol, of biodiesel plants. It has been observed that while photoautotrophic growth is favourable for biomass generation, the lipid production is enhanced in photoheterotrophic growth condition. Therefore, the feasibility of growth of “*L. subtilis* JUCHE1” using mixed carbon sources has been also be checked and has been established to be encouraging. For the implementation of the applicability of “*L. subtilis* JUCHE1” in large scale, medium scale reactor study has also been studies and important data have been generated. Since the success of the reactor design depends much on the rate of growth, kinetics have been determined with respect to carbon source both in case of photoautotrophic and photoheterotrophic conditions. For photoautotrophic growth, the multivariable growth kinetics with respect to carbon and nitrogen source as well as light intensity have been determined. Optimization of growth has also been conducted to identify the exact set of input parameters to be used in future. Besides a potential source of biomass and lipid *L. subtilis* JUCHE1is also a store house valuable pigments and carotenoids. The analysis of lipid of the cyanobacterium has revealed that the oil is rich in many valuable fatty acids. For the utilization of residual algal mass after the removal of oil and pigment pyrolysis data have also been generated. It has been established that there is a possibility of generation biochar, pyro-oil and pyro-gas. Therefore, *L. subtilis* JUCHE1can be claimed to be a very

attractive strain to be utilized in algal biorefinery. The salient findings in different trophic conditions are as follows:

10.1 Photoautotrophic Growth

10.1.1 Effect of CO₂ as inorganic carbon source on biomass growth, CO₂ fixation rate, lipid accumulation and pigment production of blue green alga *Leptolyngbya subtilis* JUCHE1

10.1.1 Determination of the kinetic parameters

- With increase in CO₂ concentrations from 5-15% v/v, the growth rate also increases and then substrate inhibition is observed beyond 15% CO₂ concentration in gas phase at 20% v/v.
- The Haldane model is valid and the values of kinetic parameters (μ_{\max} , K_s , K_I) of 0.65d⁻¹, 0.0162 g/L and 1.79 g/L respectively are observed. The value of the regression coefficient (RMSE value 0.0174)
- The maximum biomass concentration and productivity of 0.7286 g/L and 0.1857g/L/d respectively are observed for 15% inlet-CO₂ concentration on 3rd and 1st day of the culture period.

10.1.2 Determination of CO₂ fixation rate

- The maximum CO₂ fixation rate of *L. subtilis* JUCHE1 is 0.2383 g/L/d at 15% (v/v) inlet CO₂ concentration, 1.5g/L NaNO₃ and 2.5kLux.

10.1.3 Determination of Lipid content and productivity

- The highest value of lipid content is observed to be 12.5%(w/w) for 15%v/v inlet-CO₂ concentration on 3rd day.
- The highest value of lipid productivity of 0.02g/L/d is observed for 15%v/v inlet-CO₂ concentration on 3rd day.

10.1.3 Determination of pigment content

- The chlorophyll and carotenoid contents of 0.289 %(w/w) and 0.116 %(w/w) are obtained at 15%v/v CO₂ concentration from the highest biomass concentration (0.7286 g/L on 3rd day).

10.1.2 Determination of growth kinetics parameters, lipid content and CO₂ fixation rate of *L.subtilis*JUCHE1 varying concentration of NaNO₃

10.1.2.1 Determination of growth kinetics parameters

- The linearity of the double reciprocal plot with $R^2 = 0.9654$ establishes the validity of Monod model.
- From the intercept and the slope of the double reciprocal plot the values of μ_{\max} and K_s are determined to be 0.667 d^{-1} and 0.644 g/L respectively.
- The maximum biomass concentration and productivity of 0.745 g/L and 0.1738 g/L/d respectively are obtained at 2 g/L NaNO₃ concentrations on 4th and 1st day of the culture period.

10.1.2.2 Determination of CO₂ fixation rate

- The highest CO₂ fixation rate of 0.2230 g/L/d is observed on 1st day for 2 g/L of NaNO₃.

10.1.2.3 Determination of Lipid content and productivity

- The highest value of lipid content of 53.87% (w/w) is obtained at 1 g/L of NaNO₃ concentration.
- The maximum value of lipid productivity of 0.0423 g/L/d is obtained at 2 g/L of NaNO₃ concentration.

10.1.3 Determination of growth kinetic parameters, Lipid content and CO₂ fixation rate of *L.subtilis*JUCHE1 varying Light intensity

10.1.3.1 Determination of growth kinetics

- Among Steele, Aiba and Bernard and Remond models, Steele model is proved to be the fittest one to explain the dependence of growth on light intensity.
- The maximum biomass concentration and productivity are observed to be 0.7196 g/L and 0.6371 g/L/d respectively on 3rd day at 2.5 kLux .

10.1.3.2 Determination of lipid content and productivity

- The highest value of lipid content of 13.35% w/w is observed on 3rd day under the irradiance of 2.5 kLux .
- The highest values of productivity of 0.0851 g/L/d is also observed on 3rd day under the irradiance of 2.5 kLux .

10.1.4 Determination of multi-variable (CO₂-NaNO₃-I) functionality to correlate specific growth rate with the simultaneous variation of concentrations of CO₂ and NaNO₃ and light intensity

- A multi-variable kinetic model explaining the dependence of specific growth rate with respect to simultaneous variation of all three input variables, i.e., concentration of CO₂ and NaNO₃ and light intensity has been developed and validated.
- For the best fitted models, statistical parameters such as the root-mean-square error, bias factor and standard error of prediction is evaluated and their values are lie within the limit of valid models.
- Box–Behnken method of RSM is performed using three input variables (A: CO₂, B: NaNO₃ and C: light intensity) and specific growth rate(μ) of *L. subtilis* JUCHE1 as the response. From statistical summary it is observed that the p-value is less than < 0.0001 and the predicted and adjusted values of R^2 are 0.9976 and 0.9997.
- From the three-dimensional (3-D) plots along with the contour plot of AB it is found that with the increase in (B) NaNO₃ concentrations (1- 2.5g/L) along with the (A) CO₂ concentrations (0.05456 - 0.2178 g/L) the growth curve of “ μ ” simultaneously increases from 0.3594- 0.5932 d⁻¹.
- The 3D and contour plot of BC, represented an increasing trend of growth rate “ μ ” with increase in both the parameters i.e. (B) NaNO₃ concentrations and (C) Light intensity.
- From the 3D and contour plots of AC, it is observed that when both the parameters (A) CO₂ concentrations and (C) light intensity increase, the growth rates of *L. subtilis* JUCHE1 is also increased.

10.1.4 Studies on algal growth, CO₂ Capture, lipid accumulation and pigment production by *L. subtilis* JUCHE varying different wavelengths of light (Blue, Green, Yellow and Red)

10.1.4.1 Determination of biomass concentration and productivity

- Among all the wavelengths of light (Blue, Green, Yellow and Red), the highest biomass concentration and productivity of 1.2251 g/L and 1.1838 g/L/d respectively are observed under the irradiance of yellow light on 6th day of culture period.

10.1.4.1 Determination of lipid content and productivity

- The maximum lipid content of 22.15% (w/w) is obtained on 6th day of growth under yellow wavelength of light.
- The maximum lipid productivity of 0.0361 g/L/d is observed on 6th day under yellow wavelength of light.

10.1.4.2 Determination of CO₂ fixation rate

- The maximum CO₂ fixation rate of 0.3520g/L/d is achieved for yellow light on 5th day.
- The maximum CO₂ fixation rate of 3373g/L/d is observed for green light on 4th day of growth.
- The maximum CO₂ fixation rate of .2830g/L/d is observed for red light on 4th day of growth.
- The maximum CO₂ fixation rate of 0.3137g/L/d is observed for blue light on 3rd day of growth.

10.1.4.3 Determination of Chlorophyll and Carotenoid content

- Under blue light, the highest values of chlorophyll and carotenoid contents of 0.93 %w/w and 0.2728 % w/w is achieved on 6th day.

10.1.4.4 Study on the performance of Airlift photobioreactor using the most suitable wavelength with respect to Biomass, Lipid and CO₂ fixation rate

- Under semi-continuous cultivation mode, the maximum biomass concentration and productivity of 2.72g/L and 0.2224 g/L/d are observed for Internally Externally Gas-lift Photobioreactor (IEIGPBR) on 14th day and 8th day of culture periods under the irradiance of yellow light (590 nm).

10.1.4.4.1Determination of lipid content and productivity

- The highest value of lipid content and productivity of 58.86(% w/w) and 0.1043 g/L/d respectively are observed for yellow wavelength of light on 14th day and 12th day of culture periods.

10.1.4.5 Determination of CO₂ fixation rate

- It is observed that the CO₂ fixation rate increases with increase in time and reaches its maximum on 8th day and the value is 0.2855g/L/d.

10.2 Photoheterotrophic Growth of blue-green algae, *Leptolyngbya subtilis* JUCHE1 with the variation of glycerol concentrations from 0.03799- 0.15207g/L

10.2.1 Determination of growth kinetic parameters and the trends of production of biomass

- The maximum biomass concentration of 0.817 g/L is observed on 4th day at glycerol concentration of 0.1139 g/L (Equivalent to 15% v/v CO₂ concentration in gas phase),
- The maximum biomass productivity of 0.2733 g/L/d is observed on the 1st day at glycerol concentration of 0.1139 g/L (Equivalent to 15% v/v CO₂ concentration in gas phase),
- By plotting the inverse of μ against the inverse of glycerol concentration, establishes the validity of Monod model up to concentration of glycerol i.e. up to 0.1139 g/L, i.e., in the uninhibited zone of growth.
- The values of μ_{max} and K_s have been determined from the intercept and the slope of Figure 6.25 (B). As the value of $C_{S,max}$ corresponding to the maximum value of μ is 0.1139 g/L, hence the value of K_I have been determined by using the correlation, $C_{S,max} = \sqrt{K_S K_I}$ using Method-I described in Section 5.1.6 of Section 5. The values of growth kinetic parameters, namely, μ_{max} , K_s , K_I have been determined to be 0.8824 d⁻¹, 0.0261 g/L and 0.4974 g/L, respectively.
- The RMSE value has been determined to be 0.06 and is high. The Method-II, described in Section 5.1.6 of Section 5 has also been applied. But it cannot be converged with the restriction of $RMSE \leq 0.02$ with narrow adjustment of original μ'_{max} . Therefore, it appears that Haldane model is difficult to be valid in case of the heterotrophic growth on glycerol.
- Accordingly, $C_{S,crit}$, i.e., the glycerol concentration at which no growth is obtained, has been determined to be 0.25g/L. The value of $\mu_{without\ inhibition}$ at 0.152g/L has been

determined using Monod model with already determined values of μ_{\max} and K_s of 0.8824 d⁻¹, 0.0261 g/L respectively.

- Using the experimental value of μ and $\mu_{\text{without inhibition}}$ at 0.152g/L, the value of “n” has been determined to be 0.29. Overall the RMSE value has been obtained to be 0.013.

10.2.2 Determination of Lipid content and productivity

- The highest values of both lipid content and productivity of 56.34% (w/w) and 0.070248 g/L/d are observed on 4th day at the minimum glycerol concentration of 0.03799g/L (Equivalent to 5% (v/v) CO₂ in gas phase).

10.2.2 Determination of chlorophyll and carotenoid content

- Under photoheterotrophic growth, the chlorophyll and carotenoid contents of 0.186 %w/w and 0.087(%w/w) are obtained at glycerol concentration of 0.1139 g/L (Equivalent to 15%v/v CO₂ concentration) from the highest biomass concentration (0.817g/L on 4th day)

10.3 Under Photomixotrophic Growth of blue-green algae, *Leptolyngbya subtilis* JUCHE1 using both organic and inorganic carbon sources (CO₂+ Glycerol)

10.3.1 Determination of the trends of production of biomass

- The maximum biomass concentration and productivity of 0.6393 g/L and 0.248g/L/d respectively are obtained on 3rd day and 1st day using 7.5% CO₂ and 0.0569g/L glycerol (equivalent to 7.5% CO₂).

10.3.2 Determination of lipid content and productivity

- The highest lipid content and productivity of 26.71% and 0.0272g/L/d respectively is achieved using 7.5% CO₂ and 0.0569g/L glycerol (equivalent to 7.5% CO₂) on 5th day and 3rd day of culture period.

10.3.3 Determination of chlorophyll and carotenoid content

- Under photo-mixotrophic growth, the chlorophyll and carotenoid contents of 0.227 and 0.114 (%w/w) are obtained using 7.5% CO₂ and 0.0569g/L glycerol (equivalent to 7.5% CO₂) when the biomass concentration was the highest (0.6393/L on 5th day).

10.4 Pyrolysis of algal biomass for production of Bio-char, pyro-oil and pyro-gas

- It is observed that over sixty minutes the maximum weight loss of 92% w/w has been obtained at 700 °C .
- The highest yield of biochar of 29% (w/w) is obtained at 300°C.
- The maximum yield of oil and gas of 23.65% and 69.12% respectively are obtained at 700°C.
- The range of Bio-oil lies between 9.55-23.65% with increase in pyrolysis temperature from 300-700 °C.
- The yield of pyro-gas lies in between the range of 60.86-69.12% (300-700 °C) which is high.
- The thermal decomposition(TGA) profile of dry algal biomass depicts steep S- shaped curve for all the heating rates (10, 15, 20, 25 and 30 °C/min). It has also been observed that under adiabatic condition, the decomposition process can be divided into four distinct temperature zones: I: 50-275°C, II: 275-380 °C, III: 380-570 °C and IV: 570-900 °C. This indicates that the pyrolysis is expected to occur mostly from 275-570°C. After 570°C the mass-temperature profile is almost flat.
- For 500 °C char sample, the temperature range of these zones are :(1) 50-425 °C, (2) 425-620 °C, and (3) 620-900 °C, while for 700 °C char sample ranges are: zone1: 50-400°C, zone2: 400-640 °C, zone 3: 640-900 °C.
- Therefore, similar patterns of TGA plots indicates the similarity in the constituents of pyro char obtained at 500 and 700°C.
- From the GC-MS analysis of pyro-oil obtained through pyrolysis at 500°C it is found that most of the identified organic compounds in the oil are mostly fatty acids (saturated, unsaturated, polyunsaturated, volatile fatty acids), esters and amino acids.

Future scope

As discussed in Conclusion, *L. subtilis* JUCHE1 can be claimed to be a very attractive strain to be utilized in algal biorefinery.

However, further research studies should be conducted to generate more insights in the following areas:

- To study the effect of different wavelengths of light (red, green, yellow, blue) on *Leptolyngbya subtilis* JUCHE1 for production of biochemical such as DHA, EPA, ALA etc. under photoautotrophic growth should be conducted.
- Biochemical production such as Lutein, Xanthophyll, Phytoproteins using *Leptolyngbya subtilis* JUCHE1JUCHE1 under both photoautotrophic and photoheterotrophic growth should be conducted.
- The possibility of using *Leptolyngbya subtilis* JUCHE1JUCHE1 in open ponds should be explored for its integration with power plant.
- Model biorefinery system incorporating the different trophic modes of growth of *Leptolyngbya subtilis* JUCHE1JUCHE1 with the scope for production of oil, pigment, biochar, pyro-oil and other biochemicals should be explored.
- Process modeling can be carried out using standard software like ASPEN PLUS to assess the likely scenario during large scale implementation.
- Life cycle and techno economic analyses should be conducted for overall algal cultivation process.

Appendix

1. MATLAB codes have been provided below:

1.1 Aiba model

```
function Aiba_Model
phi=[0 0.9171 0.9530 1 0.9266]';
I=[0 1.45 1.95 2.49 3.2]';
fun=@(k,I)((I)/(k(1)+I+(k(2).*(I.^2))));
k0=[0.01 0.01]';
mdl=fitnlm(I,phi,fun,k0)
%c=mdl.Coefficients.Estimate;
k= nlinfit(I,phi,fun,k0)
phin=((I)/(k(1)+I+(k(2).*(I.^2))));
hold on
plot(I,phi);
plot(I,phin);
xlabel('Intensity(uE/m^2/s)'); ylabel('f_I');
legend('Experimental','Calculated');
hold off
```

1.2 Steele Model

```
function Steele_Model
%phi= $\mu/\mu_{max}$ 
phi=[0 0.917 0.953 1 0.9266]';
I=[0 1.45 1.95 2.49 3.2]';
I_opt=2.49;
phin=((I/I_opt).*exp(1-(I/I_opt)));
phin
ru = phin-phi;
```



```

normru = norm(ru);
SSE_u = normru.^2;
SST_u = norm(phin-mean(phin))^2;
R2_u = 1 - (SSE_u/SST_u)
hold on
plot(I,phi);
plot(I,phin);
xlabel('Light Intensity(kLux)'); ylabel('f_I');
legend('Expertimetal','Steele Model');
hold off

```

1.3 Bernard and Remond model

```

function Bernard_Remond_model
phi=[0 0.917 0.953 1 0.9266]';
I=[0 1.45 1.95 2.49 3.2]';
fun=@(k,I)((I)/(I+((0.4673/k(1))*((I/2.49)-1).^2)));
k0=[0.01]';
mdl=fitnlm(I,phi,fun,k0)
%c=mdl.Coefficients.Estimate;
k= nlinfit(I,phi,fun,k0);
phin=((I)/(I+((0.4673/k(1))*((I/2.49)-1).^2)));
hold on
plot(I,phi);
plot(I,phin);
xlabel('Light Intensity(kLux)'); ylabel('f_I');
legend('Expertimetal','Bernerd and Remond Model');
hold off

```

1.4 Haldane

```
function CO2
phi=[0 0.7410 0.8526 0.8662 0.8216]';
I=[0 0.05456 0.10912 0.16368 0.2178]';
fun=@(k,I)((I./(k(1)+I+(k(2).*(I.^2)))));
k0=[0.01 0.01]';
mdl=fitnlm(I,phi,fun,k0)
%c=mdl.Coefficients.Estimate;
k= nlinfit(I,phi,fun,k0)
k(2)> 0;
phin=((I./(k(1)+I+(k(2).*(I.^2)))));
hold on
plot(I,phi);
plot(I,phin);
xlabel('CO2 Concentration (g/L)'); ylabel('u/umax');
legend('Experimental','Calculated');
hold off
```